Transport of reactive solutes in heterogeneous porous formations

Promotor:	dr. ir. F.A.M. de Haan hoogleraar bodemhygiëne en -verontreiniging
Co-promotor:	dr. ir. S.E.A.T.M. van der Zee universitair hoofddocent bodemhygiëne en -verontreiniging

W.J.P. Bosma

Transport of reactive solutes in heterogeneous porous formations

Proefschrift
ter verkrijging van de graad van doctor
in de landbouw- en milieuwetenschappen
op gezag van de rector magnificus,
dr. C.M. Karssen,
in het openbaar te verdedigen
op vrijdag 11 november 1994
des namiddags te vier uur in de Aula
van de Landbouwuniversiteit te Wageningen.

The research reported in this thesis was funded by the European Community Environmental Research Program under contract number STEP-CT900031, and by the National Computing Facilities Foundation (NCF) for the use of super computer facilities with financial support from the Netherlands Organization for Scientific Research (NWO).

CIP-DATA KONINKLIJKE BIBLIOTHEEK, DEN HAAG

Bosma, W.J.P.

Transport of reactive solutes in heterogeneous porous formations / W.J.P. Bosma. - [S.l. : s.n.]
Thesis Wageningen. - With ref. - With summary in Dutch.
ISBN 90-5485-313-1
Subject headings: solute transport / soil contamination / nonlinear adsorption.

Stellingen

1. In tegenstelling tot de conclusie van Selim *et al.* (1977) heeft de volgorde van een lineair adsorberende laag en een niet-lineair adsorberende laag in een bodemkolom wel degelijk invloed op de vorm van de doorbraakcurve van een transporterende stof.

   Selim, H.M., J.M. Davidson, and P.S.C. Rao, Transport of reactive solutes through multi-layered soils, Soil Sci. Soc. Am. J., 41, 3-10, 1977.

   Dit proefschrift.

2. Juist als de gemiddelde adsorptiecoëfficiënt klein is, is de pluimvorm van een transporterende stof in een heterogeen poreus medium hier gevoelig voor.

   Dit proefschrift.

3. Gebruik van de 'Eulerian-Langrangian' methode voor niet-lineair adsorberende stoffen, in combinatie met bepaalde begin- en randvoorwaarden, levert problemen op als porieschaal dispersie verwaarloosd wordt.

   Dit proefschrift.

4. De verplaatsingssnelheid van een pluim van een eindige hoeveelheid niet-lineair preferent adsorberende stof neemt af als functie van de tijd.

   Dit proefschrift.

5. Bij een verhouding van $\alpha_T/I<1$, waar α_T de transversale dispersielengte en I de correlatielengte is, zal op de schaal van een aquifer geen concentratie-profiel waargenomen worden dat het gedrag heeft van een lopende golf.

6. In de meeste zandige aquifers kan ervan uit worden gegaan dat de verwachting van de pluimvorm van een eindige hoeveelheid niet-lineair adsorberende stof sterker beïnvloed wordt door de vorm van de adsorptie isotherm dan door ruimtelijke variabiliteit.

   Dit proefschrift.

7. Het aanvaarden van de bestuursstructuur van de onderzoekscholen en -instituten op universiteiten is een onderdeel van de ondermijning van de universitaire democratie.

8. Het is niet mogelijk om voorspellingen van statistische momenten van de verplaatsing van stoffen in heterogene poreuze media experimenteel te verifiëren.

9. Bij verdergaande drastische bezuinigingen op het hoger onderwijs en de studiefinanciering zal de prijs/kwaliteit verhouding van het Nederlandse hoger onderwijs zo'n bedenkelijk niveau bereiken dat duurdere buitenlandse universiteiten voor aankomende studenten aantrekkelijker worden.

10. Het College van Bestuur dient er op toe te zien dat de bijdrage van een 0,0 hoogleraar aan het onderzoek èn onderwijs hoger is dan de benaming van de functie suggereert.

11. Promoveren is gekkenwerk.
    11/11/1994.

12. De gelijke studieduur voor Universitair en Hoger Beroeps Onderwijs èn het promotierecht voor studenten afgestudeerd aan H.B.O. instellingen doet vermoeden dat de scheiding tussen deze twee onderwijsvormen kunstmatig is.

13. Het toepassen van het multi-functionaliteit principe bij bodemsanering kan vergeleken worden met de eis dat Rijnwater zonder zuivering drinkbaar is.

14. If you have never failed, you have never aimed high enough.
    J.P. Stenbit.

Stellingen behorend bij het proefschrift 'Transport of reactive solutes in heterogeneous porous formations' van W.J.P. Bosma, Wageningen, 11 november 1994.

Abstract

Bosma, W.J.P., **Transport of reactive solutes in heterogeneous porous formations**, Doctoral thesis, Wageningen Agricultural University, The Netherlands, 229 pages.

Transport and spreading behaviour of reactive solutes in heterogeneous porous formations is considered. Spatial variability is modeled by assuming a random space function (RSF) for the spatially variable properties. In the available literature, the effect of random spatial variability is mostly limited to considering the hydraulic conductivity as a RSF. In this thesis emphasis is given to the effects of spatial variability of physical as well as chemical properties. Linearly and nonlinearly adsorbing solutes are taken into account. Nonlinear adsorption is modeled by the Freundlich equation. The effect of local nonlinear adsorption on displacement is shown with analytical approximations for different cases. Examples are a homogeneous column with first-order degradation, a column with two layers with different adsorption behaviour and a column consisting of many layers with variable Freundlich adsorption coefficient. The concentration front in the latter one-dimensional case can successfully be described by a traveling wave front, which develops in an equivalent homogeneous column. For two-dimensional domains, displacement of linearly and nonlinearly adsorbing solutes is considered, assuming the adsorption coefficient and the hydraulic conductivity to be spatially variable. Results are given in terms of spatial and statistical moments, which describe the position and shape of concentration fronts and solute plumes. In case of linear adsorption, analytical solutions derived for the statistical moments compare well with numerical results. For a nonlinearly adsorbing solute, the boundary conditions play an important role with respect to the spreading behaviour. If the solute is continuously injected into the domain, macroscopic front spreading is determined by spatial variability. Nonlinear adsorption causes a reduction of front spreading compared with linear adsorption. Similarly, heterogeneity governs the variance of the mean plume position in case of an instantaneous or finite injection. On the other hand, the shape of the instantaneously injected plume is determined by nonlinear adsorption. A mathematical analysis for homogeneous domains can be useful for describing the plume development in heterogeneous flow domains.

Additional index words: heterogeneity, groundwater quality, stochastic hydrology, Monte Carlo simulations, traveling wave.

Voorwoord

De afgelopen vier jaar heb ik een groot deel van mijn tijd besteed aan onderzoek naar het gedrag van verontreinigende stoffen in bodem- en grondwatersystemen. Een deel van de resultaten van dit onderzoek heb ik in dit proefschrift beschreven. Hoewel ik denk dat de inhoud wetenschappelijk gezien interessante aspecten heeft en wellicht insiders zelfs zou kunnen boeien, is het boekje niet echt ontspannen leesvoer voor het slapen gaan. Daar is het ook niet voor bedoeld. Toch heb ik geprobeerd om via de inleiding en de samenvatting aan te geven wat globaal de inhoud van de tussenliggende hoofdstukken is. Misschien dat mijn volgende boek (ik heb nog geen plannen) een wat makkelijker leesbaar karakter heeft.

Ik wil in dit voorwoord ook een aantal personen bedanken die op verschillende manieren een bijdrage aan dit proefschrift hebben geleverd. In de eerste plaats wil ik mijn begeleider Sjoerd van der Zee bedanken. Voor mij was Sjoerd een ideale begeleider, vooral omdat onze interesses zeer goed aansluiten. Dat geldt zowel voor de vakinhoudelijke zaken zoals de belangstelling voor transport en heterogeniteit, als voor de behoefte aan gezelligheid. Bovendien was Sjoerd in staat om mij op de juiste momenten te inspireren en te motiveren. Mijn promotor, Frans de Haan, wil ik bedanken voor de mogelijkheden die hij mij heeft kunnen bieden en het vertrouwen dat hij mij heeft gegeven. Ik waardeer enorm de openheid die Frans toonde toen ik wat meer behoefte had aan mentale steun.

My stay at the 'Dipartimento di Ingegneria Civile ed Ambientale' of the 'Università di Trento' in Italy has been very important for the progress of my research. I am very grateful for the hospitality and friendship of both Andrea Rinaldo and Alberto Bellin. Both of them taught me a great deal about hydrology, stochastic modeling, Italian food and Italian life. Grazie tante!

Erg leuk heb ik de samenwerking met Hans van Duijn van de TU Delft gevonden. In de laatste fase van mijn onderzoek heeft hij mij het belang van de analytische wiskunde getoond, toen bleek dat er problemen waren met de numerieke berekening van de niet-lineaire gevallen. Mede dankzij zijn interesse en hulp zijn die problemen op tijd opgelost. Bovendien ben ik dankbaar voor de mogelijkheden die de vakgroep Wiskunde van de TU Delft mij heeft geboden om gebruik te kunnen maken van hun snelle computers.

In het kader van een afstudeervak hebben Stefan Gruijters, Reineke Klein Entink, Anja Pepels, Gerjon Gelling, Roy Kasteel, Robin Mulder, Eef Elzinga en Hendrik-Jan Hendricks Franssen meegewerkt aan mijn onderzoek. Ik bedank hen voor hun bijdragen en inzet. Voor de prettige sfeer op het werk en op de borrels

bedank ik de leden van de vakgroep Bodemkunde en Plantevoeding en met name de sectie bodemhygiëne en de spil van de vakgroep: het secretariaat.

Bij de afronding van het proefschrift waren Rob Roosken en Alexander Krekel nog erg behulpzaam op de computer. Dankzij hen heb ik de 'Mexico-deadline' kunnen halen. Ik ben ook blij met de hulp van Eline Bosma bij het ontwerpen van de omslag.

Nu het allemaal af is, denk ik met veel genoegen terug aan de afgelopen vier jaar. De laatste anderhalf jaar waren extra leuk dankzij de steun en gezelligheid van Mirjam.

Willem Jan Bosma
Utrecht, september 1994

Contents

Chapter 1

General introduction

1.1 Background

The physical and (bio)chemical processes in porous formations are of great interest in many areas of research. One of these areas is the field of soil and groundwater systems, which are important in view of the demand for a clean environment. Recently, in soil and groundwater research much attention has shifted to topics that are concerned with the quality of the environment. Examples of these topics are effects and causes of acid rain, adverse effects of intensive agricultural production, and processes related to the presence of contaminants in natural soil and groundwater systems. Understanding of the complex processes that occur when solutes reach the soil or groundwater would ideally enable making sound decisions with respect to land use planning, soil and groundwater remediation and economic development. To obtain this understanding, researchers use and develop different methods and tools, such as laboratory experiments, field tests and modeling approaches. Modeling of the physical and chemical processes, as used in this thesis, can extend experimental findings to situations for which experiments are impossible or difficult to conduct.

A solute that reaches a soil or groundwater system is affected by physical and (bio)chemical processes. The physical processes concern the movement of the solute, such as advection due to water flow and pore scale dispersion due to small scale variation of water velocities. The (bio)chemical processes affect the availability of the solute for physical transport phenomena. These processes include mutual reactions of various solutes present in the system (e.g., complexation), adsorption reactions of the solute with soil particles, precipitation, and biodegradation. These processes, which play a role on a local or microscopic scale,

are related and their effects on solute transport can be complicated. A complete model description of all acting processes in a soil or groundwater system may not lead to understanding of the transport problem, as effects cannot be attributed unequivocally to individual processes.

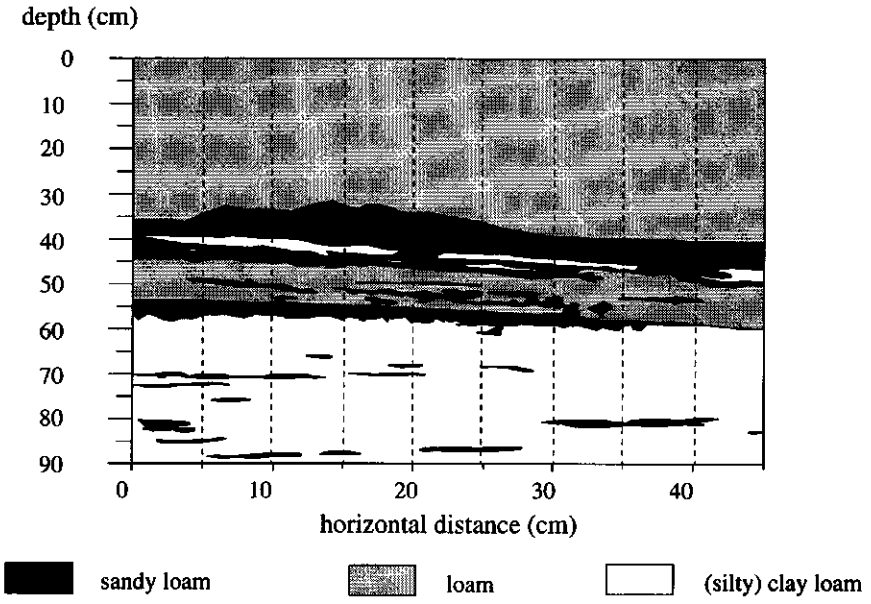

Figure 1.1 Vertical cross section of soil in the Wieringermeer, The Netherlands (from Finke and Bosma, 1993)

In addition to the local physical and chemical processes a complication in describing the fate of solutes in soil and groundwater systems is due to the natural variability of these porous formations. Deposition of soil material, rock weathering and soil morphological processes are causes of spatially variable soil properties. Figure 1.1 shows a vertical cross section of a stratified marine soil that illustrates soil heterogeneity of soil material. Variation of physical and chemical properties such as hydraulic conductivity, *p*H and organic matter content, may have a large impact on the transport behaviour of solutes. The properties vary often over distances that are much larger than the local scale. Large differences in hydraulic conductivity, for example, can lead to shorter or longer contaminant travel times than predicted on the basis of average parameters. In addition to the often unknown effects of spatial variability, an extra complication of heterogeneity lies in the fact

that the deterministic distribution of the property is often unknown.

This thesis emphasizes the combination of heterogeneity of soil properties and solute reactivity. The considered heterogeneity varies from a one-dimensional soil column with two different layers to a two-dimensional groundwater system with spatial variation of physical and chemical soil properties. The considered reactions consist of biodegradation and solute adsorption on soil particles.

The development of research in the field of solute transport stems from the time that fertilizers came into use in agriculture (Bolt, 1982). Following the formulation of the convection-dispersion equation (e.g., Lapidus and Amundsen, 1952) the number of solute displacement studies has increased considerably. Many of these studies aimed at solving the convection-dispersion equation for nonreactive and reactive solutes, subject to various initial and boundary conditions. A number of analytical solutions describing solutes moving in one-dimensional porous media, considering linear adsorption, first-order decay and zeroth-order production, were compiled by Van Genuchten and Alves (1982). Chemical complications, such as nonequilibrium and two-site adsorption, were studied by, among others, Van Genuchten *et al.* (1974), Cameron and Klute (1977), Nkedi-Kizza *et al.* (1984). One of the first attempts to model physical heterogeneity was made by assuming a dual porosity medium with a mobile and immobile zone. Examples of applications of this concept are Coats and Smith (1964) and Van Genuchten and Wierenga (1976).

The above cited works, even those that apply the dual porosity concept, describe the soil and groundwater system as a continuum with constant parameters. The irregular distribution of soil properties was investigated by Nielsen *et al.* (1973) and Biggar and Nielsen (1976). They showed effects of a spatially variable hydraulic conductivity, and demonstrated large differences between results of leaching computations with the spatially distributed parameter values and results computed with averaged values. A study of the degree of spatial variability and the effects on solute movement was performed at the experimental site in Borden, Canada (Mackay *et al.*, 1986; Sudicky, 1986).

The complexity of heterogeneity, i.e. the deterministically unknown distribution of the spatially variable property and its unknown effects, provides the incentive for approaching groundwater problems in a probabilistic framework. A detailed deterministic model description of the considered problem requires an enormous amount of data and is computationally intensive. This data requirement

is too costly for practical applications. On the other hand, the mathematical statistical model of the spatially variable property can be given in terms of a limited number of parameters by using a stochastic approach. Consequently, the results of the modeling problem are also given in statistical terms, i.e. moments (mean, variance, etc.).

Stochastic approaches are characterized by assuming a random variation of the spatially variable property in combination with a description of the spatial dependency. For example, heterogeneity of the hydraulic conductivity is often described by assuming a lognormal spatial distribution, given by the mean and the variance. The spatial dependency, or scale of heterogeneity, is typically described by a first-order autocovariance function. Early examples of stochastic approaches are Gelhar *et al.* (1979) and Dagan and Bresler (1979). Analytical expressions were derived to describe flow and nonreactive solute transport in heterogeneous media by, e.g. Gutjahr and Gelhar (1981), Dagan (1984, 1989), Gelhar and Axness (1983), and Rubin (1990). Various numerical studies have been performed to show the dispersive behaviour of nonreactive solutes (Graham and McLaughlin, 1989; Rubin, 1991*a*, *b*; Tompson and Gelhar, 1990; Bellin *et al.*, 1992).

Traditionally, the development of research dealing with heterogeneity and solute transport focused on variability of physical parameters, in most cases the hydraulic conductivity. Chemical reactions in combination with spatial variability of chemical properties have been taken into account less frequently. Dagan (1989) mentioned briefly the dispersive behaviour of linearly adsorbing solutes, considering only the case with perfect correlation between hydraulic conductivity and adsorption coefficient. Other examples of studies that considered spatial variability of linear adsorption reactions were given by Roberts *et al.* (1986), Garabedian (1987), Chrysikopoulos *et al.* (1990), Destouni and Cvetkovic (1991).

A linear description of the adsorption isotherm, however, may be a simplification of reality. Calvet *et al.* (1980) and De Haan *et al.* (1987) showed that solutes such as pesticides and heavy metals may adsorb according to a nonlinear isotherm. Van der Zee and Van Riemsdijk (1986, 1987) showed effects of spatially variable adsorption properties and solute application rates in combination with nonlinear adsorption. They used a semi-two-dimensional field (consisting of noninteracting columns) to predict the penetration depth of a nonlinearly adsorbing solute. Van Duijn and Knabner (1990) showed that with nonlinear adsorption under certain conditions a traveling wave concentration front

develops in homogeneous porous media.

The purpose of this thesis is to extend the stochastic multi-dimensional studies focused on heterogeneity to both physically and chemically heterogeneous formations, taking into account the reactivity of the solute (linear and nonlinear adsorption). To do so, some attention is given to the transport behaviour of a nonlinearly adsorbing solute in a one-dimensional system. These results are used to describe reactive solute transport in fully two-dimensional heterogeneous soil and groundwater systems.

1.2 Research objectives

The first objective of this study is to gain understanding of the behaviour of nonlinearly adsorbing solutes in heterogeneous soil and groundwater systems. With this understanding, questions can be answered with respect to the importance of the processes that play a role. In other words, is nonlinearity of adsorption important, does it lead to a different behaviour than in case of linear adsorption and is this expected difference significant? Furthermore, under what circumstances is the spreading process dominated by heterogeneity and in what cases is nonlinear adsorption more important than spatial variability? To obtain this understanding, numerical experiments are performed on one and two-dimensional soil systems. In case of spatially variable physical and chemical properties, the Monte Carlo approach is used, in which a computation is repeated a large number of times with different possible spatial realizations of the variable properties. By averaging over the ensemble, expected behaviour and a measure for the uncertainty are obtained. These analyses can also be very useful to assess the sensitivity of different parameters.

A second research objective is to derive some analytical tools that are readily applicable for estimations of concentrations, plume positions and plume growth of linearly and nonlinearly adsorbing solutes in various cases. Due to the large computational requirement of Monte Carlo analyses, numerical methods are not very suitable for applications in practice. Alternatively, analytical approximations are evaluated rapidly and they reflect directly the processes involved. Because their validity is restricted due to the underlying assumptions, their results can serve as a likely range, rather than as definite point estimates.

Several simplifications are made to fully understand the processes analyzed here. First, a single component system is assumed. No mutual reactions between reactive contaminants are taken into account. Although in many systems these reactions play an important role, they may be ignored if a large amount of solute is present. Secondly, nonlinear adsorption is described by the Freundlich adsorption isotherm, a relationship often used to describe adsorption on soil particles (Chardon, 1984; Van der Zee and Van Riemsdijk, 1987; Boekhold, 1992). Furthermore, adsorption is assumed to be fast, in other words, nonequilibrium effects are ignored. This assumption is valid when characteristic reaction times are significantly smaller than solute travel times. In a groundwater system with small water velocities, this assumption is often applicable.

An other simplification is the assumption of steady state water flow. This frequently used assumption may not apply to some cases within the characteristic time scale of the processes considered herein. Temporal variation, e.g., due to changes of head gradients by changes in precipitation and evapotranspiration, may have a large impact. In this case, however, the transport behaviour of nonlinearly adsorbing solutes in relation to spatial variability is of interest. To fully understand this problem, transient water flow is not taken into account here.

1.3 Outline of the thesis

This thesis is a compilation of several articles, published in or submitted to international scientific journals. In the first three chapters, the behaviour of a reactive solute in a one-dimensional system is considered. Chapter 2 deals with a homogeneous soil column and a nonlinearly adsorbing solute, subject to first-order (bio)degradation. An analytical approximation is presented which accounts for the increasing front retardation factor with time.

In Chapter 3, the nonhomogeneous soil column consists of two layers. The transporting solute adsorbs linearly in one layer and nonlinearly in the other. The effect of the layering order is studied and analytical approximations are given for the downstream concentration fronts.

Chapter 4 contains an analysis of the effect of chemical heterogeneity (spatial variation of the nonlinear adsorption coefficient) in one-dimensional columns. An expression for the front shape in homogeneous columns is derived

and compared with ensemble averaged front shapes for a heterogeneous column. The results are extended to a semi-two-dimensional domain characterized by noninteracting soil columns.

Further, the dispersive behaviour of a linearly adsorbing solute in fully two- and three-dimensional, physically and chemically heterogeneous porous formations is studied. In Chapter 5, an extension of the analytical solution of Dagan (1989) is derived for plume spreading in two and three dimensions. The cases of perfect positive, perfect negative correlation and no correlation between the hydraulic conductivity and adsorption coefficient are considered. In Chapter 6, the applicability of the analytical solutions derived in Chapter 5 is tested in the two-dimensional case. Numerical calculations using particle tracking techniques are performed to assess the sensitivity of various parameters.

Subsequently, the spreading behaviour of nonlinearly adsorbing solutes in two-dimensional heterogeneous formations is described. In Chapter 7, a continuous line source in either a chemically or a physically heterogeneous medium is considered. A Eulerian-Lagrangian method is used to solve the transport problem by a Monte Carlo approach. In Chapter 8, some analytical expressions are derived for the plume position and plume growth of a finite solute mass, initially present in a two-dimensional homogeneous system. Numerical computations are performed for an instantaneous solute injection, to show the applicability of this solution in physically and chemically heterogeneous cases. Furthermore, the effect of several parameters, such as the degree of nonlinearity and the degree of heterogeneity, is demonstrated and discussed.

Finally, in the last chapter some general conclusions evolving from this thesis are stated.

References

Bellin, A., P. Salandin, and A. Rinaldo, Simulation of dispersion in heterogeneous porous formations: statistics, first-order theories, convergence of computations, Water Resour. Res., 28, 2211-2227, 1992.

Biggar, J.W., and D.R. Nielsen, Spatial variability of the leaching characteristics of a field soil, Water Resour. Res., 12, 78-84, 1976.

Boekhold, A.E., Field scale behaviour of Cadmium in soil, Ph.D. Thesis, 181 pp., Wageningen Agric. Univ., The Netherlands, 1992.

Bolt, G.H., Movement of solutes in soil: principles of adsorption/exchange chromatography, in:

Soil Chemistry B. Physico-Chemical Models, edited by G.H. Bolt, pp. 285-348, Elsevier Sci. Publ., New York, 1982.

Calvet, R., M. Tercé, and J.C. Arvieu, Adsorption des pesticides par les sols et leurs constituants. III. Caractéristiques générals de l'adsorption des pesticides, Ann. Agron. 31, 239-257, 1980.

Cameron, D.A., and A. Klute, Convective-dispersive solute transport with a combined equilibrium and kinetic adsorption model, Water Resour. Res., 13, 183-188, 1977.

Chardon, W.J., Mobiliteit van cadmium in de bodem, Ph.D. Thesis, 200 pp., Wageningen Agric. Univ., The Netherlands, 1984.

Chrysikopoulos, C.V., P.K. Kitanidis, and P.V. Roberts, Analysis of one-dimensional solute transport through porous media with spatially variable retardation factor, Water Resour. Res., 26, 437-446, 1990.

Coats, K.H., and B.D. Smith, Dead-end pore volume and dispersion in porous media, Soc. Pet. Eng. J., 4, 73-84, 1964.

Dagan, G., Solute transport in heterogeneous porous formations, J. Fluid Mech., 145, 151-177, 1984.

Dagan, G., Flow and transport in porous formations, Springer-Verlag, Berlin, 1989.

Dagan, G., and E. Bresler, Solute dispersion in unsaturated heterogeneous soil at field scale, 1, Theory, Soil Sci. Soc. Am. J., 43, 461-467, 1979.

De Haan, F.A.M., S.E.A.T.M. Van der Zee, and W.H. Van Riemsdijk, The role of soil chemistry and soil physics in protecting soil quality; Variability of sorption and transport of cadmium as an example, Neth. J. Agric. Sci., 35, 347-359, 1987.

Destouni, G., and V. Cvetkovic, Field scale mass arrival of sorptive solute into the groundwater, Water Resour. Res., 27, 1315-1325, 1991.

Finke, P.A., and W.J.P. Bosma, Obtaining basic simulation data for a heterogeneous field with stratified marine soils, Hydrol. Process., 7, 63-75, 1993.

Garabedian, S.P., Large-scale dispersive transport in aquifers: Field experiments and reactive transport theory, Ph.D. thesis, Mass. Inst. of Technol., Cambridge, Mass., U.S.A., 1987.

Gelhar, L.W., and C.L. Axness, Three-dimensional stochastic analysis of macrodispersion in aquifers, Water Resour. Res., 19, 161-180, 1983.

Gelhar, L.W., A.L. Gutjahr, and R.L. Naff, Stochastic analysis of macrodispersion in a stratified aquifer, Water Resour. Res., 15, 1387-1397, 1979.

Graham, W., and D. McLaughlin, Stochastic analysis of nonstationary subsurface solute transport 1. Unconditional moments, Water Resour. Res., 25, 215-232, 1989.

Gutjahr, A.L., and L.W. Gelhar, Stochastic models of subsurface flow: infinite versus finite domains and stationarity, Water Resour. Res., 17, 337-350, 1981.

Lapidus, L., and N.R. Amundsen, Mathematics of adsorption in beds, VI, The effect of longitudinal diffusion in ion exchange and chromatographic column. J. Phys. Chem., 56, 984-988, 1952.

Mackay, D.M., D.L. Freyberg, P.V. Roberts, and J.A. Cherry, A natural gradient experiment on solute transport in a sand aquifer, 1. Approach and overview of plume movement, Water Resour. Res., 22, 2017-2029, 1986.

Nielsen, D.R., J.W. Biggar, and K.T. Erh, Spatial variability of field measured soil-water properties, Hilgardia, 42, 215-221, 1973.

Nkedi-Kizza, P., J.W. Biggar, H.M. Selim, M.Th. van Genuchten, P.J. Wierenga, J.M. Davidson, and D.R. Nielsen, On the equivalence of two conceptual models for describing ion exchange during transport through an aggregated oxisol, Water Resour. Res., 20, 1123-1130, 1984.

Roberts, P.V., M.N. Goltz, and D.M. Mackay, A natural gradient experiment on solute transport in a sand aquifer, 3. Retardation estimates and mass balances for organic solutes, Water Resour. Res., 22, 2047-2058, 1986.

Rubin, Y., Stochastic modeling of macrodispersion in heterogeneous porous media, Water Resour. Res., 26, 133-141, 1990.

Rubin, Y., Prediction of tracer plume migration in disordered porous media by the method of conditional probabilities, Water Resour. Res., 27, 1291-1308, 1991*a*.

Rubin, Y., Transport in heterogeneous porous media: Prediction and uncertainty, Water Resour. Res., 27, 1723-1738, 1991*b*.

Sudicky, E.A., A natural gradient experiment on solute transport in a sand aquifer: spatial variability of hydraulic conductivity and its role in the dispersion process, Water Resour. Res., 22, 2069-2082, 1986.

Tompson, A.F.B., and L.W. Gelhar, Numerical simulation of solute transport in three-dimensional, randomly heterogeneous porous media, Water Resour. Res., 26, 2541-2562, 1990.

Van der Zee, S.E.A.T.M., and W.H. Van Riemsdijk, Transport of phosphate in a heterogeneous field, Transp. Porous Media, 1, 339-359, 1986.

Van der Zee, S.E.A.T.M., and W.H. Van Riemsdijk, Transport of reactive solute in spatially variable soil systems, Water Resour. Res., 23, 2059-2069, 1987.

Van Duijn, C.J., and P. Knabner, Travelling waves in the transport of reactive solutes through porous media: Adsorption and binary exchange, Part 2, Report 205, Schwertpunkt programm der Deutsche Forschungsgemeinschaft, Univ. Augsburg, Inst. Mathematik, 45 pp, 1990.

Van Genuchten, M.Th., and W.J. Alves, Analytical solutions of the one-dimensional convective-dispersive transport equation, USDA Techn. Bull. 1661. 151 pp., U.S. Dept. of Agric., Washington D.C., 1982.

Van Genuchten, M.Th., and P.J. Wierenga, Mass transfer studies in sorbing porous media, I, Analytical solutions, Soil Sci.Soc. Am.J., 40, 473-480, 1976.

Van Genuchten, M.Th., J.M. Davidson, and P.J. Wierenga, An evaluation of kinetic and equilibrium equations for the prediction of pesticide movement through porous media, Soil Sci. Soc. Am. J., 38, 29-35, 1974.

Chapter 2

Analytical approximation for nonlinear adsorbing solute transport and first-order degradation*

Abstract

Under some constraints, solutes undergoing nonlinear adsorption migrate according to a traveling wave. Analytical traveling wave solutions were used to obtain an approximation for the solute concentration front, $c(z,t)$, for the situation of equilibrium nonlinear adsorption and first-order degradation. This approximation described numerically obtained fronts and breakthrough curves well. It is shown to describe fronts more accurately than a solution based on linearized adsorption. The latter solution accounts neither for the relatively steep downstream solute front nor for the deceleration in time of the nonlinear front.

2.1 Introduction

The contamination of soil and groundwater has provided a major incentive to study the fate of contaminants. Because most contaminants react with the soil matrix, the effects of such interactions on transport are of direct interest if we want to understand the observed phenomena. Whereas experimentation provides us with the phenomena to be understood, such experimental work does not suffice. Mathematical modeling gives us a tool to summarize experimental information as well as to predict the behaviour for conditions that preclude experimentation. For environmentally hazardous chemicals, experiments may also be undesirable. Practically, this is also the case for solutes that experience a large retardation which is affected by kinetics. Due to the large retardation, experimental evaluation of transport becomes time consuming and costly while it is not always feasible to

*by W.J.P. Bosma and S.E.A.T.M. van der Zee
published in: *Transport in Porous Media*, 11, 33-43, 1993.

speed up the process by e.g. large flow rates, due to the time dependency of (bio)chemical interactions. Consequently, a large number of transport models have been developed. Whereas numerical models are usually more versatile, analytical models may give more explicit understanding of the phenomena involved, and are useful for verification of numerical programs. An additional advantage of analytical solutions is that they are often evaluated more rapidly.

For one-dimensional transport, analytical solutions have been developed for different situations. For different boundary conditions Van Genuchten and Alves (1982) compiled solutions that took linear equilibrium adsorption, and zeroth as well as first order irreversible transformation rates into account.

For transport of solutes subject to kinetic adsorption onto two different sites with different rate parameters, solutions were given by Selim *et al.* (1976) and Cameron and Klute (1977). As was shown by Van Genuchten (1981) and Nkedi-Kizza *et al.* (1984), the dual-porosity model developed by Deans (1963), Coats and Smith (1964) and Van Genuchten and Wierenga (1976) is mathematically equivalent with the two-site model. Earlier, De Smedt and Wierenga (1979) showed that different solutions for the cases mentioned can be cast in the same general form. However, the solutions in each case concerned linear adsorption.

In many cases of practical interest, adsorption appears to be nonlinear. This nonlinearity may be due to variations in the background electrolyte (Cederberg *et al.*, 1985; Van Riemsdijk *et al.* 1987), but can also be observed when the background electrolyte is not varied, as was shown for heavy metals by Christensen (1980), De Haan *et al.* (1987) and Lexmond (1980) and for organic micro-pollutants by Calvet *et al.* (1980) and Friesel *et al.* (1984).

For the case of nonlinear adsorption, no analytical solutions are available for the development of the concentration front. However, for the limiting case of large displacement times (or distances) analytical traveling wave solutions were derived for several cases. Traveling wave behaviour refers to the development of a limiting front of constant shape and velocity in a homogeneous flow domain. It can be proven that (for symbols see Notation) for

$$c_0 > c_i \qquad f'(c) > 0 \qquad f''(c) < 0 \tag{2.1}$$

$$c_0<c_i \qquad f'(c)>0 \qquad f''(c)>0 \tag{2.2}$$

a traveling wave is bound to develop (Van Duijn and Knabner, 1990). An analytical solution for the front shape and velocity (after it has developed) was given for favourable Gapon divalent exchange by Reiniger and Bolt (1972) and Bolt (1982). For Langmuir adsorption, Lake and Helfferich (1978) gave an expression for the limiting front thickness. The traveling wave solution for Freundlich adsorption was given by Van der Zee and Van Riemsdijk (1987). Extending this latter result, Van der Zee (1990) gave analytical expressions for the limiting traveling wave when in the dual-porosity or two-site model the region (or site) at local equilibrium has a linear adsorption equation, whereas the region (or site) at nonequilibrium has a nonlinear (Langmuir or Freundlich) adsorption equation. The case where we have local equilibrium for both regions (one with linear and the other with nonlinear adsorption) appeared to be a special case of the one considered by Van der Zee (1990). Whereas the previously mentioned traveling wave solutions hold for steady state flow, Bond and Philips (1990) extended the work by Reiniger and Bolt (1972) and Bolt (1982) by deriving an approximation for transient unsaturated flow.

Our aim is to present an approximation for the case when adsorption is nonlinear and the solute is subject to first-order rate (bio)degradation. For this case no exact solutions are available. The analytical approximation is based on the expressions derived earlier for Freundlich waves by Van der Zee (1990), although it is equally valid for Langmuir-type adsorption. Its relevance follows from the context of organic micropollutant transport, such as pesticides (Calvet *et al.*, 1980) and chlorinated hydrocarbons (Friesel *et al.*, 1984) that often exhibit Freundlich type adsorption and are subject to (bio)chemical degradation.

2.2 Theory

We consider a solute transported in the positive z direction at steady-state flow. The solute is subject to adsorption and first-order kinetic losses. For example, such a first-order loss rate may be due to (bio)chemical degradation in the liquid phase or passive plant uptake (see, e.g., Van der Zee and Boesten (1990)). Then the mass balance equation reads

$$\theta\frac{\partial c}{\partial t}+\rho\frac{\partial s}{\partial t}=\theta D\frac{\partial^2 c}{\partial z^2}-\theta v\frac{\partial c}{\partial z}-\mu\theta c \qquad (2.3)$$

Expressing adsorption on a volumetric basis (i.e., $q=\rho s$), we assume that adsorption is at local equilibrium and given by the Freundlich equation

$$q=kc^n \qquad 0<n<1 \qquad (2.4)$$

No analytical solution exist for (2.3)-(2.4). For $\mu=0$, a traveling wave solution was developed by Van der Zee (1990). A traveling wave front is characterized by a constant shape of the front as well as a constant front velocity, provided the flow domain is physically and chemically homogeneous (for a relaxation of this constraint, consult Bond and Philips (1990)). For $0<n<1$, a traveling wave will form (at $t\rightarrow\infty$) provided (2.1) holds (Van Duijn and Knabner, 1990). This is due to the nonlinearity of adsorption, which causes relatively large concentrations to move faster through the column than relatively small concentrations (i.e., the latter experience a larger retardation factor $\tilde{R}(c)=1+q'(c)/\theta$). Hence, nonlinear adsorption has an effect that opposes dispersional front spreading. When the opposing effects of nonlinearity and pore scale dispersion are of equal force, the front ceases to flatten or steepen. Theoretically, this occurs at infinite times, but practically the limiting traveling wave front approximates the real front after relatively short times (Van der Zee, 1990).

The analytical expression of the limiting traveling wave front can be obtained after transformation by

$$\eta=z-\frac{vt}{R} \qquad R=1+\frac{\Delta q(c)}{\theta\Delta c} \qquad (2.5)$$

with R the front retardation factor and assuming

$$c(\eta)=c(z,t) \qquad q(\eta)=q(z,t) \qquad (2.6)$$

Observe that η was defined slightly different from Van der Zee (1990) where η was dimensionless. The solution of (2.3), (2.4) and (2.5) for LEA (local equilibrium assumption) valid is given by (Van der Zee, 1990)

$$c(\eta)=c_0 \quad \frac{dc}{d\eta}=0 \quad \frac{dq}{d\eta}=0; \qquad \eta=-\infty \tag{2.7a}$$

$$c(\eta)=0 \quad \frac{dc}{d\eta}=0 \quad \frac{dq}{d\eta}=0; \qquad \eta=\infty \tag{2.7b}$$

$$c(\eta)=c_0\left(1-\exp\left[\frac{\nu(R-1)}{DR}(1-n)(\eta-\eta^*)\right]\right)^{1/(1-n)} \tag{2.8}$$

assuming $\mu=0$. Discussion of the reference η^*-values was given in the original paper (Van der Zee, 1990) and is briefly summarized in the Appendix.

For the case that $\mu>0$, no traveling wave exists as the maximum concentration decreases with depth. Because this concentration controls both the experienced front retardation factor (R) and the (limiting) front steepness, both will change as the front proceeds in the positive z-direction. This is in disagreement with the definition of a traveling wave displacement.

However, it was shown that the traveling wave has developed (practically) after a small displacement of the front into the column (Van der Zee, 1990). Assuming that the solution (2.8) is valid instantaneously and that the change in the maximum concentration (at depth z) is slow, we might postulate that the traveling wave front aptly reacts to this change. In other words, the downstream front shape changes sufficiently fast to be in agreement with (2.8) at the local (at depth z) maximum concentration that can be attained in view of first-order decay. Based on this working hypothesis it is relevant to quantify the local maximum concentration that can be attained. This concentration (denoted c_0^*) follows from solving (2.3) for the situation that the downstream front has moved beyond depths of our interest. The steady-state solution for

$$\theta D\frac{\partial^2 c}{\partial z^2}-\theta v\frac{\partial c}{\partial z}-\mu\theta c=0 \tag{2.9}$$

$$c=c_0 \qquad z=0 \tag{2.10a}$$

$$\frac{dc}{dz}=0 \qquad z=\infty \tag{2.10b}$$

was given by Van Genuchten and Alves (1982; p56), i.e.,

$$c_0^*(z)=c_0 \exp\left[\frac{zv}{2D}\left(1-\sqrt{1+4\mu D/v^2}\right)\right] \tag{2.11}$$

The steady-state solution (2.11) applies to both linear and nonlinear cases, because the nonlinear term vanished by multiplication with zero i.e., when $\partial c/\partial t=0$,

$$\frac{1}{\theta}\frac{\partial q(c)}{\partial t}=(R-1)\frac{\partial c}{\partial t}=(kc_0^{n-1}/\theta)\frac{\partial c}{\partial t}=0 \tag{2.12}$$

(at steady-state described by (2.11)). Based on our working hypothesis, the terms in the exponential argument of (2.8), i.e., $R=1+(k/\theta)c_0^{n-1}$, depend on the local maximum concentration that can be attained at $\eta=0$ (the downstream front position, henceforth denoted by z^*). For the downstream front shape we therefore have to replace c_0 in R by $c_0^*(z^*)$. For the concentration levels, controlled by the pre-exponential c_0-value in (2.8) we expect that (2.11) provides a good approximation as discussed. Therefore, this c_0-value is to be replaced by the depth-dependent $c_0^*(z^*)$. Observe that this is identical with the approximation applied by Bolt (Bolt 1982; sec. 9.7) for the linear adsorption case. Finally, we need to approximate the position of the front, using (2.5). Due to the decreasing $c_0^*(z)$-values with increasing depths, the retardation factor has become depth dependent; the downstream front decelerates with increasing depth. To account for this we have to set

$$z^*=vt/\langle R(z^*)\rangle \tag{2.13}$$

where $\langle R(z^*)\rangle$ is a weighted average retardation factor for the front that has arrived at depth, z^*. An expression for $\langle R(z^*)\rangle$ is given in the Appendix. Finally, η^* in (2.8) is also concentration dependent. For the cases to be discussed, the ensuing depth dependence appeared to be small for η^* and no correction was made for this parameter.

The mentioned changes of (2.8) result in:

$$c(\eta)=c_0^*\left\{1-\exp\left[\frac{v(P-1)}{DP}(1-n)(\eta-\eta^*)\right]\right\}^{1/(1-n)} \tag{2.14}$$

$$P=1+\frac{k}{\theta}[c_0^*(z^*)]^{n-1} \tag{2.15}$$

$$\eta=z-vt/\langle R(z^*)\rangle \tag{2.16}$$

and η^* as given in the Appendix.

2.3 Illustrations

To evaluate the approximation defined by (2.14)-(2.16) for (2.3)-(2.4) numerical calculations were performed. A finite difference solution of (2.3)-(2.4) based on a Crank-Nicolson approximation of (2.3), using a Newton-Raphson iteration scheme was obtained. A fixed concentration boundary condition was used at the inlet boundary (z=0). A zero gradient boundary, well below depths of interest, was used for the downstream boundary. The initial concentration, c_i, in the column was set at a negligibly small value. Stability criteria based on a linear transport problem, as given by Van Genuchten and Wierenga (1974), were met.

For illustration and verification of the numerical solution, some reference cases for zero decay were considered first. In Figure 2.1*a* and 2.1*b* the numerical solution is shown together with the analytical traveling wave solution (for details see Van der Zee (1990)). In these cases, the parameter values as given in Table 2.1 were used. We observe that for the dispersivities assumed, which are in the range given by Frissel *et al.* (1970) for natural soils, the traveling wave soon corresponds with the numerical curves. The agreement improved fastest for the case with the largest dispersivity.

To test the accuracy of the approximation derived from the traveling wave solution, three cases were simulated that account for first order (bio)chemical transformation. Because the discrepancies between the analytical and numerical results of Figure 2.1 were largest for L_d (= D/v) equal to 1.6 cm, this value was

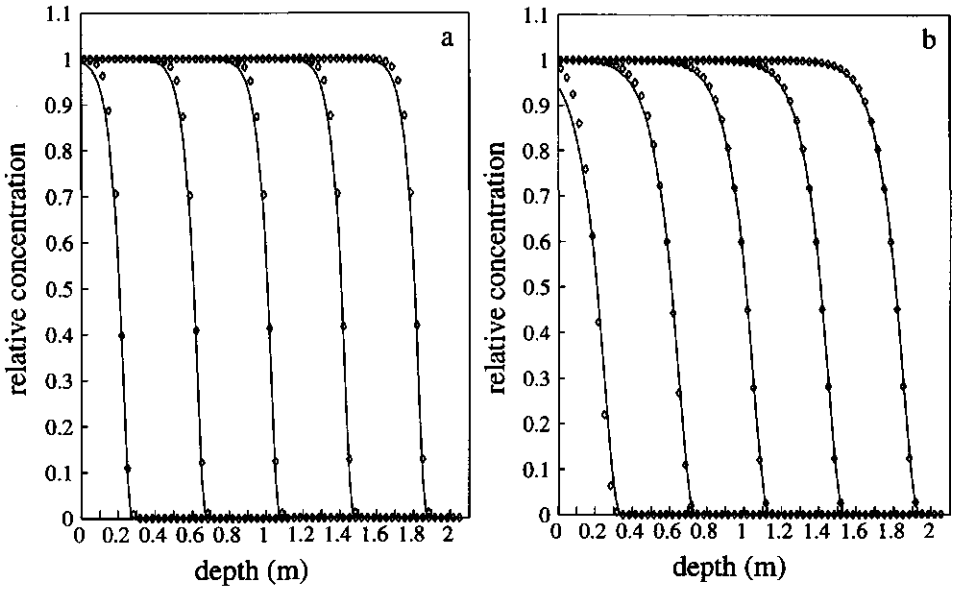

Figure 2.1 Fronts at five times for (*a*) L_d equal to 0.016 m or (*b*) 0.03 m. Solid line: analytical solution (2.7)-(2.8), Symbols: numerical approximation.

Table 2.1 Parameter values

Parameter	Fig. 2.1*a*	Fig. 2.1*b*	Fig. 2.2	Fig. 2.3	Fig. 2.4
θ	0.445	0.445	0.445	0.445	0.445
ρ (kg m^{-3})	1350	1350	1350	1350	1350
l (m)	2	2	2	2	2
v (m y^{-1})	1.9	1.9	1.9	1.9	1.9
L_d (m)	0.016	0.03	0.016	0.016	0.016
D (m^2 y^{-1})	0.03	0.057	0.03	0.03	0.03
c_0 (mol m^{-3})	0.02	0.02	0.02	0.02	0.02
c_i (mol m^{-3})	0	0	0	0	0
k (mol^{1-n} m$^{3(n-1)}$)	4.2	4.2	4.2	4.2	4.2
n	0.65	0.65	0.65	0.65	0.45
μ (y^{-1})	0	0	3.73	1.37	3.73

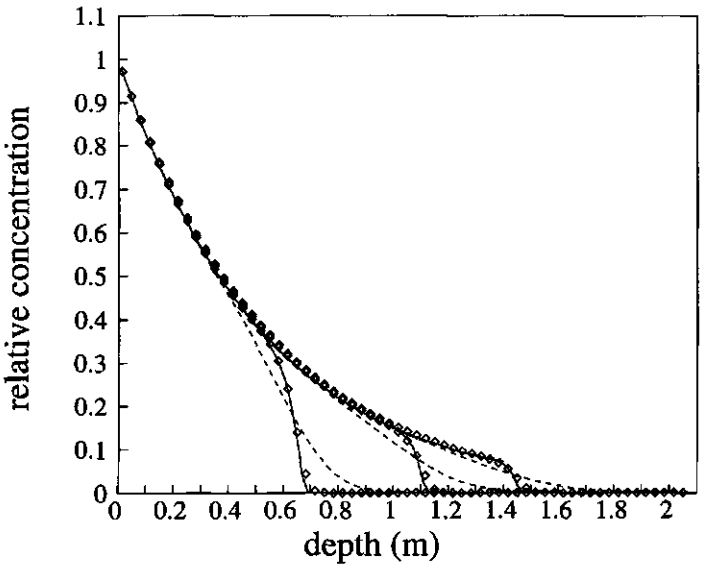

Figure 2.2 Fronts for a solute with first-order degradation. Symbols: numerical approximation; Solid line: analytical solution (2.14)-(2.16); Dashed line: analytical solution (2.17).

assumed in the additional calculations.

In Figure 2.2, the concentration-fronts are shown for three times with μ=3.73 yr^{-1} (parameters as given in Table 2.1). The numerically obtained fronts appear to be adequately described with the analytical approximation. The corresponding case where sorption was linearized, given by the analytical solution (for c_i=0)

$$\frac{c(z,t)}{c_0} = \frac{1}{2}\exp\left[\frac{(v-m)z}{2D}\right]\operatorname{erfc}\left[\frac{R_f z - mt}{2(DR_f t)^{0.5}}\right] + \frac{1}{2}\exp\left[\frac{(v+m)z}{2D}\right]\operatorname{erfc}\left[\frac{R_f z + mt}{2(DR_f t)^{0.5}}\right] \qquad (2.17)$$

with $m=v(1+4\mu D/v^2)^{1/2}$, of Van Genuchten and Alves (1982; p. 60), shows large deviations from the numerical results. The time t used for (2.17) was adapted to lead to the same downstream front position as found numerically. Apparently, the effect of adsorption nonlinearity on the downstream fronts is significant. The

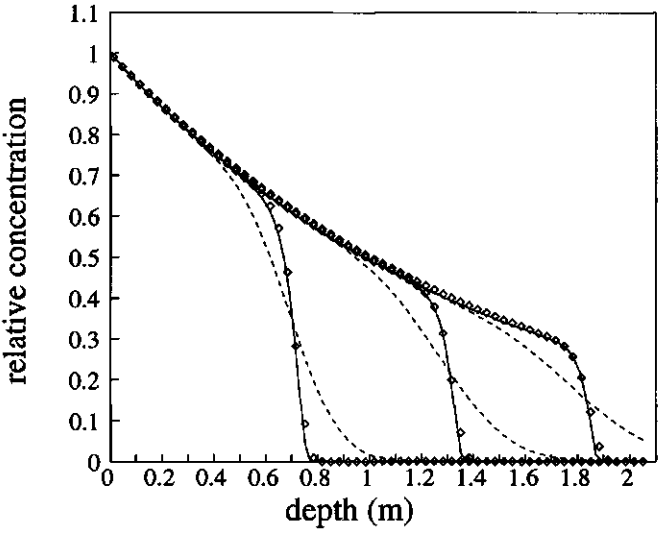

Figure 2.3 As Figure 2.2, with smaller rate parameter μ (μ=1.37 instead of 3.73).

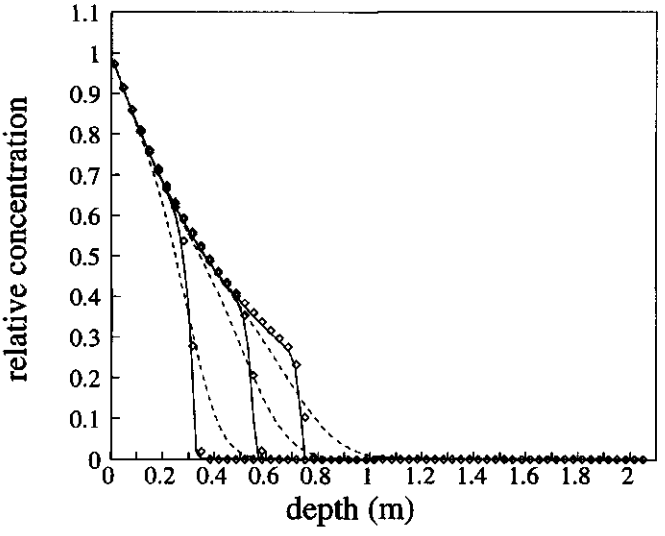

Figure 2.4 As Figure 2.2, with more pronounced nonlinearity (n=0.45 instead of n=0.65).

approximation (2.14)-(2.16) therefore improves the prediction of the front shape and front position compared with the linearized case (2.17), and may be of use despite its ad-hoc formulation.

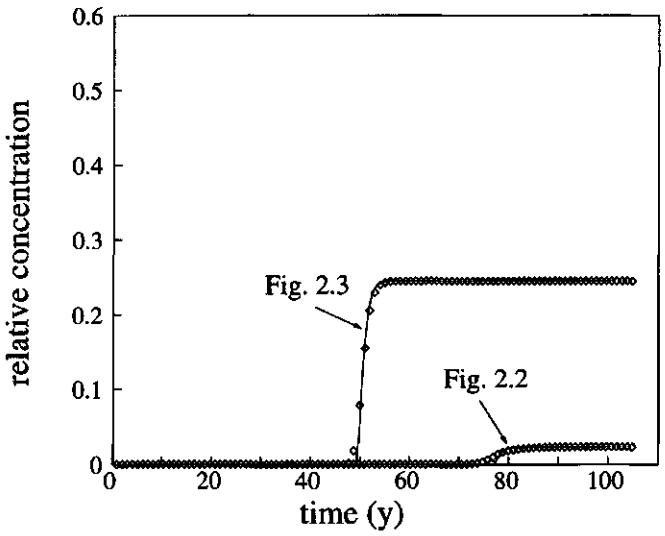

Figure 2.5 Breakthrough curve at z=2 m for cases corresponding to Figures 2.2 and 2.3. Solid line: analytical approximation of (2.14)-(2.16); Symbols: numerical approximation.

Additional situations were evaluated, one letting the decay rate parameter μ be smaller than in Figure 2.2, i.e., μ=1.37 yr^{-1}, as shown in Figure 2.3. The correspondence between numerical and analytical solutions is even slightly better. Taking μ=3.73 yr^{-1} and allowing a more pronounced nonlinearity of adsorption by setting n=0.45 gave the results of Figure 2.4. As other parameters were kept constant and c_0<1, a decrease in n resulted in a larger front retardation. The agreement of (2.14)-(2.16) with the numerical front is almost as good as for n=0.65 and significantly better than the prediction using the linearized approach. As can be seen from Figures 2.2-2.4, the front retardation factor indeed slightly increases as the front moves to larger depths. This follows from the distances between z=0 and the different front positions found for multiples of the same time lag. The good approximation of mean downstream front positions justifies the use of the depth weighted average retardation factor $\langle R(z^*)\rangle$. Additional illustrations in Figure 2.5

show that the approximation is also able to describe breakthrough curves well. The breakthrough curves correspond to the cases of Figures 2.2 and 2.3. The high degree of nonlinearity of the case corresponding to Figure 2.4 causes very low steady-state concentrations at a depth of 2 m.

2.4 Conclusions

Due to adsorption nonlinearity, concentration fronts may exhibit less dispersional spreading than in the case of linear adsorption, given particular conditions specified herein (2.1)-(2.2). Analytical solutions for such nonlinear transport can be derived for the limiting case ($t \rightarrow \infty$), which are, in a practical sense already valid after relatively short times. These solutions that describe the traveling wave that will form were used to approximate the concentration front for the case of nonlinear adsorption and a first-order transformation rate (e.g. radioactive decay or (bio)chemical degradation). Although no traveling wave forms for the latter cases, the approximations give a good description of the concentration fronts. This illustrates that, for parameter values considered, the front shape changes fast enough, subject to a local concentration change due to first-order decay, to be in agreement with a local traveling wave. Although the illustrations concerned Freundlich type adsorption, the approximation based on (2.11) will also be applicable for Langmuir adsorption, provided the appropriate traveling wave solution given by Van der Zee (1990) is used. When the nonlinear adsorption process is not at equilibrium but subject to first order kinetics, the approximation is still of use when taking into account the effective dispersion coefficient that incorporates the nonequilibrium effects, as given by Valocchi (1985) or Van der Zee (1990). However, in that case the displacement time after which a good agreement is found may be larger. The results found by linearizing the adsorption equation will give a poor description of the downstream front. Moreover, the linearized case does not predict a downstream front deceleration with increasing time. The approximation presented may be of use for predictions of transport in laboratory experiments and to verify numerical transport programs for nonlinear adsorption and first-order degradation or decay.

Appendix

For a front that has arrived at $z=z^*$ we can give an expression for the average retardation factor in the domain $0<z\leq z^*$. First define

$$z^*=vt/\frac{1}{z^*}\int_0^{z^*} R(\xi)d\xi=vt/\langle R(z^*)\rangle \tag{2.I.1}$$

R is depth-dependent because

$$R=R(c)=1+\frac{k}{\theta}[c_0^*(z)]^{n-1} \tag{2.I.2}$$

and $c_0^*(z)$ depends on (z) according to (2.11). Writing for (2.11)

$$c_0^*(z)=c_0\exp\left(\frac{z(v-m)}{2D}\right) \tag{2.I.3}$$

and

$$m=v\left(1+\frac{4\mu D}{v^2}\right)^{0.5} \tag{2.I.4}$$

we obtain for $\langle R(z^*)\rangle$

$$\langle R(z^*)\rangle=\frac{1}{z^*}\int_0^{z^*}1+\frac{k}{\theta}c_0^{n-1}\left[\exp\left(\frac{\xi(v-m)}{2D}\right)\right]^{n-1}d\xi \tag{2.I.5}$$

Integrated this yields

$$\langle R(z^*)\rangle=\frac{1}{z^*}\left[z^*+\frac{k}{\theta}\frac{2D}{(n-1)(v-m)}c_0^{n-1}\exp\left(\frac{z^*}{2D}(n-1)(v-m)\right)-\frac{k}{\theta}\frac{2D}{(n-1)(v-m)}c_0^{n-1}\right] \tag{2.I.6}$$

For a known velocity (v) and time (t) the depth (z^*) of the downstream front may be obtained by combination of (2.I.1) and (2.I.6) by simple iteration.

The reference location η^* in (2.8), where $c(\eta^*)=0$, is given by Van der Zee (1990,1991) by his (44)

$$\eta^*=-(A+G^*) \tag{2.I.7}$$

In contrast with Van der Zee (1990) η is not made dimensionless, by division with l. Therefore, in (2.I.7), A equals for LEA valid $D/v=L_d$ in the (z,t)-coordinate system instead of L_d/l. The term G^* follows from the integral (B-3) of Van der Zee (1990), i.e.,

$$G^*=L_d\frac{\theta+k\,c_0^{\,n-1}}{(1-n)k\,c_0^{\,n}}\int_0^{c_0}\ln(1-c_0^{\,n-1}\,c^{\,1-n})dc \qquad (2.I.8)$$

as can be found straightforwardly by introducing the original variables in the transformed (B-3) of Van der Zee (1990). It was found that G^* is relatively insensitive to whether c_0 or $c_0^*(z^*)$ was used to calculate G^*.

Notation

A	parameter
c	concentration (mol m^{-3})
c_0^*	depth-dependent local maximum concentration (mol m^{-3})
$\Delta c, c_0, c_i$	concentration difference, feed concentration, initial concentration (mol m^{-3})
D	pore scale diffusion/dispersion coefficient (m^2 y^{-1})
f	adsorption isotherm
f'	derivative of f to c
f''	second derivative of f to c
G^*	parameter
k	nonlinear adsorption coefficient (mol^{1-n} $m^{3(n-1)}$)
l	column length (m)
L_d	dispersivity (m)
m	parameter
n	Freundlich sorption parameter
P	function of c_0^*
Δq	change in q (mol m^{-3})
q	adsorbed amount (volumetric basis) (mol m^{-3})
q'	derivative of q to c
R	nonlinear retardation factor
$\bar{R}$	retardation factor for concentration c
R_l	linear retardation factor
$\langle R(z)\rangle$	depth-dependent average retardation factor, for front at depth z^*
s	adsorbed amount (mass basis) (mol kg^{-1})
t	time (y)
v	flow velocity (m y^{-1})
z	depth (m)
z^*	downstream front depth (m)
α	parameter
η	transformed coordinate (m)
η^*	reference point value of η (m)

θ	volumetric water fraction
μ	first-order decay parameter (y^{-1})
ξ	parameter
ρ	dry bulk density (kg m^{-3})

References

Bolt, G.H., Movement of solutes in soil: Principles of adsorption/exchange chromatography, in Soil Chemistry B, Physico-Chemical Models, edited by G.H. Bolt, pp. 285-348, Elsevier, New York, pp. 285-348, 1982.

Bond, W.J., and I.R. Philips, Approximate solutions for cation transport during unsteady, unsaturated soil water flow, Water Resour. Res., 26, 2195-2205, 1990.

Calvet, R., M. Tercé, and J.C. Arvieu, Adsorption des pesticides par les sols et leurs constituants. III. Caractéristiques générals de l'adsorption des pesticides, Ann. Agron. 31, 239-257, 1980.

Cameron, D.A., and A. Klute, Convective-dispersive solute transport with a combined equilibrium and kinetic adsorption model, Water Resour. Res., 13, 183-188, 1977.

Cederberg, G.A., R.L. Street, and J.O. Lecky, A groundwater mass transport and equilibrium chemistry model for multicomponent systems, Water Resour. Res., 21, 1095-1104, 1985.

Christensen, T.H., Cadmium sorption onto two mineral soils, Report, Dept. Sanit. Eng., Tech. Univ. of Denmark, Lingby, 1980.

Coats, K. H., and B.D. Smith, Dead-end pore volume and dispersion in porous media, Soc. Pet. Eng. J., 4, 73-84, 1964.

Deans, H.H., A mathematical model for dispersion in the direction of flow in porous media, Soc. Pet. Eng. J., 3(1), 49-52, 1963.

De Haan, F.A.M., S.E.A.T.M. van der Zee, and W.H. van Riemsdijk, The role of soil chemistry and soil physics in protecting soil quality; Variability of sorption and transport of cadmium as an example, Neth. J. Agric. Sci., 35, 347-359, 1987.

De Smedt, F., and P.J. Wierenga, A generalized solution for solute flow in soils with mobile and immobile water, Water Resour. Res., 15, 1137-1141, 1979.

Friesel, P., G. Milde, and B. Steiner, Interactions of halogenated hydrocarbons with soils, Fresenius Z. Anal. Chem., 319, 160-164, 1984.

Frissel, M.J., P. Poelstra, and P. Reiniger, Chromatographic transport through soils: III A simulation model for the evaluation of the apparent diffusion coefficient in undisturbed soils with titriated water, Plant and Soil, 33, 161-176, 1970.

Lake, L.W., and F. Helfferich, Cation exchange in chemical flooding, 2, The effect of dispersion, cation exchange, and polymer/surfactant adsorption on chemical flood environment, Soc. Pet. Eng. J., 18, 435-444, 1978.

Lexmond, Th.M., The effect of soil pH on copper toxicity to forage maize grown under field conditions, Neth. J. Agric. Sci., 28, 164-183, 1980.

Nkedi-Kizza, P., J.W. Biggar, H.M. Selim, M.Th. van Genuchten, P.J. Wierenga, J.M. Davidson, and D.R. Nielsen, On the equivalence of two conceptual models for describing ion

exchange during transport through an aggregated oxisol, Water Resour. Res., 20, 1123-1130, 1984.

Reiniger, P., and G.H. Bolt, Theory of chromatography and its application to cation exchange in soils, Neth. J. Agric. Sci., 20, 301-313, 1972.

Selim, H.M., J.M. Davidson, and R.S. Mansell, Evaluation of a two-site adsorption-desorption model for describing solute transport in soils. Proc. 1976 Summer Computer Simulation Conference, July 12-14, Washington D.C., pp. 444-448, 1976.

Valocchi, A.J., Validity of the local equilibrium assumption for modeling sorbing solute transport through homogeneous soils, Water Resour. Res., 21, 808-820, 1985.

Van der Zee, S.E.A.T.M., Analytical traveling wave solutions for transport with nonlinear and nonequilibrium adsorption, Water Resour. Res., 26, 2563-2578, 1990. (Correction, Water Resour. Res., 27, 983, 1991.)

Van der Zee, S.E.A.T.M., and J.J.T.I. Boesten, Effects of soil heterogeneity on pesticide leaching to ground water, Water Resour. Res., 27, 3051-3063, 1991.

Van der Zee, S.E.A.T.M., and W.H. van Riemsdijk, Transport of reactive solute in spatially variable soil systems, Water Resour. Res., 23, 2059-2069, 1987.

Van Duijn, C.J., and P. Knabner, Traveling waves in the transport of reactive solutes through porous media: Adsorption and binary exchange, Part 2, Report 205, Schwertpunkt programm der Deutsche Forschungsgemeinschaft, Univ. Augsburg, Inst. Mathematik, 1990.

Van Genuchten, M.Th., Analytical sollutions for chemical transport with simultaneous adsorption, zero-order production and first-order decay, J. Hydrol., 49, 213-233, 1981.

Van Genuchten, M.Th., and W.J. Alves, Analytical solutions of the one-dimensional convective-dispersive transport equation, USDA Tech. Bull. 1661. 151 pp., U.S. Dep. of Agric., Washington, D.C., 1982.

Van Genuchten, M.Th., and P.J. Wierenga, Simulation of one-dimensional solute transfer in porous media, Bull. 628, 40 pp., NMSU Agric. Exp. Stn., New Mexico State University, Las Cruces, 1974.

Van Genuchten, M.Th., and P.J. Wierenga, Mass transfer studies in sorbing porous media, I, Analytical solutions, Soil Sci.Soc. Am.J., 40, 473-480, 1976.

Van Riemsdijk, W.H., L.K. Koopal, and J.C.M. de Wit, Heterogeneity and electrolyte adsorption: Intrinsic and electrostatic effects, Neth.J.Agric.Sci., 35, 241-257, 1987.

Chapter 3

Analytical approximations for nonlinear adsorbing solute transport in layered soils*

Abstract

We consider reactive solute transport in a soil consisting of two layers that have different (bio)chemical properties. Assuming adsorption is adequately described with the Freundlich equation, the degree of adsorption nonlinearity differs. Using simple corrections the fronts are approximated analytically for the case that the top layer adsorbs nonlinearly whereas the subsoil layer adsorbs linearly (case 1) and for the case (2) that the layering order is reversed. By comparison with numerical calculations we show the adequacy of the analytical approximations as well as the effect of layering order on the subsoil front shapes. The layering order appears to affect the fronts which is in disagreement with conclusions by Selim *et al.* (1977). For the case of a layered soil with nonlinear adsorption and first-order decay, analytical approximations appear to describe the numerically computed fronts well.

3.1 Introduction

Solute transport in soil is of interest from the scope of soil and groundwater contamination. In order to understand the phenomena involved, many experimental studies have been conducted. Additionally, mathematical modeling (numerical and analytical) of the transport processes can be useful in situations where experiments cannot be carried out. For these cases many numerical models and solutions have been developed. Analytical solutions have the advantage that they reflect directly the involved phenomena and that they are evaluated rapidly. Also, analytical solutions are often used for verification of more comprehensive numerical models.

---

*by W.J.P. Bosma and S.E.A.T.M. van der Zee
published in: *Journal of Contaminant Hydrology*, 10, 99-118, 1992.

Additionally, the comparison of an analytical solution and a numerical solution can, for instance, give information with respect to efficient discretization schemes. Efficient discretization schemes can be used for numerical calculations of more complex problems, with minimum computation time.

Many analytical solutions exist for one-dimensional solute transport through homogeneous soils. Lapidus and Amundsen (1952) considered equilibrium linear adsorption in semi-infinite columns. For different boundary conditions Van Genuchten and Alves (1982) considered linear adsorption, zeroth order production and first order degradation. Dual porosity models were developed by Van Genuchten and Wierenga (1976). Nkedi-Kizza *et al.* (1984) showed the mathematical equivalence between the dual porosity model and a two-site chemical nonequilibrium model.

The above mentioned studies have considered adsorption to be described by a linear isotherm. However, as Calvet *et al.* (1980) showed for pesticides and De Haan *et al.* (1987) have shown for heavy metals such as cadmium, adsorption may be nonlinear. Under certain conditions with respect to the nonlinearity of adsorption, nonlinear adsorption leads to traveling wave fronts of constant shape traveling with constant velocity (Van Duijn and Knabner, 1990). Analytical traveling wave solutions have been developed by Van der Zee (1990), who developed a solution for the limiting traveling wave for a two site system with equilibrium linear adsorption for one site and nonequilibrium nonlinear (Langmuir or Freundlich) adsorption for the other site. Bosma and Van der Zee (1993) used the traveling wave solution to approximate the behaviour of a solute subject to nonlinear equilibrium adsorption and first-order degradation.

None of the above mentioned studies deal with solute transport in heterogenous or layered soils. Barry and Parker (1987) studied the effect of layering on solute breakthrough and front shapes, considering linear adsorption. They found that the order of layering for their linearly adsorbing systems may become irrelevant. Selim *et al.* (1977) found that also if one of the two layers adsorbs nonlinearly the layering order is insignificant.

In this paper two special cases of layered soils are considered. The first case deals with a soil consisting of a nonlinear adsorbing layer on top of a linear adsorbing layer, whereas the second case deals with the reverse situation. Our aim is to present analytical approximations for the downstream bottom layer fronts for both cases, and using these, to investigate the validity of the conclusions drawn by

Selim *et al.* (1977). Additionally, we will apply the analytical approximations to a situation with nonlinear adsorption and first-order decay in a layered soil.

3.2 Theory

We consider a solute transported in the z-direction of a layered soil. The solute is subject to equilibrium adsorption, either linear or nonlinear depending on the layer. If also first-order decay is assumed, the governing transport equation is given by (for symbols see the notation section)

$$\theta\frac{\partial c}{\partial t}+\rho\frac{\partial s_i}{\partial t}=\theta D\frac{\partial^2 c}{\partial z^2}-\theta v\frac{\partial c}{\partial z}-\mu_j\theta c \tag{3.1}$$

where μ_j is the rate constant for first order decay in the liquid phase of layer j. Index i identifies the adsorption equation for the layer considered. It is more convenient to express adsorption on a volumetric basis (i.e. $q=\rho s$) than on a mass basis, as in (3.1). Doing this, and considering first $\mu_j=0$, (3.1) can be written as

$$\theta\frac{\partial c}{\partial t}+\frac{\partial q_i}{\partial t}=\theta D\frac{\partial^2 c}{\partial z^2}-\theta v\frac{\partial c}{\partial z} \tag{3.2}$$

Depending on the stratification order of the soil column and the position of the solute, adsorption is given either by a linear isotherm (i=1):

$$q_1=k_l c \tag{3.3}$$

or by the nonlinear Freundlich isotherm (i=2):

$$q_2=kc^n \qquad 0<n<1 \tag{3.4}$$

When we consider a soil consisting of a linear adsorbing layer (i=1), an analytical solution for (3.2)-(3.3) is available (Van Genuchten and Alves, 1982). For the initial and boundary conditions for the concentration c, given by

$$c(z,t)=0 \qquad z>0 \qquad t=0 \tag{3.5a}$$

$$c(z,t)=c_0 \qquad z=0 \qquad t>0 \tag{3.5b}$$

$$\frac{dc}{dz}=0 \qquad z=\infty \qquad t>0 \tag{3.5c}$$

where LEA (Local Equilibrium Assumption) is valid, the analytical solution becomes

$$c(z,t)=c_0\left\{\frac{1}{2}\mathrm{erfc}\left[\frac{R_l z-vt}{2(DR_l t)^{1/2}}\right]+\frac{1}{2}\exp(vz/D)\mathrm{erfc}\left[\frac{R_l z+vt}{2(DR_l t)^{1/2}}\right]\right\} \tag{3.6}$$

where

$$R_l=1+\frac{k_l}{\theta} \tag{3.7}$$

However, when we assume that (i=2) and adsorption is described by (3.4), with initial and boundary conditions given by (3.5), a traveling wave solution may be derived (Van der Zee, 1990; Van Duijn and Knabner, 1990). A traveling wave is caused by the nonlinearity of adsorption. The latter causes the lower concentrations to experience a larger retardation than the higher concentrations. Therefore, the front tends to steepen, which opposes the effect of dispersional front spreading. When the opposing effects of nonlinear adsorption and dispersion are of equal force, the front shape and velocity remain constant. Although in theory a traveling wave occurs at infinite times, Van der Zee (1990) shows that after short displacement times the traveling wave solution approximates the limiting wave well. Van Duijn and Knabner (1990) show that for $0<n<1$ at $t\rightarrow\infty$ a traveling wave will form provided the following condition is met:

$$c_0>c_i \qquad f'(c)>0 \qquad f''(c)<0 \tag{3.8}$$

In this paper we consider the situation given by (3.8), where c_i=0.

Using for LEA valid the transformation (Bosma and Van der Zee, 1993)

$$\eta=z-vt/R \tag{3.9}$$

with

$$R=1+\frac{\Delta q(c)}{\theta\Delta c} \tag{3.10}$$

and assuming

$$c(\eta)=c(z,t); \qquad q(\eta)=q(z,t) \tag{3.11}$$

an analytical expression can be found of the limiting traveling wave solution. The boundary conditions are given by

$$c(\eta)=c_0 \quad \frac{dc}{d\eta}=0 \quad \frac{dq}{d\eta}=0; \qquad \eta=-\infty \tag{3.12a}$$

$$c(\eta)=0 \quad \frac{dc}{d\eta}=0 \quad \frac{dq}{d\eta}=0; \qquad \eta=\infty \tag{3.12b}$$

The solution of (3.2) and (3.4), using the boundary conditions (3.12) is

$$c(\eta)=c_0\left\{1-\exp\left[\frac{v(R-1)}{DR}(1-n)(\eta-\eta^*)\right]\right\}^{1/(1-n)} \tag{3.13}$$

The reference value η^* is discussed in Van der Zee (1990), and for LEA valid and c_i=0, η^* is derived by Bosma and Van der Zee (1993) as

$$\eta^*=-(G^*+L_d) \tag{3.14}$$

with

$$G^* = L_d \frac{\theta + kc_0^{n-1}}{(1-n)kc_0^n} \int_0^{c_0} \ln[1 - c_0^{n-1} c^{1-n}]dc \qquad (3.15)$$

where L_d is dispersivity (= D/v, assuming no molecular diffusion).

In this paper we distinguish two cases of layered soils. First, we consider a soil with a nonlinear adsorbing layer on top of a linear adsorbing layer. The second case deals with the reverse situation. In both cases an additional boundary condition needs to be defined for the interface of the two layers. We assume continuity of both concentrations and of mass fluxes. No analytical solutions exist for either layered case described above. Nevertheless, for both layered situations we attempt to describe the fronts using the mentioned analytical solutions (3.6) and (3.13).

In the first case, with a nonlinear adsorbing layer on top of a linear adsorbing layer, we assume the traveling wave solution (3.13) to hold for the top layer and (3.6) to describe the bottom layer front. In the top layer a front with a certain steepness will develop, depending on the nonlinearity of adsorption and on dispersion. With the knowledge that in practice a traveling wave front will form after short displacement times (Van der Zee, 1990), solution (3.13) can be used to describe the top layer front without modifications. However, in the bottom layer the analytical solution for linear adsorption cannot be used directly, for the thickness of the nonlinear front causes the upper boundary condition for (3.6), in this case (3.5*b*), at $z=z_L$ (z_L=boundary between top and bottom layer) to be violated. In some limiting cases (e.g. when D or n are sufficiently small) a nonlinear traveling wave front can be approximated by a shock front. If we assume that the front in the nonlinear adsorbing top layer can be represented as a shock front, a simple transformation of z and t is necessary to describe the front in the bottom layer with (3.6). These transformations are given by:

$$\zeta = z - z_L \qquad (3.16a)$$

$$\tau = t - t_L \qquad (3.16b)$$

where t_L is the time when the top layer front reaches $z=z_L$. With these transformations the boundary conditions given by (3.5) can be redefined as

$$c(\zeta,\tau)=0 \qquad \zeta>0 \qquad \tau=0 \tag{3.17a}$$

$$c(\zeta,\tau)=c_0 \qquad \zeta=0 \qquad \tau>0 \tag{3.17b}$$

$$\frac{dc}{d\zeta}=0 \qquad \zeta=\infty \qquad \tau>0 \tag{3.17c}$$

so that solution (3.6) can be rewritten as

$$c(\zeta,\tau)=c_0\left\{\frac{1}{2}\mathrm{erfc}\left[\frac{R_l\zeta-v\tau}{2(DR_l\tau)^{1/2}}\right]+\frac{1}{2}\exp(v\zeta/D)\mathrm{erfc}\left[\frac{R_l\zeta+v\tau}{2(DR_l\tau)^{1/2}}\right]\right\} \tag{3.18}$$

However, in reality the shape of the top layer front is not a shock front. The nonlinear traveling wave has a certain thickness depending on dispersivity and the nonlinearity of adsorption. When the front with the certain thickness reaches the linear adsorbing layer, front spreading continues according to linear adsorption. The starting thickness of the linear front causes wider downstream solute fronts than the fronts calculated with (3.18). By adjusting transformation (3.16), it is possible to obtain a better approximation of the downstream front using (3.18). If Δz is the travel distance necessary for the linear front to achieve the thickness of the nonlinear traveling wave, and Δt is the time necessary to travel a distance of Δz, transformation (3.16) can be rewritten as

$$\zeta=z-z_L+\Delta z \tag{3.19a}$$

$$\tau=t-t_L+\Delta t \tag{3.19b}$$

To determine Δz and Δt, expressions for the front thickness of a traveling wave and for a linear front are used, both given by Van der Zee (1990). If the front thickness of the nonlinear front is defined as δ between the concentrations $c_{i,\varepsilon}=\varepsilon\cdot c_0$ and $c_{0,\varepsilon}=(1-\varepsilon)\cdot c_0$ ($0<\varepsilon<1$), the expression is given by

$$\delta = \left[(1-n)\frac{k}{\theta}c_0^{n-1}\frac{1}{L_d R}\right]^{-1} \ln\left[\frac{1-\varepsilon^{1-n}}{1-(1-\varepsilon)^{1-n}}\right] \tag{3.20}$$

Note that the front thickness is independent of time t and depth z, and therefore independent of the thickness of the nonlinear adsorbing layer. When we choose ε=0.16, the front thickness for linear adsorption is given by

$$\delta_l = (8D\Delta z/v)^{1/2} \tag{3.21}$$

which increases as the travel distance Δz grows. The travel distance Δz can be found by setting the nonlinear front thickness (3.20) equal to the linear front thickness (3.21). The travel time Δt can be computed as

$$\Delta t = \Delta z R_l / v \tag{3.22}$$

Using (3.19) the front in the linear adsorbing bottom layer can now be approximated with (3.18) without further adaptations.

In the reverse case we consider a linear adsorbing layer on top of a nonlinear adsorbing layer. In the top layer adsorption isotherm (3.3) is valid and boundary conditions (3.5) are met. The front in the linear adsorbing top layer can now easily be described by (3.6). As in the first case, the boundary condition at z_L is violated due to the front development in the top layer. However, in this case the front that arrives at z_L is much more dispersed than the nonlinear traveling wave front of the bottom layer. Therefore, in the bottom layer longer displacement time is necessary for the traveling wave to develop. When we assume that the nonlinear adsorbing layer is thick enough for a traveling wave to develop, the downstream front can be approximated by (3.13) with a small correction.

In contrast with the first case, it is not possible to account for the deviation of the starting front thickness at $z=z_L$. Therefore, the only correction necessary has to account for the thickness of the top layer. To do this, the transformation for the traveling wave solution given by (3.9) can be replaced by

$$\eta = (z-z_L) - v(t-t_L)/R \tag{3.23}$$

in order to transform η back to z and t. With transformation (3.23) and solution

(3.13) an analytical traveling wave can be described at $z \geq z_L$. Close to z_L the approximation will be poor due to thickness of the linear adsorption front of the top layer. However, further downstream the approximation is expected to improve rapidly.

To describe transport of solutes subject to first order degradation in layered soils, the decay term $\mu_j \theta c$ does not disappear from (3.1). The governing equation (3.2) is then written as

$$\theta \frac{\partial c}{\partial t} + \frac{\partial q_i}{\partial t} = \theta D \frac{\partial^2 c}{\partial z^2} - \theta v \frac{\partial c}{\partial z} - \mu_j \theta c \tag{3.24}$$

Considering only the case with a nonlinear adsorbing layer on top of a linear adsorbing layer, an approach developed by Bosma and Van der Zee (1993) is used to solve (3.24). In order to approximate the solute fronts with first order degradation and nonlinear adsorption in a homogeneous (non-layered) soil, Bosma and Van der Zee (1993) used an adaptation of the traveling wave solution. The steady state solution, characterized by independence of the adsorption description, was utilized to quantify the local maximum concentration. This maximum concentration decreases with depth, but remains constant with time. The front shape at the downstream front position z^* could then be approximated with the traveling wave solution given by (3.13), where c_0 is substituted by the local maximum concentration that can be attained in view of first order decay, denoted by c_0^*. The local maximum concentration $c_0^*(z)$, given by Van Genuchten and Alves (1982) as the steady state solution for

$$\theta D \frac{\partial^2 c}{\partial z^2} - \theta v \frac{\partial c}{\partial z} - \mu c = 0 \tag{3.25}$$

subject to

$$c = c_0 \qquad z = 0 \tag{3.26a}$$

$$c = 0 \qquad z > 0 \tag{3.26b}$$

is derived as

$$c_0^*(z)=c_0 \exp\left[\frac{zv}{2D}\left(1-\sqrt{1+4\mu D/v^2}\right)\right] \tag{3.27}$$

Due to nonlinear adsorption the retardation factor is concentration dependent. Lower concentrations are more retarded than higher concentrations. Therefore, due to the decrease of the local maximum concentration with depth, the retardation factor R has become depth dependent. If $\langle R(z^*)\rangle$ is defined as the depth dependent average retardation factor, the approximations found by Bosma and Van der Zee (1993) are given as

$$c(\eta)=c_0^*(z)\left\{1-\exp\left[\frac{v(P-1)}{DP}(1-n)(\eta-\eta^*)\right]\right\}^{1/(1-n)} \tag{3.28}$$

with

$$P=1+(k/\theta)[c_0^*(z^*)]^{n-1} \tag{3.29}$$

and

$$\eta=z-vt/\langle R(z^*)\rangle \tag{3.30}$$

An expression for $\langle R(z^*)\rangle$ is derived by Bosma and Van der Zee (1993) and given in the Appendix.

Assuming that traveling waves react quickly to the change of the local maximum concentration, solute fronts of the nonlinear adsorbing top layer (with $\mu=\mu_1$) can be approximated with (3.28)-(3.30). Bosma and Van der Zee (1993) have demonstrated good agreement between numerical calculations and the analytical approximations for various cases. To describe the fronts in the linearly adsorbing bottom layer, a basically similar approach to the one given for non-decaying solutes is used. Transformation (3.19) accounts for the thickness of the top layer (z_L) as well as for the travel distance Δz of the linear front to obtain a thickness equal to the thickness of the top layer traveling wave front. With (3.19) the appropriate analytical solution with linear adsorption and first order degradation (for c_i=0) is given by (Van Genuchten and Alves, 1982)

$$c(\zeta,\tau)=c_0^*\left(\frac{1}{2}\exp\left[\frac{(v-m)\zeta}{2D}\right]\operatorname{erfc}\left[\frac{R_f\zeta-m\tau}{2(DR_f\tau)^{0.5}}\right]\right.$$
$$\left.+\frac{1}{2}\exp\left[\frac{(v+m)\zeta}{2D}\right]\operatorname{erfc}\left[\frac{R_f\zeta+m\tau}{2(DR_f\tau)^{0.5}}\right]\right) \qquad (3.31)$$

where

$$m=v\left(1+\frac{4\mu D}{v^2}\right)^{0.5} \qquad (3.32)$$

with $\mu=\mu_2$ for the bottom layer fronts. The concentration c_0^* is the local maximum concentration at $z=z_L-\Delta z$.

In order to use (3.31)-(3.32) to describe the bottom layer fronts, values for Δz and Δt, necessary for transformation (3.19), need to be determined. The combination of nonlinear adsorption and first order degradation causes the local maximum concentration c_0^* and the retardation factor R to be depth dependent. Consequently, the thickness of the nonlinear traveling wave front δ is dependent on Δz, due to the dependency on c_0^*. Therefore, explicit expressions for Δz and c_0^* are not available and an iterative computation is necessary. This iterative procedure is described in the Appendix. If Δz is determined, Δt can be computed with (3.22). With c_0^*, Δz, Δt, and (3.19) the solute fronts subject to first order degradation can be approximated in the linear adsorbing bottom layer with (3.31)-(3.32).

3.3 Numerical procedure

The analytical solutions (3.6) and (3.13) have been demonstrated to describe solute fronts well in the homogeneous top layer of the soil (Lapidus and Amundsen, 1952; Van der Zee, 1990; Bosma and Van der Zee, 1993). In order to verify the analytical approximations for the concentration distribution in the discussed layered soils, a numerical solution of the governing equations (3.1)-(3.4) has been used. For the cases without first order decay the correspondence between the numerical fronts and analytical fronts will be tested only for the bottom layers.

It is expected that the limiting behaviour of both analytical approximations for the bottom layer fronts is good. The correction necessary for the linear adsorption solution (case 1) will have little impact for $t \rightarrow \infty$. The traveling wave solution (case 2) is derived for $t \rightarrow \infty$ and differences at early stages will dampen out (Van Duijn and Knabner, 1990). However, at early displacement stages deviations of the numerical solution are expected. The deviation will be more distinct for the case with a linear adsorbing layer on top of a nonlinear adsorbing layer (case 2), for in this case the top layer front is much wider than the bottom layer traveling wave front.

The numerical solution is based on a finite difference Crank-Nicolson approximation of (3.2) in combination with a Newton-Raphson iteration scheme. The increments in depth z and time t were chosen to satisfy the stability and convergence criteria for linear adsorption, given by Van Genuchten and Wierenga (1974). The discretization makes it possible to specify the relevant adsorption isotherm (linear or nonlinear) for each layer. A concentration was fixed at the inlet and a flux type boundary condition was used at the outlet boundary:

$$c=c_0 \qquad z=0 \qquad t \geq 0 \tag{3.33a}$$

$$\frac{\partial c}{\partial z}=\text{finite} \qquad z \rightarrow \infty \qquad t>0 \tag{3.33b}$$

The initial condition for the numerical calculations was

$$c=c_i \qquad z>0 \qquad t=0 \tag{3.34}$$

where c_i was taken negligibly small.

To evaluate the analytical approximation in the case with a nonlinear adsorbing layer on top of a linear adsorbing layer (case 1), first the parameters R_l, R, Δz, Δt, t_L are calculated. The retardation factors R_l and R are calculated with (3.7) and (3.10), and the travel distance Δz is determined with (3.20) and (3.21). Subsequently, the travel time Δt is calculated with Δz, using (3.22), and t_L is computed as

$$t_L = z_L R / v \tag{3.35}$$

With the calculated parameter values, solution (3.18) is used to approximate the downstream fronts in the linear adsorbing bottom layer. The resulting concentrations in terms of ζ and τ can be retransformed in terms of depth z and time t with (3.19).

To use the analytical approximation in the reverse situation (case 2), the parameters R, R_l, η^*, t_L need to be calculated. The parameter G^*, necessary to determine η^* in (3.14), can analytically be calculated for particular values of n. Van der Zee (1990) has given the analytical solution of (3.15) for $n=(i+1)/(i+2)$ ($i=0,1,..,\infty$). Here, we used a numerical integration of the integral of (3.15) to compute G^* and subsequently η^*. Substitution of R_l for R in (3.35) gives t_L for this case. The downstream solute fronts in the nonlinear adsorbing bottom layer can now be approximated in terms of η with solution (3.13). With z_L the concentration values can be retransformed in terms of depth z and time t using (3.23).

Finally, transport of a pesticide through a layered soil, subject to first order degradation is calculated numerically and approximated analytically. Only the situation with a nonlinear adsorbing layer on top of a linear adsorbing layer was considered. Similar to case 2 without decay, the reverse case can simply be approximated with relevant traveling wave solution (here with first order degradation given by Bosma and Van der Zee, 1993). To use solutions (3.28) and (3.31)-(3.32) to approximate the solute fronts in the case with first order degradation and a nonlinear adsorbing layer on top of linear adsorbing layer, first the parameters R_l, $\langle R(z_L)\rangle$, $c_0^*(z_L)$, Δz, Δt, t_L, are calculated. Additionally, for each time a front is calculated in the nonlinear adsorbing top layer, the downstream front position z^* and the local maximum concentration at the downstream front position $c_0^*(z^*)$ are computed. The calculation of the average retardation factor $\langle R(z)\rangle$ at $z=z_L$, and the computations of Δz and z^* are described in the Appendix. The linear retardation factor R_l is calculated with (3.7), Δt with (3.22) and the decrease of the local maximum concentration $c_0^*(z)$ and $c_0^*(z_L)$ are determined with (3.27). With $\langle R(z_L)\rangle$ instead of R, a value for t_L can be calculated using (3.35). With solutions (3.28) and (3.31)-(3.32), and the calculated parameter values, solute fronts in the nonlinear adsorbing top layer and in the linear adsorbing bottom layer can be approximated. A retransformation of concentrations in terms of η, ζ and τ is necessary to present concentrations in terms of z and t.

The used parameter values were chosen to reflect a possible layered situation. Lexmond (1980) and De Haan *et al.* (1987) have shown that contaminants like copper and cadmium show Freundlich adsorption behaviour. To simulate transport through layered soils under field conditions, the reference values of Van der Zee (1990) were used. These values refer to transport of Cd with a feed concentration of 0.02 mol m^{-3}. The obtained Freundlich k value was k=4.4 with n=0.65, which gives a retardation factor R of 40. In order to compare both layered cases, the retardation of the linear adsorbing layer (R_l) was set equal to R. This resulted in a linear adsorption k_l of 17.4. In addition to the reference situation, calculations were performed with n=0.45 in the nonlinear adsorbing layer. For the latter calculations the Freundlich-k was adjusted to 2.0 to avoid a change of the retardation factor R in the nonlinear adsorbing top layer.

To simulate transport of a pesticide, subject to first order degradation, through a layered soil, a feed concentration of 0.02 mol m^{-3} was used. The top layer of 0.5 m represents a soil with high micro-biological activity causing a degradation rate μ_1 of 3.73 y^{-1}. In the sub-soil, consisting of a layer with a thickness of 1.5 m, a low micro-biological activity was considered. For the degradation rate of the bottom layer μ_2 a value of 0.75 y^{-1} was used. The top layer adsorbs nonlinearly with k=2.5 and n=0.5. The linear adsorption coefficient k_l of the bottom layer was equal to the reference situation without degradation, k_l=17.4. The physical and chemical parameter values used for all transport calculations are summarized in Table 3.1.

3.4 **Discussion**

Simulations based on the numerical solution of (3.2)-(3.4) have been carried out and results are shown in Figures 3.1-3.4. Figures 3.1-3.3 consider transport of Cd through a layered soil, whereas Figure 3.4 deals with transport of a pesticide, subject to first order degradation. Relative concentrations are plotted against depth z to compare the analytical approximations of the bottom layer fronts. Output is given for the times $t=\alpha\cdot\Delta t$ (α=1,2,..,9) with Δt=4.21 years.

Figure 3.1 shows the solute fronts that refer to the situation with a nonlinear adsorbing layer on top of a linear adsorbing layer. The reference situation with n=0.65 is represented by Figure 3.1*a* and 3.1*b*, whereas Figure 3.1*c* shows a

Table 3.1 Parameter values

Parameter	Unit	Reference case	Other cases	Dacay case
θ		0.445		
ρ	kg m^{-3}	1350		
l	m	2		
z_L	m	1		0.5
v	m y^{-1}	1.9		
L_d	m	0.016		
D	m^2 y^{-1}	0.03		
c_0	mol m^{-3}	0.02		
c_i	mol m^{-3}	0		
k_l		17.4		
k	mol^{1-n} $m^{3(n-1)}$	4.4	2.0	2.5
n		0.65	0.45	0.5
μ_1	y^{-1}	0		3.73
μ_2	y^{-1}	0		0.75

situation with n=0.45. In addition to the numerically calculated solute fronts Figure 3.1 shows the analytical approximation of the downstream bottom layer fronts. Figure 3.1*a* demonstrates that if solution (3.18) is used without a correction for the front thickness of the top layer front, deviations occur of the front representation during solute displacement through the column. At a relative concentration of 0.5 the deviation is negligible, for the average depth of the solute front is approximated well. However, it can be seen that the analytically approximated fronts are too steep, causing variations at the higher and lower relative concentrations. In Figure 3.1*b* the front thickness of the top layer front is used to determine Δz and Δt in (3.19). It may be seen that the agreement between the numerical and analytical approximation is good for all relative concentrations. At all times the numerical solution is approximated with better results than in Figure 3.1*a*. Especially at larger displacement times the bottom layer fronts appear to be adequately described with the analytical approximation. If nonlinearity of the top layer is increased the thickness of the top layer front will be reduced. Figure 3.1*c* shows such a case

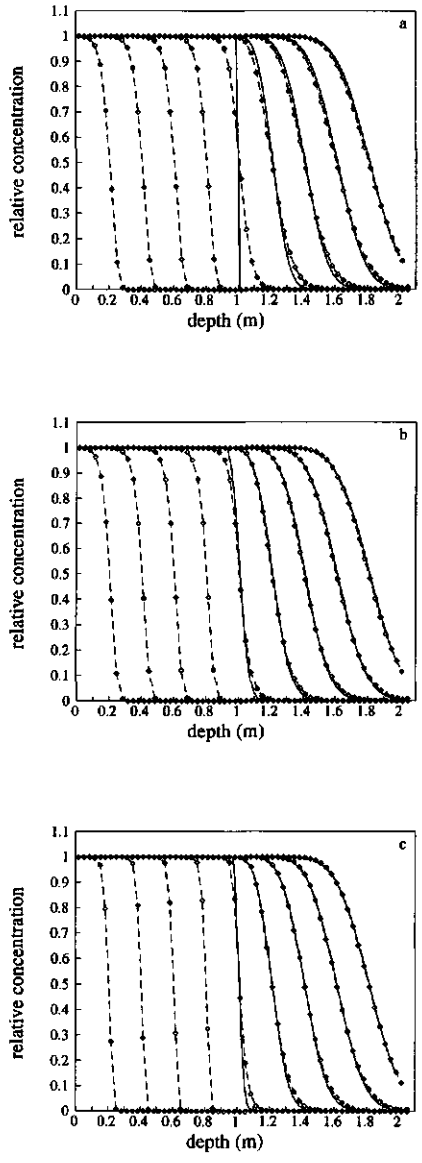

Figure 3.1 Fronts with nonlinear adsorbing layer on top of linear adsorbing layer, (*a*) for n=0.65 without correction for front thickness, (*b*) for n=0.65 with correction, and (*c*) for n=0.45 with correction. Solid line: analytical solution; Dashed line with symbols: numerical solution.

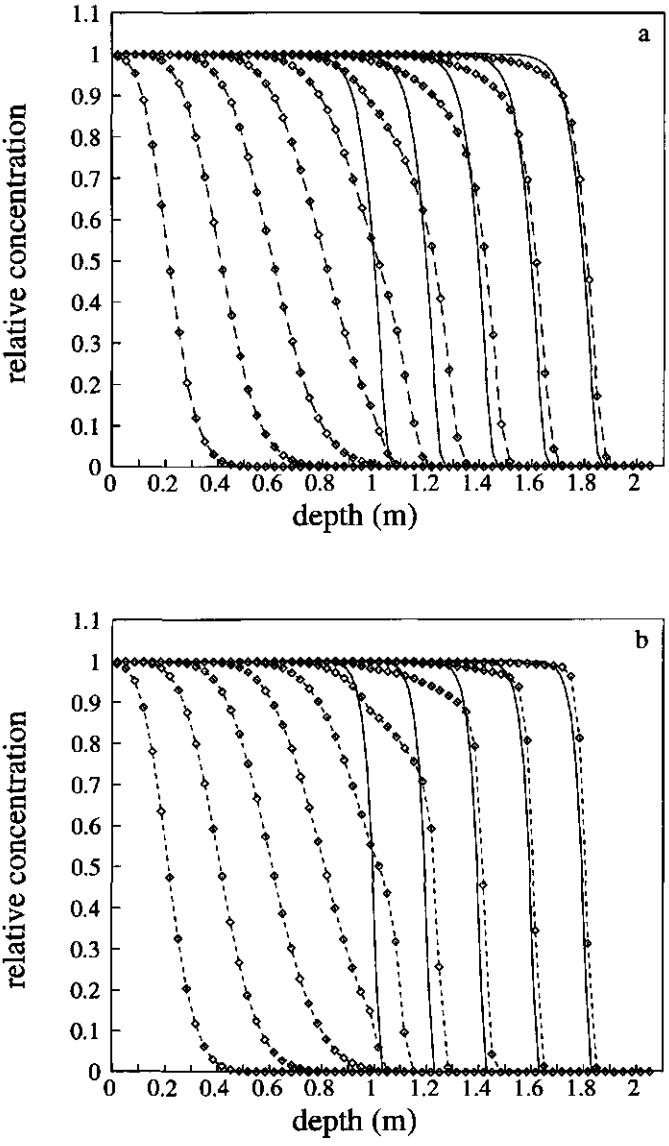

Figure 3.2 Fronts for nine times $t=\alpha\cdot\Delta t$ (α=1,2,..,9; Δt=4.21) for case with linear adsorbing layer on top of nonlinear adsorbing layer with correction for front thickness, (*a*) for n=0.65, and (*b*) for n=0.45. Solid line: analytical approximation; Dashed line with symbols: numerical solution.

with n=0.45, with the correction for the front thickness. It is visible that the bottom layer fronts are described even better, because the correction for the front thickness of the traveling wave front has less impact. It is clear that the analytical approximation holds for the situations presented here.

The effect of the correction for the front thickness of the top layer front will be larger if the traveling wave front differs more from a shock front. Therefore, situations with a larger dispersivity or a larger n value ($0<n<1$) can clearly be described more accurately with the analytical approximation in combination with the correction for the front thickness.

In the reverse case, we are considering a linear adsorbing layer on top of a nonlinear adsorbing layer. Figure 3.2 shows this case for the reference situation with n=0.65 (Figure 3.2*a*) and for the situation with n=0.45 (Figure 3.2*b*). The downstream bottom layer traveling wave fronts are approximated with (3.13) and (3.23). From Figure 3.2*a* can be seen that when the linearly spreading front enters the nonlinear adsorbing layer, it is much wider than the steep traveling wave front calculated with the analytical approximation. However, the numerically calculated front steepens rapidly and agreement between the numerical solution and the analytical approximation increases during displacement through the bottom layer. Figure 3.2*b* shows a similar simulation and approximation for n=0.45. The low n value requires the spreaded linear front to steepen even further than in Figure 3.2*a*. Corresponding to Figure 3.2*a*, at early displacement times the agreement is poor, but at the end of the column the analytical approximation describes the numerical fronts well. Only a small deviation remains. The assumption that the nonlinear adsorbing layer is long enough to develop a traveling wave seems to be justified. It is clear that in practice a traveling wave may form after short displacement times, which is in agreement with Van der Zee (1990).

A different aspect can be seen from Figures 3.1 and 3.2. The numerically calculated fronts of both Figures show different solute fronts for case 1 and case 2 even though retardation factors for both layers are equal. For the case with a nonlinear adsorbing layer on top of a linear adsorbing layer, the limiting behaviour in the bottom layer yields a (corrected) representation of a linear spreading front. The limiting behaviour of the reverse case yields a traveling wave front with a constant shape. Therefore, in the present cases (with Local Equilibrium) the layering order will be of more importance for increasing displacement times. The linear front of case 1 will continue to spread whereas the shape of the nonlinear

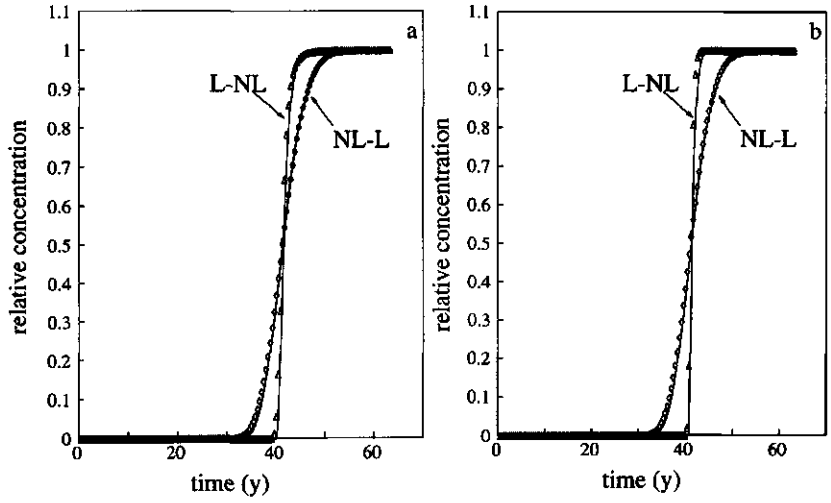

Figure 3.3 Effluent concentration distributions for both layering orders (Linear-NonLinear and NonLinear-Linear), (*a*) for n=0.65, and (*b*) for n=0.45. Solid line: analytical approximations; Symbols: numerical solution.

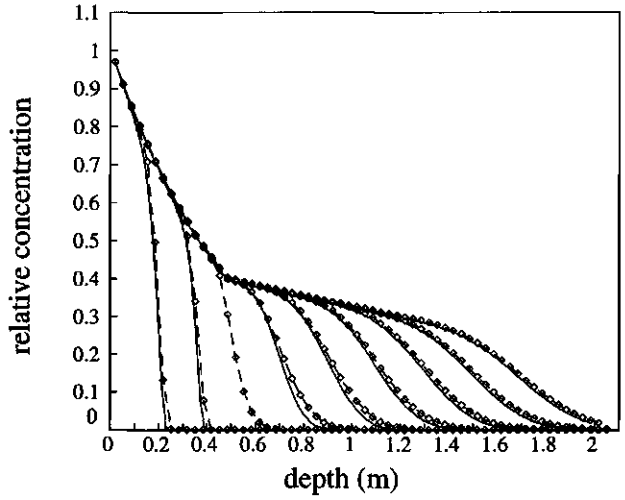

Figure 3.4 Fronts for decaying solute with linear adsorbing layer on top of nonlinear adsorbing layer with correction for front thickness. Solid line: analytical appr. (top layer: Chapter 2; Dashed line with symbols: numerical solution.

front of case 2 will remain constant. Consequently, the layering order controls the response of the solute transport system. Effluent concentration distributions, corresponding to the fronts of Figures 3.1 and 3.2, are shown in Figure 3.3. Differences in the behaviour of the two cases with different layering order are clearly visible for both n-values (n=0.65, n=0.45). These observations are in disagreement with Selim *et al.* (1977), who concluded that also with nonlinear adsorption the layering order of the soil failed to influence the shape of the effluent concentration distribution. Nonequilibrium nonlinear adsorption does not affect the finding that the layering order is important. Van der Zee (1990) has demonstrated that traveling waves also develop in situations with nonequilibrium nonlinear adsorption.

Figure 3.4 shows the solute fronts for a pesticide, subject to first order degradation, through a layered soil. The top soil adsorbs nonlinearly, whereas adsorption in the bottom layer is described by a linear isotherm. The numerically calculated fronts are approximated in the top layer with (3.28) and in the bottom layer with (3.31)-(3.32). Using (3.31)-(3.32) the correction for the thickness of the top layer front at z_L is applied. It can be seen from Figure 3.4 that both solutions approximate the numerically calculated fronts well. No analytical approximation exists for the front at α=3, for this front is partly in the top layer and partly in the bottom layer. The determination of the local maximum concentration at $z=z_L-\Delta z$ (given in the Appendix) appears to work well. As can be seen from Figure 3.4, the front retardation factor of the nonlinear adsorbing top layer indeed slightly increases as the front moves to larger depths. The distances between the average downstream position of the fronts decreases with time. This aspect is significant, because a linear adsorbing description of the top layer would have resulted in earlier breakthrough and a more dispersed front at z_L. This would have given more dispersed front shapes and larger mean front depths in the bottom layer.

3.5 Conclusions

Numerical solutions and analytical approximations were used to describe solute transport through layered soils. Two special cases without first order degradation were presented with regard to the layering order of the soil. Additionally, an extra case with first order degradation was considered. First, a soil

with a nonlinear adsorbing layer on top of a linear adsorbing layer was considered. The bottom layer fronts have been described adequately with (3.18) in combination with a correction for the front thickness of the traveling wave front. In the reverse case bottom layer fronts are approximated with the traveling wave solution. The linearly dispersed top layer fronts prevent an adequate description with traveling wave solution at early displacement times. However, the steepening of the fronts is rapid and at larger displacement times the traveling wave solution adequately approximates the bottom layer solute fronts. The numerically calculated fronts and the corresponding effluent concentration distributions of both considered cases show a distinct difference in shape. This observation disagrees with conclusions drawn by Selim *et al.* (1977) who claimed that, considering nonlinear adsorption, the layering order is of no importance to describe the effluent concentration distributions. The correction for the case with a nonlinear adsorbing layer on top of a linear adsorbing layer is adapted for a case with first order degradation. This analytical approximation also describes the numerical calculations well. The analytical approximations presented may be useful for long term predictions as well as to verify numerical transport programs for nonlinear adsorption with or without first order degradation in layered soils.

3.6 Appendix

In case of transport of a solute, subject to first order degradation, through a layered soil with a nonlinear adsorbing layer on top of a linear adsorbing layer, the downstream front position z^* is defined as

$$z^*=vt/\langle R(z^*)\rangle \tag{3.I.1}$$

where $\langle R(z^*)\rangle$, the average retardation factor in the domain $0\leq z\leq z^*$, is derived by Bosma and Van der Zee (1993) from

$$\langle R(z^*)\rangle=\frac{1}{z^*}\int_0^{z^*} R(\xi)d\xi \tag{3.I.2}$$

and

$$R(c)=1+(k/\theta)[c_0^*]^{n-1} \tag{3.I.3}$$

with c_0^* given by (3.27). Integrating (3.I.2), the expression for $\langle R(z^*)\rangle$ is given as

$$\langle R(z^*)\rangle=\frac{1}{z^*}\left[z^*+\frac{k}{\theta}\frac{2D}{(n-1)(v-m)}c_0^{n-1}\exp\left(\frac{z^*}{2D}(n-1)(v-m)\right)-\frac{k}{\theta}\frac{2D}{(n-1)(v-m)}c_0^{n-1}\right] \quad (3.I.4)$$

with

$$m=v\left(1+\frac{4\mu D}{v^2}\right)^{0.5} \quad (3.I.5)$$

For a known velocity v and time t the depth z^* of the downstream front may be obtained by combination of (3.I.1) and (3.I.4) by iteration.

To calculate the local maximum concentration c_0^* at $z=z_L-\Delta z$, the following expression is used:

$$c_0^*=c_0\exp\left(\frac{(z_L-\Delta z)v\ [1-(1+4\mu_1 D/v^2)^{1/2}]}{2D}\right) \quad (3.I.6)$$

Using the thickness of the nonlinear traveling wave front δ to determine Δz, equation (3.20) is adjusted for the case with first order degradation as

$$\delta=\left[(1-n)\frac{k}{\theta}(c_0^*)^{n-1}\frac{1}{L_d R}\right]^{-1}\ln\left[\frac{1-\varepsilon^{1-n}}{1-(1-\varepsilon)^{1-n}}\right] \quad (3.I.7)$$

Subsequently, with (3.21) Δz can be computed as

$$\Delta z=\frac{1}{8L_d}\delta^2 \quad (3.I.8)$$

However, from (3.I.7) can be seen that δ is dependent on c_0^* and therefore on Δz. The values c_0^* and Δz can be obtained by combination of (3.I.6)-(3.I.8) by iteration.

Notation

c	concentration (mol m^{-3})
c_0	feed concentration (mol m^{-3})
c_0^*	depth-dependent local maximum concentration (mol m^{-3})
c_i	initial concentration (mol m^{-3})
Δc	concentration difference (mol m^{-3})
D	pore scale dispersion coefficient ($m^2\ y^{-1}$)
f	adsorption function of c
f'	derivative of f to c

G^*	constant
k	nonlinear adsorption coefficient (mol^{1-n} m$^{3(n-1)}$)
k_l	linear adsorption coefficient
l	column length (m)
L_d	dispersivity (m)
m	parameter
n	Freundlich sorption parameter
q	adsorbed amount (volumetric basis) (mol m^{-3})
Δq	change in q (mol m^{-3})
P	function of c_0^*
R	nonlinear retardation factor
R_l	linear retardation factor
$\langle R(z) \rangle$	depth-dependent average retardation factor, for front at depth z
s	adsorbed amount (mass basis) (mol kg^{-1})
t	time (y)
t_L	time when front reaches z_L (y)
Δt	extra travel time for linear front (y)
v	velocity (m y^{-1})
z	depth (m)
z_L	boundary between two layers (m)
Δz	extra travel distance for linear front (m)
α	parameter
δ	nonlinear front thickness (m)
δ_l	linear front thickness (m)
ε	parameter
ζ	transformed z coordinate (m)
η	transformed coordinate (m)
η^*	reference point value of η (m)
θ	volumetric water fraction
μ_j	first-order decay parameter for layer j (y^{-1})
ξ	parameter
ρ	dry bulk density (kg m^{-3})
τ	transformed t coordinate (y)

References

Barry, D.A. and J.C. Parker, Approximations for solute transport through porous media with flow transverse to layering, Transport in Porous Media, 2, 65-82, 1987.

Bosma, W.J.P. and S.E.A.T.M. Van der Zee, Analytical approximation for nonlinear adsorbing solute transport and first order degradation, Transport in Porous Media, 11, 33-43, 1993.

Calvet, R., M. Tercé, and J.C. Arvieu, Adsorption des pesticides par les sols et leurs constituants.

III. Caractéristiques générals de l'adsorption des pesticides, Ann. Agron. 31, 239-257, 1980.

De Haan, F.A.M., S.E.A.T.M. Van der Zee, and W.H. Van Riemsdijk, The role of soil chemistry and soil physics in protecting soil quality; Variability of sorption and transport of cadmium as an example, Neth. J. Agric. Sci., 35, 347-359, 1987.

Lapidus, L. and N.R. Amundsen, Mathematics of adsorption in beds, VI, The effect of longitudinal diffusion in ion exchange and chromatographic column, J. Phys. Chem., 56, 984-988, 1952.

Lexmond, Th.M., The effect of soil pH on copper toxicity to forage maize grown under field conditions, Neth. J. Agric. Sci., 28, 164-183, 1980.

Nkedi-Kizza, P., J.W. Biggar, H.M. Selim, M.Th. Van Genuchten, P.J. Wierenga, J.M. Davidson, and D.R. Nielsen, On the equivalence of two conceptual models for describing ion exchange during transport through an aggregated oxisol, Water Resour. Res., 20, 1123-1130, 1984.

Selim, H.M., J.M. Davidson, and P.S.C. Rao, Transport of reactive solutes through multilayered soils, Soil Sci. Soc. Am. J., 41, 3-10, 1977.

Van der Zee, S.E.A.T.M., Analytical traveling wave solutions for transport with nonlinear and nonequilibrium adsorption, Water Resour. Res., 26, 2563-2578, 1990.

Van der Zee, S.E.A.T.M. and W.H. Van Riemsdijk, Transport of reactive solute in spatially variable soil systems, Water Resour. Res., 23, 2059-2069, 1987.

Van Duijn, C.J. and P. Knabner, Travelling waves in the transport of reactive solutes through porous media: Adsorption and binary exchange, Part 2, Report 205, Schwertpunkt programm der Deutsche Forschungsgemeinschaft, Univ. Augsburg, Inst. Mathematik, 45 pp, 1990.

Van Genuchten, M.Th. and W.J. Alves, Analytical solutions of the one-dimensional convective-dispersive transport equation, USDA Techn. Bull. 1661. 151 pp., U.S. Dept. of Agric., Washington D.C, 1982.

Van Genuchten M.Th. and P.J. Wierenga, Simulation of one-dimensional solute transfer in porous media, Agricultural Experiment Station Bulletin 628, New Mexico State University, Las Cruces, New Mexico, 40 pp, 1974.

Van Genuchten M.Th. and P.J. Wierenga, Mass transfer studies in sorbing porous media, I. Analytical solutions, Soil Sci. Soc. Am. J., 40, 473-480, 1976.

Chapter 4

Transport of reactive solute in a one-dimensional chemically heterogeneous porous medium*

Abstract

Reactive, nonlinearly adsorbing, solute transport in chemically heterogeneous soils is studied. Assuming adsorption is adequately described with the Freundlich equation, random variation of the adsorption coefficient is assumed to describe the heterogeneity. In a homogeneous case, traveling wave fronts develop, characterized by a constant velocity and a constant front shape. Using the method of moments, an analytical expression is derived to describe the constant variance of the traveling wave front. Deviations from the analytical variance and velocity, both calculated with an average adsorption coefficient, show that column scale heterogeneity has significant effects on front spreading and front movement. Expected values of front velocity and variance are computed as averages of values of 600 randomly generated columns. The nonlinear process causes small deviations from the case with average parameters. The ensemble average concentration front, representing an average front for the flow domain, shows that three mechanisms are responsible for the front spreading. At early displacement times the front spreading is caused by the thickness of the individual traveling waves. Subsequently, the effect of the internal variation of the adsorption coefficient (column scale heterogeneity) increases, whereas at large displacement times the front spreading is dominated by the different retardation coefficients of the different columns. The latter effect causes the variance to increase in proportion to t^2. An analytical approximation is derived for the ensemble average front, ignoring column scale heterogeneity.

*by W.J.P. Bosma and S.E.A.T.M. van der Zee
published in: *Water Resources Research*, 29, 117-131, 1993.

4.1 Introduction

The contamination of the environment has become a matter of considerable concern. In areas with high intensity of industry and agriculture, large concentrations of heavy metals or organic contaminants may reach the soil by atmospheric deposition or by waste disposal. These contaminated sites are a potential risk for the groundwater quality, for the quality of agricultural production, and for the quality of the drinking water supply. In order to manage our soil and groundwater resources properly, modeling tools are necessary to understand and predict movement of contaminants in the environment.

During the past decades much attention has been given to the theory and modeling of solute transport. This development has been accelerated and increased by the difficulty and high costs of field scale measurements. Much attention has been given to one-dimensional monocomponent solute transport in homogeneous media. Monocomponent models may adequately describe situations where nonreactive solutes or solutes at trace levels are present (Van der Zee, 1990*b*). A number of analytical solutions for these cases, for different boundary conditions, were given by Van Genuchten and Alves (1982), who considered linear adsorption and zeroth and first-order production and decay. Extensions were developed, taking into account the nonequilibrium aspect of the adsorption process, by Van Genuchten *et al.* (1974) and Rao *et al.* (1979).

Many transport models concern homogeneous media, but in practice soils and groundwater systems appear to be heterogeneous. One of the first efforts to describe heterogeneity was achieved by making use of the dual-porosity concept (Coats and Smith, 1964; Van Genuchten and Wierenga, 1976) and of the two-site surface adsorption concept (Cameron and Klute, 1977). In some cases heterogeneity may be treated deterministically (e.g. in case of well-defined layers with different texture or composition that are separated by relatively sharp interfaces). Valocchi (1989) studied the effect of a stratified aquifer on (two-dimensional) longitudinal solute spreading. He found that pore scale dispersion, column scale heterogeneity and adsorption kinetics are three dominating front spreading factors. However, in order to study heterogeneity in general cases a stochastic approach may be necessary. One of the first stochastic approaches for nonreactive solute transport was given by Dagan and Bresler (1979) and Bresler and Dagan (1979, 1981, 1983). By linearizing the flow equation Dagan

(1988,1989) derived an analytical solution for the spreading process of a nonreactive solute, taking into account a lognormal distribution of the hydraulic conductivity. It was shown that for a nonreactive solute, spatial variability of hydraulic conductivity accounts for a much larger solute spreading than pore scale dispersion. Bellin *et al.* (1992) validated Dagan's linear solution with extensive numerical calculations. Graham and McLaughlin (1991) applied a technique which uses field measurements to condition model results in order to improve the predictions of observed solute spreading. Successful results were obtained with this technique, although (costly) site specific measurements are necessary. A somewhat different approach to heterogeneity of soil physical parameters was given by Jury (1982), who derived a transfer function model to calculate the distribution of solute travel times.

The studies concerning heterogeneity of porous media mainly involve variable soil hydraulic properties caused by spatially variable porosity, dispersion and hydraulic conductivity. Boekhold *et al.* (1990) have shown that chemical properties which play a role in the process of adsorption, such as *p*H and organic matter content, may show highly variable distributions. Studies concerning reactive solute transport with random sorption parameters were performed by Van der Zee and Van Riemsdijk (1986, 1987), Cvetkovic and Shapiro (1990), Destouni and Cvetkovic (1991), Jury *et al.* (1986) and Chrysikopoulos *et al.* (1990). Cvetkovic and Shapiro (1990) studied the mass arrival of transporting solute taking into account spatial variability of hydraulic conductivity, of linear adsorption coefficient, and of adsorption and desorption rate parameters. Destouni and Cvetkovic (1991) showed a double peak behaviour for the mass arrival of solute into groundwater considering random hydraulic conductivity and random adsorption and desorption rate parameters. Jury *et al.* (1986) extended the transfer function model for solutes that undergo physical, chemical and biological transformations in heterogeneous systems. Van der Zee and Van Riemsdijk (1987) used a random distribution of chemical parameters to simulate solute transport in a heterogeneous field. They found that variation of the retardation factor and the water velocity causes non-Fickian front shapes for the average field concentration front. Chrysikopoulos *et al.* (1990) studied the effect of a spatially variable retardation factor on linearly adsorbing one-dimensional solute transport, focusing on column scale heterogeneity.

Most studies reported here, describing soil physical or soil chemical

heterogeneity, considered adsorption to be a linear process. However, as Calvet *et al.* (1980) showed for pesticides and De Haan *et al.* (1987) and Boekhold *et al.* (1990) have shown for heavy metals such as cadmium, adsorption may be nonlinear. For homogeneous media, Van der Zee (1990*b*) derived an analytical solution for the limited traveling wave for a two-site system with equilibrium linear adsorption for one site and nonequilibrium nonlinear adsorption for the other site. This analytical solution was adapted by Bosma and Van der Zee (1993) in order to describe solute transport subject to nonlinear adsorption and first-order decay. A first approach to model nonlinear adsorption and column scale heterogeneity was performed by studying the effect of two-layered soils on solute transport (Bosma and Van der Zee, 1992).

Our aim is to analyze the effect of chemical heterogeneity on solute transport. Although we are aware of the significance of heterogeneity of hydraulic properties, this is not included in this study. In order to obtain basic information about the effect of variable nonlinear adsorption on one-dimensional solute transport, variation of the flow velocity has been ignored. A random distribution of the adsorption coefficient has been used. The method of moments (Aris, 1956) is applied, to quantify the effect of heterogeneity on the front velocity and on the front shape. Numerically calculated front variances are compared with an analytically derived expression for the variance of a traveling wave. By studying the ensemble average front, the effect of different front spreading mechanisms is analyzed.

4.2 Theory

We consider a solute, subject to nonlinear equilibrium adsorption, transported in the z direction of a soil. Since no production or decay is assumed, the governing equation for local equilibrium assumption (LEA) valid is given by (for symbols see the notation section)

$$\theta\frac{\partial c}{\partial t}+\rho\frac{\partial s}{\partial t}=\theta D\frac{\partial^2 c}{\partial z^2}-\theta v\frac{\partial c}{\partial z} \tag{4.1}$$

assuming steady state flow. With adsorption expressed on a volumetric basis (i.e., $q=\rho s$), (4.1) can be rewritten as

$$\theta\frac{\partial c}{\partial t}+\frac{\partial q}{\partial t}=\theta D\frac{\partial^2 c}{\partial z^2}-\theta v\frac{\partial c}{\partial z} \qquad (4.2)$$

For this study nonlinear adsorption is described by the Freundlich equation, an expression often used to characterize adsorption of heavy metals and organic compounds (De Haan *et al.*, 1987; Calvet *et al.*, 1980). The Freundlich equation is given by

$$q=kc^n \qquad 0<n<1 \qquad (4.3)$$

Our aim is to study the transport of a solute through a chemically heterogeneous soil, where k is a random space function. First we describe the behaviour of a solute subject to nonlinear adsorption in a homogeneous soil. Depending on the nonlinearity of adsorption, Van Duijn and Knabner (1990) have shown that under certain conditions a traveling wave front develops in a homogeneous porous medium. These conditions are, for $c_0>c_i$, that $q'>0$ and $q''<0$, where primes denote differentiation with respect to c. Due to the nonlinearity of adsorption, lower concentrations experience a larger retardation than higher concentrations (if $0<n<1$ in the Freundlich equation (4.3)). Consequently, a relatively steep front develops as adsorption nonlinearity opposes the front spreading effect due to pore scale dispersion. If both effects, due to nonlinear adsorption and due to pore scale dispersion, are of equal force, the front shape and front velocity remain constant. Van der Zee (1990*b*) and Van Duijn and Knabner (1990) have given an analytical solution for the limiting ($t\rightarrow\infty$) front. Van der Zee (1990*b*) and Bosma and Van der Zee (1992) have shown that in practice the traveling wave solution is already valid after short displacement times.

The initial and boundary conditions used for the derivation of the analytical solution are given by

$$c(z,t)=0 \qquad z>0 \qquad t=0 \qquad (4.4a)$$

$$c(z,t)=c_0 \qquad z=0 \qquad t>0 \qquad (4.4b)$$

Bosma and Van der Zee (1993) gave the transformation to describe the concentration with respect to a moving coordinate system by

$$\eta = z - (vt/R) \tag{4.5}$$

where R, the nonlinear front retardation factor, is

$$R = 1 + \frac{\Delta q(c)}{\theta \Delta c} \tag{4.6}$$

in which $\Delta c = c_0 - c_i$ and Δq is the corresponding change in amount adsorbed. When the traveling wave front has formed we have

$$c(\eta) = c(z,t); \qquad q(\eta) = q(z,t) \tag{4.7}$$

The transformed boundary conditions for the infinite system are

$$c(\eta) = c_0 \qquad \frac{dc}{d\eta} = 0 \qquad \frac{dq}{d\eta} = 0; \qquad \eta = -\infty \tag{4.8a}$$

$$c(\eta) = 0 \qquad \frac{dc}{d\eta} = 0 \qquad \frac{dq}{d\eta} = 0; \qquad \eta = \infty \tag{4.8b}$$

The analytical traveling wave solution for (4.2)-(4.3) is given as

$$\bar{c}(\eta) = \frac{c(\eta)}{c_0} = \left\{ 1 - \exp\left[\frac{v(R-1)}{DR}(1-n)(\eta - \eta^*) \right] \right\}^{1/(1-n)} \qquad \eta \le \eta^* \tag{4.9a}$$

$$\bar{c}(\eta) = 0 \qquad \eta > \eta^* \tag{4.9b}$$

where $\bar{c}$ is the relative concentration ($0 \le \bar{c} \le 1$). The reference value η^* was discussed by Van der Zee (1990). For LEA valid and $c_i = 0$, η^* is given by (Bosma and Van der Zee, 1992)

$$\eta^* = -(G^* + L_d) \tag{4.10}$$

with the constant G^* equal to

$$G^*=L_d \frac{\theta+kc_0^{n-1}}{(1-n)kc_0^n} \int_0^{c_0} \ln[1-c_0^{n-1}c^{1-n}]dc \qquad (4.11)$$

In (4.10) and (4.11), L_d is the dispersivity (equal to D/v, assuming no molecular diffusion).

With (4.9)-(4.11) it is possible to describe transport of a solute subject to nonlinear adsorption in a homogeneous soil. In order to quantify effects of several variables (e.g., degree of nonlinearity, dispersivity) and to assess the effects of heterogeneity, the concentration distribution can be characterized in terms of spatial moments (Valocchi, 1989). The Kth moment that can be calculated to analyze the concentration front moving in the z direction is defined as

$$M_K=\int_{-\infty}^{\infty} z^K f(z)dz \qquad (4.12)$$

where $f(z)$ is the probability density function (pdf) of travel distance. To characterize the downward moving front with respect to the average front position, the Kth central moment is defined as

$$M_K{}^c=\int_{-\infty}^{\infty} (z-\mu)^K f(z)dz \qquad (4.13)$$

where μ is the first moment (M_1) given by (following (4.12))

$$\mu=M_1=\int_{-\infty}^{\infty} zf(z)dz \qquad (4.14)$$

In order to determine the moments M_K and $M_K{}^c$ with (4.12)-(4.13), an expression for $f(z)$ is required. Similar to the linear adsorption case, $\bar{c}(z,t)$ is related with the cumulative probability or distribution function of travel distance z for a continuous injection as considered here. Hence, the derivative of $\bar{c}(z,t)$ with respect to z is related with the pdf of travel distance z for the nonlinear front. In particular,

$$f(z) = -\frac{\partial \bar{c}(z,t)}{\partial z} \tag{4.15}$$

The minus sign accounts for the descending front, i.e., our choice for the direction of the z coordinate, because the zeroth moment M_0 should be normalized to unity. We obtain for the moments of (4.12) and (4.13)

$$M_K = -\int_{-\infty}^{\infty} z^K \bar{c}'(z,t)dz \tag{4.16a}$$

$$M_K{}^c = -\int_{-\infty}^{\infty} (z-\mu)^K \bar{c}'(z,t)dz \tag{4.16b}$$

where primes denote spatial derivatives.

The defined moments physically describe a concentration front. The zeroth moment (M_0) gives the amount of dissolved solute in the area of the column where the front is present. The first moment (M_1) denotes the average position of the front and, divided by time, quantifies the front velocity. The central moments are used to describe the front shape. The second central moment (M_2^c) gives the variance of the front s^2, whereas the third central moment (M_3^c) and the fourth central moment (M_4^c) are related to the skewness and the kurtosis of the concentration distribution. For this study, we are mainly interested in the first moment (M_1; average front position) and the second central moment (M_2^c; variance). Later, we will make use of the third and fourth central moments (M_3^c,M_4^c) to characterize the ensemble average concentration front of the flow domain.

If solute transport subject to nonlinear adsorption is considered, it is possible to derive an analytical expression for the variance of the front, provided (4.9) is valid, i.e., when k is constant and not a random space function (i.e. homogeneous porous medium). As mentioned earlier, a traveling wave is characterized by a constant front shape and a constant velocity. The constant front shape implies that the front variance is also invariant with time and depth. This suggests that an expression for the front variance s^2 can be derived that depends only on pore scale dispersion and on the degree of nonlinear adsorption. If, for convenience, we use the substitution $\tilde{\eta}=\eta-\eta^*$ to rewrite (4.9) as

$$\bar{c}(\tilde{\eta})=\left[1-\exp(P\tilde{\eta})\right]^m \qquad \tilde{\eta}\in<-\infty,0] \tag{4.17}$$

where

$$P=\frac{v(R-1)}{DRm} \tag{4.18}$$

and

$$m=1/(1-n) \tag{4.19}$$

an expression for the variance $s_{\tilde{\eta}}^2$ is derived with respect to the moving coordinate system $\tilde{\eta}$. Because the front shape in terms of η is equal to the front shape in terms of z, and because the substitution $\tilde{\eta}=\eta-\eta^*$ does not affect the front shape, we have the equivalence $s_{\tilde{\eta}}^2=s^2$. The variance $s_{\tilde{\eta}}^2$ can be calculated according to

$$s_{\tilde{\eta}}^2=\langle(\tilde{\eta}-\langle\tilde{\eta}\rangle)^2\rangle=\langle\tilde{\eta}^2\rangle-\langle\tilde{\eta}\rangle^2 \tag{4.20}$$

where $\langle\tilde{\eta}\rangle$ denotes the expected value of $\tilde{\eta}$, given by the first moment (M_1). With (4.15) we can evaluate $\langle\tilde{\eta}^2\rangle$ according to

$$\langle\tilde{\eta}^2\rangle=-\int_{-\infty}^{0}\tilde{\eta}^2\bar{c}'(\tilde{\eta})d\tilde{\eta} \tag{4.21}$$

with the integration limits given by -∞ and 0, in view of the $\tilde{\eta}$-domain $<-\infty,0]$ defined in (4.17). The second term on the right-hand side of (4.20) can be computed as

$$\langle\tilde{\eta}\rangle^2=\left(-\int_{-\infty}^{0}\tilde{\eta}\bar{c}'(\tilde{\eta})d\tilde{\eta}\right)^2 \tag{4.22}$$

It is not necessary to evaluate the derivative of the concentration front ($\bar{c}'(\tilde{\eta})$) for (4.21) or (4.22) because these equations can be formulated as

$$\langle g(\tilde{\eta})\rangle=-\int_{-\infty}^{0}g(\tilde{\eta})\bar{c}'(\tilde{\eta})d\tilde{\eta}=-\int_{-\infty}^{0}g(\tilde{\eta})d\bar{c}(\tilde{\eta}) \tag{4.23a}$$

$$\langle g(\tilde{\eta})\rangle = -\left[g(\tilde{\eta})\bar{c}(\tilde{\eta})\right]_{-\infty}^{0} + \int_{-\infty}^{0} \bar{c}(\tilde{\eta})dg(\tilde{\eta}) \qquad (4.23b)$$

where $g(\tilde{\eta})$ is a function of $\tilde{\eta}$ (e.g., $\tilde{\eta}^2$ in (4.21) or $\tilde{\eta}$ in (4.22)). This shows that the expected value of $g(\tilde{\eta})$ can be evaluated directly from the concentration front, $\bar{c}(\tilde{\eta})$. The integrations of (4.21)-(4.22) with $\bar{c}(\tilde{\eta})$ given by (4.17) can only be performed analytically for integer values of m. This restricts the values for n to $n=(i+1)/(i+2)$ (with $i=0,1,...,\infty$). For other n values, (4.21) and (4.22) have to be calculated numerically. To derive a general expression for $s_{\tilde{\eta}}^2$, considering only positive integer values for m, the expression for $\bar{c}(\tilde{\eta})$ given by (4.17) can be written as a series according to

$$\bar{c}(\tilde{\eta}) = 1 + \sum_{i=1}^{m} \alpha_i \exp(Pi\tilde{\eta}) \qquad (4.24)$$

with

$$\alpha_i = (-1)^i \frac{m!}{(m-i)!i!} \qquad (4.25)$$

Integrating (4.21) and (4.22) from $\tilde{\eta}$ to 0 using (4.24)-(4.25), an expression for the variance s^2 of a traveling wave front can be derived from (4.20). The obtained result is given by

$$s^2 = s_{\tilde{\eta}}^2 = -\frac{2}{P^2}\sum_{i=1}^{m}\frac{\alpha_i}{i^2} - \frac{1}{P^2}\left(\sum_{i=1}^{m}\frac{\alpha_i}{i}\right)^2 \qquad (4.26)$$

with P, m, and α_i given by (4.18), (4.19) and (4.25), respectively. With (4.26), the variance of a traveling wave for a homogeneous column, $s_{\tilde{\eta}}^2$, which is related to the thickness of the front, can be calculated. Note that $s_{\tilde{\eta}}^2$ is determined only by m and by P, which represent nonlinear adsorption and pore scale dispersion, respectively. In agreement with the traveling wave concept, $s_{\tilde{\eta}}^2$ is independent of space and time.

4.3 Numerical procedure

4.3.1 *Incorporation of heterogeneity*

In order to describe solute spreading in heterogeneous porous media one must account for the often irregular variation of transport and adsorption parameters (Mackay *et al.*, 1986*a*, *b*). To study the effect of column scale heterogeneity on solute transport, the transport and adsorption parameters may be considered variable in the vertical direction. Bosma and Van der Zee (1992) have shown the effect of layering on solute transport with nonlinear adsorption. Considering linearly and nonlinearly adsorbing layers, the layering order was found to be important in order to describe the downstream concentration front. Whereas a soil consisting of two different layers was considered (Bosma and Van der Zee, 1992), here it is our aim to show the effect of multilayered soils.

In accordance with Van der Zee (1990*a*), only variation of the adsorption parameters was considered in order to describe the effect of chemical heterogeneity, whereas variation of physical parameters such as flow velocity and dispersivity is not taken into account. The latter effects have been studied by Dagan and Bresler (1979), Bresler and Dagan (1979,1981,1983) and Amoozegar-Fard *et al.* (1982). In view of the often rather constant n value (De Haan *et al.*, 1987; Boekhold *et al.*, 1991), we have considered only the Freundlich adsorption coefficient k to be random, characterized by a probability density function (pdf). The variation of the adsorption coefficient k is given by a normal distribution $N(m_k,s_k^2)$. Similar to Black and Freyberg (1987) and Chrysikopoulos *et al.* (1990), who used a spatial correlation of their random variable, we assumed the Freundlich adsorption coefficient k to be spatially correlated according to the exponential autocorrelation function given as

$$r(\zeta)=\exp(-\zeta/\lambda) \tag{4.27}$$

where ζ is the separation distance, r is the autocorrelation and λ is the correlation scale.

To assess the effect of a spatially variable adsorption coefficient Monte Carlo simulations were performed. The random columns were finely discretized with different values for the adsorption coefficient k at each node. The columns had a prescribed probabilistic structure and each column is considered an equally

likely configuration for the actual spatial pattern of the adsorption coefficient. A one-dimensional random generator has been used to construct one-dimensional random fields of a normally distributed parameter with autocorrelation described by the first-order exponential autocorrelation function given by (4.27). Use was made of a generator, creating uncorrelated normally distributed random numbers. To improve the accuracy of the reproduction of the autocorrelation structure in the random columns, more points per correlation scale were generated than actually used in the numerical transport calculations. The remaining points were not considered during the rest of the calculations. This technique, used by Bellin (1991), has been shown to improve the results.

The variable adsorption coefficient at each discrete generation point is evaluated by

$$k=m_k+\varepsilon \tag{4.28}$$

where m_k is the average adsorption coefficient and ε is the random fluctuation of m_k with zero mean. With the fluctuations ε the autocorrelation of the adsorption coefficient can be created. Using the first order exponential autocorrelation function, the adsorption coefficient k at node i is determined by node $i-1$, i.e.,

$$k_i=\beta k_{i-1}+\varepsilon_{i-1} \tag{4.29}$$

where β is the autocorrelation coefficient for two subsequent generation points. The variance of the fluctuation of k, s_ε^2, is determined by the variance of k, s_k^2, and can easily be derived from (4.29) as

$$s_\varepsilon^2=(1-\beta^2)s_k^2 \tag{4.30}$$

With s_ε^2 it is possible to generate uncorrelated normally distributed random fluctuations with a zero mean, so that (4.29) can be used to generate a random field of k with a first order exponential autocorrelation function. With (4.30) this exponential autocorrelation function can be derived as

$$r=\beta^{|i\Delta z^*|} \tag{4.31}$$

where Δz^* is the distance between the generation points. Relating the correlation scale λ to β, (4.31) can be rewritten in terms of ζ according to (4.27). The

expression is given as

$$\lambda = -1/\ln \beta \tag{4.32}$$

With the random generator 600 possible chemically heterogeneous soil columns were generated. At each generation point of each column the k value is determined by the expected value m_k and the fluctuation ε. If the discretization of the columns used for the numerical calculations is given by Δz, these columns are constructed by selecting the k value of every jth generation point, where j is given by $\Delta z/\Delta z^*$.

4.3.2 *Solving transport equations*

A numerical solution of (4.2)-(4.3) has been developed to perform the calculations with the 600 random columns. The numerical solution is based on a finite difference Crank-Nicolson approximation of (4.2) in combination with a Newton-Raphson iteration scheme. In order to prevent oscillation the increments in depth z and time t were chosen to satisfy the criteria for linear adsorption, given by Van Genuchten and Wierenga (1974). The discretization makes it possible to specify a different adsorption coefficient for each node. A first type boundary condition was used at the inlet of the column, whereas at the outlet a flux type boundary was imposed:

$$c = c_0 \qquad z = 0 \qquad t \geq 0 \tag{4.33a}$$

$$\frac{\partial c}{\partial z} = \text{finite} \qquad z \to \infty \qquad t > 0 \tag{4.33b}$$

The initial condition for the numerical calculations was

$$c = c_i \qquad z > 0 \qquad t = 0 \tag{4.34}$$

where c_i was taken negligibly small.

The analytical solution (4.9) was derived for a zero initial concentration. The numerical approximation for that case is involved, as, due to the infinite derivative of (4.3) with respect to c at $c=0$, we must deal with a moving boundary problem.

We have taken the initial concentration negligibly small (but not zero) for the numerical approximation. This yields small deviations from the solution method proposed by Dawson and Wheeler (1990) for the same problem. These deviations are, for the chosen parameter values and the present context, insignificant.

Discretization of the soil columns is required for the numerical approximation and the implementation of chemical heterogeneity. Preliminary calculations for homogeneous columns illustrated that discretization should be done with extreme care, as otherwise s^2 for the numerical approximation does not agree with s^2 evaluated analytically with (4.26). Deviations arising from a wrong discretization were not always visible by comparing plots of front shapes, but were clearly visible by comparing limiting s^2-values ($t\rightarrow\infty$).

To evaluate the analytical solution given by (4.9) for a homogenous soil column with a constant average adsorption coefficient k, the parameters R, η^*, and G^* need to be calculated. The parameter G^*, necessary to determine η^* in (4.10), can analytically be found for particular values of n. The integral in (4.15) has been solved analytically by Van der Zee (1990*b*) for $n=(i+1)/(i+2)$ (with $i=0,1,..,\infty$). Here, we used a numerical integration of the integral in (4.11) to compute G^* and subsequently η^*.

4.3.3 *Assessment of spreading mechanisms*

Concentration distributions, calculated with the random columns using the numerical solution, give an indication of the effect of chemical heterogeneity. However, effects on the front shapes are difficult to distinguish by observing only the fronts. In a previous section we have derived an analytical expression for the variance of a traveling wave front in a homogeneous column. By computing the moments of the fronts in a chemically heterogeneous column and comparing these with the analytical moments of a homogeneous case, with the same spatially averaged k value for $0<z\leq L$ for the heterogeneous and homogeneous column, the effect of heterogeneity can be demonstrated more clearly. The adsorption coefficient k determines the front shape and the front velocity (through retardation factor R). Hence, randomness of k causes a variation in both front shape and in front velocity. Consequently, a numerical calculation of the moments described by (4.16) is necessary. The nonlinearity of adsorption causes steep fronts which may limit the accuracy of the numerical computation of the moments due to a lack of

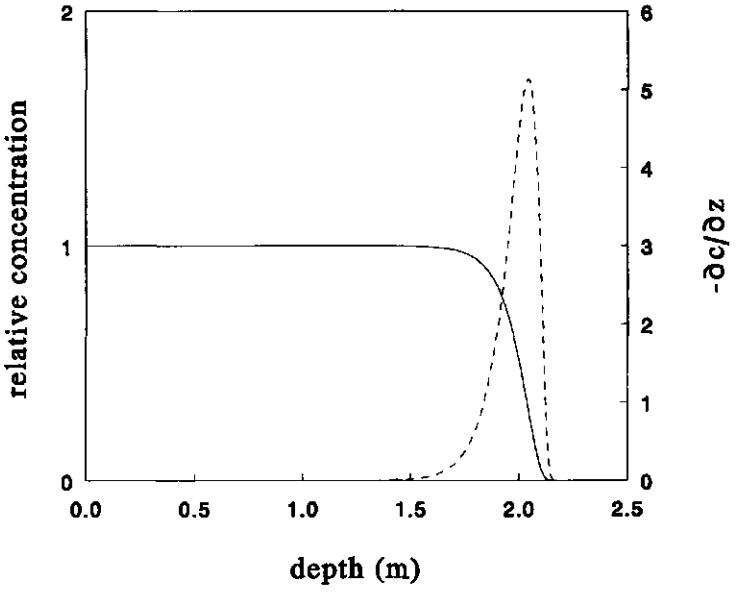

Figure 4.1 Traveling wave front (solid line) with corresponding (negative) derivative (dashed line) at time t=42 (for parameter values see Table 4.1).

points between $\bar{c}$=1 and $\bar{c}$=0. Using a rational function interpolation method to interpolate between the calculated points of the fronts, we ensured a sufficiently large number of points to define the fronts. Consequently, the moments can be calculated numerically with the trapezoidal rule for integration. Figure 4.1 shows for a homogeneous column the traveling wave front with its related density function of z, $\bar{c}'$. The dashed line in Figure 4.1, representing $\bar{c}'$, clearly has a non-Gaussian shape. The asymmetry of the front is due to the opposing effects of adsorption nonlinearity and of dispersion. Besides the asymmetric shape the non-Fickian behaviour is also clear from the time and spatial independence of the front shape for the homogeneous column considered in Figure 4.1.

Incorporation of heterogeneity of the adsorption coefficients causes several mechanisms to play a role in solute spreading. These spreading mechanisms can be characterized as follows: (1) thickness of the individual traveling wave front; (2) column scale heterogeneity of the adsorption coefficient; (3) different average retardation factors for an ensemble consisting of all columns.

The thickness of the individual traveling wave front can be assessed by

considering a homogeneous column. The front width due to dispersion and, in this case, nonlinear adsorption, may play a role in all transport cases considered in this study. If, however, an individual heterogeneous column is taken into account, both thickness of the individual front and column scale heterogeneity play a role in solute spreading. The front velocity and front variance give an impression of the impact of the heterogeneity of the adsorption coefficient. Averaging over all realizations of the velocity and variance, both as a function of depth, yields the expected behaviour of a heterogeneous column.

Additionally, an average front can be considered, representing an ensemble average front, assuming that the flow domain consists of an ensemble of parallel vertical random columns. In addition to the first two spreading mechanisms, extra spreading of the ensemble average front is caused by the variable average retardation factors for different columns. The latter spreading mechanism is caused by the numerical generation of the random columns. The fluctuation imposed on the mean value of the adsorption coefficient causes slightly different average adsorption coefficients for each column. Note that the effect of the third spreading mechanism decreases as the column length increases, because the bias in the column average k decreases with increasing number of generated points.

4.3.4 *Parameter values*

For the simulations and analytical calculations of solute transport through chemically heterogeneous soils, we have chosen to calculate transport of cadmium. De Haan *et al.* (1987) have shown that contaminants like copper and cadmium show Freundlich adsorption behaviour, and parameter values were available for Cd from Van der Zee (1990*b*). We have simulated transport of Cd with an initial concentration of 0 mol m^{-3} and a feed concentration of 0.02 mol m^{-3}. The flow parameters were kept constant in this study with the volumetric water content θ=0.445, bulk density ρ=1350 kg m^{-3}, dispersivity L_d=0.03 m, velocity v=1.9 m y^{-1}, and consequently the dispersion coefficient D=0.057 m^2 y^{-1}. Of the chemical parameters we have assumed n to be nonrandom with, for Cd, n=0.65. It is in agreement with Chardon (1984) and De Haan *et al.* (1987) that the n value is relatively insensitive for soil type differences.

The random correlated fields of k were generated with an average m_k of 4.4, with a variance s_k^2 of 0.8. This results in a coefficient of variation CV of 0.2. This

value is in a likely range, as shown by, e.g., Boekhold *et al.* (1990, 1991). The average k value gives an average retardation factor R of 40, however, the CV of R is not equal to the CV of k. The correlation scale used for the random fields was λ=0.22 m, denoting that the values of the adsorption coefficient may be considered to be uncorrelated for separation distances larger than 0.22 m. For the generation of the random columns Δz^* was $2.2 \cdot 10^{-3}$ m, creating 100 points per correlation scale. The node distance for the numerical calculations, Δz, was chosen to be $2.2 \cdot 10^{-2}$ m, which corresponds to 10 nodes per correlation scale. Consequently, this corresponds to a correlation scale of $\lambda = 10\Delta z$. The used parameter values for the transport calculations are summarized in Table 4.1.

Table 4.1 Parameter values

parameter	value	parameter	value
θ	0.445	m_k ($\text{mol}^{1-n}\ \text{m}^{3(n-1)}$)	4.4
ρ (kg m^{-3})	1350	s_k^2 ($\text{mol}^{2-2n}\ \text{m}^{6(n-1)}$)	0.8
l (m)	4	n	0.65
v (m y^{-1})	1.9	λ (m)	0.22
L_d (m)	0.03	m_k^* ($\text{mol}^{1-n}\ \text{m}^{3(n-1)}$)	4.2
D ($\text{m}^2\ \text{y}^{-1}$)	0.057	Δz (m)	$2.2 \cdot 10^{-2}$
c_0 (mol m^{-3})	0.02	Δz^* (m)	$2.2 \cdot 10^{-3}$
c_i (mol m^{-3})	0		

4.4 Results and discussion

4.4.1 *Homogeneous column*

In order to show the effect of nonlinear adsorption Figure 4.2 gives the fronts and the related variances of the fronts, for cases with linear and nonlinear adsorption. For Figure 4.2 only analytical solutions have been used. Earlier research has given evidence of the appropriateness of the used analytical solutions (Lapidus and Amundsen, 1952; Van der Zee, 1990*b*). The traveling wave fronts of

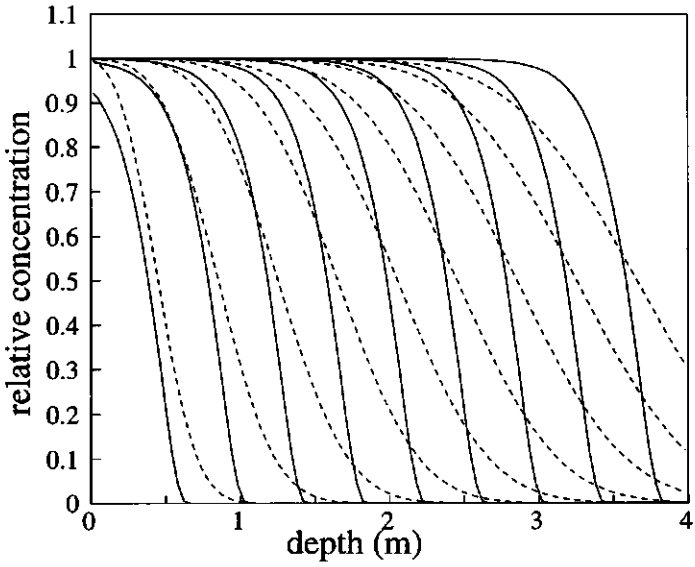

Figure 4.2 Analytically calculated fronts for nine times for case with nonlinear and linear adsorption. Solid line: traveling wave solution (4.9). Dashed line: linear solution (4.35).

Figure 4.2 have been calculated with (4.9), whereas for the case with linear adsorption use was made of a solution given by Van Genuchten and Alves (1982), i.e.,

$$\bar{c}(z,t)=\frac{1}{2}\mathrm{erfc}\left(\frac{R_l z-vt}{2(DR_l t)^{1/2}}\right)+\frac{1}{2}\exp\left(\frac{vz}{D}\right)\mathrm{erfc}\left(\frac{R_l z+vt}{2(DR_l t)^{1/2}}\right) \qquad (4.35)$$

where, in this case, R_l was set equal to R.

From Figure 4.2 can be seen that the shape and velocity of the traveling wave front become constant during the solute displacement. The analytical solution given by (4.9), used for the calculations of the traveling wave fronts of Figure 4.2, has been derived for the limiting case ($t\rightarrow\infty$), and is therefore not valid for early displacement times. Van der Zee (1990*b*) has shown that although small deviations occur between the analytical solution and the numerical approximation upon entry of the solute into the column, the solution is quickly applicable. The analytical

solution assumes an instantaneous front shape with a variance to be calculated with (4.26), whereas in practice the front shape starts as a block front that converges to the actual traveling wave. This effect causes the deviating front depths of the concentration fronts at early displacement times in Figure 4.2. At larger displacement times these deviations of the average front depths disappear.

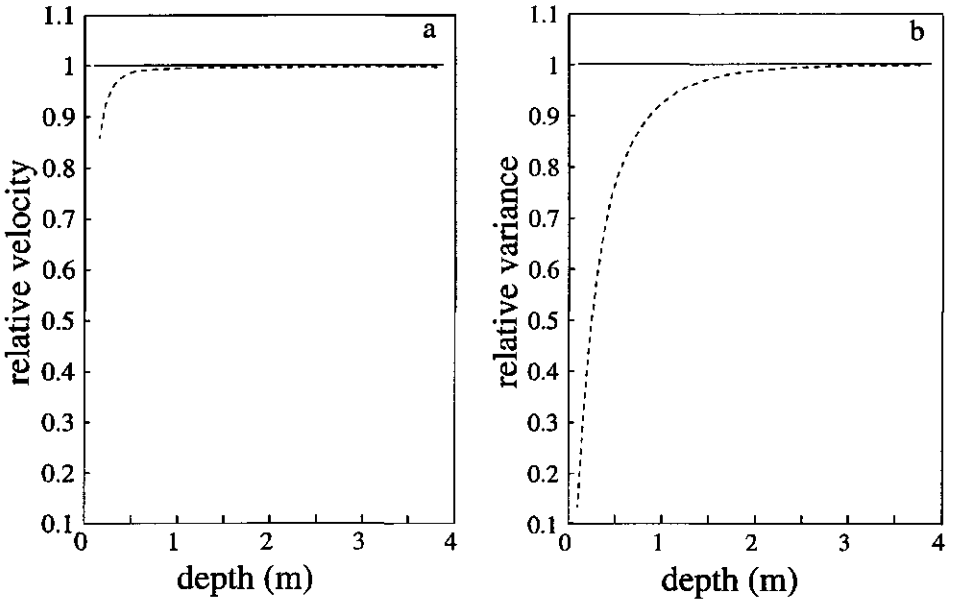

Figure 4.3 (*a*) Relative front velocity and (*b*) front variance of solute fronts in homogeneous columns. Dashed lines: numerical results, solid lines: analytical results.

In Figure 4.3 we show how the front velocity (related to the first moment) and the variance (second central moment) of the numerical solution approach the constant values of the analytical traveling wave solution. The velocity of the analytical traveling wave is determined with the retardation factor, whereas the analytical variance is computed with (4.26). For comparison, we have divided the velocities and variances by the analytical values which yields relative quantities. Figure 4.3*a* shows that the actual front starts with a velocity of zero, but rapidly approaches the velocity calculated by the analytical solution. From Figure 4.3*b* can be seen that, compared with the front velocity, more time is necessary for the numerical solution to obtain the exact thickness of the traveling wave front. However, it is clear that although the traveling wave solution is derived for $t \rightarrow \infty$,

the solution is applicable at earlier times. In fact, we will demonstrate that the reaction time of the front shape is quick enough to show differences due to a spatially variable adsorption coefficient k in the random columns.

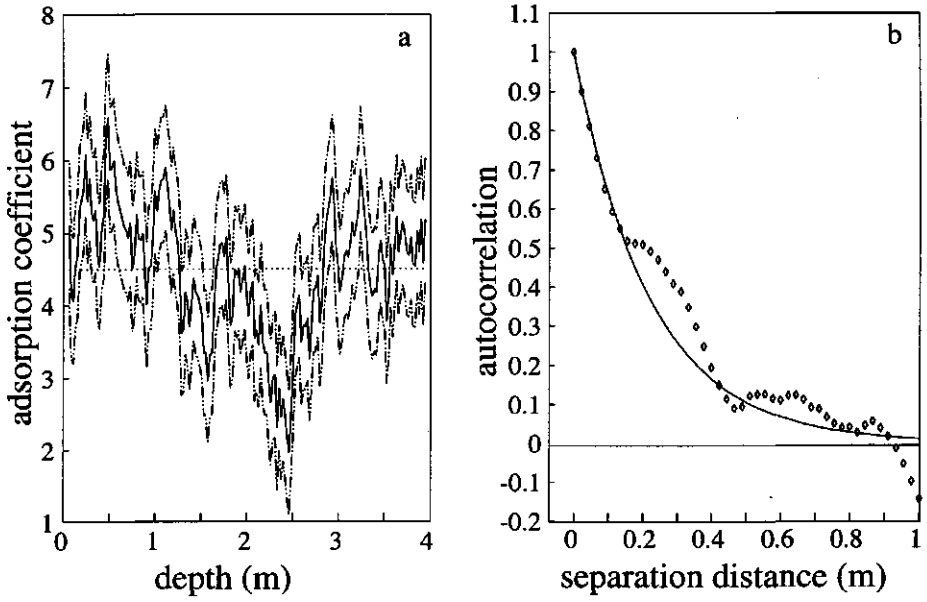

Figure 4.4 (*a*) Spatial distribution and (*b*) autocorrelation (symbols) of the adsorption coefficient of a single realization. In Figure 4.4*a*, the dashed-dotted line denotes: mean value, and the dashed line denotes distribution plus and minus standard deviation. In Figure 4.4*b*, the solid line denotes first-order autocorrelation used as input for generation of random columns.

4.4.2 *Heterogeneous column*

An analysis as given above of the front shape and front velocity of a concentration front characterized by a traveling wave is applicable to homogeneous columns. In practice, however, soils are physically and chemically heterogeneous. Looking at a single realization, randomly selected from the 600 columns with normally distributed adsorption coefficient k, we are able to obtain information about the effect of heterogeneity of nonlinear adsorption. The selected profile is a feasible representation of the ensemble of columns generated with m_k and s_k^2, as given in a previous section. The distribution of the adsorption coefficient k with

its related statistics (mean, standard deviation and autocorrelation) is given in Figure 4.4. Additionally, Figure 4.4*b* shows the first order autocorrelation function used as input for the generation of the random columns. The distribution of the adsorption coefficient k has been used to numerically calculate the solute fronts. Subsequently, we have used the average adsorption coefficient of this realization, m_k^*, to compare the numerically calculated fronts with analytically calculated fronts for the homogeneous case.

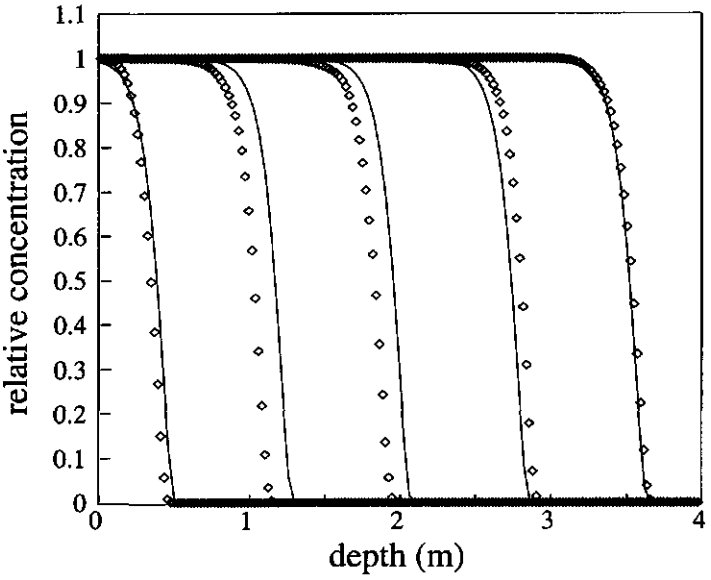

Figure 4.5 Fronts for five times $t=i\cdot\Delta t$ (i=1,2,..,5; Δt=16.8) through a chemically heterogeneous column of an individual realization. Solid line: analytical traveling wave solution with average adsorption coefficient. Symbols: numerically calculated fronts.

The results given in Figure 4.5, show that the chemical heterogeneity causes a spatially variable rate of solute transport. Due to a series of high peaks of the adsorption coefficient in the top part of the column (Figure 4.4*a*), the retardation factor increases which causes a lower solute velocity until z=2 m. A ensuing series of low adsorption parameters causes an increase of the front velocity. At the end of the column the numerical fronts coincide with the analytical fronts. This is caused by the averaging procedure of the adsorption coefficient necessary for the

analytical solution. Consequently, at z=4 m both cases have experienced the same total retardation.

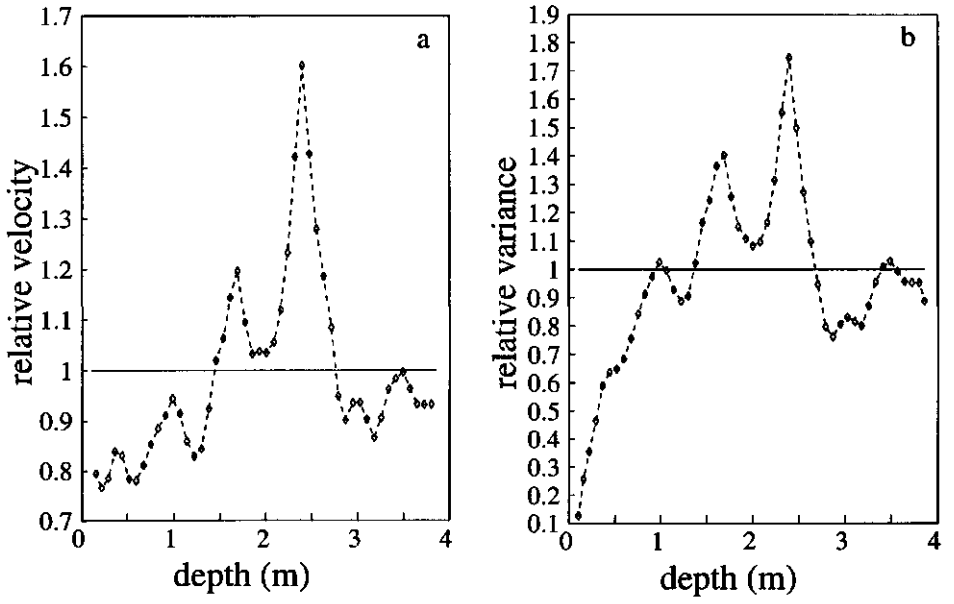

Figure 4.6 (*a*) Relative front velocity and (*b*) relative front variance of numerically calculated transport through a heterogeneous column. Dashed lines with symbols: relative velocities and variances. Solid lines: constant velocity and variance of homogeneous column with corresponding average adsorption coefficient.

The numerical and analytical fronts of Figure 4.5 give a qualitative view of the effect of chemical heterogeneity. In fact, in Figure 4.5 only the effect on the front velocity is visible, whereas differences in front shapes cannot be detected. Figure 4.6 gives the relative velocity of the front, calculated with the first moment, and the relative variance of the front, represented by the second central moment. For reasons of comparison we have chosen to represent the velocity and variance as relative quantities. Apparently, the front shape is also sensitive for the variable adsorption coefficient. The variance and velocity both have peaks at corresponding depths, indicating that a high adsorption coefficient causes steeper fronts. This observation agrees with Van der Zee (1990*b*) who showed that the effect of nonlinearity of adsorption is larger when the adsorption coefficients are larger. Hence a steeper traveling wave front results. Figures 4.5-4.6 demonstrate that

describing the concentration front in terms of moments can be very useful. Influences of a variable adsorption coefficient on the front shape are invisible in Figure 4.5, whereas the variance, with its high sensitivity, shows a clear variation of the front thickness. Similar to the variance of the homogeneous case, shown in Figure 4.3*b*, the variance of the heterogeneous realization needs more displacement time to approach the analytical value than the velocity. Nevertheless, the sensitivity of the front variance is high enough to react to the pattern of the variable adsorption coefficient, shown in Figure 4.4*a*.

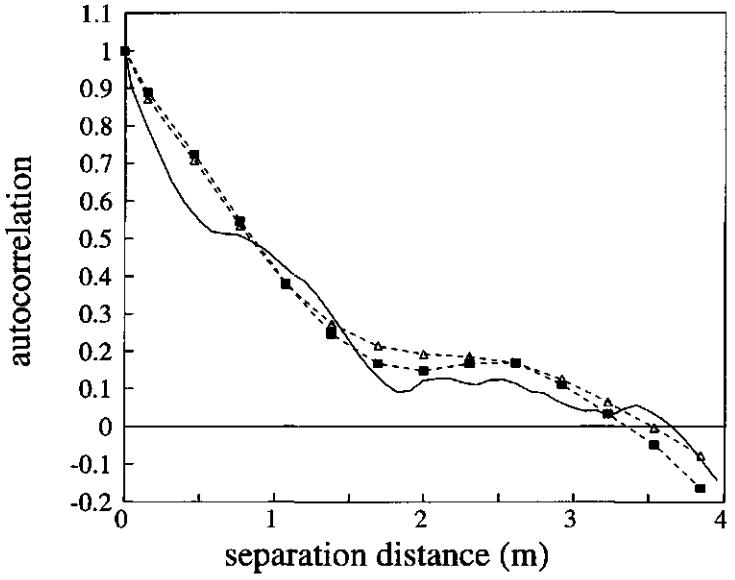

Figure 4.7 Autocorrelations of adsorption coefficient (solid line), front velocity (dashed line with triangles), and front variance (dashed line with squares).

A different way to show the effect of the spatially variable adsorption coefficient k on the concentration front is to compare the autocorrelation of the spatial distribution of the adsorption coefficient with the autocorrelation of the distribution of the front velocity and front variance. The autocorrelations of the adsorption coefficient k of the front velocity and of the front variance are given in Figure 4.7. It can be seen that all three correlations follow about the same course. The autocorrelation of the adsorption coefficient k at the lower separation distances is less than the autocorrelation of the other two quantities, indicating that at a short

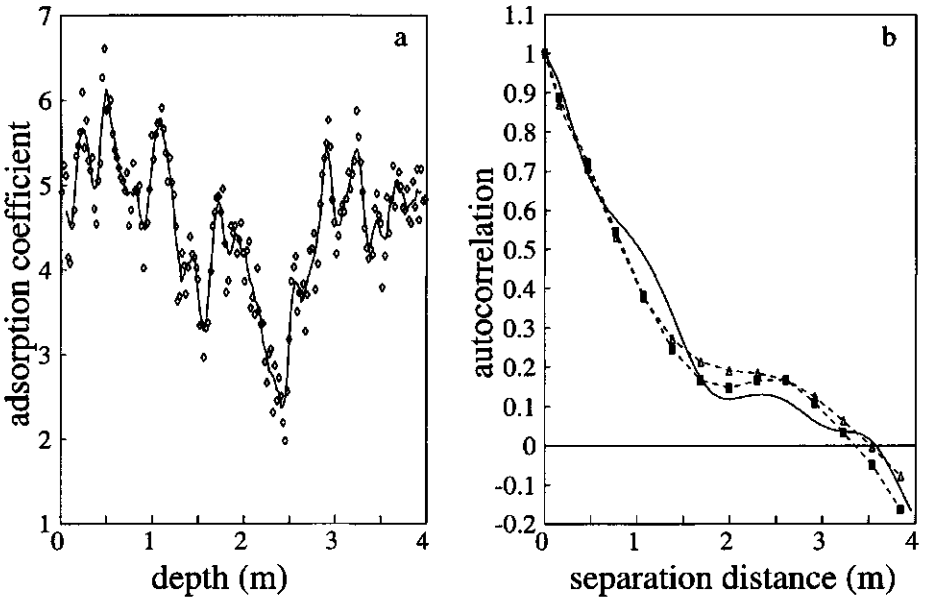

Figure 4.8 (*a*) Moving average of the adsorption coefficient k, averaged over five nodes. (*b*) Autocorrelations of moving average adsorption coefficient (solid line), front velocity (dashed line with triangles), and front variance (dashed line with squares).

distance values of the adsorption coefficient are less similar than values of the velocity and variance. This can be seen from Figures 4.4-4.6 where the distribution of the adsorption coefficient k is shown to be highly variable, even at short distances. The distributions of the front velocity and front variance show a corresponding course, but are more smoothed, causing a decrease of the small-scale variability. The smoothing is due to the fact that a concentration front is spread out over a number of nodes, whereas the values of the adsorption coefficient are node specific. If a moving average of the adsorption coefficients k is calculated, the profile of k is more smoothed, corresponding to the distributions of the front velocity and front variance. The adsorption coefficient profile, calculated as a moving average is shown in Figure 4.8*a*. Figure 4.8*b* demonstrates the corresponding autocorrelation of the moving average adsorption coefficient, compared with the autocorrelations of the front velocity and front variance. At lower separation distances the autocorrelation of the average adsorption coefficient

has increased and corresponds to the autocorrelation of the front velocity and the front variance. The small-scale heterogeneity is reduced.

In general it can be said that chemical heterogeneity of nonlinear adsorption causes deviations of the velocity and thickness of the traveling wave front. Figures 4.5-4.6 demonstrate that the heterogeneity has significant effects on single realizations of nonlinearly adsorbing solute transport. Values of front velocity and front variance are locally substantially higher or lower than the analytical values calculated with an average adsorption coefficient. If, however, adsorption would be described as a linear process, the front variances would be much larger, due to the increasing thickness of the concentration front as displacement proceeds.

4.4.3 *Expected heterogeneous column behaviour*

Due to one-dimensional chemical heterogeneity the front shape and front depth can be highly variable. A single realization has been shown to give results considerably deviating from the homogeneous case with a nonvariable single-valued adsorption coefficient. The randomness of a single realization increases the uncertainty to make predictions concerning the arrival time and front thickness at a certain point. The best prediction of front velocity and front variance is the expected value of the two quantities. The expectation characterizes the effect of the spreading mechanism denoted by column scale heterogeneity. The spreading around the expected values is a measure for the possible deviations from the expected values.

The best available estimate for the expected value of the front velocity and front variance is obtained by averaging these quantities for all 600 random columns. The average velocity and average variance are given as a function of depth in Figure 4.9. Both quantities are represented as relative quantities with respect to the analytical value for the case of a homogeneous traveling wave solution. The latter was calculated with the average adsorption coefficient. As is shown in Figure 4.9, the averaging has a smoothing effect. The deviations from the analytical value are significantly smaller compared with a single realization (Figure 4.6). In fact, if an infinite number of columns were used, the average velocity and variance curves would increase smoothly, just like in Figure 4.3 (however, not necessarily to the same value). In Figure 4.3*a* and 4.3*b* the confidence intervals are not shown, for they are equal to about 1% limiting velocity and variance,

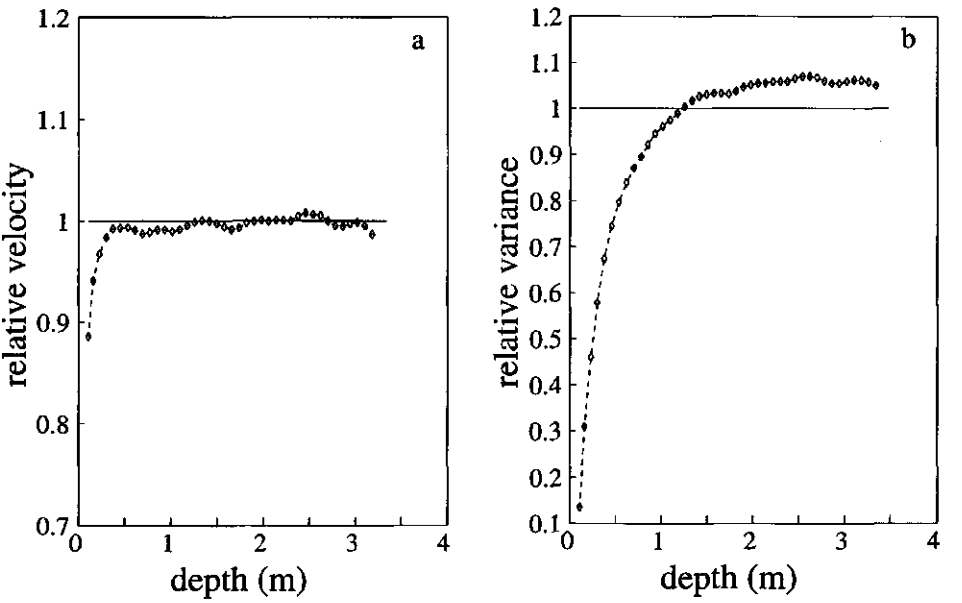

Figure 4.9 (*a*) Averaged relative front velocity and (*b*) averaged relative front variance. Dashed lines: averaged relative velocities and variances. Solid lines: constant averaged relative velocity and variance for homogenous columns with constant average adsorption coefficients.

respectively. This proves convergence of the Monte Carlo calculations. Note that, corresponding to a single realization, the expected variance tends to a constant value, typical for a traveling wave. However, if adsorption were described as a linear process, the expected variance would increase continuously with depth.

Additionally, Figure 4.9 reveals that the spreading around the analytical velocity is smaller than the spreading around the analytical variance (compare different scales). Therefore, the expected velocity will not differ much from the analytical velocity of the homogeneous case. The average variance tends towards a value larger than the analytical variance of the traveling wave front. The fact that the expected value of the variance is not equal to the value calculated with average parameters can be visualized with the frequency distributions in Figure 4.10. Here, 8000 adsorption coefficients were randomly generated, following a normal distribution (Figure 4.10*a*). With the ensemble of normally distributed adsorption coefficients and constant values of n, θ and c_0, normally distributed retardation

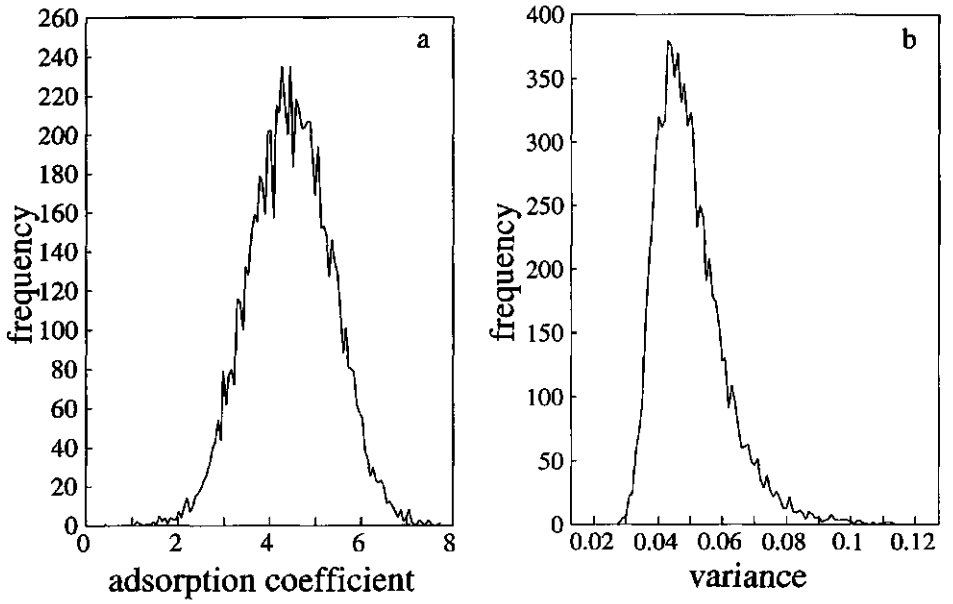

Figure 4.10 Frequency distributions of (*a*) 8000 adsorption coefficients, and of (*b*) 8000 corresponding variances, analytically calculated with (4.26).

factors have been computed according to

$$R=1+\frac{k}{\theta}c_0^{n-1} \tag{4.36}$$

where k is the random variable. If, with a normally distributed R, the front variance is calculated with (4.26) a frequency distribution is produced with a non-Gaussian shape. The frequency distribution of the front variance is given in Figure 4.10*b*. The nonlinear relationship between variance and R in (4.26) causes the shape that differs from a normal distribution. The expected value in Figure 4.10*b* is larger than the median, calculated with the analytical solution (4.26) and is shown as the solid line in Figure 4.9.

4.4.4 *Ensemble average front*

An extra effect of chemical heterogeneity can be studied by considering the

ensemble average fronts of the 600 random columns. The ensemble average front represents an average front for a flow domain, consisting of an ensemble of parallel noninteracting soil columns. Representing a field in this manner was introduced by Dagan and Bresler (1979), and applied to a chemically spatially variable field by Van der Zee and Van Riemsdijk (1987) and Destouni and Cvetkovic (1991). Considering the flow domain, we have a random distribution of the adsorption coefficient k in each column, combined with a spatial distribution of the average adsorption coefficient over the domain. The latter causes slightly different average retardation factors for each column, and therefore a variable flow domain of the transported solute. Consequently, in some columns the solute will move more rapidly than in others.

Compared with the case of column scale heterogeneity, the extra front spreading mechanism due to the spatially variable retardation factor causes a different behaviour of the ensemble average front. Whereas only two spreading mechanisms are present if column scale heterogeneity (individual front spreading and column scale heterogeneity) is considered, here we are dealing with three spreading mechanisms, which have been discussed previously.

In a previous section it has already been shown that for a homogeneous column, the thickness of a traveling wave (the first spreading mechanism) can be calculated analytically with (4.26). Since the front shape is not much affected by column scale heterogeneity, (4.26) can also be used as an estimation for the front thickness in heterogeneous columns.

To study the spreading due to column scale heterogeneity and due to the spatially variable retardation factor (second and third spreading mechanism), results are given in Figure 4.11 of the ensemble average fronts, with corresponding variance, of the heterogeneous columns and of the homogeneous columns with variable average retardation factors. Of the above mentioned spreading mechanisms, the column scale heterogeneity does not apply to the case with homogeneous columns. In the flow domain with homogeneous columns, the ensemble average fronts have been calculated with traveling wave fronts computed with different average adsorption coefficients.

The first effect visible in Figure 4.11*a* is, in contrast with a traveling wave front, that the ensemble average front has a continuously spreading character. Figure 4.11*b* verifies this with a continuously increasing variance. This can be explained by the variable retardation factor at each column, which causes a variable

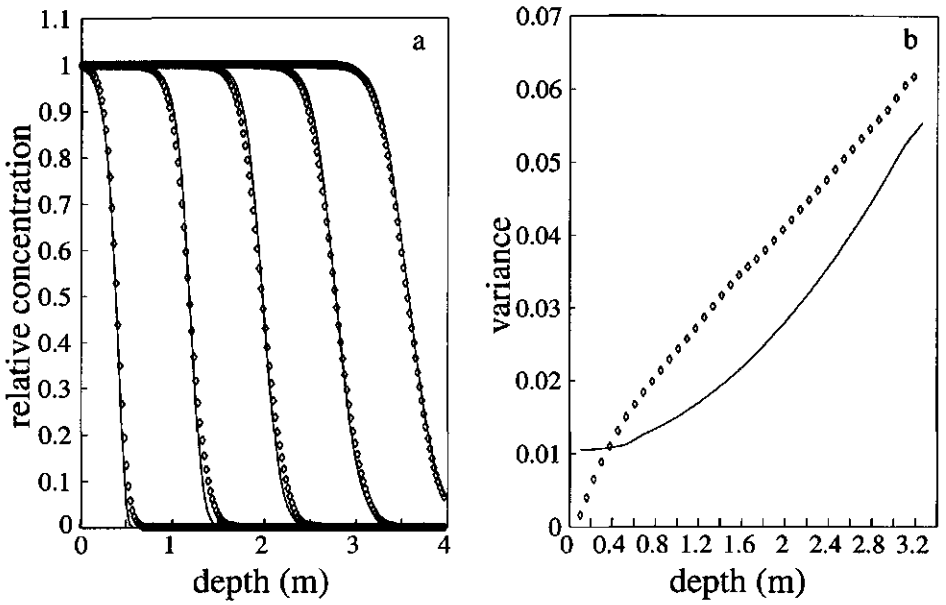

Figure 4.11 (*a*) Ensemble average fronts and (*b*) corresponding variances. Solid lines: ensemble average fronts and variances of 600 homogeneous columns with variable averaged adsorption coefficient (ignoring column scale heterogeneity). Symbols: ensemble average fronts and variances of 600 heterogeneous columns.

velocity field of the transported solute. Consequently, during displacement time, the front will spread continuously.

A different effect, visible in Figure 4.11*a*, is that there is good agreement between the ensemble average fronts of the heterogeneous columns and the fronts of the homogeneous columns with variable average retardation factors. This implies that the second spreading mechanism, the column scale heterogeneity, is of minor importance when considering ensemble average fronts. The spatial distribution of the retardation factor over the different columns predominates over the effect of front spreading. From Figure 4.11*b* can be seen that at early displacement times the effect of the average retardation factors of the different columns is still small. The variance of the ensemble average front of the homogeneous columns with variable average retardation factor is equal to the variance of the individual traveling wave, whereas the thickness of the ensemble average front of the heterogeneous columns is initially zero. At larger displacement times the effect of

column scale heterogeneity becomes relatively less important and, consequently, the relative effect of the variable average retardation factor becomes larger. The differences between the variances of the ensemble average front of the heterogeneous columns and the homogeneous columns hardly change, whereas the absolute value of the variances continuously increases. Note that Figure 4.11*b* again justifies the use of moments. The effect of column scale heterogeneity can be made clearly visible.

In addition to the second central moment, use can be made of the third and fourth central moment to assess the shape of the ensemble average concentration front. The third central moment of a concentration front can be used to quantify the skewness of the distribution function, $\bar{c}'(z,t)$. The fourth central moment is related to the kurtosis of the distribution function. The kurtosis measures the peakedness or flatness of the distribution. In order to compare the distribution functions, both skewness and kurtosis are nondimensional quantities with a value of 0 for normal distributions.

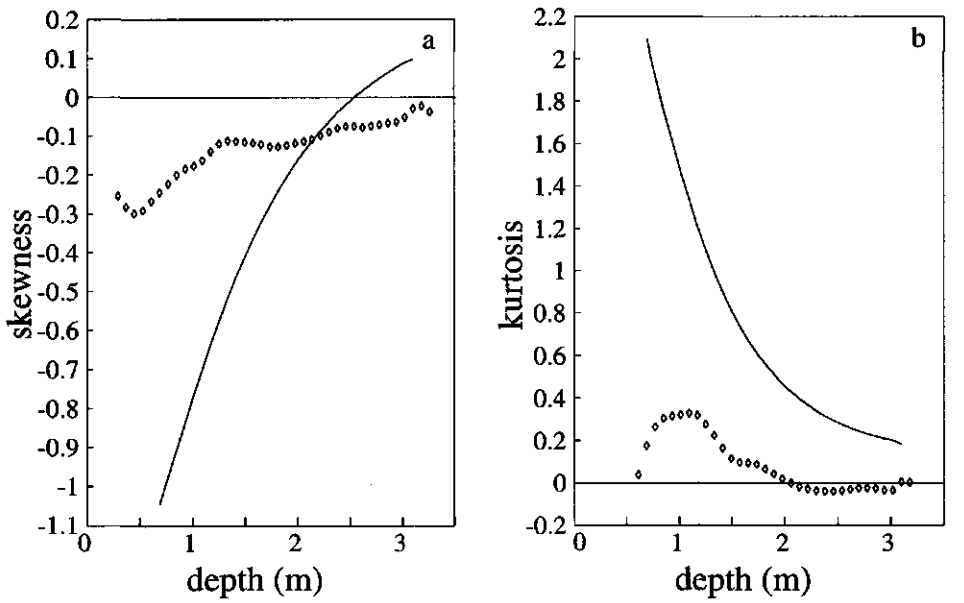

Figure 4.12 (*a*) Skewness and (*b*) kurtosis of the ensemble average fronts. Solid lines: properties of ensemble average fronts of 600 homogeneous columns with variable average adsorption coefficients. Symbols: properties of ensemble average fronts of 600 heterogeneous columns.

Figure 4.12 shows the skewness and kurtosis for the ensemble average front of 600 heterogeneous columns and for the ensemble average front of 600 homogeneous columns with different average adsorption coefficients. In Figure 4.12*a* we see that the skewness of the ensemble average front for the homogeneous columns with different average adsorption coefficients approaches a value just above the value characterising a normal distribution. The skewness increases from a negative value, that represents the skewness of a single traveling wave front. The negative skewness is due to a stronger adsorption of the lower concentrations compared to adsorption of the higher concentrations. This causes the front to be steeper at low concentrations, resulting in a negatively skewed distribution function $\overline{c}'(z,t)$. The skewness of the ensemble average front of the heterogeneous columns shows similar results. In the course of displacement the value of the normal distribution is approached. At t=0 the solution of the heterogeneous column starts as a block front, causing a less negative skewness at early displacement time compared with the skewness of the ensemble average front for the homogeneous columns. The approach to the value 0 of the fronts of the heterogeneous columns clearly demonstrates a normal behaviour of the ensemble average front.

The normal behaviour of the ensemble average front is verified by Figure 4.12*b*, which demonstrates the kurtosis of the concentration distributions. Corresponding to Figure 4.12*a*, the kurtosis for the ensemble average front calculated with homogeneous columns with different average adsorption coefficients approaches a value just above the normal value. The approach starts at the characteristic kurtosis of a single traveling wave. The kurtosis of the ensemble average front calculated with the heterogeneous columns shows a behaviour corresponding to a normal distribution.

The discrepancy between the behaviour of the ensemble average front of the homogeneous columns and a normal distribution (illustrated with skewness and kurtosis) can be attributed to the front shape of an individual traveling wave front. The steepness of the downstream part of the regular traveling wave causes the deviations of the average front from 0 in Figure 4.12 (horizontal solid line). The ensemble average front of the heterogeneous columns shows a normal behaviour due to averaging out of the irregularities of the individual fronts which develop in the heterogeneous columns (see Figure 4.6).

If column scale heterogeneity is ignored, it is possible to derive an analytical approximation for the ensemble average front. This approximation can be obtained

by adjusting the analytical solution for Fickian-type transport given by (4.35). If transport with linear adsorption in a homogeneous medium is considered, (4.35) can be rewritten in terms of the first moment (average position) and the second central moment (variance) of the front. To use (4.35) in order to describe the ensemble average front we have to account for the extra spreading due to the thickness of the individual traveling wave front.

If v^* is defined as the ensemble average front velocity ($v^*=v/R$), the mean position m_z and the variance s_z^2 of the ensemble average front can be given as

$$m_z=m_v.t \tag{4.37a}$$

$$s_z^2=s_\eta^2+(s_v.t)^2 \tag{4.37b}$$

where s_η^2 is the variance of an individual traveling wave, given by (4.26). To arrive at (4.37) we have assumed that $1/R$ is normally distributed if R is normally distributed, which in general is only valid if the coefficient of variation of R is small. With (4.37) the analytical approximation for the ensemble average front can be derived from (4.35) as

$$\bar{c}(z,t)=\frac{1}{2}\mathrm{erfc}\left(\frac{z-m_z}{s_z\sqrt{2}}\right)+\frac{1}{2}\exp\left(\frac{2m_z}{s_z^2}z\right)\mathrm{erfc}\left(\frac{z+m_z}{s_z\sqrt{2}}\right) \tag{4.38}$$

With Fickian-type transport (linear adsorption) in homogeneous columns, the variance s_z^2 is not given by (4.37*b*), but can be written as

$$s_z^2=2Dt/R_f \tag{4.39}$$

Equation (4.39) shows that s_z^2 increases linearly with time t. However, for a spatially variable retardation factor, the variance s_z^2 increases with t^2, as can be seen in (4.37*b*). This can be visualized in Figure 4.11*b*, where a parabolic course is clearly visible.

To show the applicability of (4.38), Figure 4.13 gives the results of the ensemble average front of the homogeneous columns with variable average retardation factors, approximated by the adjusted analytical solution. The corresponding variances are shown as well. Despite the assumption that $1/R$ is

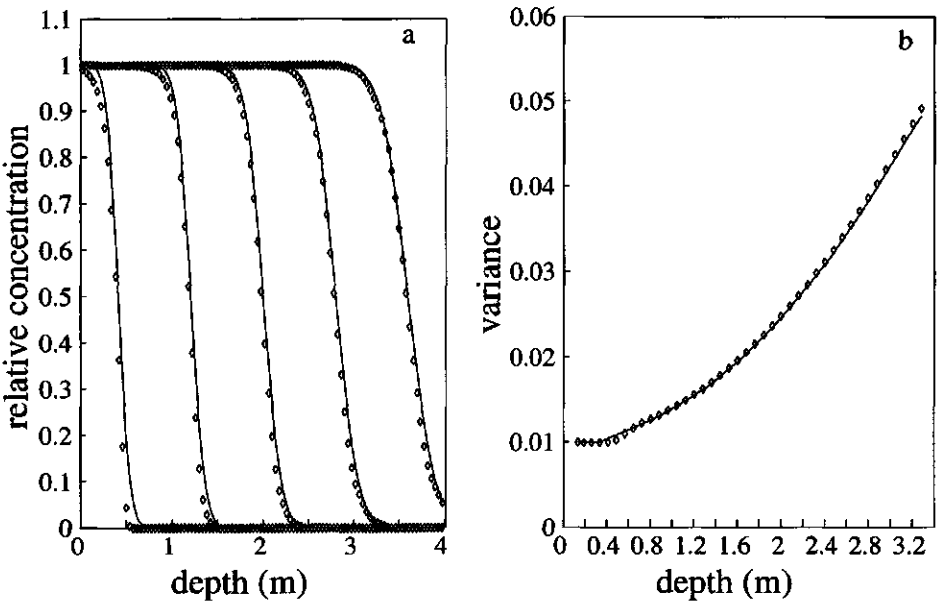

Figure 4.13 (*a*) Analytical approximation of ensemble average front and (*b*) corresponding variances, ignoring column scale heterogeneity. Solid lines: analytical approximation (4.38) and variances. Symbols: ensemble average fronts and variances of 600 homogeneous columns with variable adsorption coefficient.

normally distributed the agreement is good, although at early displacement times the ensemble average front has the shape of a traveling wave, which cannot be described adequately by a Fickian-type front.

In the above considered case, column scale heterogeneity was ignored, because the distribution of the average retardation factor produced dominant effects. However, neglecting column scale heterogeneity may not always be justified. In the case with heterogeneous columns, an extra term needs to be added to (4.37*b*) to account for the column scale heterogeneity. Although this term is unknown, it will be dependent on s_k^2, the variance of the adsorption coefficient within a single column. Whereas at large displacement times ($t \rightarrow \infty$) the spreading of the ensemble average front will be dominated by the $s_v^* t^2$ term, this term will show less dominating effects in cases with large column scale heterogeneity and small differences between columns if the limiting situation has not yet been reached.

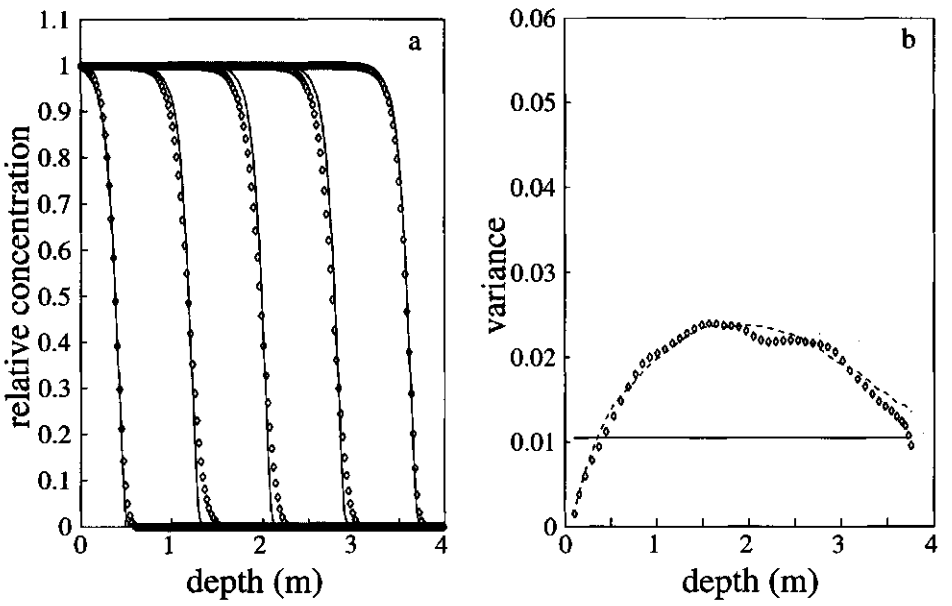

Figure 4.14 (*a*) Ensemble average fronts omitting the variable average retardation factor and (*b*) corresponding variances. Solid lines: traveling wave fronts and variance with m_k. Dashed line, Fig. 4.14b: difference between variances of Fig. 4.11b added with variance of individual traveling wave. Symbols: ensemble average fronts and variances of 600 heterogeneous columns with equal average adsorption coefficients.

The effect of column scale heterogeneity can be demonstrated more clearly if we consider the 600 randomly generated heterogeneous columns with adjusted adsorption coefficients, so that the average front retardation factors are equal in all columns. At each node the adsorption coefficients have been multiplied with a column-specific factor, in order to equalize the average adsorption coefficients of all columns. Therefore, $m_{v*}=v/R$, with R is constant and $s_{v*}^2=0$. In this situation two front-spreading mechanisms are significant: the thickness of the individual traveling wave, and the column scale heterogeneity of the adsorption coefficient. The ensemble average fronts with the corresponding variances are given in Figure 4.14. Figure 4.14*a* shows how the ensemble average front attains a shape, deviating from the Freundlich traveling wave, but remaining constant during the transport process. The continuous spreading of the ensemble average front of Figure 4.11*a* is removed and the resulting front demonstrates a significant symmetric shape. At the

end of the column the front approaches a Freundlich traveling wave front, because at that point all columns have experienced the same average adsorption coefficient.

In Figure 4.14*b* the dashed line is based on the difference of the variances of the ensemble average front with the three front-spreading mechanisms and the variances of the ensemble average front with the homogeneous columns with variable retardation factor, both given in Figure 4.11*b*. This difference represents the spreading due to the spatial distribution of the adsorption coefficients within the columns. If the difference between the two variances of Figure 4.11*b* is added to the expected thickness of the traveling wave, s_η^2, these two added spreading mechanisms approach the variances of the ensemble average front of Figure 4.14*a*. Figure 4.14*b* shows that the different front-spreading mechanisms are completely additive.

The procedure of omitting the variability of the average retardation factors demonstrates a few valuable aspects. First, it can be seen that, in this situation, the variance of the ensemble average front tends to a constant value. At the end of the column the thickness of the front decreases, which is due to the fact that at that point all columns have experienced the same average retardation factor. At the beginning of the column the curves show an equal course, for this part mainly represents the approach of the actual individual fronts to the individual traveling wave. The internal heterogeneity still has little effect.

Figure 4.14*b*, compared with Figure 4.11*b*, also gives the significance of the variance due to column scale heterogeneity. It can be seen that this front-spreading mechanism is quite relevant, although, after longer displacement times, variation of the different retardation factors between columns will dominate the front spreading process.

4.5 Conclusions

We have studied the effect of chemical heterogeneity on solute transport in one-dimensional soil columns. The heterogeneity was obtained by assuming a random variation of the Freundlich adsorption coefficient with depth. A normal distribution in combination with exponential autocorrelation was assumed. The method of moments was used to show the effect of chemical heterogeneity on the front velocity and on the front variance. This method was proven to be very

valuable, for differences in front shape could be made clearly visible. Considering a homogeneous column, an analytical expression was derived for the front variance, which is, due to nonlinear adsorption, nonvariable with space and time. For a single realization, chemical heterogeneity has significant effect. The front velocity and front variance may show large deviations from the case with average adsorption coefficient. The expected values of the front velocity and front variance, calculated as average values from 600 randomly generated columns, show a more smoothed character compared with single realizations. The front velocity shows less spreading around the case calculated with average adsorption coefficient than the front variance. The nonlinear character of the calculations causes the deviations from the case with average parameters. Considering the ensemble average front, it was shown that three front-spreading mechanisms play a role in the spreading of the front. First, the thickness of the individual fronts causes spreading, followed by an effect of the internal variation of the adsorption coefficient in the individual columns. With time, the effect of different average retardation factors of different columns increases and dominates the front spreading. It was shown that the latter spreading mechanism causes a front to spread proportionally to t^2. Due to the time dependency, the internal variation of the adsorption coefficient can, in some cases, be insignificant. Nevertheless, the steep fronts caused by nonlinear adsorption, in contrast with the continuously spreading fronts caused by linear adsorption, prove the importance of the characterization of the adsorption process.

Notation

c	concentration (mol m^{-3})
c_0	feed concentration (mol m^{-3})
c_i	initial concentration (mol m^{-3})
$\bar{c}$	relative concentration
Δc	concentration difference (mol m^{-3})
CV	coefficient of variation
D	pore scale dispersion coefficient (m^2 y^{-1})
f	probability density function
g	function
G^*	constant
k	nonlinear adsorption coefficient (mol^{1-n} $m^{3(n-1)}$)
l	column length (m)
L_d	dispersivity (m)

m	parameter
m_k	average adsorption coefficient ($mol^{1-n}\ m^{3(n-1)}$)
m_k^*	average adsorption coefficient of a single realization ($mol^{1-n}\ m^{3(n-1)}$)
m_{v^*}	average ensemble average front velocity ($m\ y^{-1}$)
m_z	average position of ensemble average front (m)
M_K	Kth moment
M_K^c	Kth central moment
n	Freundlich sorption parameter
q	adsorbed amount (volumetric basis) ($mol\ m^{-3}$)
Δq	change in q ($mol\ m^{-3}$)
P	parameter
r	autocorrelation coefficient
R	nonlinear retardation factor
R_l	linear retardation factor
s	adsorbed amount (mass basis) ($mol\ kg^{-1}$)
s^2	variance (second central moment)
s_k^2	variance of adsorption coefficient
$s_{v^*}^2$	variance of ensemble average front velocity
s_z^2	variance of ensemble average front
s_ε^2	variance of the random fluctuation
s_η^2	variance of traveling wave front
t	time (y)
v	velocity ($m\ y^{-1}$)
v^*	ensemble average front velocity ($m\ y^{-1}$)
z	depth (m)
Δz	node distance for numerical calculations (m)
Δz^*	distance between generation points for random columns (m)
α_i	parameter
β	autocorrelation coefficient for two subsequent nodes
ε	random fluctuation of adsorption coefficient k
ζ	separation distance (m)
η	transformed coordinate (m)
η^*	reference point value of η (m)
$\tilde{\eta}$	parameter ($\tilde{\eta}=\eta-\eta^*$) (m)
θ	volumetric water fraction
μ	first moment
λ	correlation scale (m)
ρ	dry bulk density ($kg\ m^{-3}$)

References

Amoozegar-Fard, A., D.R. Nielsen, and A.W. Warrick, Soil solute concentration distributions for spatially varying pore water velocities and apparent diffusion coefficients, Soil Sci. Soc. Am. J., 46, 3-9, 1982.

Aris, R., On the dispersion of a solute in a fluid flowing through a tube, Proc. R. Soc. London, Ser. A, 235, 67-77, 1956.

Bellin, A., Numerical generation of random fields with specified spatial correlation structure, Internal Report, Dept. of Civil Engineering, University of Trent, Italy, 1991.

Bellin, A., P. Salandin, and A. Rinaldo, Simulation of dispersion in heterogeneous porous formations: statistics, first-order theories, convergence of computations, Water Resour. Res., 28, 2211-2227, 1992.

Black, T.C., and D.L. Freyberg, Stochastic modeling of vertically averaged concentration uncertainty in a perfectly stratified aquifer, Water Resour. Res., 23, 997-1004, 1987.

Boekhold, A.E., S.E.A.T.M. van der Zee, and F.A.M. de Haan, Prediction of cadmium accumulation in a heterogeneous soil using a scaled sorption model, Proceedings of ModelCARE 90: Calibration and Reliability in Groundwater Modelling, conference held in The Hague, September 1990, IAHS Publ. no. 195, 1990.

Boekhold, A.E., S.E.A.T.M. van der Zee, and F.A.M. de Haan, Spatial patterns of cadmium contents related to soil heterogeneity, Water, Air, and Soil Pollution, 57-58, 479-488, 1991.

Bosma, W.J.P., and S.E.A.T.M. van der Zee, Analytical approximations for nonlinear adsorbing solute transport in layered soil, J. Contam. Hydrol., 10, 99-118, 1992.

Bosma, W.J.P., and S.E.A.T.M. Van der Zee, Analytical approximation for nonlinear adsorbing solute transport and first order degradation, Transport in Porous Media, 11, 33-43, 1993.

Bresler, E., and G. Dagan, Solute dispersion in unsaturated heterogeneous soil at field scale, 2, Applications, Soil Sci. Soc. Am. J., 43, 467-472, 1979.

Bresler, E., and G. Dagan, Convective and pore scale dispersive solute transport in unsaturated heterogeneous fields, Water Resour. Res., 17, 1685-1693, 1981.

Bresler, E., and G. Dagan, Unsaturated flow in spatially variable fields, 3, Solute transport models and their applications to two fields, Water Resour. Res, 19, 429-435, 1983.

Calvet, R., M. Tercé, and J.C. Arvieu, Adsorption des pesticides par les sols et leurs constituants. III. Caractéristiques générals de l'adsorption des pesticides, Ann. Agron. 31, 239-257, 1980.

Cameron, D.A., and A. Klute, Convective-dispersive solute transport with a combined equilibrium and kinetic adsorption model, Water Resour. Res., 13, 183-188, 1977.

Chardon, W.J., Mobiliteit van cadmium in de bodem, Ph.D. Thesis, 200 pp., Agric. Univ. Wageningen, The Netherlands, 1984.

Chrysikopoulos, C.V., P.K. Kitanidis, and P.V. Roberts, Analysis of one-dimensional solute transport through porous media with spatially variable retardation factor, Water Resour. Res., 26, 437-446, 1990.

Coats, K.H., and B.D. Smith, Dead-end pore volume and dispersion in porous media, Soc. Pet. Eng. J., 4, 73-84, 1964.

Cvetkovic, V.D. and A.M. Shapiro, Mass arrival of sorptive solute in heterogeneous porous media, Water Resour. Res., 26, 2057-2067, 1990.

Dagan, G., Time-dependent macrodispersion for solute transport in anisotropic heterogeneous aquifers, Water Resour. Res, 24, 1491-1500, 1988.

Dagan, G., Flow and transport in porous formations, Springer-Verlag, Berlin, 1989.

Dagan, G., and E. Bresler, Solute dispersion in unsaturated heterogeneous soil at field scale, 1, Theory, Soil Sci. Soc. Am. J., 43, 461-467, 1979.

Dawson, C.N., and M.F. Wheeler, Characteristic methods in modeling nonlinear adsorption in contaminant transport, in: Computational Methods in Subsurface Hydrology, edited by G. Gambolati, A. Rinaldo, C.A. Brebbia, W.G. Gray, G.F. Pinder, pp. 305-314, Springer-Verlag, New York, 1990.

De Haan, F.A.M., S.E.A.T.M. Van der Zee, and W.H. Van Riemsdijk, The role of soil chemistry and soil physics in protecting soil quality; Variability of sorption and transport of cadmium as an example, Neth. J. Agric. Sci., 35, 347-359, 1987.

Destouni, G., and V. Cvetkovic, Field scale mass arrival of sorptive solute into the groundwater, Water Resour. Res., 27, 1315-1325, 1991.

Graham, W.D., and D.B. McLaughlin, A stochastic model of solute transport in groundwater: application to the Borden, Ontario, tracer test, Water Resour. Res., 27, 1345-1359, 1991.

Jury, W.A. Simulation of solute transport using a transfer function model, Water Resour. Res., 18, 363-368, 1982.

Jury, W.A., G. Sposito, and R.E. White, A transfer function model of solute transport through soil, 1. Fundamental concepts, Water Resour. Res., 22, 243-247, 1986.

Lapidus, L., and N.R. Amundsen, Mathematics of adsorption in beds, VI, The effect of longitudinal diffusion in ion exchange and chromatographic column. J. Phys. Chem., 56, 984-988, 1952.

Mackay, D.M., W.P. Ball, and M.G. Durant, Variability of aquifer sorption properties in a field experiment on groundwater transport of organic solutes: methods and preliminary results, J. Contam. Hydrol., 1, 119-132, 1986*a*.

Mackay, D.M., D.L. Freyberg, P.V. Roberts, and J.A. Cherry, A natural gradient experiment on solute transport in a sand aquifer, 1. Approach and overview of plume movement, Water Resour. Res., 22, 2017-2029, 1986*b*.

Rao, P.S.C., J.M. Davidson, R.E. Jessup, and H.M. Selim, Evaluation of conceptual models for describing nonequilibrium adsorption-desorption of pesticides during steady-state flow in soils, Soil Sci. Soc. Am. J., 43, 22-28, 1979.

Valocchi, A.J., Spatial moment analysis of the transport of kinetically adsorbing solutes through stratified aquifers, Water Resour. Res., 25, 273-279, 1989.

Van der Zee, S.E.A.T.M., Analysis of solute redistribution in a heterogeneous field, Water Resour. Res., 26, 273-278, 1990*a*.

Van der Zee, S.E.A.T.M., Analytical traveling wave solutions for transport with nonlinear and nonequilibrium adsorption, Water Resour. Res., 26, 2563-2578, 1990*b*. (Correction, Water Resour. Res., 27, 983, 1991).

Van der Zee, S.E.A.T.M., and W.H. Van Riemsdijk, Transport of phosphate in a heterogeneous field, Transp. Porous Media, 1, 339-359, 1986.

Van der Zee, S.E.A.T.M., and W.H. Van Riemsdijk, Transport of reactive solute in spatially variable soil systems, Water Resour. Res., 23, 2059-2069, 1987.

Van Duijn, C.J., and P. Knabner, Travelling waves in the transport of reactive solutes through porous media: Adsorption and binary exchange, Part 2, Report 205, Schwertpunkt programm der Deutsche Forschungsgemeinschaft, Univ. Augsburg, Inst. Mathematik, 45 pp, 1990.

Van Genuchten, M.Th., and W.J. Alves, Analytical solutions of the one-dimensional convective-dispersive transport equation, USDA Techn. Bull. 1661. 151 pp., U.S. Dept. of Agric., Washington D.C., 1982.

Van Genuchten, M.Th., and P.J. Wierenga, Simulation of one-dimensional solute transfer in porous media, Bull. 628, 40 pp., NMSU Agric. Exp. Stn., New Mexico State University, Las Cruces, 1974.

Van Genuchten, M.Th., and P.J. Wierenga, Mass transfer studies in sorbing porous media, I. Analytical solutions, Soil Sci. Soc. Am. J., 40, 473-480, 1976.

Van Genuchten, M.Th., J.M. Davidson, and P.J. Wierenga, An evaluation of kinetic and equilibrium equations for the prediction of pesticide movement through porous media, Soil Sci. Soc. Am. J., 38, 29-35, 1974.

Chapter 5

Linear equilibrium adsorbing solute transport in physically and chemically heterogeneous porous formations 1. Analytical solutions*

Abstract

A first-order analytical solution for the transport of reactive solutes in physically and chemically heterogeneous porous media is derived and discussed. The solution relies on the assumption of chemical activity described by the local linear equilibrium assumption postulating the existence of a (spatially variable) retardation factor. Retardation factors and log permeabilities modeling heterogeneities are described statistically by random space functions with assigned correlation structure. Correlated as well as uncorrelated physical and chemical heterogeneities are studied. The analytical expressions derived reduce to Dagan's classic solution for the case of nonreactive solute transport and obey asymptotic limits already known from the literature.

5.1 Introduction

Experimental evidence and theoretical results suggest that the transport of reactive solutes in natural porous formations is dominated by the spatial variations of physical and chemical properties. Typical among these are variations in hydraulic conductivity and sorption coefficients (for an exhaustive review, see Dagan (1989)). Relevant experimental evidence is discussed in a number of recent papers (Durant and Roberts, 1986; Goltz and Roberts, 1986; Mackay *et al.*, 1986*b*; Roberts *et al.*, 1986; Garabedian, 1987; Garabedian *et al.*, 1988; LeBlanc *et al.*, 1991; Smith *et al.*, 1991). This paper addresses the problem of defining the role of heterogeneities in the description of physical and chemical properties affecting

*by A. Bellin, A. Rinaldo, W.J.P. Bosma, S.E.A.T.M. van der Zee and Y. Rubin
published in: *Water Resources Research*, 29, 4019-4030, 1993.

transport of reactive solutes.

The transport of reactive solutes through heterogeneous porous media in the case of steady state velocity field is governed by the following equation (Lapidus and Amundsen, 1952; Freeze and Cherry, 1979; Dagan, 1989):

$$\frac{\partial C(\mathbf{x},t)}{\partial t}+\frac{\partial C^*(\mathbf{x},t)}{\partial t}=\nabla\cdot[\mathbf{D}_d\cdot\nabla C(\mathbf{x},t)]-\mathbf{v}(\mathbf{x})\cdot\nabla C(\mathbf{x},t) \tag{5.1}$$

where $C(\mathbf{x}, t)$ is the solute concentration in the liquid phase, which is defined as solute mass per unit of volume, $C^*(\mathbf{x}, t)$ is the sorbed solute concentration defined as sorbed solute mass per formation solid volume; $\mathbf{D}_d$ is the tensor of pore scale dispersion, and $\mathbf{v}(\mathbf{x})$ is the heterogeneous velocity field. The statement of the problem requires also the definition of an equation which relates the solute concentrations in solid and liquid phases (Abriola, 1987; Van der Zee, 1990):

$$\frac{\partial C^*(\mathbf{x},t)}{\partial t}=K_r(\mathbf{x})[K_d(\mathbf{x})C^n(\mathbf{x},t)-C^*(\mathbf{x},t)] \tag{5.2}$$

where K_d is the partition or distribution coefficient which regulates the chemical exchange (it represents the ratio C^*/C^n under the equilibrium condition); $K_r(\mathbf{x})$ is the reaction rate parameter of solute sorption between fixed and mobile phases; and n is a coefficient typical of the process which is here assumed to be equal to one. At equilibrium (5.3) assumes the form

$$C^*(\mathbf{x},t)=K_d(\mathbf{x})\cdot C(\mathbf{x},t) \tag{5.3}$$

Equation (5.3) is theoretically valid for an instantaneous reaction, e.g., when K_r approaches infinity and (5.2) is bounded, and it is a suitable model of real life reactive transport of wide classes of solutes whenever characteristic reaction times are significantly smaller than travel times (James and Rubin, 1979; Jennings and Kirkner, 1984; Parker and Valocchi, 1986; Valocchi, 1984, 1985, 1988). Because characteristic flow times are large in many practical groundwater situations, the model (5.3), henceforth called the retardation model, is relevant.

Substituting (5.3) into (5.1), we obtain

$$\frac{\partial C(\mathbf{x},t)}{\partial t} = -\frac{1}{R(\mathbf{x})}\mathbf{v}(\mathbf{x})\cdot\nabla C(\mathbf{x},t) + \frac{1}{R(\mathbf{x})}\nabla\cdot[\mathbf{D}_d\cdot\nabla C(\mathbf{x},t)] \qquad (5.4)$$

where $R(\mathbf{x})=1+K_d(\mathbf{x})$ is known as retardation factor (e.g., Freeze and Cherry, 1979; Valocchi, 1984, 1990), since in the case of constant R the time rescaling $t^R=t/R$ transforms (5.4) into the classic convection-dispersion equation valid for passive solutes.

In the groundwater context, many transport studies have considered the effects of chemical heterogeneity (Miller and Benson, 1983; Durant and Roberts, 1986; Mackay *et al.*, 1986*b*; Roberts *et al.*, 1986; Garabedian, 1987; Van der Zee and Van Riemsdijk, 1987; Shapiro and Brenner, 1988; Valocchi, 1989; Chrysikopoulos *et al.*, 1990, 1992; Van der Zee, 1990; Destouni and Cvetkovic, 1991; Kabala and Sposito, 1991; Van der Zee and Boesten, 1991; Bosma and Van der Zee, 1993). In this paper we address the problem of combined effects of chemical and physical heterogeneities by providing an extension to Dagan's (1984) linear solution of transport of passive solutes. This solution allows a statistical characterization of chemical retardation in addition to that of the natural conductivity of the aquifer and suggests an interpretation for a few experimental findings, like the enhanced degree of anisotropy observed in dispersing plumes where heterogeneous retardation seemingly occurs. Paper 2 of this series (Bosma *et al.*, 1993) using a suitable numerical approach discusses the limits of applicability of the analytical solution.

5.2 Statistical characterization of heterogeneities

Physical heterogeneities in hydraulic parameters lead to large variations in the velocity field, which in turn cause the large spreading of solutes commonly referred to as 'macrodispersion' (Gelhar and Axness, 1983; Dagan, 1984, 1987, 1988, 1989, 1990; Gelhar, 1986; Neuman *et al.*, 1987; Barry *et al.*, 1988; Naff *et al.*, 1988; Naff, 1990; Salandin and Rinaldo, 1990; Neuman and Zhang, 1990; Zhang and Neuman, 1990; Salandin *et al.*, 1991; Rubin, 1991*a*, *b*; Bellin *et al.* 1992). The hydraulic conductivity field is usually modeled through a statistically homogeneous normally distributed random function $Y(\mathbf{x})=\ln(K(\mathbf{x}))$, where $K(\mathbf{x})$ is the hydraulic conductivity with constant mean $\langle Y\rangle$, and variance σ_Y^2 that may

display a spatial structure modeled by the isotropic, exponential model:

$$C_Y(\mathbf{r})=\langle Y'(\mathbf{x})Y'(\mathbf{x}+\mathbf{r})\rangle=C_Y(r)=\sigma_Y^2 \exp(-r) \tag{5.5}$$

where $\mathbf{r}$ and $r=|\mathbf{r}|$ are the dimensionless two-points separation distance and its modulus respectively and, $Y'=Y-\langle Y\rangle$. Here and in the following, if not explicitly stated, the space coordinates are assumed dimensionless with respect to l_Y, which is the integral scale of Y (the measure of the average distance of two uncorrelated Y values). This choice of model is supported by field studies (Freeze, 1975; Hoeksema and Kitanidis, 1984). However the basic results obtained in the following sections are not limited to this particular choice for C_Y.

Recent laboratory studies (Durant and Roberts, 1986) and field experiments (Mackay *et al.*, 1986*b*; Roberts *et al.*, 1986, Garabedian, 1987; Ball and Roberts, 1991) suggest that in the range of validity of the linear equilibrium assumption the retardation factor is spatially variable. The effect of a spatially variable retardation factor on transport in a homogeneous velocity field has been recently addressed by Chrysikopoulos *et al.* (1992). Asymptotic results have been indicated by Garabedian (1987), Garabedian *et al.* (1988) and Dagan (1989) in the case of a linear dependence between the retardation factor and the log conductivity field. Other results concerning stratified formations and formations represented by a bundle of noninteracting parallel homogeneous columns which differ with respect to fluid velocity have been obtained by Valocchi (1989), Cvetkovic and Shapiro (1990), Van der Zee and Van Riemsdijk (1987) and Destouni and Cvetkovic (1990), respectively.

To account for natural spatial variability and uncertainty of the chemical sorption coefficients, we assume the retardation coefficient to be a random space function. Furthermore, $R(\mathbf{x})$ is assumed statistically homogeneous and isotropic with constant mean, $\langle R\rangle$, variance, σ_R^2, and a spatial covariance structure, $C_R(\mathbf{r})$, depending on the lag $\mathbf{r}$.

Plausible (in some sense, limit) models of the spatial variability of the retardation factor assume $R(\mathbf{x})$ to be either perfectly correlated or uncorrelated with the log conductivity field $Y(\mathbf{x})$ (Jury, 1983; Van der Zee and Van Riemsdijk, 1987; Valocchi, 1989; Destouni and Cvetkovic, 1991). This yields for the retardation factor:

Perfect positive correlation (model A)

$$R(\mathbf{x})=1+K_d^{\,G}\exp[Y'(\mathbf{x})] \tag{5.6}$$

Perfect negative correlation (model B)

$$R(\mathbf{x})=1+K_d^{\,G}\exp[-Y'(\mathbf{x})] \tag{5.7}$$

Uncorrelated R and Y (model C)

$$R(\mathbf{x})=1+K_d^{\,G}\exp[W'(\mathbf{x})] \tag{5.8}$$

where $K_d^{\,G}$ is the geometric mean of $K_d(\mathbf{x})$ and W' is a normally distributed random space function with zero mean, variance σ_W^2 and covariance function $C_W(\mathbf{r})=\sigma_W^2 \exp(-rl_Y/l_W)$ and l_W the integral scale of $W(\mathbf{x})$.

Laboratory studies, conducted with the Borden site aquifer material, have shown for sorption of tetrachloroethane that the coefficient K_d can be related to the individual size fraction of the aquifer material (Ball and Roberts, 1991). The observed general trend is of larger K_d values for larger particle size. The same is commonly the case for $K(\mathbf{x})$ (Marsily, 1986; Dagan, 1989). Although this result seems to suggest a positive correlation between $K_d(\mathbf{x})$ and $K(\mathbf{x})$, at this stage conclusive experimental evidence for a positive linear relation between $\ln(K_d)$ and $\ln(K)$ is lacking. Moreover, the study conducted by Robin *et al.* (1991) on the spatial variability of K_d shows a weak negative correlation between $\ln(K_d)$ and $\ln(K)$. To account for significant possible variabilities, model A, the limit case of Ball and Roberts's (1991) results, and models B and C as opposite limits to Robin *et al.*'s (1991) results, are considered.

The mean and covariance structure of the retardation factor can be derived by expanding the exponential terms in Taylor series. This yields for the mean:
Models A and B

$$\langle R\rangle=1+K_d^{\,G}\exp(\sigma_Y^2/2) \tag{5.9a}$$

Model C

$$\langle R\rangle = 1 + K_d^{\,G} \exp(\sigma_W^2/2) \tag{5.9b}$$

Similarly the covariance C_R, is given by
Models A and B

$$C_R(\mathbf{r}) = (K_d^{\,G})^2 \exp(\sigma_Y^2)(\exp[C_Y(\mathbf{r})] - 1) \tag{5.10a}$$

Model C

$$C_R(\mathbf{r}) = (K_d^{\,G})^2 \exp(\sigma_W^2)(\exp[C_W(\mathbf{r})] - 1) \tag{5.10b}$$

For models A and B, the Y, R cross covariance is generally

$$C_{YR}(\mathbf{r}) = \pm K_d^{\,G} \exp(\sigma_Y^2/2) C_Y(\mathbf{r}) \tag{5.11}$$

for models A (+ sign) and B (– sign). For model C, $C_{YR}=0$ for each $\mathbf{r}$.

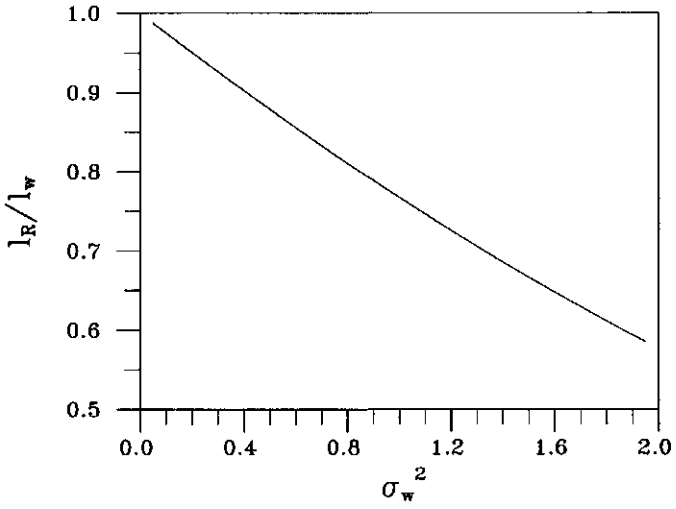

Figure 5.1 Ratio of integral scales of retardation factor and the auxiliary variable W at increasing chemical heterogeneity.

Another important quantity that characterizes the spatial variability of the retardation factor $R(\mathbf{x})$ is its integral scale I_R, a measure of the distance at which the values of R are independent, which is given by

$$I_R=\frac{1}{C_R(0)}\int_0^\infty C_R(r)dr=\frac{Ei(\sigma_W^2)-\gamma-\ln(\sigma_W^2)}{\exp(\sigma_W^2)-1} \tag{5.12}$$

where $Ei(x)=\int_{-\infty}^{x}\exp(z)/z\,dz$, $x>0$ is the exponential integral and $\gamma=0.577....$ is Euler's constant. The result (5.12), valid for model C, can be extended to the models A and B by replacing σ_W^2 with σ_Y^2 and I_W with I_Y. The ratio I_R/I_W decreases as σ_W^2 increases (Figure 5.1) implying that increasing σ_W^2 at constant I_W reduces the correlation of the field $R(\mathbf{x})$.

To summarize, we consider two types of heterogeneities: 1) the physical one, represented by the random space function $Y(\mathbf{x})$; and 2) the chemical one, which is characterized by the random space function $R(\mathbf{x})$. Different models of cross correlation (negative, positive or none) between $Y(\mathbf{x})$ and $R(\mathbf{x})$ are possible, and will be evaluated subsequently.

5.3 Analysis of the retarded velocity field

Our starting point is the mass conservation equation in absence of recharge and for steady state flow given by

$$\nabla\cdot[K(\mathbf{x})\nabla\Phi(\mathbf{x})]=0 \tag{5.13a}$$

$$\mathbf{v}(\mathbf{x})=-\frac{K_H(\mathbf{x})}{\theta}\nabla\Phi(\mathbf{x}) \tag{5.13b}$$

where Φ is the hydraulic head and θ the porosity. We define the steady head field by $\Phi(\mathbf{x})=-\mathbf{J}\cdot\mathbf{x}+\phi(\mathbf{x})$, where $\mathbf{J}$ is the expected value of the head gradient and $\phi(\mathbf{x})$ is the head fluctuation with zero mean. The linear approximation of (5.13) (Dagan, 1984) and of $R(\mathbf{x})$ yields the statistical description of the retarded velocity field $\mathbf{v}^R(\mathbf{x})=\mathbf{v}(\mathbf{x})/R(\mathbf{x})$:

$$\mathbf{v}^R(\mathbf{x})=\frac{\mathbf{V}+\mathbf{v}'(\mathbf{x})}{\langle R\rangle+R'(\mathbf{x})}=[\mathbf{V}+\mathbf{v}'(\mathbf{x})]\left[\frac{1}{\langle R\rangle}-\frac{R'(\mathbf{x})}{\langle R\rangle^2}+O\left(\frac{\sigma_R^{\,2}}{\langle R\rangle^3}\right)\right] \tag{5.14}$$

where $\mathbf{v}'(\mathbf{x})=\mathbf{v}(\mathbf{x})-\mathbf{V}$; $\mathbf{V}=\langle\mathbf{v}(\mathbf{x})\rangle$ and $R'(\mathbf{x})=R(\mathbf{x})-\langle R\rangle$ are the fluctuation around the mean value of the velocity and retarded coefficient fields, respectively.

The expansion (5.14), when truncated at first order and separated into zero- and first-order terms, gives the expressions for the expected value and the local fluctuation of the retarded velocity field:

$$\langle\mathbf{v}^R\rangle=\frac{\mathbf{V}}{\langle R\rangle}+O\left[\max\left(\frac{\sigma_R^{\,2}}{\langle R\rangle^3},\frac{\sigma_Y^{\,2}}{\langle R\rangle^2}\right)\right] \tag{5.15}$$

$$v'_j{}^R(\mathbf{x})=v_j^R(\mathbf{x})-\langle v_j^R\rangle=\frac{v'_j(\mathbf{x})}{\langle R\rangle}-\frac{V_j\,R'(\mathbf{x})}{\langle R\rangle^2}+O\left[\max\left(\frac{\sigma_R^{\,2}}{\langle R\rangle^3},\frac{\sigma_Y^{\,2}}{\langle R\rangle^2}\right)\right] \tag{5.16}$$

where v'_j and $\mathbf{V}_j$ are the fluctuation and the mean of the jth component of the velocity field. Explicit expressions for $\mathbf{V}$ and $\mathbf{v}'$, correct to first order, can be found in the literature (Dagan, 1984; Rubin, 1990; Rubin and Dagan, 1992; Zhang and Neuman, 1992).

The first-order approximation of $v'_j(\mathbf{x})$ can be obtained by retaining the first-order term in the Taylor expansion of (5.13) (Dagan, 1984; 1989):

$$\nabla^2\phi=\mathbf{J}\cdot\nabla Y' \tag{5.17a}$$

$$v'_j(\mathbf{x})=\frac{\exp(\langle Y\rangle)}{\theta}\left[J_jY'(\mathbf{x})-\frac{\partial\phi(\mathbf{x})}{\partial x_j}\right] \tag{5.17b}$$

Using (5.16) and (5.17) we obtain the retarded velocity covariance $v_{jl}^R(\mathbf{x},\mathbf{x}')=v_{jl}^R(\mathbf{r})=\langle v'_j{}^R(\mathbf{x})\,v'_l{}^R(\mathbf{x}')\rangle$ (the separation vector is $\mathbf{r}=\mathbf{x}-\mathbf{x}'$):

$$v_{jl}^{R}(\mathbf{r})=\frac{V_j V_l}{\langle R\rangle^4}C_R(\mathbf{r})-\frac{V_j V_l}{\langle R\rangle^3}\left\{2C_{YR}(\mathbf{r})-\frac{1}{J_j}\frac{\partial}{\partial r_j}C_{R\phi}(\mathbf{r})+\frac{1}{J_l}\frac{\partial}{\partial r_l}C_{R\phi}(-\mathbf{r})\right\}$$
$$+\frac{1}{\langle R\rangle^2}v_{jl}(\mathbf{r})+\max\left[O\left(\frac{\sigma_R^{\,2}}{\langle R\rangle^3}\right)^2,O\left(\frac{\sigma_Y^{\,4}}{\langle R\rangle^2}\right)\right] \qquad (5.18)$$

where $C_{R\phi}$ is the cross covariance between R and ϕ and v_{jl} is the velocity covariance function for the nonreactive case. The symmetry condition $C_{YR}(-\mathbf{r})=C_{YR}(\mathbf{r})$ is also used in (5.18). Garabedian (1987) derived equivalent expressions in Fourier space, employing a linear relationship between $K_d(\mathbf{x})$ and $\ln(K(\mathbf{x}))$.

Expressions analogous to (5.15) and (5.17) containing also the terms $\langle \mathbf{v}'R'\rangle/\langle R\rangle^2$ and $\langle v_jR'\rangle\langle v_lR'\rangle/\langle R\rangle^4$ have been obtained by Kabala and Sposito (1991). The term $\langle \mathbf{v}'R'\rangle/\langle R\rangle^2$ is neglected in (5.15) because of order $\sigma_Y^2/\langle R\rangle^2$ which is larger than the first-order expression for $\mathbf{V}$ employed in (5.15). For the same reason the term $\langle v'_jR'\rangle\langle v_lR'\rangle/\langle R\rangle^4$ of order $\sigma_Y^4/\langle R\rangle^2$ is neglected analogously to the term neglected in the expression for $v_{jl}/\langle R\rangle^2$ employed in (5.18).

The cross covariance $C_{R\phi}(\mathbf{r})$ can be computed, using a Taylor expansion in R', as

Models A and B

$$C_{R\phi}(\mathbf{r})=\pm K_d^{\,G}\exp(\sigma_Y^2/2)\,C_{Y\phi}(\mathbf{r}) \qquad (5.19a)$$

Model C

$$C_{R\phi}(\mathbf{r})=0 \qquad (5.19b)$$

where the upper and the lower signs are valid respectively for positive and negative correlations (models A and B). With reference to the models A and B by using (5.19) and (5.I.1) (Appendix I), we obtain the expression for the retarded velocity covariance after dropping higher-order terms in (5.18):

$$v'^{R}_{jl}(\mathbf{r}) = \frac{v^{R}_{jl}(\mathbf{r})}{V^2}\langle R\rangle^2 = \frac{V_j V_l}{V^2}\left\{\frac{C_R(\mathbf{r})}{\langle R\rangle^2} - 2\frac{C_{YR}(\mathbf{r})}{\langle R\rangle} \mp \frac{K_d^G}{\langle R\rangle}\exp(\sigma_Y^2/2)T_{jl}(\mathbf{r})\right\} + v'_{jl}(\mathbf{r}) \tag{5.20}$$

where $V=|\mathbf{V}|$ is the magnitude of the expected value of the velocity and $v_{jl}'=v_{jl}/V^2$ is the dimensionless form of v_{jl}. The function $T_{jl}(\mathbf{r})$ assumes the expressions for a two-dimensional and a three-dimensional isotropic log conductivity field, respectively,

$$T_{jl}(\mathbf{r}) = \sigma_Y^2\left\{\frac{2}{r^2}[(1+r)\exp(-r)-1] - \frac{\mathbf{J}\cdot\mathbf{r}}{r^2}\left(\frac{r_j}{J_j}+\frac{r_l}{J_l}\right)\cdot\left(\frac{2}{r^2}[(1+r)\exp(-r)-1]+\exp(-r)\right)\right\} \tag{5.21}$$

$$T_{jl}(\mathbf{r}) = \sigma_Y^2\left\{\frac{2}{r^3}[-2+(2+r^2+2r)\exp(-r)] - \left(\frac{r_j}{J_j}+\frac{r_l}{J_l}\right)\frac{\mathbf{J}\cdot\mathbf{r}}{r^2}\cdot\left[\frac{3}{r^3}[-2+(2+r^2+2r)\exp(-r)]+\exp(-r)\right]\right\} \tag{5.22}$$

An equivalent expression, valid for the uncorrelated case is obtained by setting $C_{R\phi}=0$ in (5.18), i.e.,

$$v'^{R}_{jl}(\mathbf{r}) = \frac{v^{R}_{jl}}{V^2}\langle R\rangle^2 = \frac{V_j V_l}{\langle R\rangle^2}C_R(\mathbf{r}) + v'_{jl}(\mathbf{r}) \tag{5.23}$$

The computation of v_{jl} as obtained by Rubin (1990) is outlined in Appendix I.

Equations (5.20), (5.23) and (5.I.1) are valid for $J_1, J_2, J_3 \neq 0$, i.e. $\mathbf{V}=(V_1, V_2, V_3)$. Equivalent expressions, valid for mean velocity directed along x_1, can be obtained by performing the limit for J_j and $V_j=\exp(\langle Y\rangle)J_j/\theta$ ($j=2, 3$) tending to

zero. Since this can be made a posteriori directly on the analytical expression of v_{jl} and X_{jl}, in the following the more general assumption J_1, J_2, $J_3 \neq 0$ is implicitly assumed in expressions involving v_{jl} and X_{jl}.

The longitudinal component of the velocity covariance function in two-dimensional case can be obtained by setting $J_2 \to 0$ in (5.20):

$$v'^{R}_{11}(\mathbf{r}) = \frac{C_R(\mathbf{r})}{\langle R \rangle^2} - 2\frac{C_{YR}(\mathbf{r})}{\langle R \rangle} \mp \frac{K_d^G}{\langle R \rangle}\exp(\sigma_Y^2/2)T_{11}(\mathbf{r}) + v'_{11}(\mathbf{r}) \tag{5.24}$$

where

$$T_{11}(\mathbf{r}) = \frac{2\sigma_Y^2}{r^2}\left\{(1+r)\exp(-r) - 1 - r_1^2\left[\frac{2}{r^2}[(1+r)\exp(-r) - 1] + \exp(-r)\right]\right\} \tag{5.25}$$

The two other components are

$$v'^{R}_{12}(\mathbf{r}) = \pm\frac{K_d^G}{\langle R \rangle}\sigma_Y^2\exp(\sigma_Y^2/2)\frac{r_1 r_2}{r^2}\left\{\frac{2}{r^2}[(1+r)\exp(-r) - 1] + \exp(-r)\right\} + v'_{12}(\mathbf{r}) \tag{5.26a}$$

$$v'^{R}_{22}(\mathbf{r}) = v'_{22}(\mathbf{r}) \tag{5.26b}$$

We observe that along the transverse direction, v_{22}^R is influenced only by the mean value of the retardation factor $\langle R \rangle$, irrespective of both the type of covariance structure assumed and the fact that R is spatially variable.

The corresponding equations for the three-dimensional case are

$$v'^{R}_{11}(\mathbf{r}) = \frac{C_R(\mathbf{r})}{\langle R \rangle^2} - 2\frac{C_{YR}(\mathbf{r})}{\langle R \rangle} \mp \frac{K_d^G}{\langle R \rangle}\exp(\sigma_Y^2/2)T_{11}(\mathbf{r}) + v'_{11}(\mathbf{r}) \tag{5.27}$$

with

$$T_{11}(\mathbf{r}) = \sigma_Y^2 \left\{ \frac{2}{r^3}[-2 + (2 + r^2 + 2r)\exp(-r)] - \frac{2r_1^2}{r^2}\left[\frac{3}{r^3}[-2 + (2 + r^2 + 2r)\exp(-r)] + \exp(-r) \right] \right\} \tag{5.28}$$

and for the other components

$$v'_{12}{}^R(\mathbf{r}) = \pm \frac{K_d^G}{\langle R \rangle} \sigma_Y^2 \exp(\sigma_Y^2/2) \frac{r_1 r_2}{r^2} \cdot \left\{ \frac{3}{r^3}[-2 + (2 + r^2 + 2r)\exp(-r)] + \exp(-r) \right\} + v'_{12}(\mathbf{r}) \tag{5.29a}$$

$$v'_{21}{}^R(\mathbf{r}) = v'_{12}{}^R(\mathbf{r}) \tag{5.29b}$$

$$v'_{13}{}^R(\mathbf{r}) = \pm \frac{K_d^G}{\langle R \rangle} \sigma_Y^2 \exp(\sigma_Y^2/2) \frac{r_1 r_3}{r^2} \cdot \left\{ \frac{3}{r^3}[-2 + (2 + r^2 + 2r)\exp(-r)] + \exp(-r) \right\} + v'_{13}(\mathbf{r}) \tag{5.30}$$

$$v'_{31}{}^R(\mathbf{r}) = v'_{13}{}^R(\mathbf{r}) \tag{5.31a}$$

$$v'_{22}{}^R(\mathbf{r}) = v'_{22}(\mathbf{r}) \tag{5.31b}$$

$$v'_{33}{}^R(\mathbf{r}) = v'_{33}(\mathbf{r}) \tag{5.31c}$$

As in the two-dimensional model, we observe that along the transverse directions the covariances v'^{R}_{22} and v'^{R}_{33} do not depend on the spatial variability of $R(\mathbf{x})$, but rather on its mean value $\langle R\rangle$. Analogously, v'^{R}_{12} and v'^{R}_{13} are independent on C_R. For the uncorrelated model in the case of mean flow in the x_1 direction,

$$v'_{11}{}^{R}(\mathbf{r}) = \frac{C_R(\mathbf{r})}{\langle R\rangle^2} + v'_{11}(\mathbf{r}) \tag{5.32a}$$

$$v'_{12}{}^{R}(\mathbf{r}) = v'_{21}{}^{R}(\mathbf{r}) = v'_{12}(\mathbf{r}) \tag{5.32c}$$

$$v'_{13}{}^{R}(\mathbf{r}) = v'_{31}{}^{R}(\mathbf{r}) = v'_{13}(\mathbf{r}) \tag{5.32d}$$

We observe that $v'_{jj}{}^{R}(\mathbf{r})=v'_{jj}(\mathbf{r})$ for j=2,3. This means that the covariances v'^{R}_{22} and v'^{R}_{33} do not depend on the variability of $R(\mathbf{x})$ but only on its mean value $\langle R\rangle$.

For two- and three-dimensional isotropic log conductivity fields, the asymptotic behaviour of (5.20) for $\mathbf{r}\to 0$ assumes the form:
Two dimensions

$$v'_{jl}{}^{R}(0) = \frac{V_j V_l}{V^2}\left\{\frac{C_R(0)}{\langle R\rangle^2} - \frac{C_{YR}(0)}{\langle R\rangle}\right\} + v'_{jl}(0) \tag{5.33a}$$

Three dimensions

$$v'_{jl}{}^{R}(0) = \frac{V_j V_l}{V^2}\left\{\frac{C_R(0)}{\langle R\rangle^2} - \frac{4}{3}\frac{C_{YR}(0)}{\langle R\rangle}\right\} + v'_{jl}(0) \tag{5.33b}$$

for the models A and B, and

$$v'_{jl}{}^{R}(0) = \frac{V_j V_l}{V^2} \frac{C_R(0)}{\langle R \rangle^2} + v'_{jl}(0) \tag{5.34}$$

for the uncorrelated model in both two and three dimensions. For mean velocity along the x_1 direction, $v'_{jl}{}^{R}$ assumes the form

$$v'_{11}{}^{R}(0) = \frac{C_R(0)}{\langle R \rangle} - \frac{C_{YR}(0)}{\langle R \rangle} + \frac{3}{8}\sigma_Y{}^2 \tag{5.35a}$$

$$v'_{12}{}^{R}(0) = v'_{12}(0) = 0 \tag{5.35b}$$

$$v'_{22}{}^{R}(0) = \frac{1}{8}\sigma_Y{}^2 \tag{5.35c}$$

for a two-dimensional isotropic log conductivity field, and

$$v'_{11}{}^{R}(0) = \frac{C_R(0)}{\langle R \rangle} - \frac{4}{3}\frac{C_{YR}(0)}{\langle R \rangle} + \frac{8}{15}\sigma_Y{}^2 \tag{5.36a}$$

$$v'_{22}{}^{R}(0) = v'_{33}{}^{R}(0) = \frac{1}{15}\sigma_Y{}^2 \tag{5.36b}$$

with all the cross terms $v'_{ij}{}^{R}=0$, $i, j\neq 0$ for the three-dimensional case.

The corresponding relationships valid for the uncorrelated model can be obtained from (5.34) by setting the appropriate value of $v'_{jl}(0)$.

The relative importance of the chemical heterogeneity compared to the variability in the flow field can be evaluated by comparing the CV of R to the CV of v_1. The coefficient of variation of the longitudinal velocity $v_1(\mathbf{x})$ and retardation factor R are

$$\mathrm{CV}[v_1(\mathbf{x})] = \frac{(\sigma_{v_1}{}^2)^{1/2}}{V_1} \tag{5.37a}$$

$$\mathrm{CV}[R(\mathbf{x})] = \frac{K_d^G \exp(\sigma_W^2/2)[\exp(\sigma_W^2) - 1]^{1/2}}{1 + K_d^G \exp(\sigma_W^2/2)} \qquad (5.37b)$$

For homogeneous, isotropic and unbounded Y fields the linear analysis (Dagan, 1984, 1989; Rubin, 1990) yields $\sigma_{v_1}^2/V_1^2=(3/8)\sigma_Y^2$ for two-dimensional flow and $\sigma_{v_1}^2/V_1^2=(8/15)\sigma_Y^2$ for three dimensional flow.

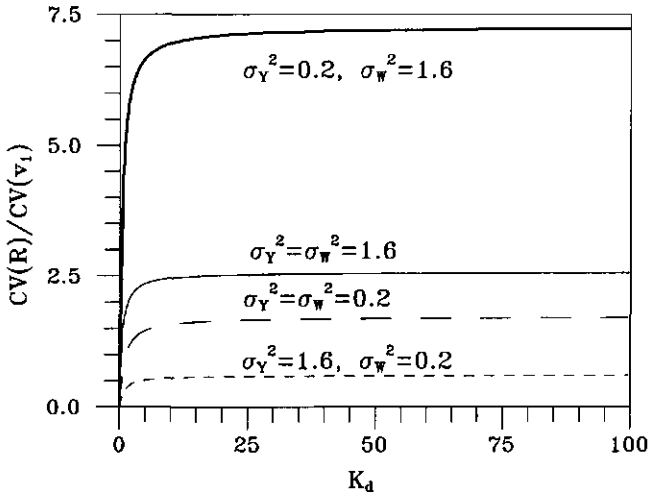

Figure 5.2 Ratio of CV of retardation factor and the longitudinal velocity for the two-dimensional isotropic case versus the average slope of isotherm K_d^G

As an example, Figure 5.2 shows $\mathrm{CV}(R)/\mathrm{CV}(v_1)$ for the model C and a two-dimensional isotropic Y field at different values of σ_Y^2 and σ_W^2. For $\sigma_Y^2 = \sigma_W^2$ the results are also applicable to models A and B in which $\mathrm{CV}(R)$ is obtained after substituting σ_W^2 by σ_Y^2 in (5.37). The most important conclusion that can be stated from inspection of Figure 5.2 is that at fixed σ_Y^2 and σ_W^2 values the physical heterogeneity dominates only for the smaller K_d^G values. The function $\mathrm{CV}(R)/\mathrm{CV}(v_1)$ is in fact an increasing function with limit for $K_d^G \to \infty$ equal to $(\exp(\sigma_W^2)-1)^{1/2}\, V_1/(\sigma_{v_1}^2)^{1/2}$. For $\sigma_Y^2 > \sigma_W^2$ a general trend that restricts the field in

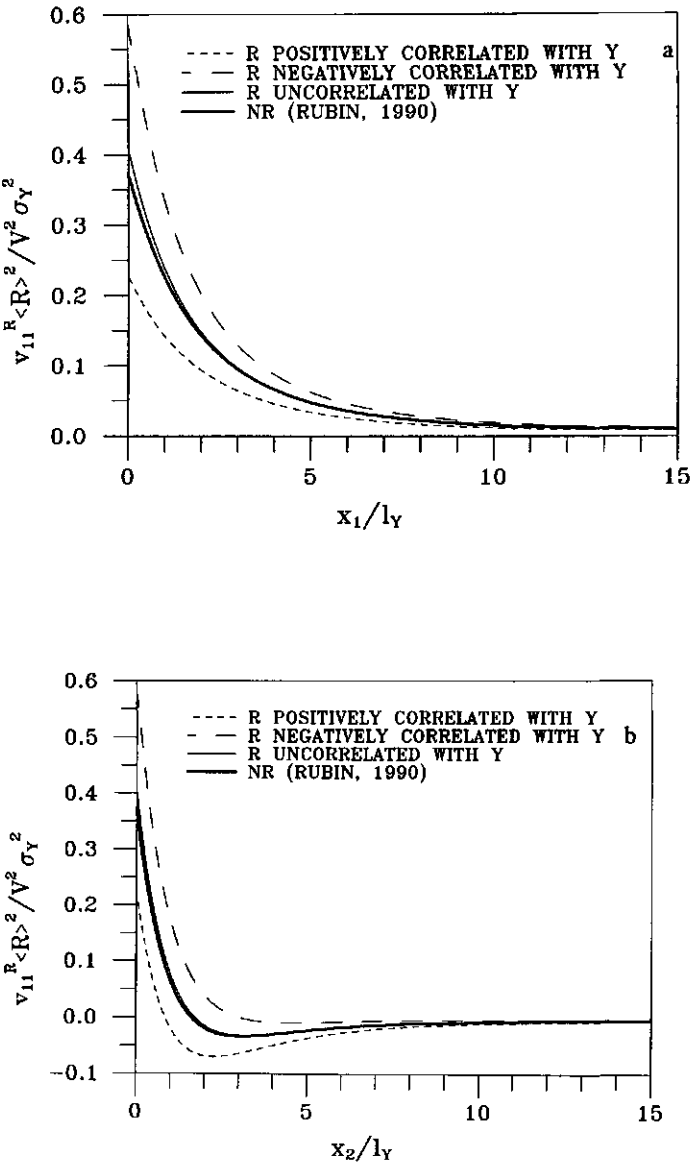

Figure 5.3 (*a*) Longitudinal velocity covariance function along the direction of the mean flow and (*b*) along the direction transverse to the mean flow ($\sigma_Y{}^2=\sigma_w{}^2=0.20$, $K_d{}^G=0.20$).

which the condition $CV(v_1) \geq CV(R)$ applies is observed. For models A and B, the condition $CV(R) > CV(v_1)$ is reached for any choice of σ_Y^2; in model C some restrictions apply. Specifically, the condition $CV(R) \geq CV(v_1)$ is not reached even at the asymptotic regime, i.e. $K_d^G \to \infty$ if $\sigma_W^2 < \ln(1+(\sigma_{v_1}^2/V_1^2))$. In this case ($\sigma_W^2 < \ln(1+(3/8)\sigma_Y^2)$ and $\ln(1+(8/15)\sigma_Y^2)$ respectively for the two- and three-dimensional isotropic cases), physical heterogeneity dominates for each value of K_d^G. In conclusion, while for models A and B either physical or chemical heterogeneities can dominate depending on K_d^G, for model C the physical heterogeneity dominates irrespectively of the K_d^G value if σ_W^2 is smaller than $\ln(1+\sigma_{v_1}^2/v_1^2)$.

As an example, the two-dimensional covariance v'^R_{11} along the x_1 and x_2-directions, together with the corresponding covariance valid for nonreactive solutes, is shown in Figure 5.3 for $K_d^G=0.20$ and $\sigma_Y^2=\sigma_W^2=0.20$. Even for small values of K_d^G the impact of the retardation factor on the covariance structure of the velocity field is remarkable. Negative correlations results in an increase of v'^R_{11} over the nonreactive case in both x_1 and x_2 directions and consequently in an increase of the retarded velocity correlation length. A perfect positive correlation leads to opposite results. This can be physically explained when we consider that the flow is channelized into the high-conductivity zones. The spreading will be enhanced or reduced if in these zones the retardation is small or large, respectively. Model C causes a relatively smaller increase of v'^R_{11} over the nonreactive case suggesting a smaller impact on transport when equivalent degrees of heterogeneity for R and v_1 are employed. However the change of v'^R_{11} introduced by model C is not negligible and it turns out that for large K_d^G, v'^R_{11} departs considerably from v'_{11} (equations (5.20), (5.35) and (5.36)).

5.4 Eulerian-Lagrangian analysis of reactive transport

The concentration distribution in the Eulerian form of (5.4) due to the motion of a particle of mass $dM=C_0 d\mathbf{a}$ injected at the time $t=0$ in the position $\mathbf{x}=\mathbf{a}$ is described by the equivalent Lagrangian formulation (Taylor, 1921; Dagan, 1989):

$$dC(\mathbf{x},\ t;\ \mathbf{a}) = \frac{dM}{\theta}\delta[\mathbf{x} - \mathbf{X}_t^R(t;\ \mathbf{a})] \tag{5.38}$$

where $\mathbf{X}_t^R$ represents the Lagrangian coordinates of the particle originated at the position $\mathbf{a}$ at time t=0 and δ denotes the Dirac distribution. The vector $\mathbf{X}_t^R$ can be written as

$$\mathbf{X}_t^R(t;\ \mathbf{a}) = \mathbf{X}^R(t,\ \mathbf{a}) + \mathbf{X}_d(t) \tag{5.39}$$

where $\mathbf{X}_d$ is a Brownian motion displacement associated with an underlying isotropic pore scale dispersion process (e.g., Dagan, 1989). Since the spatial variability of $R(\mathbf{x})$ and $Y(\mathbf{x})$ takes place over scales larger than the characteristic pore scale dimension, $\mathbf{X}_d$ may be assumed as statistically independent of both R and Y. The trajectory $\mathbf{X}^R(t, \mathbf{a})$ reflects the combined effects of the heterogeneity of the velocity field, and the spatial variability of the retardation factor.

For a steady flow $\mathbf{X}^R$, assumes the following form:

$$\mathbf{X}^R(t;\ \mathbf{a}) = \mathbf{a} + \int_0^t \mathbf{v}^R[\mathbf{X}_t^R(\tau,\ \mathbf{a})]d\tau = \mathbf{a} + \frac{\mathbf{V}}{\langle R\rangle}\ t + \frac{1}{\langle R\rangle}\int_0^t \left\{ \mathbf{v}'[\mathbf{X}_t(\tau,\ \mathbf{a})] - \frac{\mathbf{V}}{\langle R\rangle}R'[\mathbf{X}_t^R(\tau,\ \mathbf{a})]\right\} d\tau \tag{5.40}$$

Upon validity of ergodic assumptions (Dagan, 1990), the statistical representation relies on the description of moments. Usually this description is limited to the first two moments, i.e. the mean $\langle \mathbf{X}^R\rangle$ and the covariance X_{jl}^R. The expected value of the trajectory is obtained from (5.40) by averaging as

$$\langle \mathbf{X}^R(t)\rangle = \mathbf{a} + \mathbf{V}t/\langle R\rangle \tag{5.41}$$

The total particle displacement covariance $X_{t,jl}^R$ is given by the following expression:

$$X_{t,\ jl}^R(t) = X_{jl}^R(t) + X_{d,\ jl} \tag{5.42}$$

where $X_{d,jl}$ represents the pore scale dispersion effect and X_{jl}^R denotes the effect of physical and chemical heterogeneities:

$$X_{jl}^{R}(t) = 2\int_0^t (t-\tau) v_{jl}^{R}[\langle \mathbf{X}^{R}(\tau)\rangle]\, d\tau \tag{5.43}$$

Notice that, in accordance with Dagan's theory (1984), the covariance samples the mean trajectory $\langle \mathbf{X}^R \rangle$ rather than the actual trajectory. This approximation proves to be reasonable (from numerical experimentation on passive solute transport) for $\sigma_Y^2 \leq 1.6$ (Bellin *et al.* 1992).

Substitution of (5.20) into (5.43) and integration with respect to time yields for models A and B the final expression of X_{jl}^R valid for a two-dimensional isotropic log conductivity field:

$$X'^{R}_{jl}(t') = \frac{2V_jV_l}{V^2}\left(\frac{K_d^G}{\langle R\rangle}\right)^2 \exp(\sigma_Y^2)\{[Ei(\sigma_Y^2) - \gamma - \ln(\sigma_Y^2)]t'$$

$$+ \sum_{m=1}^{\infty} \frac{(\sigma_Y^2)^m}{m^2 m!}\exp(-mt') - \sum_{m=1}^{\infty} \frac{(\sigma_Y^2)^m}{m^2 m!}\} \mp \frac{2V_jV_l}{V^2}\frac{K_d^G}{\langle R\rangle}\sigma_Y^2 \exp(\sigma_Y^2/2)$$

$$\cdot\{2[\exp(-t') + \ln(t') - Ei(-t') + \gamma - 1]$$

$$-\left(\frac{V_j}{J_j} + \frac{V_l}{J_l}\right)\frac{\mathbf{J}\cdot\mathbf{V}}{V^2}[-t' + 2\ln(t') - 2Ei(-t') + 2\gamma - 1 + \exp(-t')]\} + X'_{jl}(t') \tag{5.44}$$

The corresponding expression valid for the uncorrelated model is

$$X'^{R}_{jl}(t') = \frac{X_{jl}^{R}(t)}{l_Y^2} = \frac{2V_jV_l}{V^2}\left(\frac{K_d^G}{\langle R\rangle}\right)^2 \exp(\sigma_W^2)\left(\frac{l_W}{l_Y}\right)^2$$

$$\cdot\left\{\frac{l_Y}{l_W}[Ei(\sigma_W^2) - \gamma - \ln(\sigma_W^2)]t' + \sum_{m=1}^{\infty}\frac{(\sigma_W^2)^m}{m^2 m!}\right.$$

$$\left.\cdot \exp\left[-m\frac{l_Y}{l_W}t'\right] - \sum_{m=1}^{\infty}\frac{(\sigma_W^2)^m}{m^2 m!}\right\} + X'_{jl}(t') \tag{5.45}$$

$$j,\ l = 1,\ 2$$

In (5.45) $t'=tV/\langle R\rangle l_Y$ and $X'_{jl}=X_{jl}/l_Y^2$ are the dimensionless time and displacement covariance function respectively. The presence of $m!$ in the denominator of the series in (5.45) assures their uniform and fast convergence and allows rapid calculation of the infinite sums (for $\sigma_W^2=0.20$ and $t'=0$ the ratio of the fifth to the first term is $O(10^{-7})$).

Analogous expressions can be derived for the three-dimensional case:

$$X'_{jl}(t') = \frac{2V_jV_l}{V^2}\left(\frac{K_d^G}{\langle R\rangle}\right)^2 \exp(\sigma_Y^2)\{[Ei(\sigma_Y^2)-\gamma-\ln(\sigma_Y^2)]t' + \sum_{m=1}^{\infty}\frac{(\sigma_Y^2)^m}{m^2m!}\exp(-mt') - \sum_{m=1}^{\infty}\frac{(\sigma_Y^2)^m}{m^2m!}\} \pm \frac{2V_jV_l}{V^2}\frac{K_d^G}{\langle R\rangle}\sigma_Y^2\exp(\sigma_Y^2/2) \cdot \left\{\left[\frac{3\mathbf{J}\cdot\mathbf{V}}{V^2}\left(\frac{V_j}{J_j}+\frac{V_l}{J_l}\right)-2\right]\left[-\frac{t'}{2}+1+\frac{1}{t'}(\exp(-t')-1)\right] + \left(\frac{V_j}{J_j}+\frac{V_l}{J_l}\right)\frac{\mathbf{J}\cdot\mathbf{V}}{V^2}[\exp(-t')+t'-1]-2[\exp(-t')+t'-1]\right\} + X'_{jl}(t') \quad (5.46)$$

for the models A and B. In the uncorrelated case, equation (5.45), with the suitable three-dimensional expression for X'_{jl}, applies.

The limits for small and large t' are discussed in Appendix II. As for the nonreactive case (Dagan, 1989), X_{jl} grows as t'^2 and t' for small and large t', respectively. For models A and B the dispersion coefficient, defined as $D'_{jl}=0.5\mathrm{d}X'_{jl}(t')/\mathrm{d}t'$, assumes for large t' the forms

$$D'^{\,R}_{jl}(t') = \frac{V_jV_l}{V^2}\left[\frac{C_R(0)}{\langle R\rangle^2}\frac{l_R}{l_Y} - \frac{C_{YR}(0)}{\langle R\rangle}\left(\frac{V_j}{J_j}+\frac{V_l}{J_l}\right)\frac{\mathbf{J}\cdot\mathbf{V}}{V^2}\right] + \frac{1}{2}\frac{dX'_{jl}(t')}{dt'}\Bigg|_{t'\gg 1} \qquad t'\gg 1 \quad (5.47)$$

$$D'^{R}_{jl}(t') = \frac{V_j V_l}{V^2}\left\{\frac{C_R(0)}{\langle R\rangle^2}\frac{l_R}{l_Y} - \frac{C_{YR}(0)}{\langle R\rangle}\cdot\left[1+0.5\frac{\mathbf{J}\cdot\mathbf{V}}{V^2}\left(\frac{V_j}{J_j}+\frac{V_l}{J_l}\right)\right]\right\} + \frac{1}{2}\frac{dX'_{jl}(t')}{dt'}\bigg|_{t'\gg 1} \qquad t'\gg 1 \tag{5.48}$$

for the two- and three-dimensional cases, respectively.

The dispersion coefficient reaches for large t' a constant asymptotic value which is larger or smaller than the corresponding value for the nonreactive case depending on whether model B or A is chosen. Model C is characterized by an increase of the dispersion coefficient over the corresponding value for the nonreactive case:

$$D'^{R}_{jl}(t') = \frac{V_j V_l}{V^2}\frac{C_R(0)}{\langle R\rangle^2}\frac{l_R}{l_Y} + \frac{1}{2}\frac{dX'_{jl}(t')}{dt'}\bigg|_{t'\gg 1} \qquad t'\gg 1 \tag{5.49}$$

As an example and without lack of generality we consider the case where the mean velocity is directed along the x_1 direction, i.e. $\mathbf{V}=(V, 0)$ for a two-dimensional flow domain. The general expression for the displacement covariances (5.44) yields, for the models A and B

$$X'^{R}_{11}(t') = 2\left(\frac{K_d^G}{\langle R\rangle}\right)^2 \exp(\sigma_Y^2)\{[Ei(\sigma_Y^2)-\gamma-\ln(\sigma_Y^2)]t' + \sum_{m=1}^{\infty}\frac{(\sigma_Y^2)^m}{m^2 m!}\exp(-mt') - \sum_{m=1}^{\infty}\frac{(\sigma_Y^2)^m}{m^2 m!}\} \mp \frac{4K_d^G}{\langle R\rangle}\sigma_Y^2\exp(\sigma_Y^2/2)$$
$$\cdot\{t'-\ln(t')+Ei(-t')-\gamma\} + \sigma_Y^2\{2t'-3\ln(t')+(3/2) - 3\gamma + 3\left[Ei(-t') + \frac{\exp(-t')(1+t')-1}{t'^2}\right]\} \tag{5.50}$$

and for the uncorrelated model,

$$X'_{11}{}^{R}(t') = 2\left(\frac{K_d^G}{\langle R\rangle}\right)^2 \exp(\sigma_W{}^2)\left(\frac{l_W}{l_Y}\right)^2 \left\{\frac{l_Y}{l_W}[Ei(\sigma_W{}^2) - \gamma - \ln(\sigma_W{}^2)]t' + \sum_{m=1}^{\infty}\frac{(\sigma_W{}^2)^m}{m^2 m!}\exp\left[-m\frac{l_Y}{l_W}t'\right] - \sum_{m=1}^{\infty}\frac{(\sigma_W{}^2)^m}{m^2 m!}\right\}$$
$$+\sigma_Y{}^2\left\{2t' - 3\ln(t') + (3/2) - 3\gamma + 3\left[Ei(-t') + \frac{\exp(-t')(1+t') - 1}{t'^{\,2}}\right]\right\} \quad (5.51)$$

For all models A to C the transverse second moment is given by

$$X'_{22}{}^{R}(t') = X'_{22}(t') = \sigma_Y{}^2\{\ln(t') - (3/2) + \gamma - Ei(-t') + 3\left[\frac{1}{t'^{\,2}} - \frac{\exp(-t')(1+t')}{t'^{\,2}}\right]\} \quad (5.52)$$

For $K_d^G \to 0$ (5.50) and (5.51) reduce to Dagan's (1984) solution for nonreactive solutes. From (5.52) we also observe that along the direction transverse to the mean flow the behaviour of the second moments X'^{R}_{22} does not change with respect to the nonreactive case. In fact, this moment can be computed by rescaling time as $t^R = t/\langle R\rangle$ in the passive solute solution. The modification of the second moment X_{11} mainly depends on the square of the ratio of K_d^G and $\langle R\rangle$ and on $\sigma_W{}^2$ ($\sigma_Y{}^2$ for the models A and B). Observing that for $\sigma_W{}^2$ constant the ratio $K_d^G/\langle R\rangle$ tends rapidly to its asymptotic constant value, we conclude that beyond a certain value any increase in K_d^G affects dispersing plumes only by mean retardation. This effect is magnified by large values of K_d^G.

In conclusion, the spatial variability of the retardation coefficient affects only the longitudinal dispersion. This result is also suggested from field experiments (e.g., Mackay *et al.*, 1986*a*, Garabedian, 1987, Garabedian *et al.*, 1988).

The limit behaviour of (5.50), (5.51), and (5.52) (see appendix II) is

$$X'_{11}{}^{R}(t') = \left\{ \frac{C_R(0)}{\langle R \rangle^2} - \frac{C_{YR}(0)}{\langle R \rangle} + \frac{3}{8}\sigma_Y^2 \right\} t'^{\,2} + O(t'^{\,3}) \qquad t' \ll 1 \tag{5.53}$$

$$X'_{22}{}^{R}(t') = \frac{1}{8}\sigma_Y^2 t'^{\,2} + O(t'^{\,3}) \qquad t' \ll 1 \tag{5.54}$$

$$X'_{11}{}^{R}(t') = 2\left\{ \frac{l_R}{l_Y} \frac{C_R(0)}{\langle R \rangle^2} - 2\frac{C_{YR}(0)}{\langle R \rangle} + \sigma_Y^2 \right\} t' + \left\{ 4\frac{C_{YR}(0)}{\langle R \rangle} - 3\sigma_Y^2 \right\} \ln(t')$$

$$+ \left\{ \sigma_Y^2 \left[\frac{3}{2} - 3\gamma \right] + 4\gamma \frac{C_{YR}(0)}{\langle R \rangle} - 2\frac{C_R(0)}{\langle R \rangle^2 (\exp(\sigma_Y^2) - 1)} \sum_{m=1}^{\infty} \frac{(\sigma_Y^2)^m}{m^2 m!} \right\} \qquad t' \gg 1 \tag{5.55}$$

$$X'_{22}{}^{R}(t') = \sigma_Y^2 [\ln(t') + 0.933] \qquad t' \gg 1 \tag{5.56}$$

The asymptotic behaviour for the uncorrelated case follows from these equations by setting $C_{YR}=0$ and by substitution of σ_Y^2 with σ_W^2 from (5.II.3), (5.II.4), (5.II.6), and (5.II.8). We notice again that the chemical reaction affects the transverse form of the plume only by a constant reduction factor $\langle R \rangle^2$ which corresponds to rescaling the time by $t^R = t/\langle R \rangle$ (see equations (5.54), (5.56)).

The time evolution of the dimensionless second moment $X'_{11}(t')$ with $K_d^G = 0.20$ and $\sigma_Y^2 = \sigma_W^2 = 0.20$ for a two-dimensional isotropic random field is shown in Figure 5.4*a*. The uncorrelated case is close to Dagan's (1984) solution for passive solute. For the models A and B we observe large differences of opposite effects between the uncorrelated and the nonreactive cases. It seems possible to conclude that for small values of $\sigma_Y^2/\langle R \rangle^2$ and $\sigma_R^2/\langle R \rangle^3$, although the impact of model C cannot be neglected, the foremost impact on the behaviour of the plume moments is caused by the interaction between $\mathbf{v}'$ and R' which is absent in the uncorrelated case. For $(\sigma_R^2/\langle R \rangle) < \sigma_Y^2$ the proposed linear solution is of $O(\sigma_Y^2/\langle R \rangle^2)$,

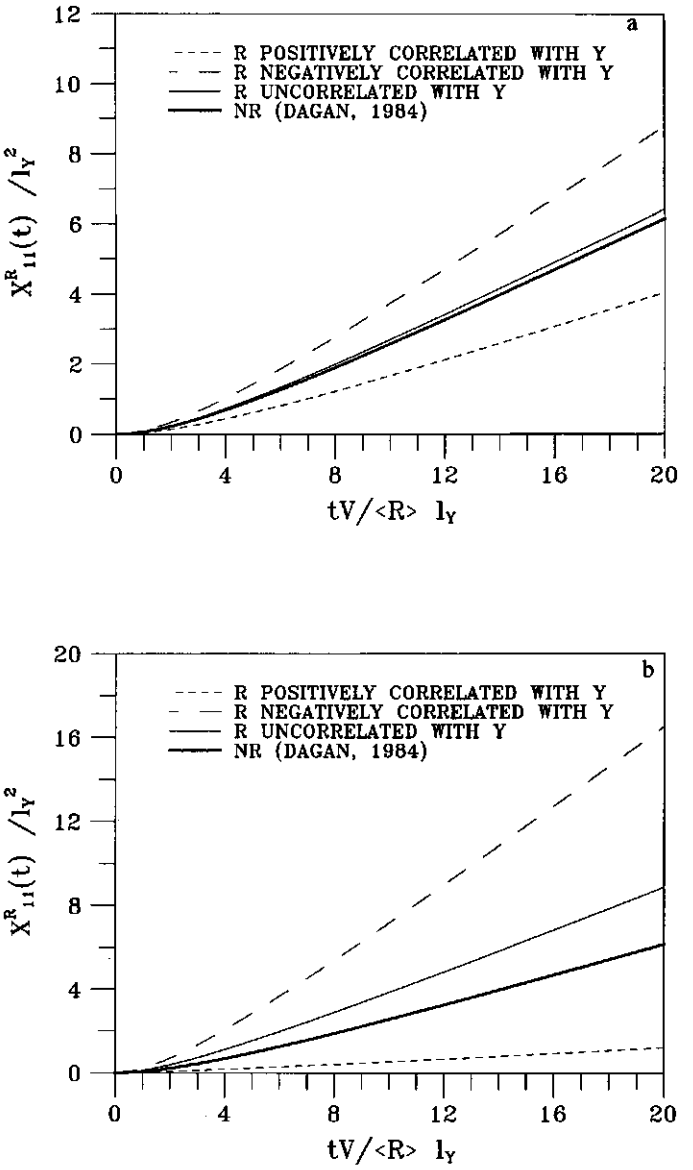

Figure 5.4 Variance of longitudinal displacements (5.50) and (5.51) for the different cases; (*a*) $\sigma_Y^2=\sigma_W^2=0.20$ and $K_d^G=0.20$; (*b*) as in (*a*) with $K_d^G=1.26$.

i.e. it is dominated by the order of approximation of the velocity field. When $(\sigma_R^2/\langle R\rangle)>\sigma_Y^2$, the solution is of $O(\sigma_R^2/\langle R\rangle^3)$. Figure 5.4*b* illustrates the impact of larger K_d^G values on $X'_{11}(t)$ (K_d^G=1.26, corresponding to the case in which CV(R) is equal to or greater than CV(v_1)). We observe that for the case discussed the value of $\sigma_R^2/\langle R\rangle^3$ is 0.03. From Figures 5.4*a* and 5.4*b* we conclude that when CV(R)≤CV(v_1) the model C shows a smaller impact on X_{11} than the models A and B. This impact, however, depends on σ_W^2 and K_d^G and in some cases it has a considerable effect on the longitudinal dispersion. In fact, for solutes characterized by large K_d^G the increase of X_{11} can be large even for small σ_W^2 (Figure 5.4*b*). A full set of numerical experiments is given in part 2 of this two paper series (Bosma *et al.*, 1993).

5.5 Conclusions

The following conclusions are worth mentioning:

1. A first-order analytical solution of transport in heterogeneous porous formations has been obtained. The innovation is the incorporation of chemical heterogeneity in addition to the physical heterogeneity embedded in classic solutions available in the literature. The retardation factor has been assumed to model this class of reactive transport processes, i.e. travel times are much larger than the times characteristic of reaction rates.

2. Chemical and physical heterogeneities are assumed as random space functions with assigned correlation structure. The random fields are either mutually correlated or uncorrelated. Two common models of perfect correlation are considered as an example.

3. The analytical solution for the variances of the retarded plumes shows that heterogeneous retardation has often a large impact on longitudinal spreading. Transverse variances are unaffected by the heterogeneity of retardation. The present results allow for a possible explanation of experimental results where very elongated plumes for retarded transport are observed. They also allow inference of the type of correlation between retardation factor and permeability by comparing field results of longitudinal variances, given the major impact that the type of functional dependence shows on the outcome of the transport process.

5.6 Appendix I

The velocity covariance function $v_{ji}(\mathbf{r})$ in (5.20) and (5.23) was obtained using the first-order approximation by Dagan (1984) and Rubin (1990) in the form

$$v_{ji}(\mathbf{r}) = \frac{\exp(2\langle Y\rangle)}{\theta^2}\left\{J_j J_i C_Y(\mathbf{r}) - J_j \frac{\partial}{\partial r_i} C_{Y\phi}(-\mathbf{r}) + J_i \frac{\partial}{\partial r_j} C_{Y\phi}(\mathbf{r}) - \frac{\partial^2}{\partial r_j\, \partial r_i}\Gamma(\mathbf{r})\right\} \qquad (5.I.1)$$

where $\Gamma(\mathbf{r})=\sigma_\phi^2-C_\phi(\mathbf{r})$ is the variogram of the stationary head fluctuations.

For a two-dimensional isotropic log conductivity field with exponential covariance structure C_Y, $C_{Y\phi}$ and Γ assume the following expressions:

$$C_{Y\phi}(\mathbf{r}) = \sigma_Y^2 \frac{\mathbf{J}\cdot\mathbf{r}}{r^2}[(1+r)\exp(-r)-1] \qquad (5.I.2)$$

$$\Gamma(\mathbf{r}) = \tfrac{1}{2}\sigma_Y^2 |\mathbf{J}|^2\left\{\left[2\frac{(\mathbf{J}\cdot\mathbf{r})^2}{|\mathbf{J}|^2 r^2}-1\right]\left[\frac{1}{2}+\frac{\exp(-r)(r^2+3r+3)-3}{r^2}\right]\right.$$
$$\left. -Ei(-r)+\ln r+\exp(-r)-0.4228\right\} \qquad (5.I.3)$$

where $r=|\mathbf{r}|/l_Y$. In (5.I.2) and (5.I.3), $C_{Y\phi}$ and Γ are made dimensionless by l_Y and l_Y^2.

For a three-dimensional isotropic log conductivity field the cross covariance and the piezometric head variogram are, respectively,

$$C_{Y\phi}(\mathbf{r}) = \sigma_Y^2 \frac{\mathbf{J}\cdot\mathbf{r}}{r^3}[(r^2+2r+2)\exp(-r)-2] \qquad (5.I.4)$$

and

$$\Gamma(\mathbf{r}) = |\mathbf{J}|^2\sigma_Y^2\left\{\frac{1}{3}-\frac{1}{r^3}[-4+r^2+\exp(-r)(4+4r+r^2)]\right.$$
$$\left. +\frac{(\mathbf{J}\cdot\mathbf{r})^2}{r^5\, J^2}\exp(-r)[12-12\exp(r)+12r+5r^2+r^2\exp(r)+r^3]\right\} \qquad (5.I.5)$$

The solution of (5.I.1), valid for a two-dimensional isotropic log conductivity field with mean velocity directed along x_1, has been proposed by Rubin (1990), and we refer to his paper for the details of the analytical expression. The general expression for a three-dimensional anisotropic fields has been derived by Rubin and Dagan (1992).

5.7 Appendix II

The limits for small and large t' (e.g., $t'\ll 1$ and $t'\gg 1$) assume for the two-dimensional case the following form:

$$X'^{R}_{jl}(t') = \frac{V_j V_l}{V^2}\left\{\frac{C_R(0)}{\langle R\rangle^2} - \frac{C_{YR}(0)}{\langle R\rangle}\right\} t'^{2} + X'_{jl}(t')\big|_{t'\ll 1} + O(t'^{3}) \qquad t'\ll 1 \qquad (5.\text{II}.1)$$

$$\begin{aligned} X'^{R}_{jl}(t') = \frac{2V_j V_l}{V^2}\Bigg\{ & \left[\frac{C_R(0)}{\langle R\rangle^2}\frac{l_R}{l_Y} - \frac{C_{YR}(0)}{\langle R\rangle}\left(\frac{V_j}{J_j}+\frac{V_l}{J_l}\right)\frac{\mathbf{J}\cdot\mathbf{V}}{V^2}\right] t' \\ & - \frac{2C_{YR}(0)}{\langle R\rangle}\left[1-\left(\frac{V_j}{J_j}+\frac{V_l}{J_l}\right)\frac{\mathbf{V}\cdot\mathbf{J}}{V^2}\right]\ln(t') \\ & - \frac{1}{\exp(\sigma_Y^2)-1}\frac{C_R(0)}{\langle R\rangle^2}\sum_{m=1}^{\infty}\frac{(\sigma_Y^2)^m}{m^2 m!} - \frac{C_{YR}(0)}{\langle R\rangle} \\ & \cdot\left[2\gamma - 2 - \left(\frac{V_j}{J_j}+\frac{V_l}{J_l}\right)\frac{\mathbf{V}\cdot\mathbf{J}}{V^2}(2\gamma-1)\right]\Bigg\} + X'_{jl}(t')\big|_{t'\gg 1} \qquad t'\gg 1 \end{aligned} \qquad (5.\text{II}.2)$$

valid for the models A and B and

$$X'^{R}_{jl}(t') = \frac{V_j V_l}{V^2}\frac{C_R(0)}{\langle R\rangle^2} t'^{2} + X'_{jl}(t')\big|_{t'\ll 1} + O(t^3) \qquad t'\ll 1 \qquad (5.\text{II}.3)$$

$$\begin{aligned} X'^{R}_{jl}(t') = \frac{2V_j V_l}{V^2}\Bigg\{ & \frac{C_R(0)}{\langle R\rangle^2}\frac{l_R}{l_Y}t' - \left(\frac{l_W}{l_Y}\right)^2 \frac{1}{\exp(\sigma_W^2)-1} \\ & \cdot \frac{C_R(0)}{\langle R\rangle^2}\sum_{m=1}^{\infty}\frac{(\sigma_W^2)^m}{m^2 m!}\Bigg\} + X'_{jl}(t')\big|_{t'\gg 1} \qquad t'\gg 1 \end{aligned} \qquad (5.\text{II}.4)$$

for the uncorrelated model. Here l_R and $C_R(0)=\sigma_R^2$ are respectively the integral scale and the variance of the retardation factor.

Correspondingly for the three-dimensional case we obtain

$$X'^{R}_{jl}(t') = \frac{V_j V_l}{V^2}\left\{\frac{C_R(0)}{\langle R\rangle^2} - \frac{4}{3}\frac{C_{YR}(0)}{\langle R\rangle}\right\} t'^{\,2} + X'_{jl}(t')\big|_{t'\ll 1} + O(t'^{\,3}) \qquad t' \ll 1 \tag{5.II.5}$$

for the models A and B, and

$$X'^{R}_{jl}(t') = \frac{V_j V_l}{V^2}\frac{C_R(0)}{\langle R\rangle^2} t'^{\,2} + X'_{jl}(t')\big|_{t'\ll 1} + O(t'^{\,3}) \qquad t' \ll 1 \tag{5.II.6}$$

for the uncorrelated model.

The limit for $t' \gg 1$ of (5.46) and (5.45) result in

$$X'^{R}_{jl}(t') = \frac{2V_j V_l}{V^2}\left\{\left[\frac{C_R(0)}{\langle R\rangle^2}\frac{l_R}{l_Y} - \frac{C_{YR}(0)}{\langle R\rangle}\left[1 + 0.5\frac{\mathbf{J}\cdot\mathbf{V}}{V^2}\left(\frac{V_j}{J_j} + \frac{V_l}{J_l}\right)\right]\right] t' \right.$$
$$\left. - \frac{C_R(0)}{\langle R\rangle^2}\frac{1}{\exp(\sigma_Y^2) - 1}\sum_{m=1}^{\infty}\frac{(\sigma_Y^2)^m}{m^2 m!} + \frac{2C_{YR}(0)}{\langle R\rangle}\frac{\mathbf{J}\cdot\mathbf{V}}{V^2}\left(\frac{V_j}{J_j} + \frac{V_l}{J_l}\right)\right\} + X'_{jl}(t')\big|_{t'\gg 1} \qquad t' \gg 1 \tag{5.II.7}$$

for the models A and B, and

$$X'^{R}_{jl}(t') = \frac{2V_j V_l}{V^2}\left\{\frac{C_R(0)}{\langle R\rangle^2}\frac{l_R}{l_Y} t' - \left[\frac{C_R(0)}{\langle R\rangle^2}\frac{1}{\exp(\sigma_W^2) - 1}\sum_{m=1}^{\infty}\frac{(\sigma_W^2)^m}{m^2 m!}\right]\right\} + X'_{jl}(t')\big|_{t'\gg 1} \qquad t' \gg 1 \tag{5.II.8}$$

for the model C. Both the two- and three-dimensional models show the same type of variability for small and large t'. This is in agreement with the asymptotic expressions developed by Dagan (1984) for the nonreactive case.

Notation

a	particle injection coordinate (L)
C	concentration of solute in aqueous phase (ML^{-3})
C^*	concentration of solute in solid phase (ML^{-3})
CV	coefficient of variation
C_R	covariance function of the retardation factor
C_Y	covariance function of hydraulic log conductivity
$C_{R\Phi}$	cross covariance function of the retardation factor R and hydraulic head Φ

C_{YR}	cross covariance function of hydraulic log conductivity and retardation factor R
$C_{Y\Phi}$	cross covariance function of hydraulic log conductivity and hydraulic head Φ (L)
C_0	solute concentration of the injected particle (ML^{-3})
$\mathbf{D}_d$	tensor of pore scale dispersion (L^2T^{-1})
dM	mass of solute particle (M)
δ	Dirac distribution
da	volume of the particle (L^3)
dC	solute concentration of the particle (ML^{-3})
Ei	exponential integral
Φ	hydraulic head (L)
ϕ	fluctuation around the mean of the hydraulic head (L)
γ	Euler's constant
$\mathbf{J}$	mean head gradient
K_r	reverse reaction rate coefficient (T^{-1})
K_d	slope of the isotherm that regulate the chemical exchange
K_H	hydraulic conductivity (LT^{-1})
K_d^G	geometrical mean of $K_d(\mathbf{x})$
l_Y	integral scale of the hydraulic log conductivity (L)
l_R	integral scale of the retardation factor (L)
l_W	integral scale of the auxiliary function used for the uncorrelated case
n	coefficient of chemical exchange
$\mathbf{r}$	dimensionless spatial lag
r	modulus of the dimensionless spatial lag
R	retardation factor
R'	fluctuation around the mean of the retardation factor
$\langle R \rangle$	mean of the retardation factor
σ_Y^2	variance of the hydraulic log conductivity
σ_R^2	variance of the retardation factor
σ_W^2	variance of the auxiliary function used for the uncorrelated case
t	time (T)
t'	dimensionless time
$\mathbf{v}$	velocity (LT^{-1})
$\mathbf{V}$	mean velocity (LT^{-1})
$\mathbf{v}'$	fluctuation around the mean of the velocity (LT^{-1})
$\mathbf{v}^R$	retarded velocity (LT^{-1})
v_{jl}	velocity covariance tensor (L^2T^{-2})
v'_{jl}	dimensionless velocity covariance tensor
v_{jl}^R	retarded velocity covariance tensor (L^2T^{-2})
v'^R_{jl}	dimensionless retarded velocity covariance tensor
W	auxiliary function used for the uncorrelated model
$\mathbf{x}$	space coordinate (L)
$\mathbf{X}_d$	Brownian motion displacement (L)
$\langle \mathbf{X}^R \rangle$	mean retarded trajectory of the particle (L)

X^R_{jl}	covariance tensor of the residual displacements (L^2)
$X_{d,jl}$	covariance tensor of the Brownian motion displacement (L^2)
$X^R_{t,jl}$	covariance tensor of the total residual displacements (L^2)
Y	hydraulic log conductivity
$\langle Y \rangle$	mean hydraulic log conductivity
Y'	fluctuation around the mean of the hydraulic log conductivity
θ	formation porosity
∇	gradient operator
$\nabla\cdot$	divergence operator
∂	partial derivative operator

References

Abriola, L.M., Modeling contaminant transport in the subsurface: An interdisciplinary challenge, Rev. Geophys., 25, 125-134, 1987.

Ball, W.P., and P.V. Roberts, Long term sorption of halogenated organic chemicals by aquifer material, 1, Equilibrium, Environ. Sci. Technol., 25, 1223-1236, 1991.

Barry D.A., J. Coves, and G. Sposito, On the Dagan model of solute transport in groundwater: Application to the Borden site, Water Resour. Res., 24, 1805-1817, 1988.

Bellin A., P. Salandin, and R. Rinaldo, Simulation of dispersion in heterogeneous porous formations: Statistics, first-order theories, convergence of computations, Water Resour. Res., 28, 2211-2227, 1992.

Bosma W.J.P., and S.E.A.T.M. Van der Zee, Transport of reacting solute in a one-dimensional chemically heterogeneous porous medium, Water Resour. Res., 29, 117-131, 1993.

Bosma, W.J.P., A. Bellin, S.E.A.T.M. van der Zee, and A. Rinaldo, Linear equilibrium adsorbing solute transport in physically and chemically heterogeneous porous formations, 2, Numerical results, Water Resour. Res., 29, 4031-4043, 1993.

Chrysikopoulos C.V., P.K. Kitanidis, and P.V. Roberts, Analysis of one-dimensional solute transport through porous media with spatially variable retardation factor, Water Resour. Res., 26, 437-446, 1990.

Chrysikopoulos C.V., P.K. Kitanidis, and P.V. Roberts, Generalized Taylor-Aris moment analysis of the transport of sorbing solutes through porous media with spatially periodic retardation factor, Transport in Porous Media, 7, 163-185, 1992.

Cvetkovic, V.D., A.M. Shapiro, Mass arrival of sorptive solute in heterogeneous porous media, Water Resour. Res., 26, 2057-2067, 1990.

Dagan G., Solute transport in heterogeneous porous formations, J. Fluid Mech., 145, 151-177, 1984.

Dagan G., Theory of solute transport by groundwater, Annu. Rev. Fluid Mech., 19, 183-215, 1987.

Dagan G., Time-dependent macrodispersion for solute transport in anisotropic heterogeneous aquifers, Water Resour. Res., 24, 1491-1500, 1988.

Dagan G., Flow and Transport in Porous Formations, Springer-Verlag, New-York, 1989.

Dagan G. Transport in heterogeneous porous formations: Spatial moments, ergodicity and effective dispersion, Water Resour. Res., 26, 1281-1290, 1990.

Destouni G., and V. Cvetkovic, Field scale mass arrival of sorptive solute into the groundwater, Water Resour. Res., 27, 1315-1325, 1991.

Durant, M. G., and P.V. Roberts, Spatial variability of organic solute sorption in the Border aquifer, Tech. Rep. 303, Dept. of Civ. Eng., Stanford Univ., Stanford, Calif., 1986.

Freeze R.A., A stochastic conceptual analysis of one-dimensional groundwater flow in nonuniform homogeneous media, Water Resour. Res., 11, 725-741, 1975.

Freeze R.A., and J.A. Cherry, Groundwater, Prentice Hall, Englewood Cliffs, N.J., 1979.

Garabedian, S. P., Large scale dispersive transport in aquifers: Field experiments and reactive transport theory, Ph.D. Thesis, Mass. Inst. of Technol., Cambridge, Mass., 1987.

Garabedian S.P., L.W. Gelhar, and M.A. Celia, Large scale dispersive transport in aquifers: Field experiments and reactive transport theory, Tech. Rep. 315, 290 pp., Ralph M. Parsons Lab., Dep. of Civ. Eng., Mass. Inst. of Technol., Cambridge, 1988.

Gelhar L.W., Stochastic subsurface hydrology from theory to applications, Water Resour. Res., 22, 135S-145S, 1986.

Gelhar L.W., and C.L. Axness, Three-dimensional stochastic analysis of macrodispersion in aquifers, Water Resour. Res., 19, 161-180, 1983.

Golz M.N., and P.V. Roberts, Interpreting organic transport data from a field experiment using physical nonequilibrium models, J. Contam. Hydrol., 1, 77-93, 1986.

Hoeskema, R.J., and P.K. Kitanidis, An application of the geostatistical approach to the inverse problem in two-dimensional groundwater modeling, Water Resour. Res., 20, 1003-1020, 1984.

James R.V., and J. Rubin, Applicability of the local equilibrium assumption to transport through soils of solutes effected by ion exchange, in Chemical Modeling in Aqueous Systems, edited by E.A. Jenne, pp. 225-235, American Chemical Society, Washington, D.C., 1979.

Jennings A.A., and D.J. Kirkner, Instantaneous equilibrium approximation analysis, J. Hydraul. Eng., 110, 1700-1717, 1984.

Jury, W.A., Chemical transport modelling: current approaches and unresolved problems, in chemical mobility and reactivity in soil systems, report, Soil Sci. Soc. Am. J., Madison, Wis., 1983.

Kabala, Z.J., and G. Sposito, A stochastic model of reactive solute transport with time varying velocity in a heterogeneous aquifer, Water Resour. Res., 27, 341-350, 1991.

Lapidus, L., and N.R. Amundsen, Mathematics of adsorption in beds, VI, The effect of longitudinal diffusion in ion exchange and chromatographic columns, J. Phys. Chem., 56, 984-988, 1952.

LeBlanc D.R., S.P. Garabedian, K.M. Hess, L.W. Gelhar, R.D. Quadri, K.G. Stollenwerk, and W.W. Wood, Large scale natural gradient tracer test in sand and gravel Cape Cod, Massachusetts, 1, Experimental design and observed tracer movement, Water Resour. Res., 27, 895-910, 1991.

Mackay, D.M., D.L. Freyberg, P.V. Roberts, and J.A. Cherry, A natural gradient experiment on solute transport in a sand aquifer, 1, Approach on overview and plume movement, Water Resour. Res., 22, 2017-2029, 1986*a*.

Mackay, D.M., W.P. Ball, and M.G. Durant, Variability of aquifer sorption properties in a field experiment on groundwater transport of organic solutes: Methods and preliminary results, J. Contam. Hydrol., 1, 119-132, 1986*b*.

Marsily, G., de, Quantitative Hydrogeology, Academic, San Diego, Calif., 1986.

Miller, C. T., and L.V. Benson, Simulation of solute transport in chemically reactive heterogeneous system: Model development and application, Water Resour. Res., 19, 381-391, 1983.

Naff, R.L., On the nature of the dispersive flux in saturated heterogeneous porous media, Water Resour. Res., 26, 1013-1026, 1990.

Naff, R. L., T.C. Yeh, and M.W. Kemblowski, A note on the recent natural gradient tracer test at the Borden site, Water Resour. Res., 24, 2099-2103, 1988.

Neuman, S.P., and Y.K. Zhang, A quasi-linear theory of non-Fickian and Fickian subsurface dispersion, 1, Theoretical analysis with application to isotropic media, Water Resour. Res., 26, 887-902, 1990.

Neuman, S.P., C.L. Winter, and C.M. Newman, Stochastic theory of field-scale Fickian dispersion in anisotropic porous media, Water Resour. Res., 23, 453-466, 1987.

Parker, J.C., and A.J. Valocchi, Constraints on the validity of equilibrium and first-order kinetic transport models in structured soils, Water Resour. Res., 22, 399-407, 1986.

Roberts, P.V., M.N. Goltz, and D.M. Mackay, A natural gradient experiment on solute transport in a sand aquifer, 3, Retardation estimates and mass balances for organic solutes, Water Resour. Res., 22, 2047-2058, 1986.

Robin M.J.L., E.A. Sudicky, R.W. Gillham, and R.G. Kachanoski, Spatial variability of strontium distribution coefficients and their correlation with hydraulic conductivity in the Canadian forces base Borden aquifer, Water Resour. Res., 27, 2619-2632, 1991.

Rubin Y., Stochastic modeling of macrodispersion in heterogeneous porous media, Water Resour. Res., 26, 133-141, 1990. (Correction, Water Resour. Res., 26, 2631, 1990.)

Rubin Y., Prediction of tracer plume migration in disordered porous media by the method of conditional probabilities, Water Resour. Res., 27, 1291-1308, 1991*a*.

Rubin Y., Transport in heterogeneous porous media: Prediction and uncertainty, Water Resour. Res., 27, 1723-1738, 1991*b*.

Rubin Y., and G. Dagan, A note on head and velocity covariances in three-dimensional flow through heterogeneous anisotropic porous media, Water Resour. Res., 28, 1463-1470, 1992.

Salandin, P., and Rinaldo A., Numerical experiments on dispersion in heterogeneous porous media, In: Computational Methods in Subsurface Hydrology, edited by G. Gambolati *et al*., pp. 495-501, Springer-Verlag, New York, 1990.

Salandin P., A. Rinaldo, and G. Dagan, A note on transport in stratified formations by flow tilted with respect to the bedding, Water Resour. Res., 27, 3009-3017, 1991.

Shapiro, M., and H. Brenner, Dispersion of a chemically reactive solute in a spatially periodic model of a porous medium, Chem. Eng. Sci., 43, 551-571, 1988.

Smith R. L., R.W. Harvey, and D.R. LeBlanc, Importance of closely spaced vertical sampling in delineating chemical and microbiological gradients in groundwater studies J. of Contam. Hydrol., 7, 285-300, 1991.

Taylor G.I., Diffusion by continuous movements, Proc. London Math. Soc., Ser. 2, 20, 196-212, 1921.

Valocchi, A.J., Describing the transport of ion exchanging contaminants using an effective K_d approach, Water Resour. Res., 20, 499-503, 1984.

Valocchi, A.J., Validity of the local equilibrium assumption for modeling sorbing solute transport through homogeneous soils, Water Resour. Res., 21, 808-820, 1985.

Valocchi, A.J., Theoretical analysis of deviations from local equilibrium during sorption solute transport through idealized stratified aquifers, J. of Contam. Hydrol., 2, 191-207, 1988.

Valocchi, A.J., Spatial moment analysis of the transport of kinetically adsorbing solutes through stratified aquifers, Water Resour. Res., 25, 273-279, 1989.

Valocchi, A.J., Numerical simulation of the transport of adsorbing solutes in heterogeneous aquifers, In: Computational Methods in Water Resources, edited by G. Gambolati *et al.*, pp. 373-382, Springer-Verlag, New York, 1990.

Van der Zee, S.E.A.T.M., Analytical traveling wave solutions for transport with nonlinear and nonequilibrium adsorption, Water Resour. Res., 26, 2563-2578, 1990. (Correction, Water Resour. Res., 27, 983, 1991.)

Van der Zee, S.E.A.T.M., and J.J.T.I. Boesten, Effect of soil heterogeneity on pesticide leaching to groundwater, Water Resour. Res., 27, 3051-3063, 1991.

Van der Zee, S.E.A.T.M., and W.H. Van Riemsdijk, Transport of reactive solute in spatially variable soil systems, Water Resour. Res., 23, 2059-2069, 1987.

Zhang D., and S.P. Neuman, Comment on "A note on head and velocity covariances in three-dimensional flow through heterogeneous anisotropic porous media" by Y. Rubin and G. Dagan, Water Resour. Res., 28, 3343-3344, 1992.

Zhang Y.K., and S.P. Neuman, A quasi-linear theory of non-Fickian and Fickian subsurface dispersion, 2, Application to anisotropic media and the Borden site, Water Resour. Res., 26, 903-913, 1990.

Chapter 6

Linear equilibrium adsorbing solute transport in physically and chemically heterogeneous porous formations 2. Numerical results*

Abstract

Numerical Monte Carlo simulations were conducted to assess dispersion of reactive solutes in two-dimensional physically and chemically heterogeneous porous media, using random fields with assigned correlation structure for hydraulic conductivity and linear adsorption coefficient. Conditions under which linearization of adsorption is valid are discussed. Lognormal distributions of hydraulic conductivity and adsorption coefficient were assumed. Calculations have been performed for positive and negative correlation between hydraulic conductivity and adsorption coefficient, and for uncorrelated cases. Effects of varying different properties including mean and average sorption coefficient, physical and chemical integral scale and variance of hydraulic conductivity on dispersive behaviour are shown. A larger mean sorption coefficient enhances plume spreading in uncorrelated and in negatively correlated cases. In positively correlated cases counteracting effects of physical and chemical heterogeneity play an important role. The outcome of these counteracting effects depends on the mean, variance, and integral scales of the spatially variable properties. The analytical solutions, derived in paper 1 (Bellin *et al.*, 1993), reveal a good agreement with the numerical results in a significant range of heterogeneities. The generally surprisingly good agreement of the analytical solutions with the numerically obtained results can possibly be attributed to opposing effects of nonlinearities neglected in the derivation of the analytical solutions. In case of strong physical heterogeneity the analytical solutions perform slightly better than in case of strong chemical heterogeneity.

*by W.J.P. Bosma, A. Bellin, S.E.A.T.M. van der Zee and A. Rinaldo
published in: *Water Resources Research*, 29, 4031-4043, 1993.

6.1 Introduction

From an environmental point of view, solute transport and its implications are an important area of research. In recent years, much attention has been addressed towards characterization of spatial variability of field-scale properties because of increasing evidence of its prominent role on field- and basin-scale transport. Experimental results have demonstrated the existence of heterogeneity of soil physical (Biggar and Nielsen, 1976; Bresler and Dagan, 1983; Sudicky, 1986; Freyberg, 1986; Golz and Roberts, 1986; Hess *et al.*, 1992) and soil chemical (Boekhold and Van der Zee, 1992; Mackay *et al.*, 1986*a*) parameters. Large solute transport experiments (Mackay *et al.*, 1986*b*; Freyberg, 1986; LeBlanc *et al.*, 1991) have shown the impact of spatially variable parameters, which emphasizes the need for understanding the effects of heterogeneity at local and regional scales (Dagan, 1986).

Considerable theoretical progress has been made with respect to flow and transport in physically heterogeneous porous media. Stochastic methods have been used to derive analytical expressions to describe flow and nonreactive solute transport in heterogeneous media by, e.g., Gutjahr and Gelhar (1981), Dagan (1984, 1988, 1989), Gelhar and Axness (1983), Garabedian (1987), Neuman *et al.* (1987), Rubin (1990), Rubin and Dagan (1992). Use of a stochastic approach enables incorporation of uncertainty, resulting in expressions for first- and higher-order moments of the expected plume behaviour. Various numerical studies have been done to show the applicability of analytical approaches and to demonstrate the dispersive behaviour of nonreactive transport in heterogeneous formations (e.g., Graham and McLaughlin, 1989; Rubin, 1990, 1991*a*, 1991*b*; Tompson and Gelhar, 1990; Ababou *et al.*, 1989; Bellin *et al.*, 1992). Numerical approaches based on stochastic theory often use uncoupled flow calculations and particle tracking schemes to compute dispersion of a mass of solute in porous formations. This technique was used by Freeze (1975), Rubin (1990), Salandin and Rinaldo (1990), Valocchi (1989) and Bellin *et al.* (1992).

The above cited works primarily focused on heterogeneity of physical parameters, usually incorporated in a lumped variable, e.g., hydraulic conductivity. Less frequently, heterogeneity of soil chemical parameters has been taken into consideration. Examples where only spatial variability of chemical properties of the porous medium was taken into account, are given by Van der Zee (1990*a*),

Chrysikopoulos *et al.* (1990, 1992), and Bosma and Van der Zee (1993). In the work by Chrysikopoulos *et al.* (1990, 1992) analytical expressions were derived for linearly adsorbing solute transport in one- and three-dimensional porous media with spatially variable retardation factor. Van der Zee (1990*a*) and Bosma and Van der Zee (1993) considered nonlinearly adsorbing solute transport in chemically heterogeneous porous media. Van der Zee (1990*a*) used a semi-two-dimensional approach, assuming that heterogeneity in the horizontal plane dominates the heterogeneity in the direction of flow, to derive analytical expressions for the redistribution of a solute initially present in the topsoil. Bosma and Van der Zee (1993) performed numerical Monte Carlo simulations to assess the effect of column scale heterogeneity on one- and semi-two-dimensional dispersive behaviour. Both physical and chemical heterogeneity were taken into account by Van der Zee and Van Riemsdijk (1987), Dagan (1989), Russo (1989*a*, 1989*b*), Cvetkovic and Shapiro (1990), Destouni and Cvetkovic (1991), Kabala and Sposito (1991), and Bellin *et al.* (1993). The approaches used differ in the assumed correlation between physical and chemical properties, as well as in whether transport in multi-dimensional porous media was assumed, whether linear or nonlinear, equilibrium or nonequilibrium adsorption was assumed, and whether first-order decay was assumed. Also, results were obtained either analytically or numerically.

One- and semi-two-dimensional approaches were used by Van der Zee and Van Riemsdijk (1987), Russo (1989*a*, 1989*b*), and Destouni and Cvetkovic (1991). Russo (1989*a*, 1989*b*) examined the effect of spatial variability of physicochemical interactions on transport of Na/Ca-chloride salts through a one-dimensional unsaturated soil. It was concluded that heterogeneity of soil properties in the unsaturated zone may enhance the heterogeneity of the field response. Van der Zee and Van Riemsdijk (1987) derived analytical expressions for the penetration depth of a nonlinearly adsorbing solute, considering a semi-two-dimensional field with spatially variable water velocity, adsorption coefficient and applied amount. The semi-two-dimensional field was modeled as an ensemble of noninteracting parallel stream tubes. Destouni and Cvetkovic (1991) showed double peak behaviour of the breakthrough of a kinetically linearly adsorbing solute in a semi-two-dimensional field with spatially variable water velocity and sorption rate coefficients.

Fully two- and three-dimensional analytical approaches were given by Dagan (1989), Cvetkovic and Shapiro (1990), Kabala and Sposito (1991), and Bellin *et al.* (1993). Dagan (1989) derived the asymptotic behaviour of dispersion of linearly

adsorbing solutes in heterogeneous media with spatially variable retardation factor perfectly correlated with spatially variable hydraulic conductivity. Cvetkovic and Shapiro (1990) considered nonequilibrium linear adsorption and examined perfectly correlated and uncorrelated sorption rate coefficients and hydraulic conductivity. They averaged the position of the solute in the transverse direction to derive an expression for the arrival time at a plane perpendicular to the direction of transport. Kabala and Sposito (1991) examined the behaviour of a solute subject to spatially variable adsorption and first-order decay in a heterogeneous velocity field. They showed that the effective solute velocity differs from the ensemble average solute velocity. Bellin *et al.* (1993) extended Dagan's (1989) theory for the dispersion of linearly adsorbing solutes in physically and chemically heterogeneous porous media. They derived expressions for the second-order moments of transport under ergodic conditions to assess the longitudinal and transverse spreading behaviour as a function of time. Perfectly correlated and uncorrelated cases were considered.

This paper deals with numerical experiments to show the effect of spatially variable hydraulic conductivity in combination with spatially variable sorption coefficient. Parameters that are used to describe the heterogeneities (i.e., mean sorption coefficient, correlation between physical and chemical properties, length of integral scales, variances of spatially variable parameters) are varied in the numerical calculations. The numerical experiments are limited to a two-dimensional domain due to computational restrictions. Additionally, the performance and applicability of the analytical solutions derived in paper 1 (Bellin *et al.*, 1993) are shown for the considered cases.

6.2 Mathematical formulation of the problem

We consider transport of a reacting solute in a chemically and physically heterogeneous two-dimensional porous medium. The physical heterogeneity is represented by a spatially variable hydraulic conductivity whereas the chemical heterogeneity is due to a spatially variable adsorption coefficient. Although basically heterogeneity of these parameters is deterministic and caused by spatially variable physical and chemical properties, the complexity of heterogeneous structures and the problem of accounting for the variability and uncertainty call for a stochastic approach. Using such an approach, the spatially variable parameters

are considered random space functions (RSF) with correlation (Dagan, 1989).

6.2.1 *Heterogeneous flow*

To assess water flow through heterogeneous porous formations, several physical properties can be assumed spatially variable. According to experimental results (Freeze, 1975; Biggar and Nielsen, 1976; Warrick *et al.*, 1977), physical properties may be modeled by a lognormal distribution. Numerous studies have been performed with a lognormally distributed hydraulic conductivity (e.g., Dagan, 1984, 1988, 1989; Gelhar and Axness, 1983; Shapiro and Cvetkovic, 1988; Bellin *et al.*, 1992) and a lognormally distributed scaling factor (e.g., Bresler and Dagan, 1979, 1983).

In view of generally accepted concepts we assume a lognormally spatially variable hydraulic conductivity $K(\mathbf{x})$ (LT^{-1}), with $\mathbf{x}=(x_1,x_2)$ (L). Similar to the procedure in paper 1 (Bellin *et al.*, 1993) we assumed a normally distributed log conductivity Y, defined as $Y(\mathbf{x})=\ln[K(\mathbf{x})]$, with constant mean $\langle Y\rangle$ and variance σ_Y^2. To complete the necessary information of the stochastic variable Y, an isotropic exponential covariance function is assumed, defined as $C_Y(\mathbf{r})=\langle Y'(\mathbf{x})Y'(\mathbf{x}+\mathbf{r})\rangle$ with $Y'(\mathbf{x})=Y(\mathbf{x})-\langle Y\rangle$ and given by (Black and Freyberg, 1987; Dagan, 1989; Bellin *et al.*, 1992; Bosma and Van der Zee, 1993; Bellin *et al.*, 1993)

$$C_Y(\mathbf{r})=\sigma_Y^2 \exp\left(\frac{-|\mathbf{r}|}{l_Y}\right) \tag{6.1}$$

where $\mathbf{r}$ is the planar distance vector between two positions in the heterogeneous domain (L) and l_Y is the integral scale of the log conductivity (L). Equation (6.1) therefore describes the degree of correlation of two Y values at a distance $|\mathbf{r}|$.

Transport of reacting solute in heterogeneous porous media is governed by advection and diffusion. To describe advection of a moving solute, the water velocity at each point in the domain should be known. The random space function hydraulic conductivity causes the water velocity $\mathbf{v}(\mathbf{x})$ to be a RSF as well. To obtain a velocity field in a heterogeneous porous medium, Darcy's law in combination with the mass balance equation needs to be solved. The large difference in the characteristic times of flow and transport allows water flow to be considered in a steady state condition. Following this hypothesis, the velocity at position $\mathbf{x}$ can be obtained from Dagan (1989):

$$\nabla^2\phi+\nabla Y\cdot\nabla\phi=\mathbf{J}\cdot\nabla Y \tag{6.2}$$

$$\Phi(\mathbf{x})=-\mathbf{J}\cdot\mathbf{x}+\phi(\mathbf{x}) \tag{6.3}$$

$$\mathbf{v}(\mathbf{x})=-\frac{K(\mathbf{x})}{\theta}\nabla\Phi(\mathbf{x}) \tag{6.4}$$

where Φ is the hydraulic head (L), $\mathbf{J}$ is the mean head gradient $\mathbf{J}=(J,0)$, ϕ is the random head fluctuation (L) with zero mean, and θ is the porosity. The statistical characterization of the velocity field viewed through (6.4) and (6.2) as a homogeneous random function is assumed complete with the knowledge of the first two moments, e.g., the mean $\langle v_i\rangle$ (i=1, 2) and the covariance function $v_{ij}(\mathbf{r})=\langle(v_i(\mathbf{x})-\langle v_i\rangle)(v_j(\mathbf{x}+\mathbf{r})-\langle v_j\rangle)\rangle$, where $v_i(\mathbf{x})$ is the ith component of the velocity at point $\mathbf{x}$ (Dagan, 1988; Rubin, 1990; Rubin and Dagan, 1992).

6.2.2 *Sorption model formulation*

Sorption at relatively low solute concentrations is usually dominated by surface complexation and/or electrostatic exchange. A recent review was given by Goldberg (1992). At low levels, where the solute of interest hardly affects the equilibria for other compounds, the Freundlich equation, usually given as $C^*=K_FC^n$ (with C and C^* being the solute concentration in the liquid and in the solid phase (ML^{-3}), respectively, and K_F ($M^{1-n}L^{3(n-1)}$) and n being Freundlich parameters), and the linear model, $C^*=K_dC$, where K_d is the sorption coefficient, are particularly useful. Since the sorption of heavy metals and pesticides is commonly weak to moderately nonlinear (Calvet *et al.*, 1980; Chardon, 1984), a linearization of the Freundlich equation is favoured for low concentrations. The cause for this is the non-Lipschitz behaviour of $C^*=K_FC^n$ for C=0 which is physico-chemically unrealistic. Recently, it was shown by Boekhold *et al.* (1993) that cadmium sorption by a sandy soil at low concentrations is practically linear. Although the assumption of linearity affects the transport behaviour (Van der Zee, 1990*b*; Van Duijn and Knabner, 1992), it is not a point of interest in this study.

The parameter K_d reflects all parameters that were not accounted for

explicitly in the linear adsorption model, i.e., all but the concentration of the solute of interest. Because the adsorption maximum C_m^* for permeable (e.g., sandy) media commonly depends on f_{om}, the organic matter content, this is also the case for K_d. In fact, this was often shown to be the case for pesticides (Boesten, 1986). Boekhold *et al.* (1993) showed for Cd that K_d depended on f_{om}, *p*H, and other ionic solutes that either form complexes with Cd or compete for sorption sites on the matrix surface. It is plausible that these parameters affecting K_d are random space functions (Beckett and Webster, 1971). A demonstration was given by Boekhold *et al.* (1991) with regard to f_{om} and K_d. They also showed that at larger concentrations (where $n < 1$) the Freundlich equation gave good predictions of spatially variable sorption when the dependence of K_F on f_{om} and *p*H was accounted for. The covariance functions of f_{om} and *p*H revealed different integral scales.

To model heterogeneity of the adsorption coefficient K_d, similar to the hydraulic conductivity K, a lognormal distribution is used. Because no a priori reasons exist to assume either negative or positive correlation between sorption parameters and the hydraulic conductivity (Destouni and Cvetkovic, 1991), several cases of correlation have been studied.

Regarding the cross correlation of K_d and hydraulic conductivity, generally valid statements are not easily made. For different solutes, different factors (e.g., *p*H, redox potential, ionic strength, matrix composition, cationic and anionic solution composition) may control the K_d-value (Boekhold *et al.*, 1993; Goldberg, 1992; Bolt, 1982). Whereas some factors may be positively correlated with hydraulic conductivity (such as clay content) negative or zero correlations are also feasible. Although in most practical situations the correlation between overall K_d and hydraulic conductivity may appear to be most likely in the range of negative to mildly positive (Robin *et al.*, 1991), there are no a priori reasons to exclude perfect (positive or negative) correlations.

If no correlation between K_d and K is assumed, heterogeneity of the adsorption coefficient can be described according to

$$K_d(\mathbf{x}) = K_d^G \exp[W(\mathbf{x})] \tag{6.5}$$

where K_d^G is the geometric mean of K_d and W is a normally distributed random variable with zero mean and variance σ_W^2. The autocovariance of W, C_W, is defined similar to (6.1):

$$C_W(\mathbf{r})=\sigma_W^2 \exp(\frac{-|\mathbf{r}|}{l_W}) \tag{6.6}$$

with l_W being the integral scale of W.

We adopted a general functional model to describe perfect correlation between hydraulic conductivity and adsorption, given by

$$K_d(\mathbf{x})=K_d^{\,G}[\exp(Y(\mathbf{x}))]^{\beta} \tag{6.7}$$

We account for various extreme cases that encompass likely correlations that may be revealed experimentally in the future. These are as follows: Case A is perfect positive correlation ($\beta>0$), and case B is perfect negative correlation ($\beta<0$). For $\beta=0$ we are dealing with the trivial case of homogeneous adsorption. With linear homogeneous adsorption, behaviour is similar to the nonreactive case (Dagan, 1989; Bellin *et al.*, 1992) except for a rescaling in time. If the cases $\beta=-1$ and $\beta=1$ are considered, (6.7) corresponds with the models used by Van der Zee and Van Riemsdijk (1987), Destouni and Cvetkovic (1991) and Bellin *et al.* (1993).

Assuming a stationary velocity field and linear adsorption, transport of a reactive solute in a two-dimensional physically and chemically heterogeneous porous medium is described by the following equations:

$$\frac{\partial C(\mathbf{x},t)}{\partial t}+\frac{\partial C^*(\mathbf{x},t)}{\partial t}=\nabla\cdot[\mathbf{D}_d\cdot\nabla C(\mathbf{x},t)]-\mathbf{v}(\mathbf{x})\cdot\nabla C(\mathbf{x},t) \tag{6.8}$$

$$C^*(\mathbf{x},t)=K_d(\mathbf{x})\cdot C(\mathbf{x},t) \tag{6.9}$$

where $\mathbf{D}_d$ is the tensor of pore-scale dispersion (LT^{-2}) and $\mathbf{v}(\mathbf{x})$ is the heterogeneous velocity field (LT^{-1}).

Transport in heterogeneous porous media can be represented in terms of spatial moments (Valocchi, 1989; Dagan, 1989). Assuming the ergodic hypothesis to be valid, the first- and second-order spatial moments are equal to the statistical mean and variance of the particle trajectory, given by

$$<X_j(t)>=\int_{-\infty}^{\infty} X_j(t) f(\mathbf{X}) d\mathbf{X} \tag{6.10}$$

$$X_{jl}(t)=\int_{-\infty}^{\infty} (X_j(t)-<X_j(t)>)(X_l(t)-<X_l(t)>) f(\mathbf{X}) d\mathbf{X} \tag{6.11}$$

where $\mathbf{X}$ is the particle displacement (L) and $f(\mathbf{X})$ is the probability density function of the trajectory $\mathbf{X}$.

Bellin *et al.* (1993) extended Dagan's (1989) theory by deriving analytical solutions for the first and second longitudinal and transverse moments for the above correlated (for $\beta=-1$ and $\beta=1$) and uncorrelated cases. Their solutions were based on the linearized flow equation and on first-order approximations of adsorption. Therefore, the solutions are only valid for small σ_Y^2 and σ_W^2. The assumptions correspond to those used by Dagan (1988, 1989) to derive first-order analytical solutions for the nonreactive case. For easy reference, the expressions derived in paper 1 (Bellin *et al.*, 1993) for the second-order moments in the longitudinal (X_{11}) and transverse (X_{22}) directions are given here, i.e.,

$$X_{11}(\tau)=2\frac{(K_d^G)^2 l_Y^2}{<R>^2}\exp(\sigma_Y^2)\left([Ei(\sigma_Y^2)-\gamma-\ln(\sigma_Y^2)]\tau+\sum_{m=1}^{\infty}\frac{(\sigma_Y^2)^m}{m^2 m!}\exp(-m\tau)-\right.$$

$$\left.\sum_{m=1}^{\infty}\frac{(\sigma_Y^2)^m}{m^2 m!}\right)\mp\frac{4K_d^G l_Y^2}{<R>}\sigma_Y^2\exp(\sigma_Y^2/2)(\tau-\ln(\tau)+Ei(-\tau)-\gamma)+$$

$$\sigma_Y^2 l_Y^2\left(2\tau-3\ln(\tau)+(3/2)-3\gamma+3(Ei(-\tau)+\frac{\exp(-\tau)(1+\tau)-1}{\tau^2})\right) \tag{6.12}$$

for the correlated cases (minus sign for positive correlation and plus sign for negative correlation), and

$$X_{11}(\tau)=2\frac{(K_d^G)^2}{<R>^2}\exp(\sigma_W^2)l_W^2\cdot$$
$$\left(\frac{l_Y}{l_W}[Ei(\sigma_W^2)-\gamma-\ln(\sigma_W^2)]\tau+\sum_{m=1}^{\infty}\frac{(\sigma_W^2)^m}{m^2m!}\exp(-m\frac{l_Y}{l_W}\tau)-\sum_{m=1}^{\infty}\frac{(\sigma_W^2)^m}{m^2m!}\right)+$$
$$\sigma_Y^2 l_Y^2\left(2\tau-3\ln(\tau)+(3/2)-3\gamma+3(Ei(-\tau)+\frac{\exp(-\tau)(1+\tau)-1}{\tau^2})\right) \qquad (6.13)$$

for the uncorrelated cases. The expression for the transverse second-order moment is, for correlated and uncorrelated cases, given by

$$X_{22}(\tau)=\sigma_Y^2 l_Y^2\left(\ln(\tau)-(3/2)+\gamma-Ei(-\tau)+3(\frac{1}{\tau^2}-\frac{\exp(-\tau)(1+\tau)}{\tau^2})\right) \qquad (6.14)$$

In (6.12)-(6.14), τ is dimensionless time ($\tau=tV/<R>l_Y$), γ (≈ 0.577) is Euler's constant and $Ei(x)=\int_{-\infty}^{x}\exp(z)/z dz$ is the exponential integral. Observe that the transverse second-order moment (6.14) is influenced only by chemical heterogeneity through the mean retardation factor $<R>$ in τ.

6.3 **Numerical experiments**

6.3.1 *Monte Carlo approach*

Numerical simulations of transport in heterogeneous porous media may conveniently employ a Monte Carlo approach through which many independent realizations are generated, depending on the problem and the scale of heterogeneity. Bellin *et al.* (1992) demonstrated that as $\sigma_Y^2>1$ as many as 1500 realizations were necessary to stabilize the more sensitive transverse second moment. The approach utilised in this study is similar to the method used by Bellin *et al.* (1992).

For each case a series of Monte Carlo simulations was performed, using independent realizations of the same random fields. Four phases can be distinguished in each simulation: (1) generation of the random conductivity field,

(2) solution of the flow equation to obtain the heterogeneous velocity field, (3) generation of the random adsorption field, and (4) calculation of solute transport.

The two-dimensional domain was discretized in triangular elements. Two adjacent elements contained the same value for the random variables. An efficient fast Fourier transform method (Gutjahr, 1989) was used to generate the random fields with prescribed correlation structure. The velocity field was obtained by solving the fully nonlinear flow equation (6.2)-(6.4) by a Galerkin finite element method (Bellin *et al.*, 1992). The generated random field of the adsorption coefficient and the calculated heterogeneous velocity field combine to the retarded velocity field, $\mathbf{v}^R(\mathbf{x})=\mathbf{v}(\mathbf{x})/R(\mathbf{x})$, with $R(\mathbf{x})$ being the spatially variable retardation coefficient given by $R(\mathbf{x})=1 + K_d(\mathbf{x})$. It is worthwhile noting that approximations used to derive the analytical solutions (Bellin *et al.*, 1993) do not play a role in the numerical calculations.

Once the retarded velocity field is available, transport can be calculated by a particle-tracking scheme. A particle, which represents a certain amount of mass injected in the area, moves according to (Hockney and Eastwood, 1988; Tompson and Gelhar, 1990; Bellin, 1992)

$$\mathbf{X}(t+\Delta t)=\mathbf{X}(t)+\mathbf{v}^R(\mathbf{X}(t))\cdot\Delta t \tag{6.15}$$

where $\mathbf{X}$ is the position of the particle. In (6.15) we neglected both molecular diffusion and pore-scale dispersion because the latter is assumed to be of less importance than the effect of the heterogeneous velocity field (Dagan, 1989; Bellin *et al.*, 1992).

In each Monte Carlo realization the trajectory of only one single particle is recorded as a function of time. In contrast with numerical approaches in which many particles are tracked in one realization, the approach with one particle per realization guarantees independent trajectories of all particles. Using this approach, the ergodic requirement (Dagan, 1988, 1989) is fully satisfied. The statistical moments (mean trajectory and longitudinal and transverse second moments) represent the spatial moments of a plume traveling in a heterogeneous domain and injected in a source of a size which is in the transverse direction much larger than the scale of heterogeneity (Dagan, 1990; Bellin *et al.*, 1992).

The statistical moments of the trajectories are calculated numerically according to

$$<X_j(t)> = \frac{1}{MC}\sum_{i=1}^{MC} X_j^i(t) \tag{6.16}$$

$$X_{jj}(t) = \frac{1}{MC}\sum_{i=1}^{MC} (X_j^i(t) - <X_j(t)>)^2 \tag{6.17}$$

where j denotes either the longitudinal (j=1) or transverse (j=2) direction and the amount of Monte Carlo realizations is given by MC. The second order moments X_{jl}, with $j \neq l$, have not been taken into account. An important aspect of this study deals with the ability of the analytical solutions for physical and chemical heterogeneous porous media (6.12)-(6.14) to describe X_{11} and X_{22} calculated with (6.16)-(6.17) for different heterogeneous cases.

6.3.2 *Simulation cases*

Although our interest is the effect of physical and chemical heterogeneity on displacement behaviour of a solute plume, some attention is given to the circumstances under which either physical or chemical heterogeneity dominates the transport process. Randomness of the field parameters hydraulic conductivity and sorption coefficient is considered. Spatially variable grain size distributions, organic matter content, *p*H and microscopic mechanisms determine the heterogeneity of both physical and chemical parameters. From a transport point of view, heterogeneity of the hydraulic conductivity and the sorption coefficient results in a spatially variable flow field with a spatially variable retardation factor. As was shown by a simple approximation (Dagan, 1989), the coefficient of variation of the longitudinal velocity (CV_v), which represents the basic spreading mechanism for the nonreactive case, depends only on σ_Y^2. The relative importance of physical and chemical heterogeneity can be assessed quantitatively by comparing the coefficients of variation (CV) of the velocity and the retardation factor. These parameters are considered representative for physical and chemical heterogeneity, respectively.

Bellin *et al.* (1993) showed that for the reactive case the mean sorption coefficient plays an important role in the heterogeneity of the retarded velocity field. This is due to defining the retardation factor as $1 + K_d$, which causes K_d^G to remain in the expression for CV_R, given for the uncorrelated case by

$$CV_R=\frac{K_d^G[\exp(0.5\,\sigma_W^2)][\exp(\sigma_W^2)-1]^{0.5}}{1+K_d^G\exp(0.5\,\sigma_W^2)} \tag{6.18}$$

For the correlated cases CV_R is given by (6.18) with σ_Y^2 instead of σ_W^2. Because the main spreading is the result of the random retarded velocity field, the variation coefficient of the velocity field should be compared with the variation coefficient of the retardation factor. Note that generally these variation coefficients are different from the variation coefficients of the field parameters K and K_d.

The mean sorption coefficient plays an especially important role if the solute is not strongly sorbed, i.e., if K_d^G is small (Bellin *et al.*, 1993). Little sorption can be relevant in all kinds of environmental circumstances, depending on *p*H, organic matter content, and background electrolyte concentration. Calculations have been performed with three values of K_d^G, namely, 0.2, 1.26, and 10.0. These values were chosen to represent a small (K_d^G=0.2) and a large (K_d^G=10.0) mean sorption coefficient, and to include the intermediate case for which $CV_R=CV_v$ if $\sigma_Y^2=\sigma_W^2=0.2$ (K_d^G=1.26). The latter case describes the situation where physical and chemical heterogeneity are equal from a transport point of view. From the point of view of field parameters, the condition for equal degrees of physical and chemical heterogeneity is met if the coefficients of variation of K and K_d are the same. This condition is fulfilled if $\sigma_Y^2=\sigma_W^2$; the value of K_d^G is not relevant.

To show the effect of correlation and the performance of the analytical solutions (6.12)-(6.14), computations of correlated and uncorrelated cases have been performed. For the correlated cases, σ_Y^2=0.2 has been used. Equation (6.7) was used to determine the spatially variable sorption field. Positive correlation was simulated with β=1, whereas negative correlation was described with β=−1. Positively and negatively correlated calculations were performed for K_d^G=0.2, K_d^G=1.26 and K_d^G=10.0 (σ_Y^2=0.2).

The computations of the uncorrelated cases were used to study the effect of K_d^G, l_Y/l_W, σ_W^2 and σ_Y^2. A reference case with K_d^G=1.26, σ_Y^2=0.2, σ_W^2=0.2 and $l_Y=l_W$ was defined so that $CV_R=CV_v$. The effect of the mean sorption coefficient was obtained by varying K_d^G of the reference case (K_d^G=0.2, K_d^G=10.0). The effect of the integral scale was examined with respect to the reference case with equal degree of physical and chemical heterogeneity. Cases with $l_Y=0.5l_W$, $l_Y=l_W$, and $l_Y=2l_W$ were simulated. For these cases, l_Y was kept constant and l_W was varied. The

effect of the degree of chemical heterogeneity was assessed for σ_W^2=0.05, 0.2, 0.8, and 1.6. The remaining variables were similar to the reference case (K_d^G=1.26, σ_Y^2=0.2, l_Y=l_W).

A large degree of physical heterogeneity was simulated with σ_Y^2=1.6 for all three K_d^G values (0.2, 1.26, 10.0). The remaining variables for these calculations were σ_W^2=0.2 and l_Y=l_W. A complete overview of the simulated cases is given in Table 6.1.

Table 6.1 Simulation cases

case	K_d^G	σ_Y^2	σ_W^2	l_Y/l_W	Correlation
A1	0.2	0.2	0.2	1.0	no
A2	0.2	0.2		1.0	+
A3	0.2	0.2		1.0	–
A4	0.2	1.6	0.2	1.0	no
B1	1.26	0.2	0.2	1.0	no
B2	1.26	0.2		1.0	+
B3	1.26	0.2		1.0	–
B4	1.26	0.2	0.2	0.5	no
B5	1.26	0.2	0.2	2.0	no
B6	1.26	0.2	0.05	1.0	no
B7	1.26	0.2	0.8	1.0	no
B8	1.26	0.2	1.6	1.0	no
B9	1.26	1.6	0.2	1.0	no
C1	10.0	0.2	0.2	1.0	no
C2	10.0	0.2		1.0	+
C3	10.0	0.2		1.0	–
C4	10.0	1.6	0.2	1.0	no

In addition to the above parameters, which determine heterogeneity of physical and chemical properties, other parameters were kept constant in all calculations. The size of the domain, expressed in integral scales, was $36l_Y$ in the

x_1-direction and $18l_Y$ in the x_2-direction. To minimize the effects of boundaries in the transport calculations, an inner core region was defined. The need for an inner core region, first detected by Rubin and Dagan (1989), is illustrated by Bellin *et al.* (1992) who showed the boundary effect on the velocity covariance. If a particle leaves the inner core, the realization is not taken into account. The size of the inner core ($29l_Y \times 11l_Y$) was large enough to lead to only a few cancelled realizations. The coordinates of the particle injection point are given by $\mathbf{x}_0=(5l_Y,9l_Y)$. A sketch of the used domain is shown in Figure 6.1.

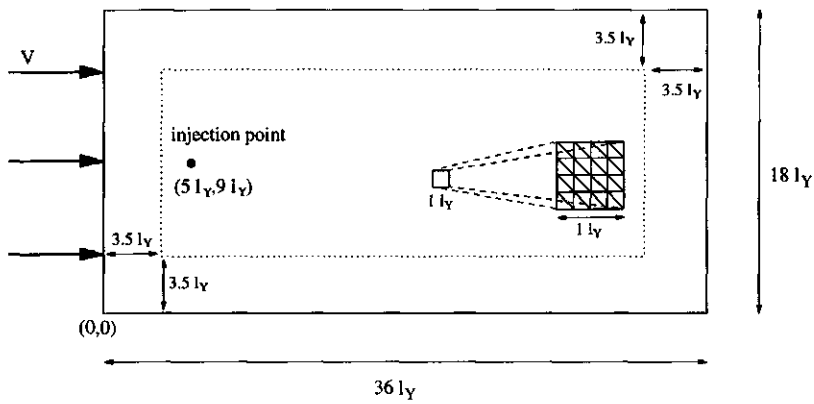

Figure 6.1 Schematic representation of the two-dimensional transport domain.

In the calculations the time step was continuously modified in order to prevent the particle to cross the cell boundaries within the time step. Similar to the calculations performed by Bellin *et al.* (1992), the boundary conditions used were no flux at $x_2=0$ and $x_2=18l_Y$ and unit specific discharge in the x_1-direction at the nodes $(0,x_2)$ and $(36l_Y,x_2)$. The condition $\phi=0$ is imposed for the node $\mathbf{x}=(0,0)$. The dimensionless mean water velocity was 1 and 0 in the x_1 and x_2 directions respectively.

6.4 Results and discussion

Plume spreading of the cases given in Table 6.1 were assessed by calculation of the second order moments, X_{11} and X_{22}, as a function of time given by (6.17). For the sake of comparison, X_{11}, X_{22} are shown in dimensionless form by dividing X_{11} and X_{22} by l_Y^2. Time is made dimensionless by multiplying t with $V/\langle R\rangle l_Y$, where V is the mean Eulerian velocity and $\langle R\rangle$ is the mean retardation coefficient given by $1 + K_d^G \exp(\sigma_W^2/2)$. In case of perfect correlation (positive or negative) $\langle R\rangle$ is given by $1 + K_d^G \exp(\sigma_Y^2/2)$.

In addition to the effects of variation of physical, chemical, and statistical properties, the results are compared with the analytical solutions (6.12)-(6.14), for both correlated and uncorrelated cases. Similar to discussions given by Bellin *et al.* (1992) with respect to physical heterogeneity, comparison with an analytical solution gives insight on the effect of the assumptions made to derive the first-order approximations for the cases with physical and chemical heterogeneity.

In this paper we give full attention to plume spreading. The effect of physical and chemical heterogeneity on the mean position of the plume, denoted by its first-order moment, is not studied. The first-order approximation of the mean trajectory, expressed by $\langle X_1(t)\rangle = Vt/\langle R\rangle$, predicts only an effect of $\langle R\rangle$. Numerical results for both nonreactive and reactive cases show small deviations from the analytical solution (Bellin, 1992; Bellin *et al.*, 1992). Larger deviations are observed for larger degrees of heterogeneities. However, these effects cannot be decomposed from effects that can be attributed to numerical inaccuracies (Bellin *et al.*, 1992).

6.4.1 *Effect of the mean sorption coefficient*

The effects of the mean sorption coefficient are illustrated in Figure 6.2. Values for X_{11} and X_{22} as a function of time are plotted for the cases A1, B1 and C1. Case A1 represents the case of little sorption and C1 of strongly adsorbed solutes and for case B1, K_d^G is chosen such that (with $\sigma_Y^2=\sigma_W^2=0.2$) the variation coefficients of R and v are of the same order. Additionally, the numerical results from Bellin *et al.* (1992) which describe the nonreactive case (with physical heterogeneity only) are shown. The effect of chemical heterogeneity is apparent in Figure 6.2*a*. For $K_d^G=0.2$ a very small increase of plume spreading in the

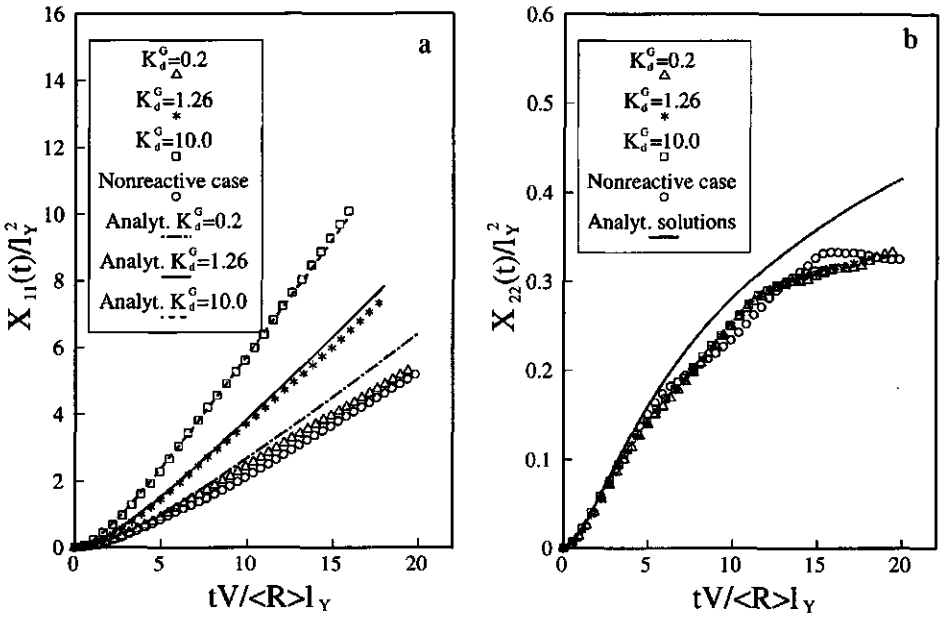

Figure 6.2 Analytical (lines) and numerical (symbols) results of displacement in (*a*) the longitudinal and (*b*) transverse direction for various mean sorption coefficients (cases A1, B1, C1).

longitudinal direction can be seen with respect to the nonreactive case. The effects of chemical heterogeneity are in that case dominated by physical heterogeneity effects. Longitudinal plume spreading is enhanced by chemical heterogeneity for larger K_d^G values. The case with equal degrees of physical and chemical heterogeneity reveals that chemical heterogeneity cannot be ignored. Values for X_{11} are in this case significantly larger than for the nonreactive case. For large K_d^G values the chemical heterogeneity dominates the spreading process in the longitudinal direction. It is worthwhile mentioning that in view of Figure 5.2 (paper 1, Bellin *et al.* (1993)), a continued increase of K_d^G will not increase X_{11} due to insensitivity of CV_R for K_d^G if K_d^G>10.0 (with unaltered σ_w^2). Figure 6.2*b* shows that the effects in the transverse direction are quite different. Corresponding to the analytical expression of the transverse second- order moment (6.14), X_{22} is affected by chemical heterogeneity only by the scaling of time (division by <*R*>). The numerical results of the nonreactive case and the cases A1, B1 and C1 all follow

the same pattern, which agrees with the analytical results of paper 1 (Bellin *et al.*, 1993). The deviating behaviour of X_{11} from the nonreactive case and the similar behaviour of X_{22}, causes a different expected plume behaviour for nonreactive and reactive solutes. Such different plume shapes were found in field experiments described by, among others, Mackay *et al.* (1986*b*).

Figure 6.2 also contains the results from the analytical solutions (6.13)-(6.14). The longitudinal moments, X_{11}, are well described by (6.13). First-order assumptions made in the derivations of (6.13)-(6.14) have a minor effect on X_{11} for a relatively mild degree of heterogeneity (σ_W^2=0.2). Interestingly, the agreement between analytical and numerical results improve as K_d^G increases. Hence, Figure 6.2*a* suggests a possibly compensative effect of the neglected higher-order terms in the linear expansion of $\mathbf{v}(\mathbf{x})/R(\mathbf{x})$, used in the derivations of the analytical solutions (6.13)-(6.14), if K_d^G values increase.

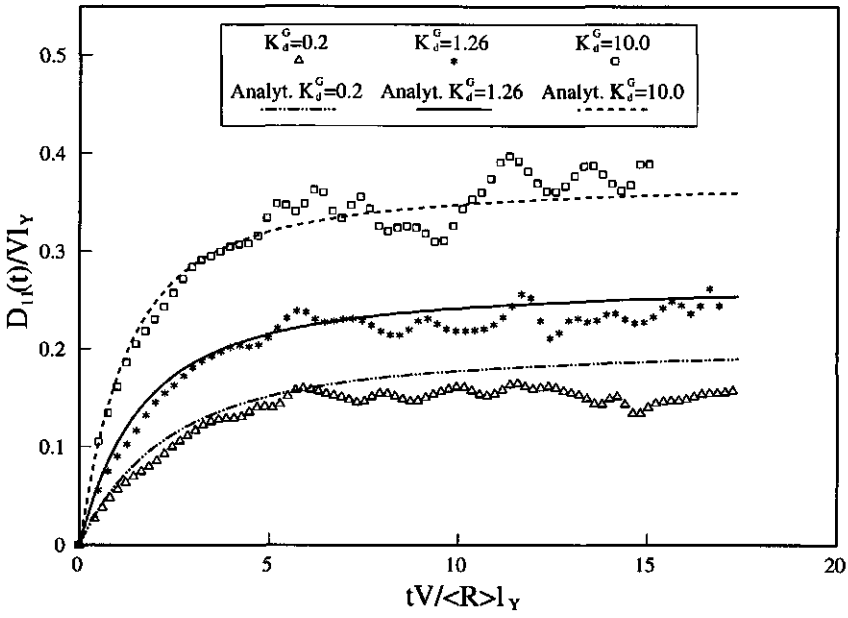

Figure 6.3 Dispersion coefficients obtained by numerical differentiation for various mean sorption coefficients (cases A1, B1, C1).

In Figure 6.2*b*, the curves of the analytical solutions of the cases shown are equal, which is in agreement with the theory. Despite some overestimation the analytical solutions (Dagan, 1989; Bellin *et al.*, 1993) describe the numerical

results reasonably well.

An alternative way to describe the numerical and analytical results is given in Figure 6.3. We demonstrate here the macroscopic longitudinal dispersion coefficient obtained by a numerical derivative of the calculated variances (i.e., $D_{11}=1/2dX_{11}/dt$). Despite some sensitivity for fluctuations, due to the calculation of the first derivative, the agreement between the analytical and numerical results is very good. The results show that for $K_d^G=0.2$ the limiting dispersion coefficient is slightly overestimated and that the agreement improves as K_d^G increases.

6.4.2 *Effect of correlation*

The results shown in Figure 6.2 and 6.3 were obtained for the uncorrelated case. To show the effect of perfect positive and negative correlation, results of cases A1, A2, A3, B1, B2, B3, C1, C2, and C3 are presented in Figure 6.4 for various mean sorption coefficients. We see that in the longitudinal direction plume spreading is enhanced if K and K_d are negatively correlated, as is expected from the theory. Large conductivities combined with low sorption on one hand, and low conductivities combined with high sorption on the other, cause large solute spreading. This enhancement is stronger if the mean sorption coefficient K_d^G is large. In the case of positive correlation between K and K_d the effects are somewhat different. As expected, for all cases, plume spreading in the longitudinal direction is smaller for the positively correlated case than for the uncorrelated case. However, the difference between the uncorrelated case and the positively correlated case is disproportionately different in the three cases considered ($K_d^G=0.2$, 1.26, 10.0). In fact, in Figure 6.5 one can infer that in the case of positive correlation X_{11} is larger for $K_d^G=0.2$ than for the cases with $K_d^G=1.26$ and $K_d^G=10.0$. Since we are dealing with two opposing effects, caused by physical and chemical heterogeneity, it is important to realize their magnitude. In the case with $K_d^G=0.2$, the effect of chemical heterogeneity is quite small, and therefore physical heterogeneity is not strongly affected by the opposing chemical heterogeneity. In the case of equal physical and chemical heterogeneity ($K_d^G=1.26$), the effects are more balanced, and plume spreading in the longitudinal direction is relatively small. If chemical heterogeneity is larger than physical heterogeneity ($K_d^G=10.0$), X_{11} is slightly larger than if $K_d^G=1.26$. Effects of physical heterogeneity are countered, but effects of the relatively large mean sorption coefficient remain, with the resulting increase of the

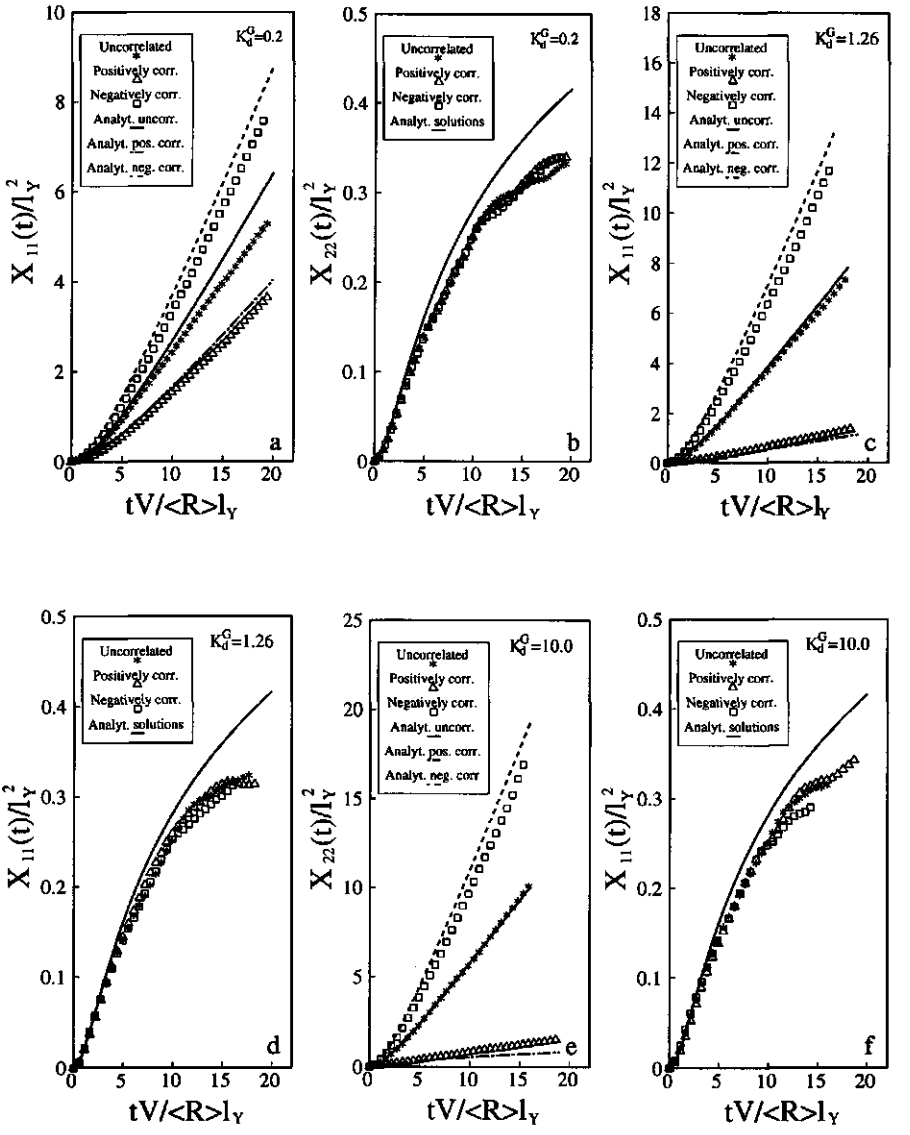

Figure 6.4 Analytical (lines) and numerical (symbols) results of displacement in (*a*), (*c*), (*e*) the longitudinal and (*b*), (*d*), (*f*) transverse direction for positively correlated, negatively correlated and uncorrelated cases. Fig. 6.4*a,b*: cases A1, A2, A3; Fig. 6.4*c,d*: cases B1, B2, B3; Fig. 6.4*e,f*: cases C1, C2, C3.

longitudinal plume spreading. The chemical heterogeneity itself enhances longitudinal spreading if K_d^G increases. Part of this enhancement is reduced by the positive correlation, causing large velocities at positions with strong adsorption and low velocities at positions with weak adsorption. Similar to the results of Figure 6.2, correlation (positive or negative) does not have an effect on spreading in the transverse direction.

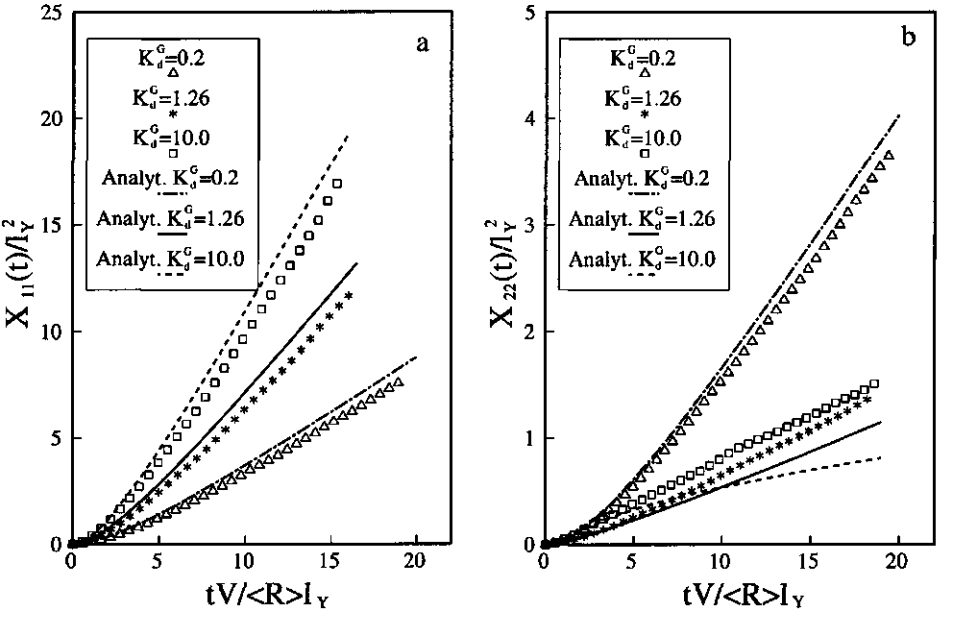

Figure 6.5 Analytical (lines) and numerical (symbols) results of displacement in the longitudinal direction for (*a*) negatively correlated and (*b*) positively correlated cases for various mean sorption coefficients (Fig. 6.5*a*: cases A3, B3, C3; Fig. 6.5*b*: cases A2, B2, C2).

The above results show that correlation between physical and chemical parameters cannot be ignored. Although perfect correlation is unlikely to be found in the field, the results imply that moderate correlation may have a distinct effect as well. In Figures 6.4 and 6.5 the analytical solutions for the various cases are also shown. It can be seen that in the longitudinal direction, in general, the analytical results match the numerical results. Considering the negatively correlated cases, the analytical solution slightly overestimates the numerically calculated values. Although the performance of the analytical solution does not improve as

K_d^G increases, as was observed for the uncorrelated case (Figure 6.2), the deviations of X_{11} for larger K_d^G are relatively small. This may also be attributed to the compensative effect of the neglected higher-order terms in the derivation of the analytical solutions. Errors due to these effects may be enhanced by the negative correlation between K and K_d. Higher K_d^G values cause a slight increase of the overestimation of the analytical solution.

If K and K_d are positively correlated, the effects are opposite. An increase of K_d^G causes, compared with the uncorrelated case, a decrease of the analytical solution with respect to the numerical results, resulting in an underestimation for K_d^G>1.26. Nevertheless, the deviations on an absolute scale are small (observe the scale in Figure 6.5*b*), because positive correlation reduces the solute spreading. The better agreement of the analytical and numerical results for K_d^G=0.2 can be explained with the minor role of chemical heterogeneity if K_d^G is small.

6.4.3 *Effect of integral scales*

The integral scale is an important parameter to describe the spatial structure of a spatially variable property. In combination with the mean and variance, it influences the effect of the heterogeneous variable. The integral scale is intuitively defined as a measure for the distance between two points beyond which the property is practically uncorrelated (Dagan, 1989).

The effect of the integral scale of the spatially variable chemical parameter can be revealed with cases B1, B4 and B5. The integral scale could not be multiplied by a factor larger than 2, due to limits of the domain size. Figure 6.6 shows numerical and analytical results of the cases B1, B4 and B5 and the numerical results of the nonreactive case (Bellin *et al.*, 1992). As expected, in Figure 6.6*a* we show that a decrease of the chemical integral scale (l_W) reduces spreading in the longitudinal direction. This reduction cannot continue beyond the lower limit represented by the nonreactive case (i.e., no chemical heterogeneity). On the other hand, an increase of l_W enhances plume spreading in the longitudinal direction. A larger chemical integral scale generally increases the distance between large and small adsorption coefficients and therefore between quickly and more slowly moving particles. This results in larger longitudinal second-order moments. The results of the analytical solution show that for larger l_W the numerical results are described well. For cases with lower chemical integral scales (i.e., l_Y/l_W=1,

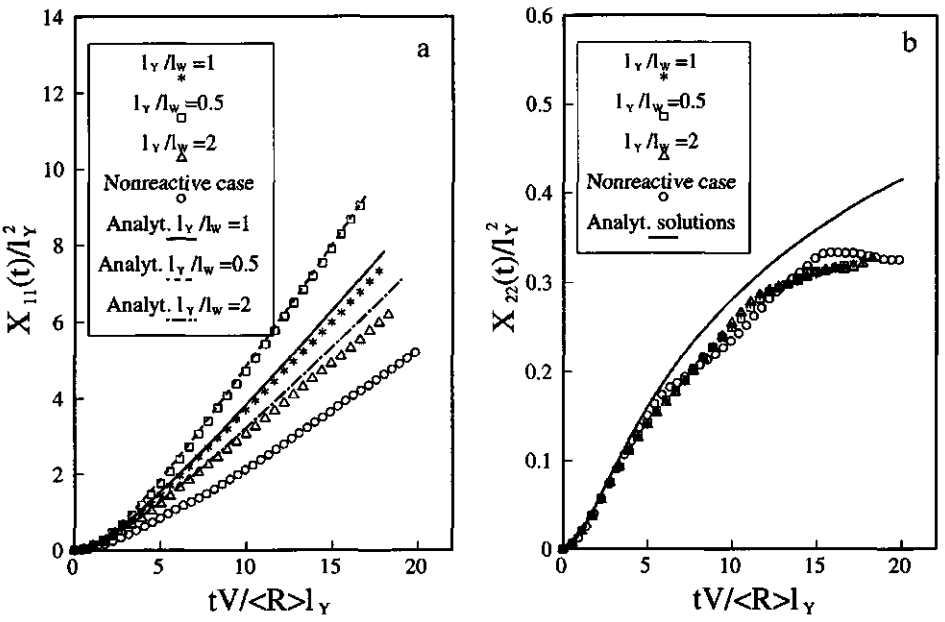

Figure 6.6 Analytical (lines) and numerical (symbols) results of displacement in (*a*) the longitudinal and (*b*) transverse direction for various ratios of integral scales (l_Y/l_w) (cases B1, B4, B5).

l_Y/l_w=2), the analytical solution somewhat overestimates the results of the numerical calculations.

The second-order moment in the transverse direction, X_{22}, is not sensitive to a change of the chemical integral scale (see Figure 6.6*b*). The transverse dispersion is determined by physical heterogeneity only, which was not altered in these cases. These results agree with derivations of Bellin *et al.* (1993) who showed no functional relationship between X_{22} and l_w.

6.4.4 *Effect of* σ_Y^2 *and* σ_w^2

The parameter which has been given the most attention in studies regarding transport in heterogeneous porous media is the variance of the spatial variable log conductivity, σ_Y^2 (Dagan, 1988, 1989; Bellin *et al.*, 1992; Shapiro and Cvetkovic, 1988; Cvetkovic and Shapiro, 1989; Valocchi, 1990; Rubin, 1990; Selroos and

Cvetkovic, 1992). This parameter is used to describe the degree of physical heterogeneity. Due to the properties of the lognormal distribution, the variation coefficient of Y is a function of σ_Y^2 only ($CV_Y=[\exp(\sigma_Y^2)-1]^{0.5}$), Van der Zee and Boesten (1991)). Similarly, the parameter σ_W^2 determines the degree of chemical heterogeneity. Results from Figures 6.2-6.6 show that chemical heterogeneity may have a large impact on spreading in the longitudinal direction. Therefore to demonstrate the effect of the degree of heterogeneity, several values of σ_W^2 and σ_Y^2 have been used. Cases B1, B6, B7 and B8 have been computed to demonstrate the effect of various degrees of chemical heterogeneity. Additionally, the effect of a large degree of physical heterogeneity ($\sigma_Y^2=1.6$) is considered for three sorption levels (cases A4, B9, and C4).

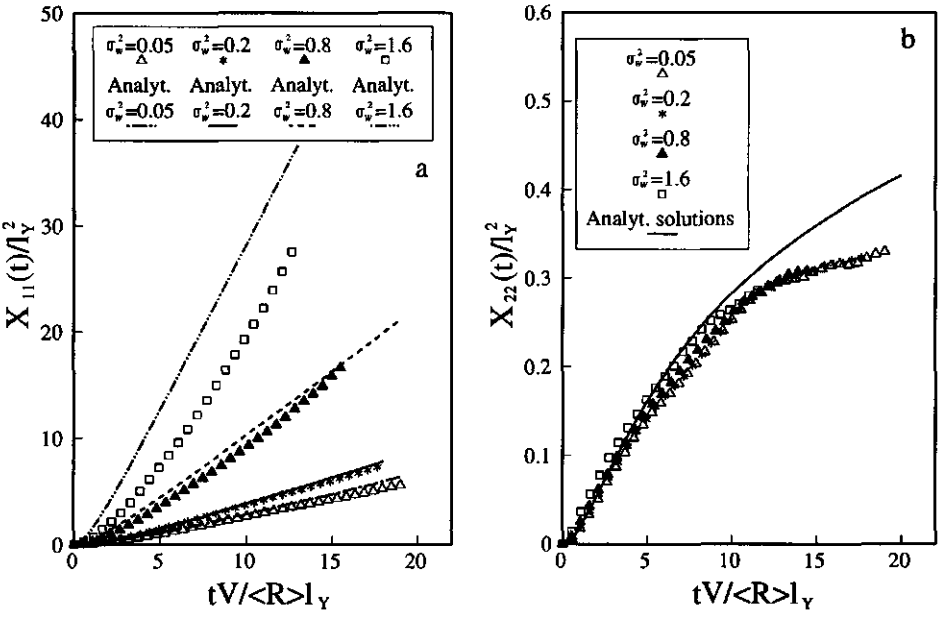

Figure 6.7 Analytical (lines) and numerical (symbols) results of displacement in (*a*) the longitudinal and (*b*) transverse direction for various degrees of chemical heterogeneity (σ_W^2) (cases B1, B6, B7, B8).

Figure 6.7 reveals the longitudinal and transverse second-order moment for four degrees of chemical heterogeneity, obtained by changing σ_W^2 with $K_d^G=1.26$. From the results in the longitudinal direction it can be seen that indeed different

σ_W^2 values modify the spreading behaviour. A strong increase of X_{11} values is the result of a relatively mild increase of σ_W^2. For the case with σ_Y^2=0.2 (valid for all cases shown in Figure 6.7) and σ_W^2=1.6, chemical heterogeneity dominates the spreading process. On the other hand, Figure 6.7*b* once again demonstrates the independence of transverse spreading from chemical heterogeneity. It can be seen that the numerical results in the transverse direction are not as smooth as the X_{11} results. Bellin *et al.* (1992) already noticed slower convergence for the moments in the transverse direction in the nonreactive case.

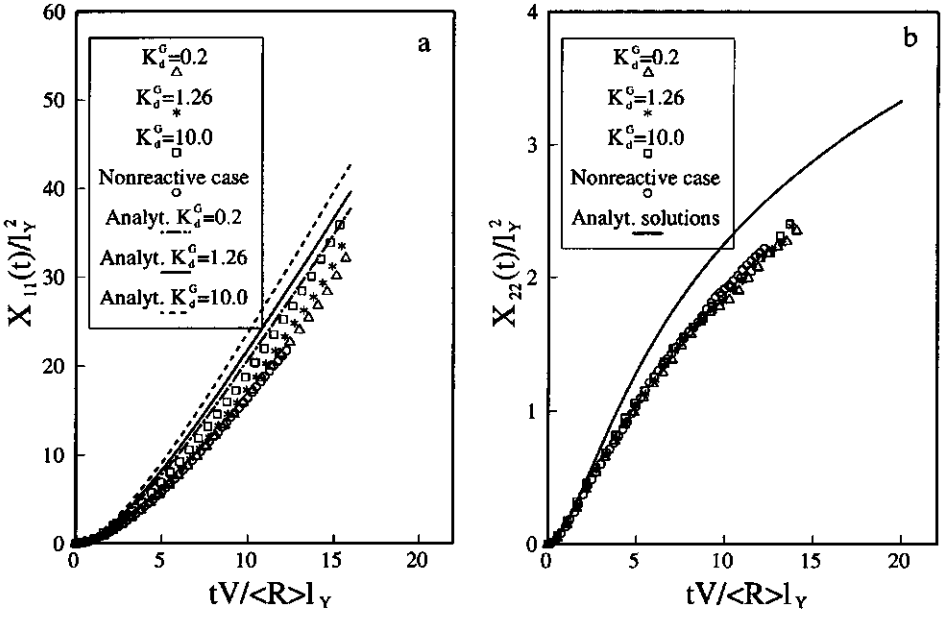

Figure 6.8 Analytical (lines) and numerical (symbols) results of displacement in (*a*) the longitudinal and (*b*) transverse direction with large physical heterogeneity (σ_Y^2=1.6) for various mean sorption coefficients (cases A4, B9, C4).

The analytical results in Figure 6.7*a* show that if σ_W^2 increases, larger deviations occur between the numerical results and the analytical solution. Errors due to first-order approximations, are enhanced if the degree of heterogeneity increases. Apparently, if K_d^G=1.26 and σ_W^2=1.6, the higher-order effects are not strong enough to compensate for the overestimation of the analytical solution. Smaller deviations are observed in Figure 6.8 where results are shown for cases

A4, B9, and C4, with σ_Y^2=1.6, σ_W^2=0.2 and K_d^G=0.2, 1.26 and 10.0. Figure 6.8*a* illustrates that the analytical solution performs better for large σ_Y^2 than for large σ_W^2 values. With σ_Y^2=1.6, plume spreading in the longitudinal direction is more profound compared with cases where σ_Y^2=0.2 (Figures 6.2-6.6). Interestingly, varying the K_d^G values has only a minor impact on spreading in the longitudinal direction. Physical heterogeneity dominates, and only changes in σ_W^2 will enhance front spreading due to chemical heterogeneity. This agrees with results of Figure 5.2 (paper 1, Bellin *et al.* (1993)), which show that CV_R/CV_v is hardly affected by K_d^G if σ_Y^2=1.6 and σ_W^2=0.2. However, whether spreading in the longitudinal direction is dominated by either physical of chemical heterogeneity cannot be determined only by taking into account the chosen values for σ_Y^2 and σ_W^2. Previous sections have illustrated that the impact of correlation and of integral scales cannot be ignored.

Figure 6.8*b* shows that an increase of σ_Y^2 influences the amount of spreading in the transverse direction. The X_{22} values are significantly higher compared with cases computed with σ_Y^2=0.2 (e.g., Figure 6.2*b*). Again, changing K_d^G has no effect on X_{22}. Results from the analytical solution demonstrate that an increasing degree of physical heterogeneity hardly affects the applicability of the solution. The deviations found in all figures between the analytical solutions derived by Bellin *et al.* (1993) and the actual numerical results are not significantly larger than the corresponding deviations for the nonreactive case (Rubin, 1990; Bellin *et al.*, 1992). This justifies the use of the analytical solution for correlated and uncorrelated cases with physical and chemical heterogeneity in the parameter range considered herein.

6.5 Conclusions

Numerical simulations were performed to assess the effect of physical and chemical heterogeneity on reactive solute transport. Physical heterogeneity was modeled by assuming a random variation with spatial correlation of the hydraulic log conductivity. Chemical heterogeneity was described in a similar manner assuming a random variation of the natural logarithm of the sorption coefficient. The results of the numerical Monte Carlo calculations were compared with analytical solutions for uncorrelated and for correlated cases (correlation between

the hydraulic conductivity and the adsorption coefficient). Several values of the sorption coefficient, different ratios of chemical and physical integral scales, and several values for σ_Y^2 and σ_W^2 were considered. Solute spreading was described in terms of the second-order moments in the longitudinal and the transverse direction. We conclude from the results that stronger sorption (larger K_d^G) enhances the spreading in the longitudinal direction, for cases with both uncorrelated and correlated sorption coefficient and hydraulic conductivity. In case of positively correlated K_d and K, longitudinal spreading is reduced with respect to the uncorrelated and negatively correlated case. The parameters K_d^G, σ_W^2, l_W, σ_Y^2, and l_Y determine the contribution of chemical and physical heterogeneity. If both contributions are of equal magnitude, a minimal degree of solute spreading is observed. Increasing the chemical integral scale enhances longitudinal solute spreading due to a larger distance between quickly and slowly moving particles. As expected, enhanced longitudinal spreading is also observed with larger coefficients of variation of either the hydraulic conductivity or the sorption coefficient (by increasing σ_Y^2 and σ_W^2). In agreement with analytical findings in paper 1 (Bellin *et al.*, 1993), chemical heterogeneity only influences the time scale of the transverse solute spreading. Differences in correlation, K_d^G, σ_W^2, and integral scale do not increase or decrease values of the transverse second-order moment. Moreover, we conclude that the analytical solutions can describe solute displacement in physically and chemically heterogeneous porous media for a wide range of parameter values. An increase of the mean sorption coefficient generally improves the performance of the analytical solution, due to a compensative effect of the neglected higher-order terms as K_d^G increases. If σ_Y^2 and σ_W^2 increase, the analytical solution overestimates the numerically obtained results. However, with σ_W^2 up to 0.8 and σ_Y^2 up to 1.6, the analytical solution still agrees well with the numerical calculations. Despite some overestimation the numerical results of the transverse second-order moment are all well described by the analytical solution.

References

Ababou, R., D. McLaughlin, L.W. Gelhar, and A.F.B. Tompson, Numerical simulation of three-dimensional saturated flow in randomly heterogeneous porous media, Transp. Porous Media, 4, 549-565, 1989.

Beckett, P.H.T., and R. Webster, Soil variability: a review, Soils Fert., 34, 1-15, 1971.

Bellin, A., Un contributo allo studio del trasporto di soluti passivi e reattivi in formazioni porose eterogenee, Ph.D. thesis, Universitá di Trento, Italy, 1992.

Bellin, A., P. Salandin, and A. Rinaldo, Simulation of dispersion in heterogeneous porous formations: statistics, first-order theories, convergence of computations, Water Resour. Res., 28, 2211-2227, 1992.

Bellin, A., A. Rinaldo, W.J.P. Bosma, S.E.A.T.M. Van der Zee, and Y. Rubin, Reactive transport in chemically and physically heterogeneous porous formations, Water Resour. Res., 1993.

Biggar, J.W., and D.R. Nielsen, Spatial variability of the leaching characteristics of a field soil, Water Resour. Res., 12, 78-84, 1976.

Black, T.C., and D.L. Freyberg, Stochastic modeling of vertically averaged concentration uncertainty in a perfectly stratified aquifer, Water Resour. Res., 23, 997-1004, 1987.

Boekhold, A.E., and S.E.A.T.M. Van der Zee, Significance of soil chemical heterogeneity for spatial behaviour of cadmium in field soils, Soil Sci. Soc. Am. J., 56, 747-754, 1992.

Boekhold, A.E., S.E.A.T.M. Van der Zee, and F.A.M. de Haan, Spatial patterns of cadmium contents related to soil heterogeneity, Water, Air, and Soil Pollution, 57-58, 479-488, 1991.

Boekhold, A.E., E.J.M. Temminghoff, and S.E.A.T.M. Van der Zee, Influence of electrolyte composition and *p*H on cadmium sorption by an acid sandy soil, J. Soil Sci., 44, 85-96, 1993.

Boesten, J.J.T.I., Behaviour of herbicides in soil: simulation and experimental assessment, Ph.D. thesis, 263 pp., Wageningen Agric. Univ., the Netherlands, 1986

Bolt, G.H., Movement of solutes in soil: principles of adsorption/exchange chromatography, in: Soil Chemistry B. Physico-Chemical Models, edited by G.H. Bolt, pp. 285-348, Elsevier Sci. Publ., New York, 1982.

Bosma, W.J.P., and S.E.A.T.M. Van der Zee, Transport of reacting solute in a one-dimensional chemically heterogeneous porous medium, Water Resour. Res., 29, 117-131, 1993.

Bresler, E., and G. Dagan, Solute dispersion in unsaturated soil at field scale: II. Application. Soil Sci. Soc. Am. J., 43, 467-472, 1979.

Bresler, E., and G. Dagan, Unsaturated flow in spatially variable fields, 2. Application of water flow models to various fields, Water Resour. Res, 19, 429-435, 1983.

Calvet, R., M. Tercé, and J.C. Arvieu, Adsorption des pesticides par les sols et leurs constituants. III. Caractéristiques générals de l'adsorption des pesticides, Ann. Agron. 31, 239-257, 1980.

Chardon, W.J., Mobiliteit van cadmium in de bodem, Ph.D. thesis, 200 pp., Wageningen Agricultural University, The Netherlands, 1984.

Chrysikopoulos, C.V., P.K. Kitanidis, and P.V. Roberts, Analysis of one-dimensional solute transport through porous media with spatially variable retardation factor, Water Resour. Res., 26, 437-446, 1990.

Chrysikopoulos, C.V., P.K. Kitanidis, and P.V. Roberts, Generalized Taylor-Aris moment analysis of the transport of sorbing solutes through porous media with spatially-periodic retardation factor, Transp. Porous Media, 7, 163-185, 1992.

Cvetkovic, V.D., and A.M. Shapiro, Solute advection in stratified formations, Water Resour. Res., 25, 1283-1289, 1989.

Cvetkovic, V.D., and A.M. Shapiro, Mass arrival of sorptive solute in heterogeneous porous media, Water Resour. Res., 26, 2057-2067, 1990.

Dagan, G., Solute transport in heterogeneous porous formations, J. Fluid Mech., 145, 151-177, 1984.

Dagan, G., Statistical theory of groundwater flow and transport: pore to laboratory, laboratory to formation, and formation to regional scale, Water Resour. Res., 22, 20S-134S, 1986.

Dagan, G., Time-dependent macrodispersion for solute transport in anisotropic heterogeneous aquifers, Water Resour. Res, 24, 1491-1500, 1988.

Dagan, G., Flow and transport in porous formations, Springer-Verlag, Berlin, 1989.

Dagan, G., Transport in heterogeneous formations: spatial moments, ergodicity and effective dispersion, Water Resour. Res., 26, 1281-1290, 1990.

Destouni, G., and V. Cvetkovic, Field scale mass arrival of sorptive solute into the groundwater, Water Resour. Res., 27, 1315-1325, 1991.

Freeze, R.A., A stochastic-conceptual analysis of one-dimensional groundwater flow in nonuniform homogeneous media, Water Resour. Res., 11, 725-741, 1975.

Freyberg, D.L., A natural gradient experiment on solute transport in a sand aquifer, 2. Spatial moments and the advection and dispersion of nonreactive tracers, Water Resour. Res., 22, 2031-2046, 1986.

Garabedian, S.P., Large-scale dispersive transport in aquifers: Field experiments and reactive transport theory, Ph.D. thesis, Mass. Inst. of Technol., Cambridge, Mass., U.S.A., 1987.

Gelhar, L.W., and C.L. Axness, Three-dimensional stochastic analysis of macrodispersion in aquifers, Water Resour. Res., 19, 161-180, 1983.

Goldberg S., Use of surface complexation models in soil chemical systems, Adv. in Agronomy Vol. 47, edited by D.L. Sparks, pp. 234-329, 1992.

Goltz, M.N., and P.V. Roberts, Interpreting organic transport data from a field experiment using physical nonequilibrium models, J. Contam. Hydrol., 1, 77-93, 1986.

Graham, W., and D. McLaughlin, Stochastic analysis of nonstationary subsurface solute transport 1. Unconditional moments, Water Resour. Res., 25, 215-232, 1989.

Gutjahr, A.L., Fast Fourier Transforms for random field generation, project report, contract 4-RS of Los Alamos National Laboratory, N. M. Inst. of Min. and Technol., Socorro, 1989.

Gutjahr, A.L., and L.W. Gelhar, Stochastic models of subsurface flow: infinite versus finite domains and stationarity, Water Resour. Res., 17, 337-350, 1981.

Hess, K.M., S.H. Wolf, and M.A. Celia, Large-scale natural gradient tracer test in sand and gravel, Cape Cod, Massachusetts 3. Hydraulic conductivity variability and calculated macrodispersivities, Water Resour. Res., 28, 2011-2027, 1992.

Hockney, R.W., and J.W. Eastwood, Computer simulation using particles, Adam Higler, Bristol, England, 1988.

Kabala, Z.J., and G. Sposito, A stochastic model of reactive solute transport with time-varying velocity in a heterogeneous aquifer, Water Resour. Res., 27, 341-350, 1991.

LeBlanc, D.R., S.P. Garabedian, K.M. Hess, L.W. Gelhar, R.D. Quadri, K.G. Stollenwerk, and W.W. Wood, Large-scale natural gradient tracer test in sand and gravel, Cape Cod, Massachusetts 1. Experimental design and observed tracer movement, Water Resour. Res., 27, 895-910, 1991.

Mackay, D.M., W.P. Ball, and M.G. Durant, Variability of aquifer sorption properties in a field experiment on groundwater transport of organic solutes: methods and preliminary results, J. Contam. Hydrol., 1, 119-132, 1986*a*.

Mackay, D.M., D.L. Freyberg, P.V. Roberts, and J.A. Cherry, A natural gradient experiment on solute transport in a sand aquifer, 1. Approach and overview of plume movement, Water Resour. Res., 22, 2017-2029, 1986*b*.

Neuman, S.P., C.L. Winter, and C.M. Newman, Stochastic theory of field-scale Fickian dispersion in anisotropic porous media, Water Resour. Res., 23, 453-466, 1987.

Robin, M.J.L., E.A. Sudicky, R.W. Gillham, and R.G. Kachanoski, Spatial variability of strontium distribution coefficients and their correlation with hydraulic conductivity in the Canadian Forces Base Borden Aquifer, Water Resour. Res., 27, 2619-2632, 1991.

Rubin, Y., Stochastic modeling of macrodispersion in heterogeneous porous media, Water Resour. Res., 26, 133-141, 1990.

Rubin, Y., Prediction of tracer plume migration in disordered porous media by the method of conditional probabilities, Water Resour. Res., 27, 1291-1308, 1991*a*.

Rubin, Y., Transport in heterogeneous porous media: Prediction and uncertainty, Water Resour. Res., 27, 1723-1738, 1991*b*.

Rubin, Y., and G. Dagan, Stochastic analysis of boundary effects on head spatial variability in heterogeneous aquifers 2. Impervious boundary, Water Resour. Res., 25, 707-712, 1989.

Rubin, Y., and G. Dagan, A note on head and velocity covariances in three-dimensional flow through heterogeneous anisotropic porous media, Water Resour. Res., 28, 1463-1470, 1992.

Russo, D. Field-scale transport of interacting solutes through the unsaturated zone 1. Analysis of the spatial variability of the transport properties, Water Resour. Res., 25, 2475-2485, 1989*a*.

Russo, D. Field-scale transport of interacting solutes through the unsaturated zone 2. Analysis of the spatial variability of the field response, Water Resour. Res., 25, 2487-2495, 1989*b*.

Salandin, P., and A. Rinaldo, Numerical experiments on dispersion in heterogeneous porous media, in: Computational Methods in Subsurface Hydrology, edited by G. Gambolati et al., pp. 495-501, Springer-Verlag, New York, 1990.

Selroos, J.O., and V.D. Cvetkovic, Modeling solute advection coupled with sorption kinetics in heterogeneous formations, Water Resour. Res., 28, 1271-1278, 1992.

Shapiro, A.M., and V.D. Cvetkovic, Stochastic analysis of solute arrival time in heterogeneous porous media, Water Resour. Res., 24, 1711-1718, 1988.

Sudicky, E.A., A natural gradient experiment on solute transport in a sand aquifer: spatial variability of hydraulic conductivity and its role in the dispersion process, Water Resour. Res., 22, 2069-2082, 1986.

Tompson, A.F.B., and L.W. Gelhar, Numerical simulation of solute transport in three-dimensional, randomly heterogeneous porous media, Water Resour. Res., 26, 2541-2562, 1990.

Valocchi, A.J., Spatial moment analysis of the transport of kinetically adsorbing solutes through stratified aquifers, Water Resour. Res., 25, 273-279, 1989.

Van der Zee, S.E.A.T.M., Analysis of solute redistribution in a heterogeneous field, Water Resour. Res., 26, 273-278, 1990*a*.

Van der Zee, S.E.A.T.M., Analytical traveling wave solutions for transport with nonlinear and nonequilibrium adsorption, Water Resour. Res., 26, 2563-2578, 1990*b*. (Correction, Water Resour. Res., 27, 983, 1991.)

Van der Zee, S.E.A.T.M., and J.J.T.I. Boesten, Effects of soil heterogeneity on pesticide leaching to groundwater, Water Resour. Res., 27, 3051-3063, 1991.

Van der Zee, S.E.A.T.M., and W.H. van Riemsdijk, Transport of reactive solute in spatially variable soil systems, Water Resour. Res., 23, 2059-2069, 1987.

Van Duijn, C.J., and P. Knabner, Travelling waves in the transport of reactive solutes through porous media: Adsorption and binary exchange - Part 2, Transp. Porous Media, 8, 199-226, 1992.

Warrick, A.W., G.J. Mullen, and D.R. Nielsen, Scaling field-measured soil hydraulic properties using a similar media concept, Water Resour. Res., 13, 355-362, 1977.

Chapter 7

Dispersion of a continuously injected, nonlinearly adsorbing solute in chemically or physically heterogeneous porous formations*

Abstract

In this paper we consider transport of a nonlinearly adsorbing solute in a two-dimensional porous medium. The solute is continuously injected along a line source with a size equal to the transverse dimension of the domain. Adsorption is described by the Freundlich isotherm. The domain is assumed to be spatially variable and variation of hydraulic conductivity and adsorption coefficient is considered separately. Solute transport is solved by a mixed Eulerian-Lagrangian method. It is shown that nonlinear adsorption adds an extra requirement of taking into account pore scale dispersion while using Eulerian-Lagrangian solution methods. Solute dispersion is characterized in terms of spatial moments, where the pdf is the derivative of the transversely averaged concentration field. Results of numerical calculations are obtained for nonlinear and linear adsorption. It is shown that for large displacements an increase of pore scale dispersion leads to a decrease of average front spreading in case of nonlinear adsorption. The nonlinearity of adsorption opposes the local spreading in the longitudinal direction, whereas transverse spreading decreases the average front spreading. For larger displacements the front variance increases linearly with time. If transverse mixing is of the order of magnitude of the scale of heterogeneity, the front variance approaches a constant value, i.e. a traveling wave becomes apparent.

7.1 Introduction

Many numerical and analytical studies have demonstrated the relevance of spatial variability for dispersion of reactive and nonreactive solutes in porous

*by W.J.P. Bosma and S.E.A.T.M. van der Zee
accepted for publication by: *Journal of Contaminant Hydrology.*

formations (e.g., Gelhar and Axness, 1983; Dagan, 1984, 1988, 1989; Garabedian, 1987; Rubin, 1990; Cvetkovic and Shapiro, 1989; Destouni and Cvetkovic, 1991; Bellin *et al.*, 1992; Bellin *et al.*, 1993; Bosma *et al.*, 1993; Tompson, 1993; Bosma *et al.*, 1994*a*). In studies by Gelhar and Axness (1983), Dagan (1984, 1988), and Rubin (1990) nonreactive solutes were considered and they focused on the spatial variability of soil physical parameters. More recent work by Bellin *et al.* (1993), Bosma *et al.* (1993), Cvetkovic and Shapiro (1989), and Destouni and Cvetkovic (1991) have also considered the reactivity of the solute. Spatial variability of adsorption parameters and reaction rate constants was taken into account. Whereas interest has been focused mainly on linearly adsorbing solutes, Tompson (1993) and Bosma *et al.* (1994*a*) used nonlinear relationships to describe the solute adsorption isotherm. Tompson (1993) compared effects of various relationships in a three-dimensional study, demonstrating important qualitative nonlinear behaviour. Bosma *et al.* (1994*a*) described expected plume behaviour of an instantaneously injected solute in two-dimensional porous media, using a Monte Carlo approach.

One of the important effects of nonlinear adsorption, shown by Bosma *et al.* (1994*b*), is the relevance of the way of solute injection. An instantaneously injected plume moves with a decreasing average velocity, which is in contrast with a linearly adsorbing solute. Bosma and Van der Zee (1993) showed for a one-dimensional problem that in case of a continuous injection of a nonlinearly adsorbing solute the front moves at the same velocity as the linearly adsorbing solute. The front shape, however, is different in these cases.

The purpose of this study is to assess the dispersive behaviour of a continuously injected, nonlinearly adsorbing solute in heterogeneous formations. The source is located along a line with a size equal to the transverse dimension of the flow domain. A similar study was performed by Bosma and Van der Zee (1993), in which transverse spreading was not taken into account, as the flow domain consisted of a large number of noninteracting stream tubes, representing a semi-two-dimensional domain. An important aspect here is to study the effect of the transverse solute displacement. Accordingly, the effect of nonlinear adsorption is studied and compared to results of linearly adsorbing solutes. Additional calculations are performed to assess the influence of the degree of heterogeneity. Cases with either chemical or physical heterogeneity are considered in order to decompose the effects of both phenomena.

7.2 Formulation of the problem

Transport of an adsorbing solute in a two-dimensional porous medium can be described by

$$\frac{\partial c(\mathbf{x},t)}{\partial t}+\frac{\partial q(\mathbf{x},t)}{\partial t}=\nabla\cdot[\mathbf{D}\cdot\nabla c(\mathbf{x},t)]-\mathbf{v}(\mathbf{x})\cdot\nabla c(\mathbf{x},t) \qquad \mathbf{x}=(x_1,x_2) \tag{7.1}$$

where c is the amount of solute in the liquid phase (ML^{-3}), $\mathbf{D}$ is the pore scale dispersion tensor (LT^{-2}), $\mathbf{v}$ is the heterogeneous velocity field (LT^{-1}) and $\mathbf{x}$ and t are space (L) and time (T) variables. The amount of solute in the solid phase (on a volumetric base) q (ML^{-3}), is related to the concentration in solution, according to

$$q(\mathbf{x},t)=K_F(\mathbf{x})\,[c(\mathbf{x},t)]^n \tag{7.2}$$

With (7.1)-(7.2), no production or decay of the solute is assumed and kinetic sorption effects are not taken into account. The latter assumption can, for several solutes, be made in view of the characteristic time scale of the transport processes in groundwater systems. The nonlinear relationship (7.2), known as the Freundlich equation, is often used to describe adsorption of heavy metals and pesticides with $0<n<1$ (De Haan *et al.*, 1987; Calvet *et al.*, 1980).

The equations (7.1)-(7.2) describe reactive solute transport in physically and chemically heterogeneous porous media. The sorption coefficient K_F ($M^{1-n}L^{3(n-1)}$) is spatially variable due to spatial variability of soil properties like *p*H, organic matter content, and clay content. In (7.2) the parameter n is assumed constant. Chardon (1984) found, for solutes like cadmium and copper, very small changes in n values for different soil types.

In a physically and chemically heterogeneous domain, the elements of the dispersion tensor $\mathbf{D}$ are given by (Bear and Verruijt, 1987),

$$D_{ij}=\alpha_T V\delta_{ij}+(\alpha_L-\alpha_T)\frac{V_iV_j}{V} \tag{7.3}$$

where i and j denote the principal directions of flow, δ_{ij} is the Kronecker delta, V is the mean velocity ($V=|\mathbf{v}|$), α_L and α_T are the longitudinal and transverse dispersivities (L).

In this study we analyze the behaviour of a nonlinearly adsorbing solute in a physically or chemically heterogeneous two-dimensional porous medium, continuously injected along a line source perpendicular to the direction of flow. Initially, no solute is present, i.e. $c(\mathbf{x},t=0)=0$. The continuous line source is described by $c(x_1=0,x_2,t)=c_0$, where c_0 is the feed concentration (ML^{-3}).

Steady state water flow is described by the mass conservation equation, i.e.

$$\nabla\cdot[K(\mathbf{x})\nabla\Phi(\mathbf{x})]=0 \tag{7.4a}$$

$$\mathbf{v}(\mathbf{x})=-K(\mathbf{x})/\theta\nabla\Phi(\mathbf{x}) \tag{7.4b}$$

where K is the hydraulic conductivity (LT^{-1}), Φ is the hydraulic head (L) and θ is the water filled porosity. Typical boundary conditions used to solve (7.4) are constant hydraulic heads at two opposite domain boundaries and no flow conditions at the other boundaries. In a physically heterogeneous domain, the hydraulic conductivity is spatially variable.

Effects of spatial variation of soil properties can be characterized with spatial moments (Valocchi, 1989). Prediction of concentrations at specific points in the flow domain is subject to a large degree of uncertainty (Dagan, 1989) and it is often sufficient to calculate the first- and second-order spatial moments to characterize the position and shape of the solute body or solute plume. For a continuously injected solute plume the spatial moments are defined as

$$m(t)=-\int_{\mathbf{R}^2} c'(\mathbf{x},t)d\mathbf{x} \tag{7.5}$$

$$\mu_j(t)=-\frac{1}{m(t)}\int_{\mathbf{R}^2} x_j\, c'(\mathbf{x},t)d\mathbf{x} \tag{7.6}$$

$$\sigma_{jl}^2(t)=-\frac{1}{m(t)}\int_{\mathbf{R}^2} (x_j-\mu_j(t))(x_l-\mu_l(t))\, c'(\mathbf{x},t)d\mathbf{x} \tag{7.7}$$

In (7.5)-(7.7), the probability density function (pdf) is given by the negative derivative of $c(\mathbf{x},t)$, because $c(\mathbf{x},t)$ is related to the distribution function of the

travel distance x_j. Accordingly, the spatial moments of a continuously injected plume describe the part of the plume where the concentration changes from the initial concentration to the feed concentration of the plume, i.e. the concentration front. The spreading behaviour of a continuously injected plume was characterized earlier in this manner by Bosma and Van der Zee (1993). However, in that study the flow domain was one-dimensional, thus excluding transverse dispersion effects, whereas here this limitation is not effective.

The zeroth-order moment, given by the expression (7.5), describes the total mass in the liquid phase (M) of the domain in which the front is present, μ_j is the position of the centre of mass in the x_1 or x_2 direction (L), and σ_{jl}^2 is the second central moment or front variance (L^2). Bosma *et al.* (1993) considered the second order moments with $j=l$ and $j,l=1,2$. In this study, only the longitudinal moments ($j=l=1$) are of interest, for we consider a line source with a dimension equal to the transverse dimension of the flow domain.

7.3 Numerical procedure

7.3.1 *Eulerian-Lagrangian approach*

Spatial variation of the adsorption coefficient and the hydraulic conductivity is incorporated by assuming a lognormal distribution of K_F and K, according to

$$K_F(\mathbf{x})=\exp[W(\mathbf{x})] \tag{7.8a}$$

$$K(\mathbf{x})=\exp[Y(\mathbf{x})] \tag{7.8b}$$

where W and Y are normally distributed random variables with mean $\langle W\rangle$ and $\langle Y\rangle$ and variance σ_W^2 and σ_Y^2. The spatial correlation of the adsorption coefficient is modeled by an isotropic exponential covariance function (Gelhar and Axness, 1983; Dagan, 1989)

$$C_W(\mathbf{r})=\sigma_W^2\exp\left(\frac{-|\mathbf{r}|}{l_W}\right) \tag{7.9a}$$

$$C_Y(\mathbf{r})=\sigma_Y^2\exp(\frac{-|\mathbf{r}|}{l_Y}) \qquad (7.9b)$$

where $|\mathbf{r}|$ is the lag distance (L) and l_W and l_Y are the integral scales of W and Y (L).

The solution of the transport equations (7.2)-(7.3) with initial and boundary condition (7.5) is not trivial, because chemical or physical heterogeneity, nonlinearity of adsorption and continuous solute injection reduce the applicability of many known Eulerian and Lagrangian numerical methods. Eulerian methods are in general not suitable for advection dominated problems with spatially variable soil properties, whereas the continuous injection of the solute does not allow to make optimal use of straightforward Lagrangian methods. In this study, a mixed Eulerian-Lagrangian method was used. Similar approaches, which solve the advection part with a Lagrangian particle tracking method and the dispersion part with an Eulerian finite difference or finite element method, were described by Neuman (1984), Cheng *et al.* (1984), Farmer (1987) and Yeh (1990).

To use the mixed Eulerian-Lagrangian method to solve the transport problem, (7.1)-(7.2) can be reformulated, according to

$$R_c(\mathbf{x},t)\frac{\partial c(\mathbf{x},t)}{\partial t}=\nabla\cdot[\mathbf{D}\cdot\nabla c(\mathbf{x},t)]-\mathbf{v}(\mathbf{x})\cdot\nabla c(\mathbf{x},t) \qquad (7.10)$$

$$R_c(\mathbf{x},t)=1+\frac{dq}{dc}=1+nK_F(\mathbf{x})[c(\mathbf{x},t)]^{n-1} \qquad (7.11)$$

where, due to nonlinearity of adsorption, R_c is the concentration dependent retardation coefficient. Equation (7.10) can be rewritten as

$$\frac{Dc(\mathbf{x},t)}{Dt}=\frac{1}{R_c(\mathbf{x},t)}\nabla\cdot[\mathbf{D}\cdot\nabla c(\mathbf{x},t)] \qquad (7.12)$$

where $Dc(\mathbf{x},t)/Dt$ is the substantial derivative,

$$\frac{Dc(\mathbf{x},t)}{Dt} = \frac{\partial c(\mathbf{x},t)}{\partial t} + \frac{\mathbf{v}(\mathbf{x})}{R_c(\mathbf{x},t)} \nabla c(\mathbf{x},t) \tag{7.13}$$

The substantial derivative (7.13) describes the concentration change along a streamline in the considered flow domain. Equation (7.13) allows calculation of the concentration change due to advection alone. This part is the Lagrangian part of the problem and it requires the discretization of the injected mass into particles which move along a streamline. Accordingly, each particle is associated with a position and a concentration. During each time step the new position of each particle, due to advection alone, is proportional to the length of the time increment and the velocity at the location of the particle. The velocity at a specific location in the domain is determined by interpolation of the velocities in the Eulerian grid points in the surrounding area of the particle location. The dispersion part of (7.10), represented by (7.12), can be solved using an Eulerian finite difference approximation of (7.12). This yields a concentration change in each grid cell rather than a concentration change of each particle. This procedure requires transformation of particle concentrations to concentrations at fixed grid cells.

7.3.2 *Limitations of Eulerian-Lagrangian approach to nonlinear adsorption*

Previous applications of the Eulerian-Lagrangian method to transport problems (Neuman, 1984; Cheng *et al.*, 1984; Farmer, 1987) were limited to nonreactive or linearly adsorbing solutes. Applying an Eulerian-Lagrangian method to solute transport problems subject to nonlinear adsorption causes a few difficulties. First, the concentration dependency of the retardation coefficient requires the use of the concentration of the previous time step to determine R_c for the current time step. The error caused by this problem can be minimized by using small time steps.

A second consequence of nonlinear adsorption is the requirement of pore scale dispersion or molecular diffusion in the transport calculations. The concentration dependency of the retardation coefficient, shown in (7.11), which is used to determine the retarded velocity field introduces errors if pore scale dispersion or molecular diffusion is ignored. With (7.11) can be seen that each concentration has a different retardation coefficient and that R_c increases if c decreases. This increase causes a self sharpening front with an average retardation

coefficient that depends only on the initial and the feed concentration (c_i and c_0, respectively), for a chemically homogeneous medium given by

$$\langle R \rangle = 1 + \frac{q_0 - q_i}{c_0 - c_i} \tag{7.14}$$

which reduces to (if c_i=0) (Bosma and Van der Zee, 1993)

$$\langle R \rangle = 1 + K_F c_0^{n-1} \tag{7.15}$$

However, if R_c is calculated for a case with no pore scale dispersion or molecular diffusion, the concentration along a streamline is either equal to c_i or c_0. Calculation of R_c with (7.11) will lead to an overestimation of the front velocity. An increasing amount of pore scale dispersion or molecular diffusion enhances local spreading of concentrations, which reduces the error of the average front retardation coefficient. The described problem shows that one of the major advantages of mixed Eulerian-Lagrangian methods, i.e. applicability to transport problems with Peclet numbers ranging from 0 to infinity (Yeh, 1990; Neuman, 1984; Cheng 1984), is no longer valid for nonlinearly adsorbing solutes. The range of Peclet numbers that can be covered depends on discretization, degree of nonlinearity of the adsorption isotherm, average adsorption coefficient and degree of heterogeneity of physical and chemical properties.

7.3.3 *Monte Carlo procedure*

To assess the expected behaviour, calculations are performed by a Monte Carlo approach. During a Monte Carlo iteration a realization of a random field with spatial correlation is generated and the velocity field is obtained. In case of chemical heterogeneity, a random K_F field is generated and the solution of the velocity field **v** is straightforward. With physical heterogeneity a random K field is obtained, followed by the solution of (7.4) with a suitable finite difference method. The mixed Eulerian-Lagrangian method is used to solve the transport problem (7.10)-(7.11). The solution of (7.10)-(7.11) is the concentration field as a function of time, $c(\mathbf{x},t)$. Effects of spatially variable properties are not easily depicted from a concentration field. Moreover, in a two-dimensional case it is difficult to visually show the effect as a function of time. Spatial moments can be

more useful for this purpose (Valocchi, 1989). Because we are dealing with a solute injected along a line source, our interest is focused only on moments in the longitudinal direction. The pdf in (7.5)-(7.7) is obtained by averaging the concentration field in the transverse direction. This yields a one-dimensional concentration distribution of which the first and second central moment (variance) can be calculated with a numerical integration method, described earlier by Bosma and Van der Zee (1993). The first moment describes the depth of the front and the variance is a measure for the width of the concentration front. Figure 7.1 shows a two-dimensional concentration field with the corresponding averaged concentration distribution and the pdf obtained with numerical differentiation.

In this study we analyze the effects of nonlinear adsorption and heterogeneity on the movement and spreading of a continuously injected solute in a two-dimensional domain. Results of a nonlinearly adsorbing solute will be compared with the linear adsorption case. The numerical calculations are performed for a two-dimensional domain with a length and width of 33.3 integral scales. Initially, no solute is present in the domain and the feed concentration c_0 is 0.02. We consider a strongly adsorbed solute with an average retardation coefficient, $\langle R\rangle=1+(c_0)^{n-1}\cdot\exp(\langle W\rangle+\sigma_W^2/2)$, of 40. With a constant n of 2/3 for the nonlinear case $\langle W\rangle$ is adapted for different values of σ_W^2. For the linearly adsorbing solute, n=1 and $\langle W\rangle$ is adjusted accordingly to obtain an average retardation coefficient of 40. The mean water velocity is 1 in the longitudinal and 0 in the transverse direction.

In the cases of chemical heterogeneity (σ_Y^2=0), we consider values of σ_W^2 from 0.086 to 0.8. In the physically heterogeneous case (σ_W^2=0), several computations have been performed with σ_Y^2=0.022 up to 0.8. The problem of combined physical and chemical heterogeneity has not been taken into account due to numerical limitations that particularly play a role with continuous injection and nonlinear adsorption. In the computed cases effects of different degrees of chemical and physical heterogeneity are assessed by variation of σ_W^2 and σ_Y^2. Subsequently, the effects of the longitudinal and transverse dispersivity is shown. The longitudinal dispersivity was shown to be important for the development of a traveling wave concentration front in the one-dimensional case (Van der Zee, 1990; Bosma and Van der Zee, 1993). An important issue is whether, and under which circumstances a traveling wave will develop in a two-dimensional heterogeneous porous medium.

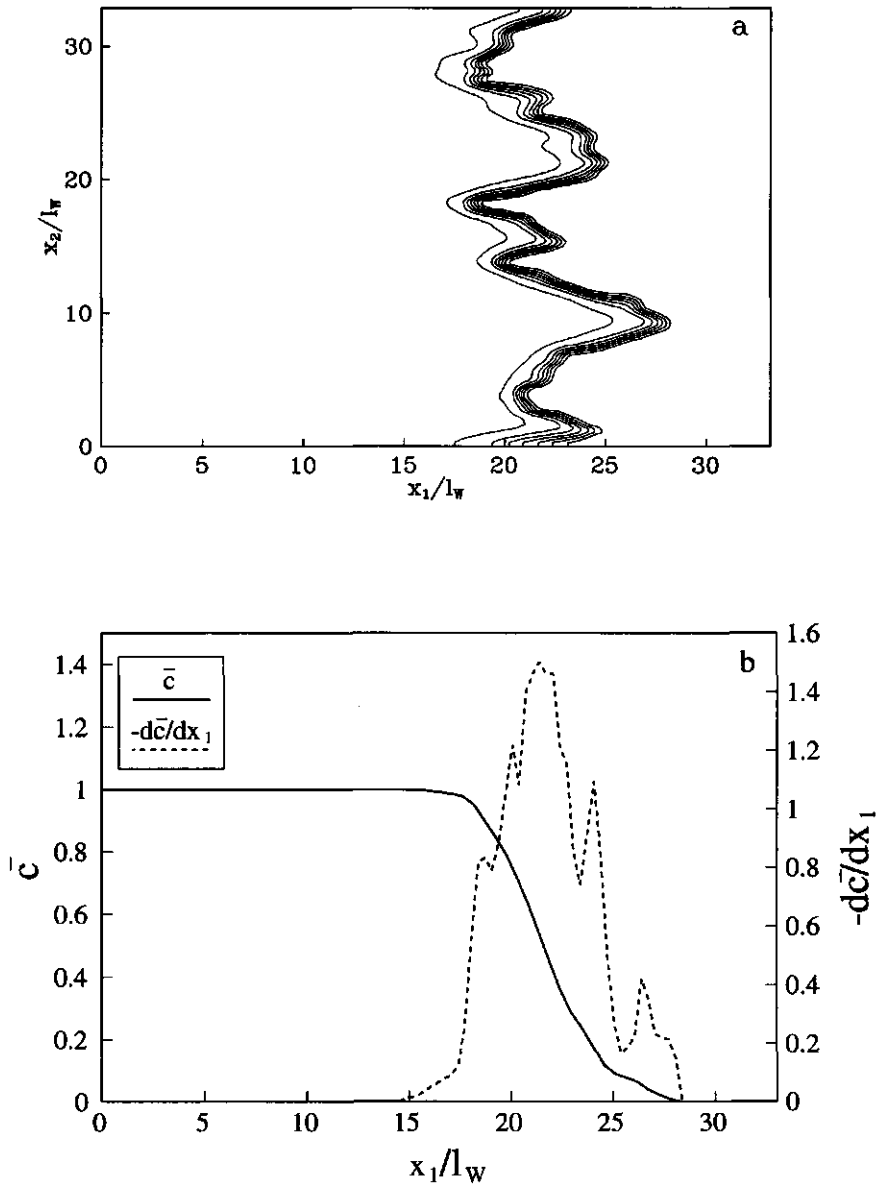

Figure 7.1 Iso-concentration lines (*a*) and averaged concentration front with corresponding pdf (*b*) for case with chemical heterogeneity (σ_w^2=0.2) and nonlinear adsorption.

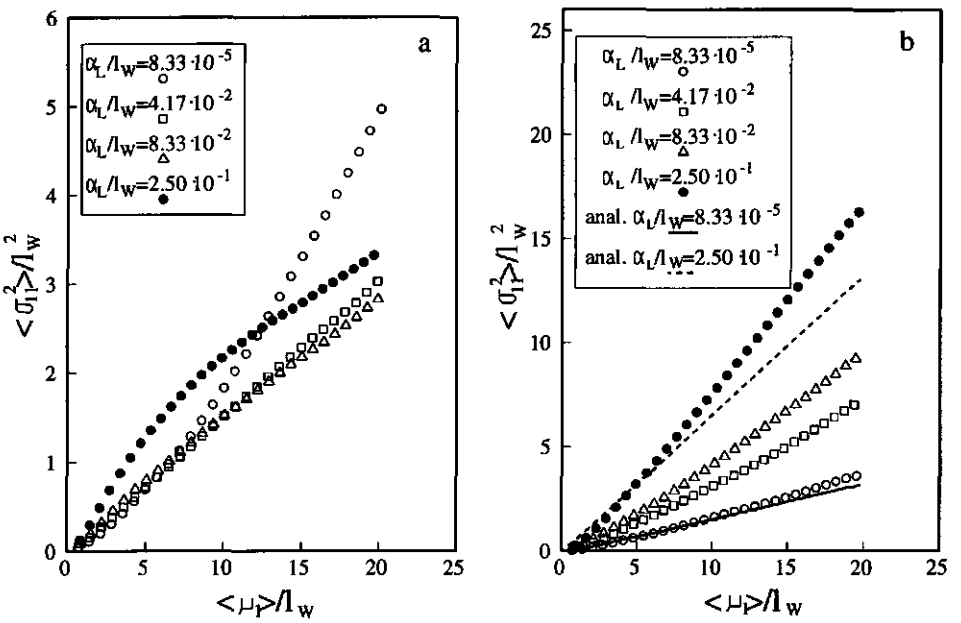

Figure 7.2 Mean front variance for nonlinear (*a*) and linear (*b*) adsorption with chemical heterogeneity (σ_w^2=0.0864) for various dispersivities, α_L/α_T=2. Lines in Fig. 7.2*b* represent the analytical solution of Bellin *et al.* (1993).

7.4 **Results and discussion**

7.4.1 *Chemical heterogeneity*

The effect of several values of the longitudinal and transverse dispersivities for a mild degree of chemical heterogeneity, σ_w^2=0.086, is shown in Figure 7.2. In this figure, the mean front variance $\langle\sigma_{11}^2\rangle$ is obtained by averaging over the Monte Carlo realizations. The results are shown as a function of the longitudinal front displacement, $\langle\mu_1\rangle$. In these cases, with a continuous injection, this is equivalent to dimensionless time because of a constant mean front velocity. For all shown cases the ratio α_L/α_T= 2. In Figure 7.2*a*, we see the results for the case of nonlinear adsorption. In case of very small pore scale dispersion, i.e. α_L=8.33·10$^{-5}l_W$, there is little effect of nonlinear adsorption. The results for this combination of α_L and α_T are similar to the results for linear adsorption (Fig. 7.2*b*).

In general, the downstream effect of nonlinear adsorption is a local steepening of the front due to stronger adsorption of lower concentrations. However, in this case locally the fronts remain steep due to a negligible degree of pore scale dispersion. The spreading of the averaged concentration front is determined only by the spatial variability of the adsorption coefficient. Consequently, the analytical solution of Bellin *et al.* (1993), derived for linearly adsorbing solutes, can be applied to describe the results with small pore scale dispersion.

If we consider the cases with an increasing amount of pore scale dispersion, the effect of nonlinear adsorption becomes more apparent. In case of linear adsorption (Fig. 7.2*b*), an increase of pore scale dispersion enhances the spreading of the averaged concentration front. This effect allows the summation of the contribution of pore scale dispersion and heterogeneity to obtain an effective macroscopic dispersion coefficient (Dagan, 1989). This is demonstrated by the analytical results, given by the expression of Bellin *et al.* (1993) added to the contribution of pore scale dispersion. In case of nonlinear adsorption, however, pore scale dispersion has an opposite effect. For large displacements, the averaged fronts tend to steepen with larger pore scale dispersion, resulting in decreasing $\langle\sigma_{11}{}^2\rangle$ with increasing dispersion. This effect is caused by the mutual effect of transverse dispersion and nonlinear adsorption. In the one-dimensional case, Van der Zee (1990) and Bosma and Van der Zee (1993) showed the traveling wave behaviour, i.e. steep fronts with a constant front shape. They demonstrated that the longitudinal spreading due to pore scale dispersion is resisted by nonlinear adsorption. Consequently, in the two-dimensional case transverse spreading becomes relatively more important, which causes the decrease of the front variance. Heterogeneity still dominates the front spreading process, resulting in a linear increase of the front variance as a function of the displacement. Nevertheless, the slope of the increasing variance is reduced with increasing pore scale dispersion.

For smaller displacements, the effect of pore scale dispersion corresponds more to the expectation of increasing front variance with increasing dispersivity. At a certain point, the effects of nonlinear adsorption and, consequently, transverse dispersion become more apparent, causing a slower increase of the variance. For larger dispersivity, $\alpha_L=0.25l_W$, this effect is clearly illustrated. Larger front variances at small travel times due to longitudinal dispersion are followed by a slow increase of $\langle\sigma_{11}{}^2\rangle$ as a function of the displacement.

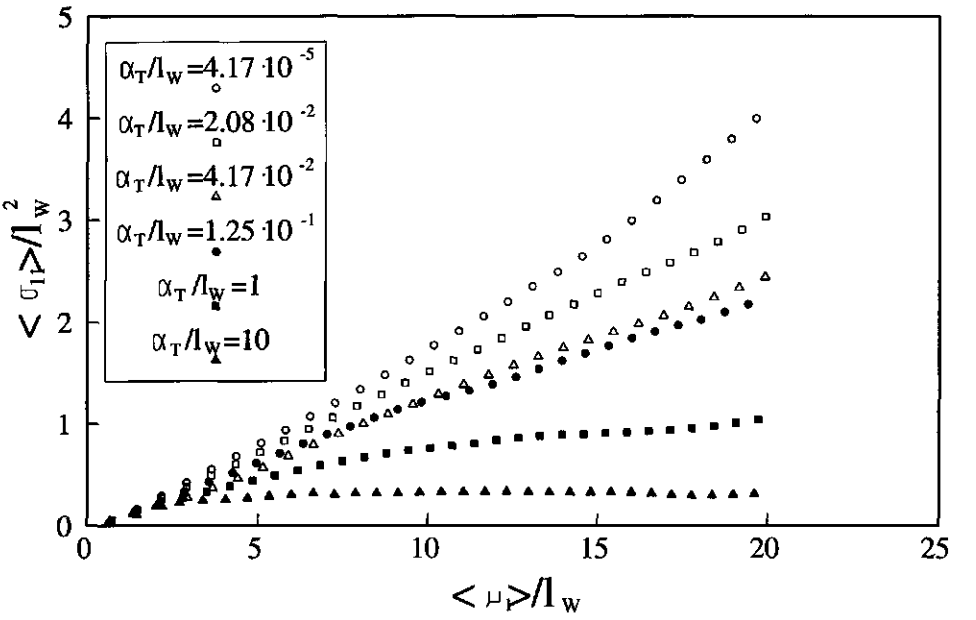

Figure 7.3 Mean front variance for nonlinear adsorption with chemical heterogeneity (σ_W^2=0.0864) for various transverse dispersivities, $\alpha_L=4.7\cdot10^{-2}l_W$.

The effect of the transverse dispersivity is illustrated more explicitly in Figure 7.3. Here, results of averaged front variances are shown for nonlinear adsorption with σ_W^2=0.086 and $\alpha_L=4.17\cdot10^{-2}l_W$ for different values of α_T. Corresponding to the results of Figure 7.2, we see a decreasing variance with an increasing α_T. For large transverse dispersivities, i.e. $\alpha_T=1l_W$ and $\alpha_T=10l_W$, we see that the front variance approaches a constant value. In that case, the heterogeneous porous medium is effectively homogeneous and a traveling wave front will develop. For the case with infinitely large transverse dispersivity, the value of the front variance can be obtained from the analytical expression derived by Bosma and Van der Zee (1993). Note that in practical cases these values of transverse dispersivities are not applicable and that front spreading is determined by the combination of spatial variability and transverse dispersion.

The effect of pore scale dispersion and nonlinear adsorption was shown in Figures 7.2 and 7.3 for a mild degree of heterogeneity. Figure 7.4 shows results of similar calculations for σ_W^2=0.2 (Fig. 7.4*a*) and σ_W^2=0.8 (Fig. 7.4*b*). The results

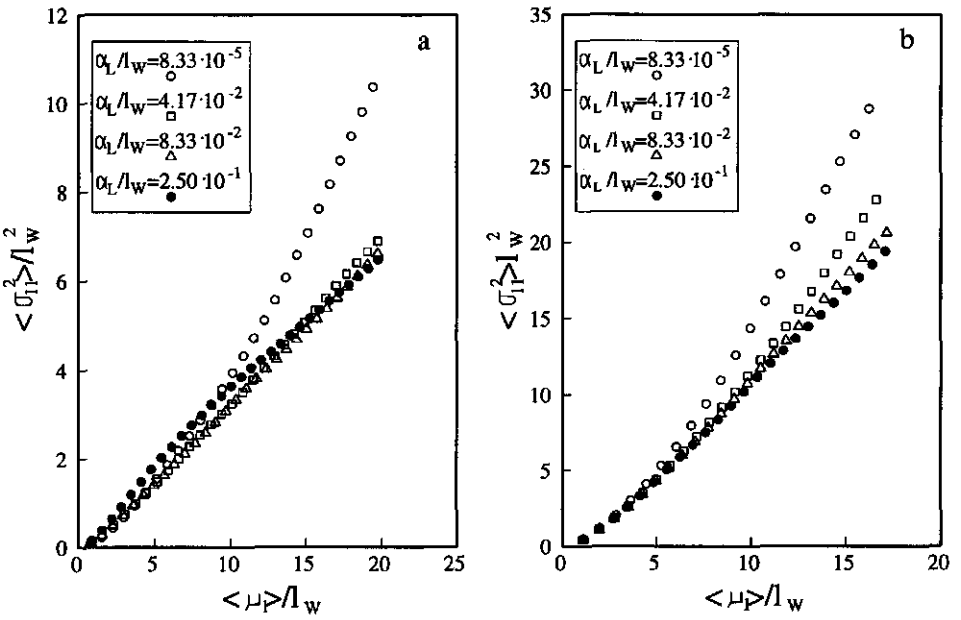

Figure 7.4 Mean front variance for nonlinear adsorption with chemical heterogeneity, σ_w^2=0.2 (*a*) and σ_w^2=0.8 (*b*) for various dispersivities, α_L/α_T=2.

show that an increasing degree of heterogeneity strongly enhances the degree of front spreading (compare the vertical axes of Figures 7.2 and 7.4). We see that also for larger degree of heterogeneity pore scale dispersion causes a reduction of the averaged front variance. For σ_w^2=0.2 there is still a slight increase visible at small travel distances with increasing α_L. For σ_w^2=0.8 the spatial variability of K_F dominates the front spreading, even at small travel distance. Similar to the other cases the variance is reduced for larger displacements. For larger variances, however, this reduction is less pronounced and less effective.

The effect of heterogeneity, with constant pore scale dispersion, is demonstrated in Figure 7.5. Here we show the results of the nonlinear adsorption case with α_L=8.33·10$^{-5}l_w$ (Fig. 7.5*a*) and α_L=8.33·10$^{-2}l_w$ (Fig. 7.5*b*) for different values of σ_w^2. In all cases α_L/α_T=2. In Figure 7.5*a* the results of the analytical solution of Bellin *et al.* (1993) for linear adsorption are also given. This solution is applicable here because in case of small pore scale dispersion the averaged front variance is not affected by nonlinear adsorption (with a continuous injection). Only

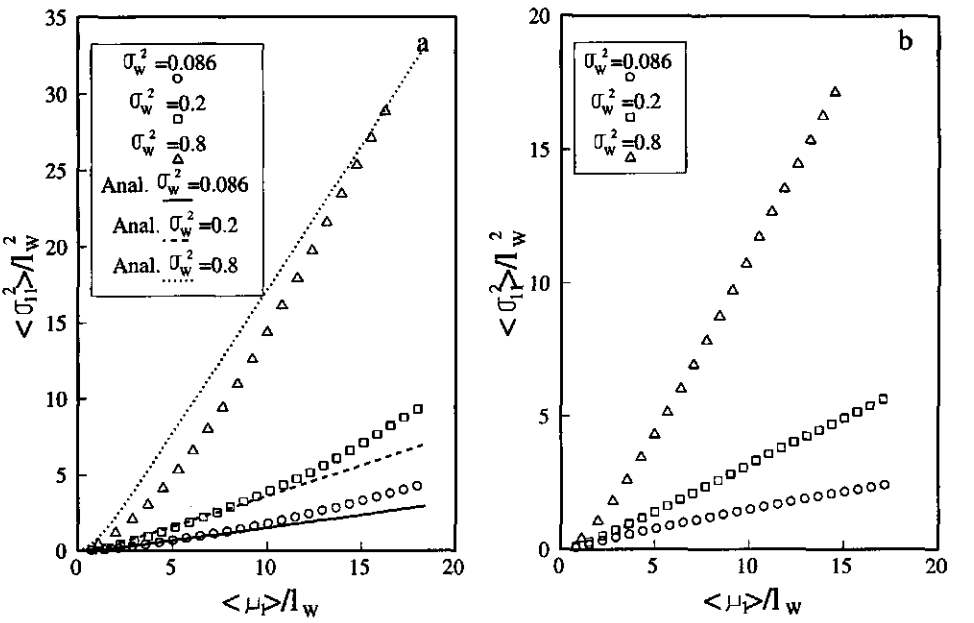

Figure 7.5 Mean front variance for nonlinear adsorption with $\alpha_L=8.33\cdot10^{-5}l_w$ (*a*) and $\alpha_L=8.33\cdot10^{-2}l_w$ (*b*) for various degrees of chemical heterogeneity. Lines in Fig. 7.5*a* represent the analytical solution of Bellin *et al.* (1993) for linear adsorption.

the displacement is affected through the front retardation coefficient. The enhancing effect of σ_w^2 again becomes apparent in Figure 7.5*a*. The analytical and numerical results agree reasonably well, although there is a slight deviation in growth rate of the expected front variances. These deviations are of the same order of magnitude as the deviations shown by Bosma *et al.* (1993) for larger degrees of chemical heterogeneity. In case of larger pore scale dispersion (Fig. 7.5*b*), the analytical solution is not applicable. Compared with results of Figure 7.5*a* there is a clear decrease of front variances due to increasing transverse spreading and effects of nonlinear adsorption on the longitudinal direction. The dominating effect of the degree of heterogeneity is still apparent, resulting in a linearly increase of the front variances with the front displacement at large travel times.

7.4.2 *Physical heterogeneity*

In the previous paragraph we have shown the effect of chemical heterogeneity and nonlinear adsorption on the front spreading of a continuously injected solute. To assess the separate effects of physical heterogeneity, several computations have been performed with a spatially variable hydraulic conductivity. Corresponding to the cases with chemical heterogeneity we have studied the effects of pore scale dispersion and of the degree of heterogeneity.

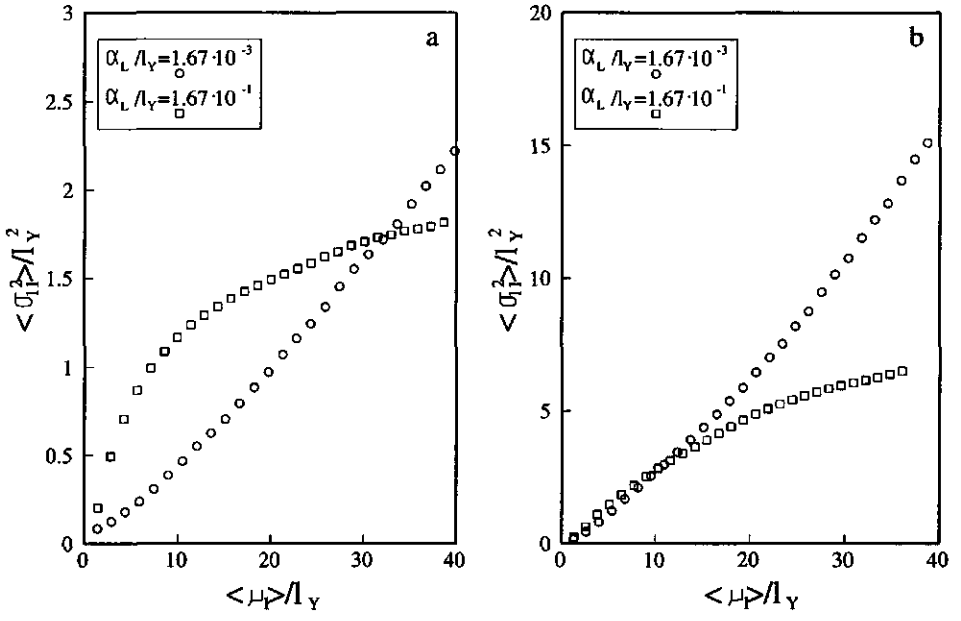

Figure 7.6 Mean front variance for nonlinear adsorption with physical heterogeneity, $\sigma_Y^2=0.02$ (*a*) and $\sigma_Y^2=0.2$ (*b*) for various dispersivities, $\alpha_L/\alpha_T=2$.

In Figure 7.6 we show the mean front variance, obtained by averaging over many Monte Carlo realizations, for two values of pore scale dispersion. In all shown cases $\alpha_L/\alpha_T=2$. The results are given for two mild degrees of physical heterogeneity, i.e. $\sigma_Y^2=0.02$ (Fig. 7.6*a*) and $\sigma_Y^2=0.2$ (Fig. 7.6*b*). The results in Figure 7.6 correspond to the results with chemical heterogeneity. In Figure 7.6*a* we see a clear example of the effect of increasing pore scale dispersion with nonlinear adsorption. At small displacements, an increase of $\langle\sigma_{11}^2\rangle$ is visible due to the

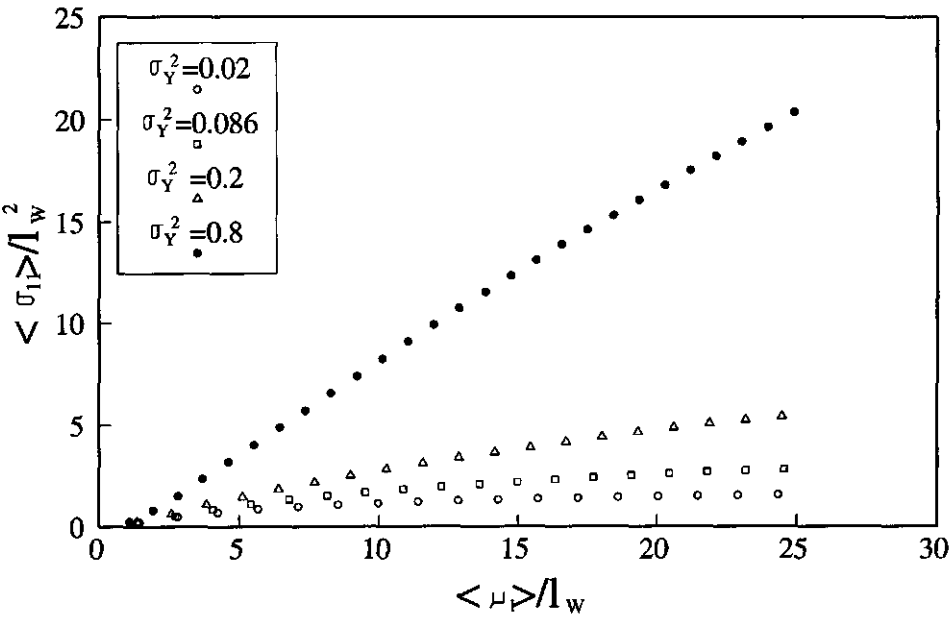

Figure 7.7 Mean front variance for nonlinear adsorption with α_L=0.167l_Y for various degrees of physical heterogeneity.

spreading effect of longitudinal dispersion. At larger displacements, the front steepening effect of nonlinear adsorption becomes more profound and counteracts the longitudinal spreading. Transverse spreading becomes more important, resulting in a slower increase of the front variance with respect to the case with small pore scale dispersion. The effect is rather large due to a small degree of physical heterogeneity.

With a larger degree of heterogeneity (Fig. 7.6*b*), the results are similar. Increasing pore scale dispersion only slightly enhances front spreading at small displacements, and at larger displacements the effect of nonlinear adsorption becomes apparent. This results in a slower increase of $\langle\sigma_{11}{}^2\rangle$ as a function of the front displacement, compared with the case with small pore scale dispersion. Although in this case, with larger $\sigma_Y{}^2$, the effect of α_L is negligible at small displacements, at large displacements the variance reduction is substantial. Both figures show that at large travel times spatial variability of the hydraulic conductivity dominates the front spreading process, resulting in a linear increase

of $\langle\sigma_{11}^2\rangle$ as a function of the displacement.

In Figure 7.7 we demonstrate the effect of several degrees of physical heterogeneity on front spreading. In all shown cases $\alpha_L=0.167I_Y$ and $\alpha_L/\alpha_T=2$. The results of this figure correspond to results with various degrees of chemical heterogeneity. There is a profound enhancement of front spreading with increasing physical heterogeneity. Whereas for $\sigma_Y^2=0.02$ and $\sigma_Y^2=0.086$ some effects of pore scale dispersion and nonlinear adsorption are still visible for small displacements (compare the shape of the curves with Figure 7.6*a*), this is not the case for $\sigma_Y^2=0.8$. Here, also at small displacements spatial variability of the hydraulic conductivity dominates the front spreading, resulting in a linear increase of $\langle\sigma_{11}^2\rangle$ with $\langle\mu_1\rangle$. For larger displacements, nonlinear adsorption and pore scale dispersion decrease the slope, and therefore the rate of growth of the average front spreading.

7.5 Conclusions

We considered the spreading of a reactive solute, continuously injected in two-dimensional either chemically or physically heterogeneous porous formations. Solute adsorption was described by the nonlinear Freundlich isotherm. The solute was injected along a line source with a dimension equal to the transverse dimension of the flow domain. In the chemically heterogeneous case, the adsorption coefficient K_F was assumed randomly variable according to a lognormal distribution with an isotropic exponential autocovariance function. Variation of the hydraulic conductivity K was modeled in a similar way in the physically heterogeneous case. Spatial moments are used to describe the position and the spreading of the averaged concentration front. Due to the continuous injection, the pdf, which is necessary to compute the spatial moments, is obtained by the derivative of the concentration front.

Results are obtained by numerical solution of the transport problem. The combination of continuous injection, nonlinear adsorption, spatial variability and multi-dimensionality limits application of a straightforward technique. The calculations have been performed with a mixed Eulerian-Lagrangian method. The convective part of the problem is solved by a Lagrangian approach, using particles to represent the solute mass. The concentration change due to pore scale dispersion is obtained by an Eulerian finite difference method. Application of such methods

to cases with continuous injection and nonlinear adsorption ($0<n<1$) requires pore scale dispersion to enforce a local front spreading. Without local front spreading, the front retardation coefficient is underestimated, resulting in an overestimation of the front velocity.

The results of the chemically heterogeneous cases have shown the distinct effect of the contribution of nonlinear adsorption and pore scale dispersion. Whereas in case of linear adsorption an increase of pore scale dispersion enhances the longitudinal spreading of the front, in case of nonlinear adsorption longitudinal spreading is hindered by the front steepening effect. Local transverse spreading becomes relatively more important and the average front spreading is reduced. For small displacements, larger dispersivities enhance the front spreading (especially for small degrees of heterogeneity), but at larger displacements the effects of nonlinear adsorption cause a reduction of the front variances. At large displacements, the variance grows linearly with time but the slope is decreased due to the combination of pore scale dispersion and nonlinear adsorption.

Calculations with variable transverse dispersivities confirm the front spreading phenomena for continuous injection, pore scale dispersion and nonlinear adsorption. Moreover, these calculations show that in an effectively homogeneous two-dimensional case (α_T>>integral scale) the front variance approaches a constant value, which implies effectively a traveling wave type behaviour.

Results from additional computations in physically heterogeneous domains corroborate the findings of the chemically heterogeneous domain. In the considered cases, the effects of physical and chemical heterogeneity are of equal order of magnitude. The combined effect of pore scale dispersion and nonlinear adsorption is also apparent with spatially variable hydraulic conductivities.

References

Bear, J., Hydraulics of groundwater, McGraw Hill, New York, 1979.

Bellin, A., P. Salandin, and A. Rinaldo, Dispersion in heterogeneous porous formations: statistics, first-order theories, convergence of computations, Water Resour. Res., 28, 2211-2227, 1992.

Bellin, A., A. Rinaldo, W.J.P. Bosma, S.E.A.T.M. van der Zee, and Y. Rubin, Linear equilibrium adsorbing solute transport in physically and chemically heterogeneous porous formations, 1. Analytical solutions, Water Resour. Res., 29, 4019-4030, 1993.

Bosma, W.J.P., and S.E.A.T.M. van der Zee, Transport of reacting solute in a one-dimensional chemically heterogeneous porous medium, Water Resour. Res., 29, 117-131, 1993.

Bosma, W.J.P., A. Bellin, S.E.A.T.M. van der Zee, and A. Rinaldo, Linear equilibrium adsorbing solute transport in physically and chemically heterogeneous porous formations, 2. Numerical results, Water Resour. Res., 29, 4031-4043, 1993.

Bosma, W.J.P., S.E.A.T.M. Van der Zee, and C.J. Van Duijn, Plume development of a nonlinearly adsorbing solute in heterogeneous porous formations, Water Resour. Res., submitted, 1994*a*.

Bosma, W.J.P., S.E.A.T.M. van der Zee, A. Bellin, and A. Rinaldo, Instantaneous injection of a nonlinearly adsorbing solute in a heterogeneous aquifer, in: Transport and reactive processes in aquifers, edited by T.H. Dracos and F. Stauffer, pp. 411-417, A.A. Balkema, Rotterdam, 1994*b*.

Calvet, R., M. Tercé, and J.C. Arvieu, Adsorption des pesticides par les sols et leurs constituants. III. Caractéristiques générals de l'adsorption des pesticides, Ann. Agron. 31, 239-257, 1980.

Chardon, W.J., Mobiliteit van cadmium in de bodem, Ph.D. thesis, 200 pp., Wageningen Agricultural University, The Netherlands, 1984.

Cheng, R.T., V. Casulli, and S.N. Milford, Eulerian-Lagrangian solution of the convection-dispersion equation in natural coordinates, Water Resour. Res., 20, 944-952, 1984.

Cvetkovic, V.D., and A.M. Shapiro, Solute advection in stratified formations, Water Resour. Res., 25, 1283-1289, 1989.

Dagan, G., Solute transport in heterogeneous porous formations, J. Fluid Mech., 145, 151-177, 1984.

Dagan, G., Time-dependent macrodispersion for solute transport in anisotropic heterogeneous aquifers, Water Resour. Res, 24, 1491-1500, 1988.

Dagan, G., Flow and transport in porous formations, Springer-Verlag, Berlin, 1989.

De Haan, F.A.M., S.E.A.T.M. Van der Zee, and W.H. Van Riemsdijk, The role of soil chemistry and soil physics in protecting soil quality; Variability of sorption and transport of cadmium as an example, Neth. J. Agric. Sci., 35, 347-359, 1987.

Destouni, G., and V. Cvetkovic, Field scale mass arrival of sorptive solute into the groundwater, Water Resour. Res., 27, 1315-1325, 1991.

Farmer, C.L., Moving point techniques, in: Advances in transport phenomena in porous media (J. Bear and M.Y. Corapcioglu, Eds.), NATO ASI Series #128, Nyhoff, Boston, 952-1004, 1987.

Garabedian, S.P., Large-scale dispersive transport in aquifers: Field experiments and reactive transport theory, Ph.D. thesis, Mass. Inst. of Technol., Cambridge, Mass., U.S.A., 1987.

Gelhar, L.W., and C.L. Axness, Three-dimensional stochastic analysis of macrodispersion in aquifers, Water Resour. Res., 19, 161-180, 1983.

Neuman, S.P., Adaptive Eulerian-Lagrangian finite element method for advection-dispersion, Int. J. Num. Meth. Eng., 20, 321-337, 1984.

Rubin, Y., Stochastic modeling of macrodispersion in heterogeneous porous media, Water Resour. Res., 26, 133-141, 1990.

Tompson, A.F.B., Numerical simulation of chemical migration in physically and chemically heterogeneous porous media, Water Resour. Res., 29, 3709-3726, 1993.

Valocchi, A.J., Spatial moment analysis of the transport of kinetically adsorbing solutes through stratified aquifers, Water Resour. Res., 25, 273-279, 1989.

Van der Zee, S.E.A.T.M., Analytical traveling wave solutions for transport with nonlinear and nonequilibrium adsorption, Water Resour. Res., 26, 2563-2578, 1990. (Correction, Water Resour. Res., 27, 983, 1991.)

Yeh, G.T., A Lagrangian-Eulerian method with zoomable hidden fine-mesh approach to solving advection-dispersion equations, Water Resour. Res., 26, 1133-1144, 1994.

Chapter 8

Plume development of a nonlinearly adsorbing solute in heterogeneous porous formations*

Abstract

Transport of nonlinearly adsorbing solutes in homogeneous and heterogeneous porous formations is considered. Initially, a fixed amount of solute is assumed to be present in the domain. Transport is characterized in terms of the first and second spatial moments. Nonlinear equilibrium adsorption is described by the Freundlich isotherm, with the Freundlich exponent n, $0<n<1$. By asymptotic balancing, we derive first order approximations of the limiting behaviour of the plume position and plume growth as a function of time for the homogeneous case. In the heterogeneous case, we consider random variation of a physical (log conductivity) and a chemical (log adsorption coefficient) parameter, both with an isotropic exponential covariance function. Expected behaviour of the relevant spatial moments is obtained by applying a Monte Carlo approach. Individual realizations are solved numerically with a particle tracking scheme in which nonlinear adsorption is accounted for by a time dependent retarded velocity. We assess the effects of varying certain transport parameters, such as the degree of physical and chemical heterogeneity, degree of nonlinearity, the adsorption coefficient and the degree of correlation between hydraulic conductivity and adsorption coefficient. Results of the homogeneous case for a strong degree of nonlinearity show good agreement between the numerical calculations and the limiting analytical expressions. Nonlinear adsorption is shown to have a strong effect on the shape of the plume, especially in longitudinal direction. For the heterogeneous case, the analytical expressions predict well the time dependence of the growth rate of the spatial moments. Variation of the transport parameters demonstrates a dominating effect of the degree of nonlinearity on the plume dimensions, which is hardly affected by the degree of heterogeneity, correlation and the adsorption coefficient. The variance of the mean plume position is affected by all parameters. Although the degree of heterogeneity has a strong impact, the longitudinal and transverse

*by W.J.P. Bosma, S.E.A.T.M. van der Zee and C.J. van Duijn
submitted for publication to *Water Resources Research.*

variances are reduced with respect to the linear adsorption case, due to the large size of nonlinear plumes.

8.1 Introduction

In natural soil and groundwater systems, variation of formation materials causes heterogeneity of physical and chemical properties. It is widely recognized that solute transport is strongly affected by this spatial variability. The effect of a spatially variable hydraulic conductivity on solute dispersion has been thoroughly studied analytically (e.g., Gelhar and Axness, 1983; Neuman *et al.*, 1987; Garabedian, 1987; Dagan, 1982, 1984, 1989) and numerically (e.g., Rubin 1990; Bellin *et al.*, 1992). Both analytical and numerical approaches commonly use stochastic methods to account for the spatially variable hydraulic conductivity. Additionally, existence of spatial variability of soil chemical parameters has been demonstrated by Mackay *et al.* (1986) and Boekhold and Van der Zee (1992). The strong impact of variation of chemical properties on solute transport (e.g., Van der Zee and Van Riemsdijk, 1987; Chrysikopoulos *et al.*, 1990, 1992; Destouni and Cvetkovic, 1991; Bosma and Van der Zee, 1993; Bellin *et al.*, 1993; Bosma *et al.*, 1993; Tompson, 1993) justifies the increasing attention given to chemical heterogeneity. The approaches differ with respect to the chemistry considered. Chrysikopoulos *et al.* (1990, 1992), Bellin *et al.* (1993) and Bosma *et al.* (1993) considered linear equilibrium adsorption, whereas Destouni and Cvetkovic (1991) took into account the spatial variability of parameters which describe linear nonequilibrium adsorption. Van der Zee and Van Riemsdijk (1987) and Bosma and Van der Zee (1993) described the effects of nonlinear adsorption on solute transport. Tompson (1993) studied the behaviour of several equilibrium adsorbing compounds, including a nonlinearly adsorbing solute, in a one realization case in a three-dimensional domain. Bellin *et al.* (1993), Bosma *et al.* (1993) and Tompson (1993) considered both physical and chemical heterogeneity.

In this paper, we study plume development of an initially present finite amount of nonlinearly adsorbing solute. Bosma *et al.* (1994) showed the relevance of the difference between instantaneous and continuous solute injection in case of nonlinear adsorption. Based on an asymptotic method developed by Dawson *et al.* (1994), see also Grundy *et al.* (1994), analytical expressions are derived for the limiting behaviour of the time dependence of plume displacement and plume

growth in homogeneous porous media. The applicability of the analytical expressions to homogeneous and physically and chemically heterogeneous cases is illustrated. Several parameters that affect nonlinear adsorption and physical and chemical heterogeneity are varied to assess their influence on expected plume dimensions and on variation of the plume position.

8.2 Formulation of the problem

Reactive solute transport in heterogeneous porous media is the result of a spatially variable velocity field and a spatially variable retardation coefficient. The spatial variability of the fluid velocity is determined by the hydraulic conductivity, which has been shown to vary strongly in space (Sudicky, 1986). The spatially variable retardation is caused by spatially variable soil parameters such as *p*H and organic matter content (Boekhold *et al.*, 1993). This variation is often modeled by considering the spatially variable property as a random space function (Dagan, 1989; Bellin *et al.*, 1992; Bosma *et al.*, 1993).

In this paper we consider reactive solute transport in a two-dimensional physically and chemically heterogeneous porous medium. Let the domain be the entire (x_1,x_2) plane. The fluid velocity $\mathbf{v}(\mathbf{x})$, with $\mathbf{x}=(x_1,x_2)$ (L), is obtained from the stochastic differential equations (Dagan, 1989)

$$\nabla^2\phi+\nabla Y\cdot\nabla\phi=\mathbf{J}\cdot\nabla Y \tag{8.1}$$

$$\Phi(\mathbf{x})=-\mathbf{J}\cdot\mathbf{x}+\phi(\mathbf{x}) \tag{8.2}$$

$$\mathbf{v}(\mathbf{x})=-K(\mathbf{x})/\theta\ \nabla\Phi(\mathbf{x}) \tag{8.3}$$

where Φ is the hydraulic head (L), $\mathbf{J}$ the mean head gradient with $\mathbf{J}=(J,0)$, ϕ the random head fluctuation (L) with zero mean, θ the constant water filled porosity. Furthermore, K is the hydraulic conductivity (LT^{-1}) and Y is the log conductivity, i.e. $Y=\ln(K)$. Equation (8.1) implies $\mathrm{div}(\theta\mathbf{v})=0$. In using (8.1)-(8.3), we assumed water flow to be at steady state during the transport process.

From mass conservation we obtain the solute transport equation

$$\frac{\partial c(\mathbf{x},t)}{\partial t}+\frac{\partial q(\mathbf{x},t)}{\partial t}=\nabla\cdot[\mathbf{D}\cdot\nabla c(\mathbf{x},t)]-\mathbf{v}(\mathbf{x})\cdot\nabla c(\mathbf{x},t) \tag{8.4}$$

where c is the solute concentration in the liquid phase (ML^{-3}) and q the amount of solute in the solid phase (ML^{-3}), t is time (T), $\mathbf{v}(\mathbf{x})$ the heterogeneous velocity field (LT^{-1}), and $\mathbf{D}$ the tensor of pore scale dispersion (LT^{-2}) with only non zero diagonal terms D_{11} and D_{22}. We consider equilibrium nonlinear adsorption which is described by the Freundlich isotherm,

$$q(\mathbf{x},t)=K_F(\mathbf{x})\,[c(\mathbf{x},t)]^n \tag{8.5}$$

in which the adsorption coefficient $K_F(\mathbf{x})$ ($M^{1-n}L^{3(n-1)}$) is spatially variable, due to spatially variable soil properties (Bosma *et al.*, 1993; Boekhold *et al.*, 1993). The power n is assumed to satisfy $0<n<1$.

To assess the effects of heterogeneity and of nonlinearity of adsorption on transport, we analyze the displacement of a given, fixed amount of solute which initially may be arbitrarily distributed in the (x_1,x_2) plane. That is, we shall investigate solutions of (8.4)-(8.5) for $-\infty<x_1,x_2<\infty$ and $t>0$, subject to the initial condition

$$c(\mathbf{x},0)=c_0(\mathbf{x}) \qquad (\mathbf{x}=x_1,x_2)\in\mathbf{R}^2 \tag{8.6}$$

where c_0 represents the initially given solute distribution (ML^{-3}). It is required to satisfy the integrability condition

$$M=\int_{\mathbf{R}^2}[c_0(\mathbf{x})+K_F(\mathbf{x})c_0(\mathbf{x})^n]d\mathbf{x} \quad <\infty \tag{8.7}$$

where θM denotes the amount of solute present in the flow domain, i.e. both in solution and adsorbed. Equations (8.4)-(8.5) and condition (8.7) imply

$$\int_{\mathbf{R}^2}[c(\mathbf{x},t)+K_F(\mathbf{x})c(\mathbf{x},t)^n]d\mathbf{x} \;=\; M \quad \text{for all } t>0 \tag{8.8}$$

expressing the fact that the total amount of solute in conserved. This is in contrast with earlier work (Bosma and Van der Zee, 1993), where continuous injection of

solutes was considered.

In a heterogeneous domain, the often unknown deterministic distribution of parameters limits the interest in the precise plume behaviour as a function of position and time. On the contrary, one is generally interested in the development in terms of certain average quantities such as the mass, the centre of mass and the spatial variance. They are given by the spatial moments (Valocchi, 1989; Dagan, 1989)

$$m(t)=\int_{\mathbf{R}^2} c(\mathbf{x},t)d\mathbf{x} \tag{8.9}$$

$$\mu_i(t)=\frac{1}{m(t)}\int_{\mathbf{R}^2} x_i c(\mathbf{x},t)d\mathbf{x} \tag{8.10}$$

$$\sigma_{ij}^{\ 2}(t)=\frac{1}{m(t)}\int_{\mathbf{R}^2} (x_i-\mu_i)(x_j-\mu_j)c(\mathbf{x},t)d\mathbf{x} \tag{8.11}$$

where $c(\mathbf{x},t)$ can be regarded as the pdf. In (8.9) the zeroth order moment m describes the total mass in the liquid phase (M). Observe that due to the nonlinearity of adsorption, $m(t)$ decreases with increasing time. Furthermore, μ is the position of the plume centroid (L) and σ^2 describes the mass distribution around the mean position of the plume (L^2). In (8.10)-(8.11), the subscripts i and j denote the principal directions of the moments. In our analysis the moments of interest are limited to μ_1, μ_2, $\sigma_{11}^{\ 2}$ and $\sigma_{22}^{\ 2}$, where the subscripts 1 and 2 refer to the longitudinal and transverse direction with respect to the mean direction of flow, respectively.

For transport of a nonlinearly adsorbing solute in a heterogeneous porous medium, no analytical expressions are yet available for the development of the various moments as a function of time. However, in section 3, asymptotic expressions for large time will be derived for the time dependency of the growth rate of the various moments for a two-dimensional homogeneous case. Subsequently, these expressions will be tested numerically for several degrees of nonlinearity, and the applicability to heterogeneous cases will be examined.

8.3 Plume development in a homogeneous domain

In this section we consider the solute transport in a two-dimensional homogeneous domain. Assuming that the fluid flow is one-dimensional and directed along the positive x_1-axis, we are led to consider the initial value problem

$$\frac{\partial}{\partial t}[c+K_F c^n]+V\frac{\partial c}{\partial x_1}=D_{11}\frac{\partial^2 c}{\partial x_1^2}+D_{22}\frac{\partial^2 c}{\partial x_2^2} \tag{8.12}$$

for $-\infty<x_1,x_2<\infty$, $t>0$ and

$$c(x_1,x_2,0)=c_0(x_1,x_2) \quad \text{for } -\infty<x_1,x_2<\infty \tag{8.13}$$

where c_0 satisfies (8.7) and c satisfies the mass-invariance condition (8.8). In (8.12), all coefficients are considered as being constant and positive. To simplify the discussion we first eliminate the constants from (8.12) by the redefinitions

$$\begin{aligned} u&=(K_F)^{\frac{1}{n-1}}c \qquad & \tilde{t}&=\frac{V}{\alpha_L}t \\ \tilde{x}_1&=\frac{x_1}{\alpha_L} & \tilde{x}_2&=\frac{x_2}{\sqrt{\alpha_L\alpha_T}} \end{aligned} \tag{8.14}$$

where

$$\alpha_L=\frac{D_{11}}{V} \quad \text{and} \quad \alpha_T=\frac{D_{22}}{V} \tag{8.15}$$

This yields the dimensionless problem

$$\frac{\partial}{\partial t}[u+u^n]+\frac{\partial u}{\partial \tilde{x}_1}=\frac{\partial^2 u}{\partial \tilde{x}_1^2}+\frac{\partial^2 u}{\partial \tilde{x}_2^2} \tag{8.16}$$

for $-\infty<\tilde{x}_1,\tilde{x}_2<\infty$, $t>0$ and

$$u(\tilde{x}_1,\tilde{x}_2,0)=u_0(\tilde{x}_1,\tilde{x}_2)=(K_F)^{\frac{1}{n-1}}c_0(\alpha_L\tilde{x}_1,\sqrt{\alpha_L\alpha_T}\tilde{x}_2) \tag{8.17}$$

for $-\infty<\tilde{x}_1,\tilde{x}_2<\infty$. With the scaling from (8.14), the mass conservation equation (8.8) becomes

$$M_u=\int_{R^2}[u+u^n]d\tilde{\mathbf{x}}=\frac{M}{\alpha_L^{3/2}\alpha_T^{1/2}(K_F)^{1/1-n}} \tag{8.18}$$

The large time behaviour of solutions of the initial value problem (8.16), (8.17), subject to (8.18) for all $t\geq 0$, is investigated in detail by Dawson *et al.* (1994). Their results and methods are based on Grundy *et al.* (1994) where a one-dimensional version of (8.16) is studied. In both papers limit profiles are considered for all $n>0$.

For n in the range $0<n<1$, the asymptotic result is the following. At large times, i.e. if $t\to\infty$, the term $u+u^n$ in the time derivative can be replaced by u^n (since $u\to 0$ as $t\to\infty$) and the $\tilde{x}_1$-diffusion can be disregarded with respect to the $\tilde{x}_1$-convection. Thus the scaled solute distribution converges to a solution of a reduced transport equation and it selects the unique solution for which initially the mass M_u is concentrated at the origin of the $\tilde{x}_1,\tilde{x}_2$ plane. To be precise, let $u(\tilde{x}_1,\tilde{x}_2,t)$ satisfy (8.16)-(8.18). Then

$$u(\tilde{x}_1,\tilde{x}_2,t)\to u_s(\tilde{x}_1,\tilde{x}_2,t) \quad \text{as } t\to\infty \tag{8.19}$$

where u_s is the fundamental solution of the reduced equation with the same mass, i.e. u_s satisfies

$$\frac{\partial u^n}{\partial t}+\frac{\partial u}{\partial \tilde{x}_1}=\frac{\partial^2 u}{\partial \tilde{x}_2^2} \quad \text{for } -\infty<\tilde{x}_1,\tilde{x}_2<\infty,\ t>0 \tag{8.20}$$

and

$$u^n(\tilde{x}_1,\tilde{x}_2,0)=M_u\delta(\tilde{x}_1,\tilde{x}_2) \quad \text{for } -\infty<\tilde{x}_1,\tilde{x}_2<\infty \tag{8.21}$$

where $\delta(\tilde{x}_1,\tilde{x}_2)$ denotes the two-dimensional Dirac distribution at the origin.

The solution u_s of (8.20)-(8.21) can be captured in terms of similarity variables. If we set (see Dawson *et al.*, 1994)

$$u_s(\tilde{x}_1,\tilde{x}_2,t)=t^{-\frac{3}{3-n}}M_u^{\frac{2}{3-n}}v(\eta,\zeta) \tag{8.22}$$

with

$$\eta=\frac{\tilde{x}_1}{t^{\frac{2n}{3-n}}M_u^{\frac{2(1-n)}{3-n}}} \quad \text{and} \quad \zeta=\frac{\tilde{x}_2}{t^{\frac{n}{3-n}}M_u^{\frac{1-n}{3-n}}} \tag{8.23}$$

then we obtain for v the time-independent partial differential equation

$$\frac{3n}{3-n}v^n+\frac{2n}{3-n}\eta\frac{\partial v^n}{\partial\eta}+\frac{n}{3-n}\zeta\frac{\partial v^n}{\partial\zeta}-\frac{\partial v}{\partial\eta}+\frac{\partial^2 v}{\partial\zeta^2}=0 \tag{8.24}$$

Solving this equation in $\mathbf{R}^2$, i.e. for $-\infty<\eta,\zeta<\infty$, subject to the conditions

$$v\geq 0 \quad \text{and} \quad \int\int_{\mathbf{R}^2} v^n(\eta,\zeta)d\eta d\zeta=1 \tag{8.25}$$

and substituting the result into (8.22), yields the required fundamental solution of the reduced transport equation. Note that the ensuing v-problem only depends on the Freundlich power n because all other physical constants have been scaled to one by the transformations (8.14), (8.22) and (8.23). Unfortunately, no explicit solution could be found. Nevertheless, based on analytical and numerical techniques, Dawson *et al.* (1994) were able to give a fairly complete picture of the solution and presented a numerical example of (8.24)-(8.25) for the case n=0.5. It is shown here in Figure 8.1 for completeness. Note that in this figure a different scaling is used for v and for the independent variable η and ζ; they did not incorporate the total mass M_u into the variables. It is found by solving the time dependent problem (8.16)-(8.17) and by plotting the solution at large times in the appropriate scaled variables.

We are now in a position to give the large time expressions for the different spatial moments. Combining (8.19), (8.22) and (8.23) and expressing the results in terms of the original physical variables, we find that as $t\rightarrow\infty$

$$(i) \qquad \mu_1(t)\rightarrow\left(\frac{M}{K_F}\right)^{\frac{2(1-n)}{3-n}}\left(\frac{1}{\alpha_T}\right)^{\frac{1-n}{3-n}}\left(\frac{Vt}{K_F}\right)^{\frac{2n}{3-n}}\mu_\eta(n) \tag{8.26}$$

where the constant $\mu_\eta(n)$ is given by

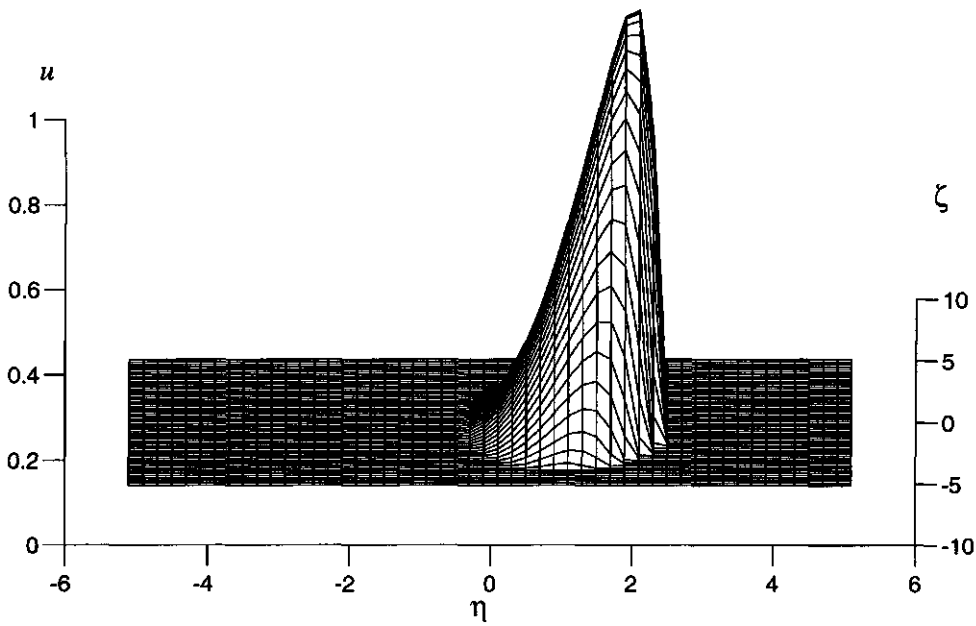

Figure 8.1 Numerical solution of initial value problem (8.16)-(8.17) in the scaled variables $v=t^{3/(3-n)}u$, $\eta=\tilde{x}_1 t^{-2n/(3-n)}$, $\zeta=\tilde{x}_2 t^{-n/(3-n)}$, with n=0.5 and M_u=8. The solution is shown here at t=3000 as a three-dimensional object viewed from different directions. Here the initial value u_0=1 on the square of side 2 with centre at origin and u_0=0 elsewhere (after Dawson *et al.*, 1994).

$$\mu_\eta(n)=\frac{\iint_{\mathbf{R}^2}\eta v(\eta,\zeta)d\eta d\zeta}{\iint_{\mathbf{R}^2} v(\eta,\zeta)d\eta d\zeta} \tag{8.27}$$

(ii)
$$\sigma_{11}^2(t)\rightarrow\left(\frac{M}{K_F}\right)^{\frac{4(1-n)}{3-n}}\left(\frac{1}{\alpha_T}\right)^{\frac{2(1-n)}{3-n}}\left(\frac{Vt}{K_F}\right)^{\frac{4n}{3-n}}\sigma_\eta^2(n) \tag{8.28}$$

where the constant $\sigma_\eta^2(n)$ is given by

$$\sigma_\eta^2(n)=\frac{\iint_{\mathbf{R}^2}(\eta-\mu_\eta(n))^2\,\nu(\eta,\zeta)d\eta d\zeta}{\iint_{\mathbf{R}^2}\nu(\eta,\zeta)d\eta d\zeta} \tag{8.29}$$

(iii)
$$\sigma_{22}^2(t)\rightarrow\left(\frac{M}{K_F}\right)^{\frac{2(1-n)}{3-n}}(\alpha_T)^{\frac{2}{3-n}}\left(\frac{Vt}{K_F}\right)^{\frac{2n}{3-n}}\sigma_\zeta^2(n) \tag{8.30}$$

where the constant $\sigma_\zeta^2(n)$ is given by

$$\sigma_\zeta^2(n)=\frac{\iint_{\mathbf{R}^2}\zeta^2\,\nu(\eta,\zeta)d\eta d\zeta}{\iint_{\mathbf{R}^2}\nu(\eta,\zeta)d\eta d\zeta} \tag{8.31}$$

The coefficients $\mu_\eta(n)$, $\sigma_\eta^2(n)$ and $\sigma_\zeta^2(n)$ have to be determined from the solution of the ν-problem. This was done by Dawson *et al.* (1994) for the case n=0.5. They found

$$\mu_\eta(0.5)=0.656 \qquad \sigma_\eta^2(0.5)=0.052 \qquad \sigma_\zeta^2(0.5)=0.853 \tag{8.32}$$

8.4 **Numerical procedure**

8.4.1 *Incorporation of heterogeneity*

We incorporate spatial variability of soil physical and soil chemical parameters into our numerical calculations with a procedure equal to the one used by Bosma *et al.* (1993). A random variation of the hydraulic conductivity and the adsorption coefficient was applied assuming a normal distribution of the log conductivity Y and the log adsorption coefficient W, the latter defined as $W(\mathbf{x})=\ln[K_F(\mathbf{x})]$. The distributions of Y and W are characterized by their means $\langle Y\rangle$ and $\langle W\rangle$ and their variances σ_Y^2 and σ_W^2. Spatial dependency of Y and W is modeled with an autocovariance function, defined for example for Y as

$C_Y(\mathbf{r})=\langle Y'(\mathbf{x})Y'(\mathbf{x}+\mathbf{r})\rangle$ with the fluctuation of Y, $Y'(\mathbf{x})=Y(\mathbf{x})-\langle Y\rangle$. An isotropic exponential relationship is used to describe C_Y and C_W, i.e.

$$C_Y(\mathbf{r})=\sigma_Y^2 \exp(\frac{-|\mathbf{r}|}{l_Y}) \tag{8.33a}$$

$$C_W(\mathbf{r})=\sigma_W^2 \exp(\frac{-|\mathbf{r}|}{l_W}) \tag{8.33b}$$

where $\mathbf{r}$ is the planar distance vector (L) between two positions in the domain and l_Y and l_W are the integral scales of Y and W (L), respectively.

With the assumed distributions and autocovariance, random fields of Y and W can be generated to obtain heterogeneous K and K_F fields. The log conductivity and log adsorption coefficient fields with prescribed correlation structure are generated with a fast Fourier transform method (Gutjahr, 1989). In view of the discussions by Bosma *et al.* (1993) and Tompson (1993), regarding correlation of hydraulic conductivity and adsorption coefficient, we consider cases with no correlation and with perfect (positive and negative) correlation between K and K_F. In case of no correlation the random adsorption coefficient field is computed according to

$$K_F(\mathbf{x})=K_F^G \exp[W'(\mathbf{x})] \tag{8.34}$$

where K_F^G is the geometric mean of the Freundlich adsorption coefficient, i.e. $K_F^G=\exp(\langle W\rangle)$. In case of positive or negative correlation $K_F(\mathbf{x})$ is obtained from $Y'(\mathbf{x})$, according to

$$K_F(\mathbf{x})=K_F^G \exp[Y'(\mathbf{x})]^\beta \tag{8.35}$$

where β determines the correlation, i.e. $\beta=1$ accounts for perfect positive correlation and if $\beta=-1$, K and K_F are perfectly negatively correlated (Bosma *et al.*, 1993).

8.4.2 *Solving the equations*

For each calculation first the random fields of K and K_F are generated. Consequently, the flow equation is solved to obtain the heterogeneous velocity field, followed by the solution of the transport problem. The approach used, regarding the size and discretization of the two-dimensional domain and the computation of the velocity field $\mathbf{v}(\mathbf{x})$, is described earlier by Bellin *et al.* (1992) and Bosma *et al.* (1993). We briefly summarize the main features of the approach.

The flow equation is solved by a Galerkin finite element method on a two-dimensional domain discretized in triangular elements. The random fields were generated so that two adjacent elements contained the same value for the random variables. The boundary conditions used, were no flux on the upper and lower boundaries of the domain (x_2=0 and x_2=18l_Y) and unit specific discharge in the x_1 direction (at x_1=0 and x_1=36l_Y). The condition ϕ=0 is imposed for node $\mathbf{x}$=(0,0). Consequently, the mean velocity $\langle\mathbf{v}\rangle$=(V,0), with V=1. To minimize the effect of the boundary conditions, use is made of an inner core region in which solute transport takes place (see Bosma *et al.*, 1993).

The nonlinearity of adsorption requires an adjustment of the transport approaches of Bellin *et al.* (1992) and Bosma *et al.* (1993). Similar to these previously applied approaches, we use a particle tracking scheme to calculate the solute displacement in the heterogeneous domain. However, whereas Bellin *et al.* (1992) and Bosma *et al.* (1993) could represent the injected mass by one single particle, this is not possible if nonlinear adsorption is considered. To compute the transport of a nonlinearly adsorbing solute by a particle tracking scheme, we write (8.4) in terms of the total mass of a solute (on a volumetric base, ML^{-3}), i.e. $T(\mathbf{x},t)$=$c(\mathbf{x},t)$+$q(\mathbf{x},t)$. If we define a retardation coefficient $\tilde{R}(\mathbf{x},t)$ as

$$\tilde{R}(\mathbf{x},t)=\frac{T(\mathbf{x},t)}{c(\mathbf{x},t)}=1+\frac{q(\mathbf{x},t)}{c(\mathbf{x},t)}=1+K_F(\mathbf{x})[c(\mathbf{x},t)]^{n-1} \tag{8.36}$$

we can write (8.4) according to

$$\frac{\partial T(\mathbf{x},t)}{\partial t}=\nabla\cdot\left[\mathbf{D}\cdot\nabla\left(\frac{T(\mathbf{x},t)}{\tilde{R}(\mathbf{x},t)}\right)\right]-\mathbf{v}(\mathbf{x})\cdot\nabla\left(\frac{T(\mathbf{x},t)}{\tilde{R}(\mathbf{x},t)}\right) \tag{8.37}$$

Writing the mass balance equation in terms of total amount of solute implies the assumption of equilibrium adsorption. The retardation coefficient $\tilde{R}$ is related to the concentration dependent retardation coefficient $R_c=1+nK_F(\mathbf{x})c^{n-1}$, as used by Bosma and Van der Zee (1994), according to

$$\tilde{R}=\frac{1}{c}\int_0^c R_c(s)ds \tag{8.38}$$

where $\tilde{R}$ is actually a cell averaged retardation coefficient.

The numerical procedure pursued here to solve (37) is similar to the approach of Tompson (1993). The total mass present in the two-dimensional domain is distributed over a large amount of particles. Each particle represents a constant mass, m_p. Tracking of the particles enables a recording of the exact position of the particle as a function of time, given by $\mathbf{X}(t)$ (L). The displacement of the particle, subject to nonlinear adsorption, in a physically and chemically heterogeneous domain can be calculated with

$$\mathbf{X}(t+\Delta t)=\mathbf{X}(t)+\mathbf{v}^{\tilde{R}}(\mathbf{X}(t),t)\cdot\Delta t+\mathbf{X}_d(\mathbf{X}(t),t,\Delta t) \tag{8.39}$$

where Δt is the time step of the numerical calculation and $\mathbf{v}^{\tilde{R}}$ is the retarded velocity (LT^{-1}) associated with the position of the particle, given by $\mathbf{v}^{\tilde{R}}(\mathbf{x},t)=\mathbf{v}(\mathbf{x})/\tilde{R}(\mathbf{x},t)$. In case of linear adsorption, the retarded velocity is only dependent on the position. In our analysis with nonlinearly adsorbing solutes, the retarded velocity is dependent on the concentration and therefore on position and time. In (8.39), $\mathbf{X}_d$ is the displacement of the particle (L) due to molecular diffusion and pore scale dispersion. This displacement is computed for an individual particle as

$$\mathbf{X}_d(\mathbf{X}(t),t,\Delta t)=\mathbf{B}\cdot\mathbf{Z}\sqrt{2\Delta t/\tilde{R}(\mathbf{X}(t),t)} \tag{8.40}$$

where

$$\mathbf{B}\cdot\mathbf{B}^T=\begin{pmatrix} D_{11} & 0 \\ 0 & D_{22} \end{pmatrix} \tag{8.41}$$

and $\mathbf{Z}$ is a vector which contains two random numbers with zero mean and unit variance.

In contrast with the position of a particle, the cell averaged retardation coefficient $\tilde{R}$, necessary to compute $\mathbf{v}^{\tilde{R}}$ and $\mathbf{X}_d$, is a volume averaged quantity. In the numerical procedure, the total mass accumulated in one cell during the previous time step is used to obtain the concentration and, subsequently, the retardation coefficient. The particles present in one cell experience the same retardation coefficient and retarded velocity. Note that due to the nonlinearity of adsorption an iteration scheme is necessary to compute the cell concentration from the total mass present in the cell.

In each calculation a large amount of particles is released at the injection area. During each time step the velocity, retardation coefficient and pore scale dispersion associated with the position of each particle is obtained and used to compute the displacement according to (8.39). The fine spatial discretization (Bosma *et al.*, 1993) allows the use of a cell constant value for the velocity $\mathbf{v}$ and the cell averaged retardation coefficient $\tilde{R}$. The time step is continuously modified to prevent a particle displacement to be larger than a fraction (0.25) of the discretization distance ($\Delta x_1=\Delta x_2=0.25 l_Y$) . Test calculations have been performed to minimize the effects of discretization of time (Δt), space (Δx_1, Δx_2) and mass (number of particles N).

8.4.3 *Evaluation of moments*

Plume development of an instantaneously injected solute can be characterized by the spatial moments, given by the expressions (8.9)-(8.11). They describe the position and plume dimensions in the longitudinal and transverse directions. In a previous section, analytical expressions have been derived for the time dependency of the growth rate of the first and second order moments in homogeneous two-dimensional porous media. The derived expressions describe the limiting ($t\rightarrow\infty$) behaviour. In order to test, for several degrees of nonlinearity, the usefulness of the expressions for time scales relevant to transport problems and to

study the plume behaviour in heterogeneous media, a numerical evaluation of the moments is necessary.

For a single realization, the spatial moments can be derived from trajectories of individual particles, according to

$$m(t)=\sum_{i=1}^{N}\frac{m_p}{\tilde{R}_i} \tag{8.42a}$$

$$\langle X_j(t)\rangle=\frac{1}{m(t)}\sum_{i=1}^{N}X_j(t)_i\frac{m_p}{\tilde{R}_i} \tag{8.42b}$$

$$X_{jj}(t)=\frac{1}{m(t)}\left(\sum_{i=1}^{N}X_j(t)_i^2\frac{m_p}{\tilde{R}_i}-\frac{\left[\sum_{i=1}^{N}X_j(t)_i\frac{m_p}{\tilde{R}_i}\right]^2}{m(t)}\right) \tag{8.42c}$$

where $\tilde{R}_i$ is the cell averaged retardation coefficient associated with particle i. Particles present in one cell all experience the same retardation coefficient. In (8.42) $\langle X_j\rangle$ represents the centroid of the plume (L) and X_{jj} describes the trajectory covariance with respect to the mean centroid (L^2). The covariances X_{jl} with $j\neq l$ are not taken into account.

In general, prediction of an individual realization is not possible, due to the unknown deterministic spatially variable parameters and due to the small size of the injection area. Of more interest is the expected behaviour which can be obtained from the statistical moments (mean and variance) of results of an ensemble of independent Monte Carlo realizations. Only if the size of the solution area is very large with respect to the scale of heterogeneity, expected behaviour can be obtained from a single realization (Dagan, 1991). The expected plume centroid and plume covariances can be obtained from

$$\langle\langle X_j(t)\rangle\rangle = \frac{1}{MC}\sum_{i=1}^{MC}\langle X_j(t)\rangle_i \qquad (8.43a)$$

$$\langle X_{jj}(t)\rangle = \frac{1}{MC}\sum_{i=1}^{MC} X_{jj}(t)_i \qquad (8.43b)$$

where MC is the size of the Monte Carlo ensemble.

The second order statistical moments can be used to describe the variation within an ensemble of realizations. For the mean centroid these can be defined as

$$s^2_{\langle X_j\rangle}(t) = \frac{1}{MC}\sum_{i=1}^{MC}(\langle X_j(t)\rangle_i - \langle\langle X_j(t)\rangle\rangle)^2 \qquad (8.44)$$

The variance of the mean centroid is a measure for the area where the plume is located. If a plume remains small during the displacement, which may be valid for linear adsorption with a small initial plume size with respect to the scale of heterogeneity, the variance of the mean centroid can be described by the trajectory covariance derived for ergodic conditions (Dagan, 1989). Bellin *et al.* (1993) derived, assuming ergodic conditions, analytical expressions for the trajectory covariance $X_{jj}(t)$ of a linearly adsorbing solute in a physically and chemically heterogeneous porous medium. For non-ergodic conditions and linear adsorption, for instance if the solute is injected in a small area (point injection), these expressions can be used to approximate $s^2_{\langle X_j\rangle}$. A small deviation occurs due to molecular diffusion and pore scale dispersion.

8.4.4 *Simulation cases*

In addition to the calculations with the purpose to study the behaviour of a nonlinearly adsorbing solute plume in homogeneous and heterogeneous porous formations, extra computations have been performed to show the effect of several parameters. Effects of the degree of nonlinearity, determined by n, of the mean Freundlich adsorption coefficient $K_F{}^G$, of the degree of physical and chemical heterogeneity ($\sigma_Y{}^2$, $\sigma_W{}^2$) and of correlation between K and K_F are studied.

In all calculations transport of a solute resembling cadmium is simulated and the injected mass is 0.4 in the injection point a of the domain (see Bosma *et al.*,

1993). This mass is divided over 2000 particles, sufficient to describe the moments accurately during the plume displacement. The cases with physical and chemical heterogeneity consisted of 500 realizations, a number which has been shown to be sufficient to stabilize the highest order moments of interest.

The considered cases differed with respect to the parameters n, K_F^G, σ_Y^2, σ_W^2 and correlation between K and K_F. For the homogeneous case ($\sigma_Y^2=\sigma_W^2=0$) the performance of the analytical expressions is tested for $n=0.5$ with $K_F=3.26$. We simulated transport of a strongly adsorbed solute, in view of the assumption that was made to derive the analytical expressions (8.26)-(8.31), i.e. the adsorbed mass is much larger than the mass in solution. Furthermore, for $n=0.5$ we have given the absolute levels of the limiting spatial moments. Pore scale dispersion is assumed to be an effect of spatial variability of the hydraulic conductivity. In case of physical heterogeneity, small values of dispersivities were used to account for small scale dispersion and molecular diffusion ($\alpha_L=\alpha_T=10^{-3}l_Y$). In the homogeneous case, longitudinal and transverse spreading is accounted for by larger dispersivities, i.e. $\alpha_L=\alpha_T=10^{-1}l_Y$.

Whereas for linear adsorption it is possible to define an average retardation coefficient, the dependence of $\tilde{R}$ on c, K_F^G and n in the instantaneously injected nonlinear case limits the possibilities of comparison between different cases on the basis of adsorption parameters. These cases can be compared on the basis of displacements (mean plume centroids), yielding effective retardation coefficients (Tompson, 1993). Nevertheless, because the mean adsorption coefficient has a distinct effect on the trajectory covariance in the linear adsorption case (Bosma *et al.*, 1993), additional calculations with different K_F^G values for the nonlinear case ($n=0.65$) have been done ($K_F^G=0.01$, $K_F^G=0.1$, $K_F^G=3$ and $K_F^G=10$). For a moderate degree of physical heterogeneity ($\sigma_Y^2=0.2$) computations have been performed with $n=0.35$, $n=0.5$, $n=0.65$ and $n=0.8$. The corresponding adsorption coefficients are chosen so that initially the retardation coefficients are equal for all cases, i.e. $\tilde{R}=3.37$. Chemical heterogeneity is not taken into account while studying the effect of n. In that case the value of n influences the spatial variability of the retardation coefficient so that effects of the degree of nonlinearity cannot be decomposed from effects of chemical heterogeneity. For $n=0.65$ extra calculations were done to show the effect of increasing degree of physical and chemical heterogeneity (σ_Y^2 and σ_W^2 up to 1.6). Finally, for $n=0.65$, $K_F^G=3$ and $\sigma_Y^2=\sigma_W^2=0.2$ we show the effect of positive and negative correlation between K and K_F.

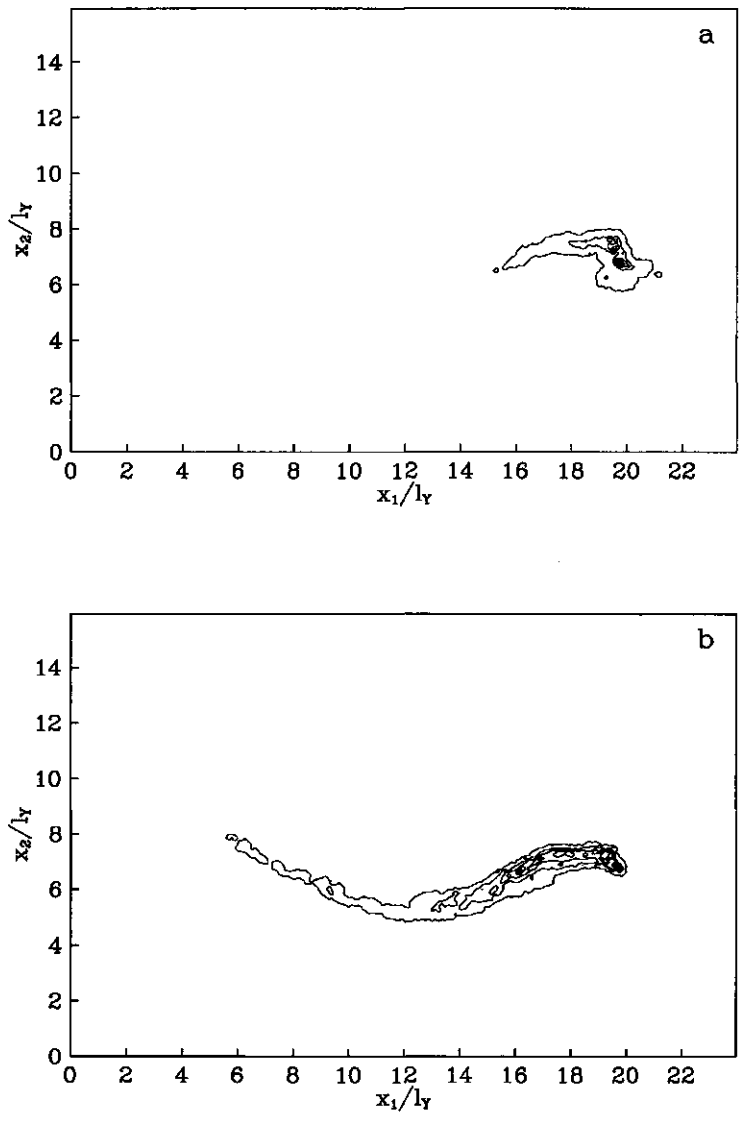

Figure 8.2 Contour plots of solute concentration of linearly (*a*) and nonlinearly (*b*) adsorbing instantaneously injected solute in a physically and chemically heterogeneous porous medium (σ_Y^2=1.6, σ_w^2=0.2).

8.5 Results and discussion

8.5.1 *Qualitative plume behaviour*

Effects of nonlinear adsorption for a one-dimensional homogeneous case were shown by Bosma *et al.* (1994). The decreasing plume velocity and the asymmetrical plume shape were made apparent. Tompson (1993) has shown snapshots of linearly and nonlinearly adsorbing plumes in three-dimensional heterogeneous formations. As an illustration of the effects of nonlinear adsorption and physical and chemical heterogeneity in two-dimensional domains, some contour plots of concentration distributions at a certain time are given in Figure 8.2. In both the linear and nonlinear cases σ_Y^2=1.6 and σ_W^2=0.2. The retardation coefficient of the linear case is 26.3, which is constant in time and equal for all concentrations. For the nonlinear case, with n=0.35, M=0.4 and initially $\tilde{R}$=3.37, the spreading of the concentrations causes increasing retardation coefficients and, consequently, a decreasing plume velocity. In Figure 8.2 the plumes have covered roughly the same distance, however the nonlinear case requires more time to reach this distance. The profound effect of nonlinear adsorption on the shape of the plume is striking. Whereas the transverse dimensions do not differ much from the linear case, in the longitudinal direction nonlinearity (with $0<n<1$) causes long individual plumes. The downstream part tends to a sharp front, which is in agreement with Van der Zee (1990) and Bosma and Van der Zee (1993), while the upstream part shows considerable tailing. The physical heterogeneity, causing irregular streamlines, gives rise to the winding of the long plume through the two-dimensional domain. The plume windings hinder the exact calculation of the spatial moments using the distributed positions of particles. With (8.42*b*) the longitudinal and transverse spatial covariances are computed with respect to the mean centroid, which underestimates the longitudinal and overestimates the transverse covariances with respect to the actual centroid. Calculating the spatial moments with respect to the actual centroid is difficult and the introduced error is, especially for the longitudinal moment, small for a moderate degree of physical heterogeneity. Similar problems were encountered by Dagan (1991) who considered a linear adsorbing solute injected in long narrow strips of a finite length.

8.5.2 *Expected plume development*

For a quantitative view of plume development in two-dimensional domains, plume centroids and longitudinal and transverse trajectory covariances are computed for individual plumes with (8.42). The expected behaviour is calculated by ensemble averaging, according to (8.43).

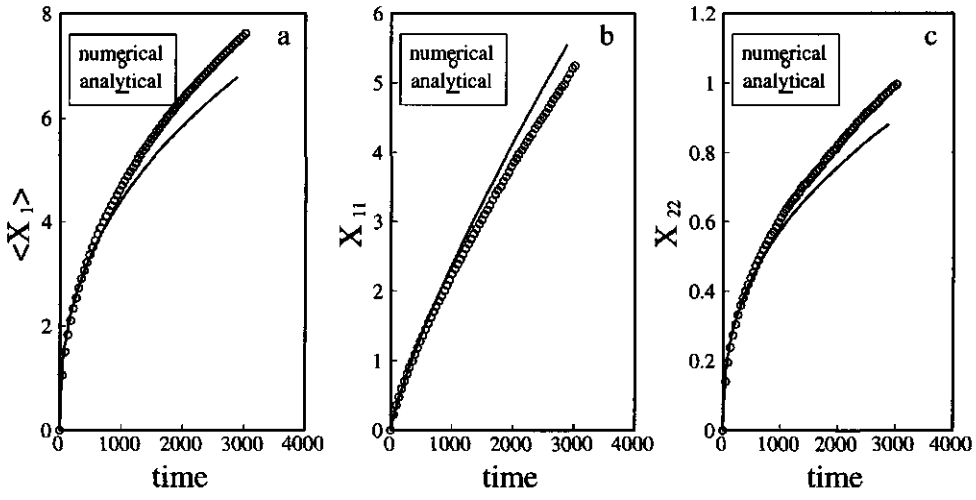

Figure 8.3 Development of the first (*a*), second longitudinal (*b*) and second transverse (*c*) spatial moments for the homogeneous case with n=0.5; Solid lines are limiting behaviour analytically derived in (8.26)-(8.32).

Figure 8.3 shows the expected spatial moments for the homogeneous case with n=0.5. The analytically derived solid lines represent the limiting behaviour of the spatial moments. From the results in Figure 8.3 we see that there is good agreement between the numerical results and the analytical expressions for limiting behaviour of moment growth. Some deviations are visible for large travel times. The analytical results underestimate the numerical results of $\langle X_1 \rangle$ and X_{22}, whereas X_{11} is overestimated. These relatively small differences can be a result of numerical inaccuracies as well as of errors due to assumptions necessary to derive the

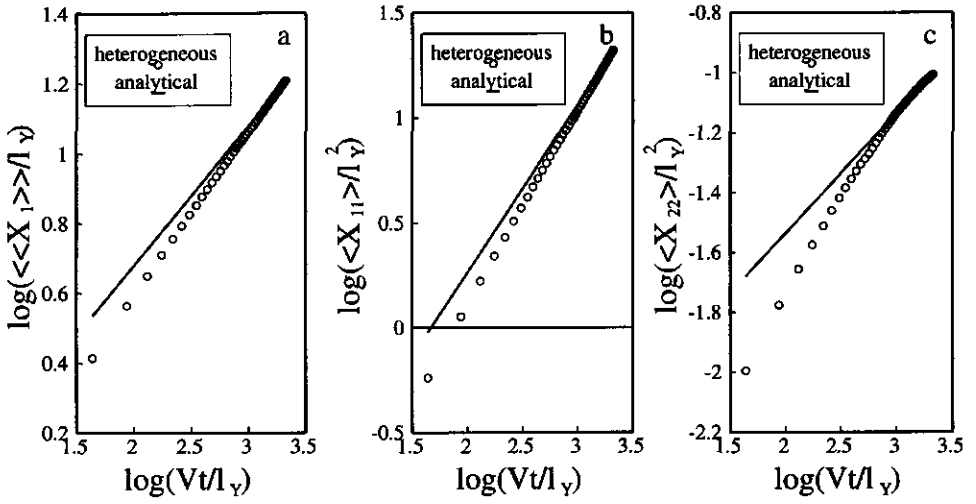

Figure 8.4 Development of the logarithm of the first (*a*), second longitudinal (*b*) and second transverse (*c*) spatial moments for the heterogeneous case (σ_Y^2=0.2, σ_W^2=0) with n=0.5; Solid lines are fitted limiting behaviour analytically derived in (8.26)-(8.31).

analytical approximations. Note that even for a moderate degree of sorption with large transverse dispersion the effective retardation is very high. Calculations witheven stronger degrees of nonlinearity (n<0.5) revealed a strong plume immobilization due to large retardation coefficient.

To show the applicability of the expressions (8.26)-(8.31) to a heterogeneous case, in Figure 8.4 the logarithm of the expected spatial moments of a physically heterogeneous case (σ_Y^2=0.2) with n=0.5 is shown. The slopes of the analytical results represent the limiting behaviour of the time dependence of the growth rate of the spatial moments. The absolute level of the analytical results are unknown, but the lines are drawn so that they intersect the results of the heterogeneous case where limiting behaviour is most likely. We see that even for heterogeneous cases the expressions can be very useful to predict the development of the plumes. The slopes of the heterogeneous and analytical results demonstrate good agreement. If a point on the curve is known, e.g. a measurement of the plume position or size,

the position and the growth rate of the plume as a function of time can be computed analytically.

The results of Figures 8.3 and 8.4 refer to the spatial moments of the plume as a function of time in case of homogeneous porous formations. To show the effect of various parameters in heterogeneous cases, the second spatial moments are plotted as a function of the displacement, given by the expected plume position $\langle\langle X_1 \rangle\rangle$. In this way, we account for the nonlinear growth rate (see (8.26)-(8.31)) of the mean centroid.

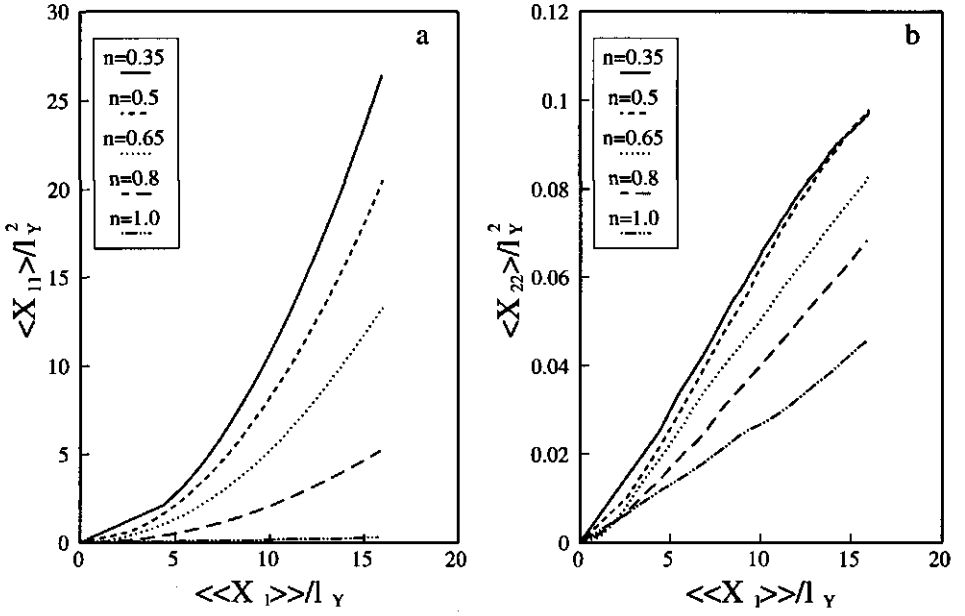

Figure 8.5 Expected longitudinal (*a*) and transverse (*b*) spatial moments for physically heterogeneous case (σ_Y^2=0.2, σ_W^2=0) for various degrees of nonlinearity.

Figure 8.5 shows the contribution of nonlinearity on the expected longitudinal and transverse spatial moments in a physically heterogeneous and chemically homogeneous porous medium (σ_Y^2=0.2, σ_W^2=0). The physical heterogeneity causes irregularly shaped streamlines with a spatially variable flow velocity and flow direction. The large effect of nonlinear adsorption on the longitudinal plume dimension is striking. Even for n=0.8 there is a large increase of $\langle X_{11} \rangle$ with respect to the linear case (n=1). Although tailing occurs for all values

of n (n<1), the lengths of the plumes are also clearly different for different n values.

The transverse plume dimensions are only slightly affected by nonlinearity. Transverse plume spreading is determined by pore scale dispersion and by physical heterogeneity. An effect of (nonlinear) adsorption is not expected. However, the results of Figure 8.5*b* show an enhanced transverse plume spreading as n decreases. Two effects play a role, both being the result of the shape of the plumes. The large size of the individual plumes causes a transverse spreading along the entire length of the plume. The second effect is caused by the winding of the plume. The transverse dimension with respect to the expected centroid is larger than the transverse plume shape with respect to the actual centroid. Both effects are more pronounced if the plumes are longer and, therefore, if n is smaller.

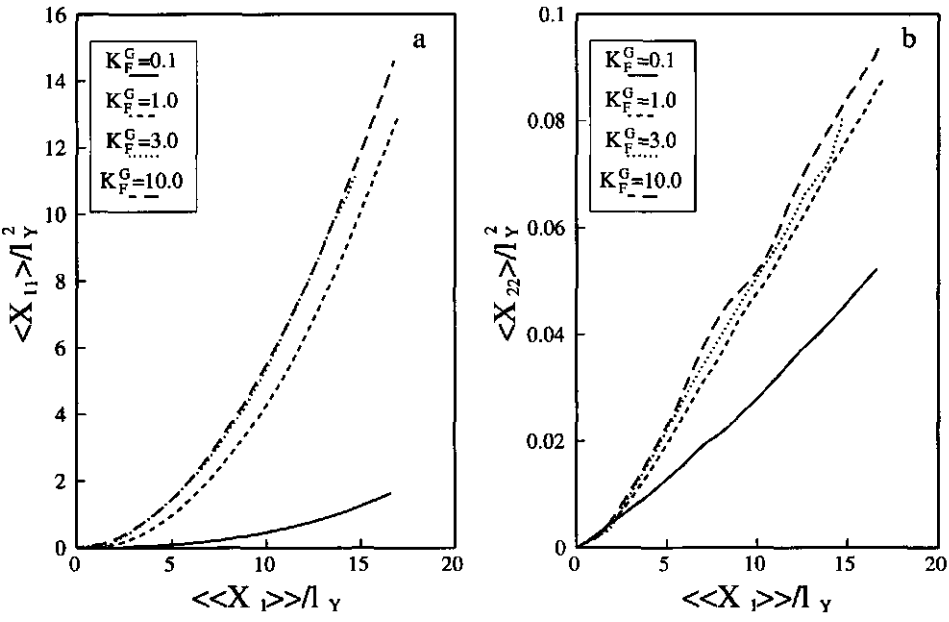

Figure 8.6 Expected longitudinal (*a*) and transverse (*b*) spatial moments for physically and chemically heterogeneous case ($\sigma_Y^2=\sigma_W^2=0.2$) for various mean adsorption coefficients (n=0.65).

Results of Bosma *et al.* (1993) showed for the linear case with small adsorption a large effect of the mean adsorption coefficient on the trajectory

covariance. This effect was due to the increasing coefficient of variation of the retardation coefficient if the adsorption coefficient increases. This effect, which plays also a role in the nonlinear case, decreases if K_F^G is large, because then $1+K_F^G \approx K_F^G$. In Figure 8.6 the results are given for the expected spatial moments for different mean adsorption coefficients with n=0.65 and $\sigma_Y^2=\sigma_W^2$=0.2. In general, we see small differences for different values of K_F^G. This is caused by the increasing retardation with decreasing concentration during the plume spreading. Only for very small K_F^G values the are visible effects. The contribution of adsorption on solute transport is smaller if K_F^G decreases, which reduces the effect of nonlinearity. Consequently, the expected plume length is smaller for K_F^G=0.05 and K_F^G=0.25, causing smaller longitudinal spatial moments. In the transverse direction similar effects are visible. Effects of different plume lengths, as described above with regard to the results of Figure 8.5, play a similar role. With large K_F^G values, the effect of nonlinear adsorption is more pronounced.

Considering both the longitudinal and transverse spatial moments, it seems that except for small K_F^G values, there is no effect of the mean adsorption coefficient. Obviously, the velocity of the plume is affected, but this is accounted for by showing the results as a function of the plume displacement.

The effect of correlation on the plume dimensions is demonstrated in Figure 8.7. The results have been obtained with n=0.65, $\sigma_Y^2=\sigma_W^2$=0.2 and K_F^G=3. In the negatively correlated cases, areas with low adsorption coefficients occur in areas with large hydraulic conductivities and vice versa. This is expected to enhance the spreading of solutes (Bellin *et al.*, 1993; Bosma *et al.*, 1993), contrary to the effects of positive correlation. However, the results of $\langle X_{11} \rangle$ show that nonlinearity affects the plume shape in such a manner that correlation has a minor impact on the longitudinal plume shape. The plume is long, due to strong retardation of low concentrations and enhancing or balancing effects of negative or positive correlation cause small differences of $\langle X_{11} \rangle$.

In the transverse direction no significant effect is visible. Transverse spreading is enhanced by physical heterogeneity and, as was shown above (Figures 8.5-8.6), by nonlinear adsorption, provided $\sigma_Y^2>0$. In this case, there may be a small effect due to longer plumes, similar to the cases with variable n. This effect, however, is not significant because of the low impact of correlation on $\langle X_{11} \rangle$.

Previous results have shown the dominance of the degree of nonlinearity on the plume dimensions, especially in the longitudinal direction. The effect of

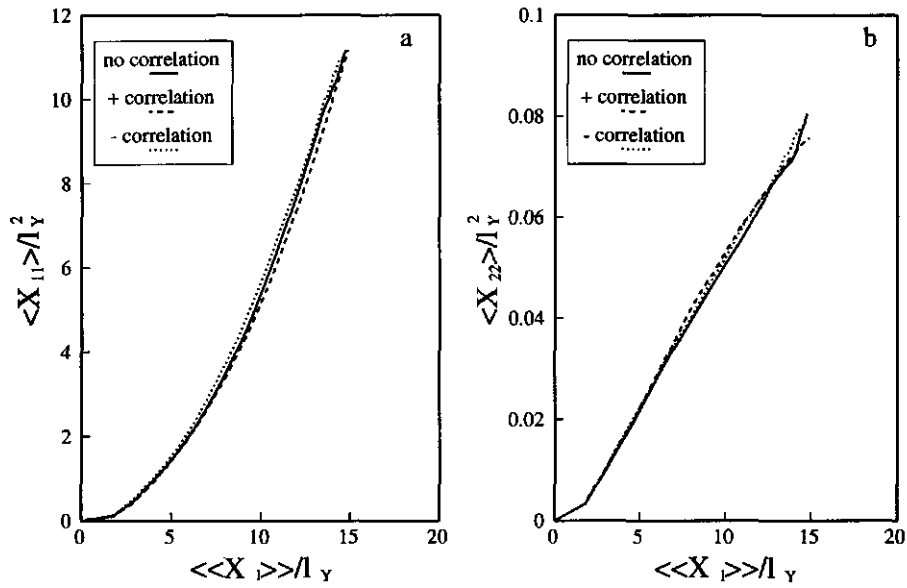

Figure 8.7 Expected longitudinal (*a*) and transverse (*b*) spatial moments for physically and chemically heterogeneous case ($\sigma_Y^2=\sigma_W^2=0.2$) with correlated and uncorrelated K_H and K_F^G (n=0.65, K_F^G=3).

physical and chemical heterogeneity on the expected shape of the plume is assessed by varying σ_Y^2 and σ_W^2. We have considered σ_Y^2 and σ_W^2 varying from 0.2 to 1.6. Additionally, the chemically homogeneous case ($\sigma_W^2=0$) is shown with $\sigma_Y^2=0.2$. Due to the lognormal distributions, a variation coefficient of the spatially variable parameter, defined as the standard deviation divided by the mean, can be obtained directly, i.e. $CV=[\exp(\sigma^2)-1]^{0.5}$ (Van der Zee and Boesten, 1991). This means that in the considered cases the variation coefficients of vary from 0 to 2.0. For the physical heterogeneity, relationships of Dagan (1989) can be used to compute the resulting variation coefficient of the velocity field **v**, which is one of the contributors to spreading of the solute plume. Quantification of the other contribution, i.e. the variation coefficient of the retardation coefficient (Bosma *et al.*, 1993), is more complex in the nonlinear case. The variation coefficient of $\tilde{R}$ is not only dependent on the spatial variability of K_F, but also on the degree of variation of the concentration $c(\mathbf{x},t)$. The time dependence of $\tilde{R}$ hinders a comparison of the degree of physical and chemical heterogeneity on the basis of

v and $\tilde{R}$, as was done by Bosma *et al.* (1993). In this case we compare the variation coefficients of the actual field measured parameters K and K_F, through σ_Y^2 and σ_W^2.

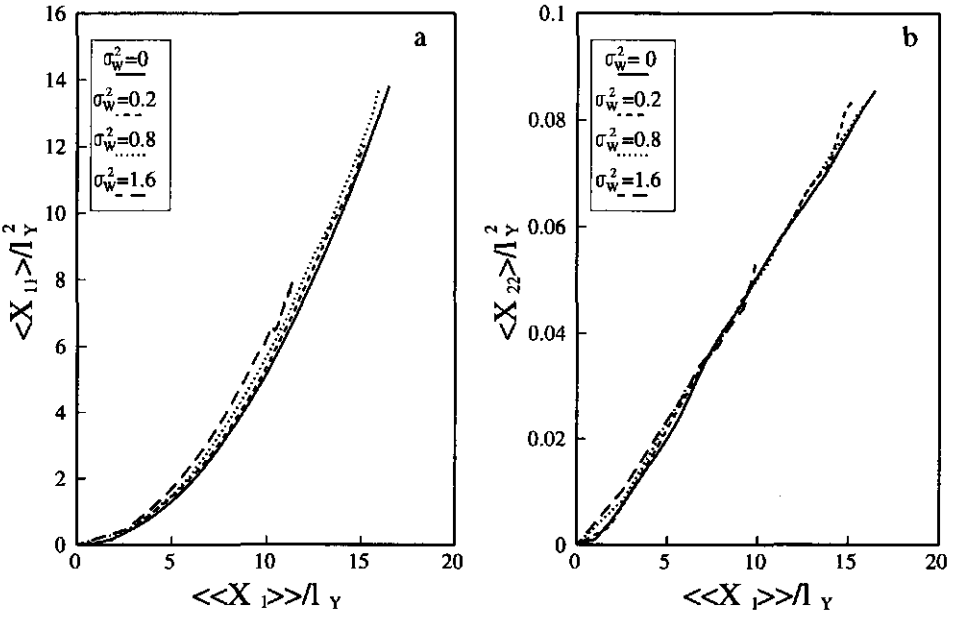

Figure 8.8 Expected longitudinal (*a*) and transverse (*b*) spatial moments for physically heterogeneous case (σ_Y^2=0.2) for various degrees of chemical heterogeneity (n=0.65, K_F^G=3).

In Figure 8.8 the expected longitudinal and transverse plume dimensions are given in a physically heterogeneous domain (σ_Y^2=0.2) for several degrees of chemical heterogeneity (n=0.65). The insensitivity of the longitudinal second spatial moment for chemical heterogeneity in a physically homogeneous domain is striking. Small differences between the different cases are visible. Once again, the nonlinearity dominates the long shape of the plume. In the transverse direction, chemical heterogeneity does not affect the second order moment. Transverse spreading is dominated by physical heterogeneity and the small differences in plume lengths due to different degrees of chemical heterogeneity have no effect on $\langle X_{22} \rangle$.

The effect of physical heterogeneity can be obtained from Figure 8.9.

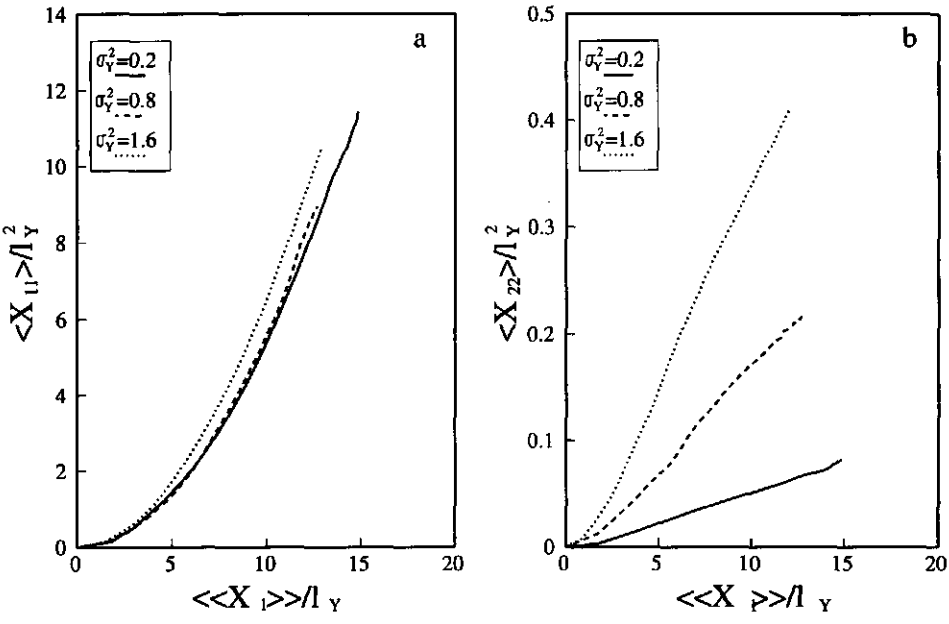

Figure 8.9 Expected longitudinal (*a*) and transverse (*b*) spatial moments for chemically heterogeneous case (σ_W^2=0.2) for various degrees of physical heterogeneity (n=0.65, K_F^G=3).

Compared with Figures 8.8, we see the impact of nonlinear adsorption on the longitudinal moments prevails. The effect of physical heterogeneity is comparable to the effect of chemical heterogeneity, only minor enhancement of the longitudinal plume dimension with increasing σ_Y^2 is visible. The enhancement of the transverse moments with increasing σ_Y^2 is caused by the increasing irregularity of the streamlines. In the longitudinal direction the plume shape is dominated by nonlinear adsorption.

8.5.3 *Variation of plume position*

In the previous paragraph we showed and discussed the expected position and growth of the plume, both as a function of time and displacement. With the time dependence of the velocity of the plume, i.e. $d\langle\langle X_1\rangle\rangle/dt \sim t^{(3n-3)/(3-n)}$, the expected position of the plume in a heterogeneous medium can be estimated. From a

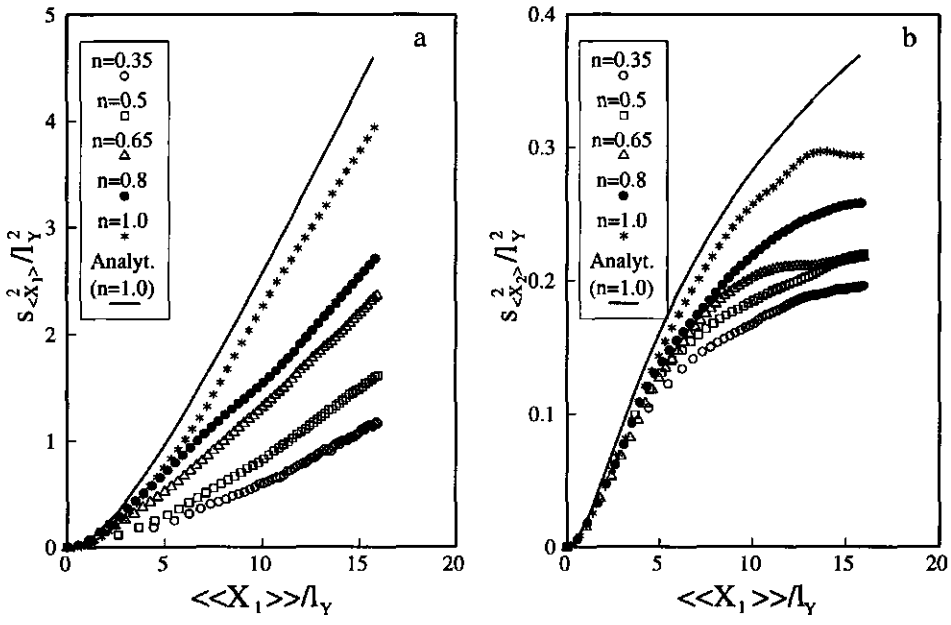

Figure 8.10 Variance of longitudinal (*a*) and transverse (*b*) plume position for physically heterogeneous case (σ_Y^2=0.2, σ_W^2=0) for various degrees of nonlinearity; Solid lines in (*a*) and (*b*) are analytical results from Bellin *et al.* (1993) and Dagan (1989), respectively.

practical point of view interest is usually focused on one realization. In that case, information about the (un)certainty of the expected position of the plume may be relevant. A quantification of this uncertainty is the variance of the mean centroid $s^2_{\langle X_j \rangle}$, given by (8.44), which can be considered as a measure for the area where the plume is located.

In Figure 8.10 we show the effect of the degree of nonlinearity on the variance of the mean centroid, both in the longitudinal and transverse direction. The results show that there is a significant effect of nonlinearity on $s^2_{\langle X_1 \rangle}$. We see a clear reduction of $s^2_{\langle X_1 \rangle}$ of the nonlinear cases with respect to the linear case. Apparently, the large plume size in longitudinal direction decreases $s^2_{\langle X_1 \rangle}$, as a prominent variation of the downstream position of the plume is compensated by the plume tail. Indeed, we see larger $s^2_{\langle X_1 \rangle}$ values for smaller plumes, i.e. if n increases (see $\langle X_{11} \rangle$ in Figure 8.5*a*).

In Figure 8.10 also analytical results of Bellin *et al.* (1993) and Dagan

(1989) are shown for the linear case. Applying these expressions for the trajectory covariance to describe $s^2_{\langle X_j \rangle}$ implies the assumption that plumes remain small with respect to the degree of heterogeneity. In the longitudinal direction we see a good agreement between the numerical and the analytical results. As can be seen in Figure 8.2*a*, the plume size remains relatively small, even for large degrees of physical heterogeneity. In the transverse direction spreading of a linearly adsorbing solute is purely due to physical heterogeneity (Dagan, 1989; Bellin *et al.*, 1993). Therefore, the analytical expression for nonreactive solutes (Dagan, 1989) is used to approximate $s^2_{\langle X_2 \rangle}$. The overestimation of the analytical solution with respect to the numerical results of n=1 is of equal order of magnitude as in Bellin *et al.* (1992) and Bosma *et al.* (1993). Although transverse spreading is mainly physically determined, there is an effect of nonlinearity as $s^2_{\langle X_2 \rangle}$ is also reduced because of the larger plume size if n decreases. A larger degree of nonlinearity increases the reduction of the variance in the transverse direction.

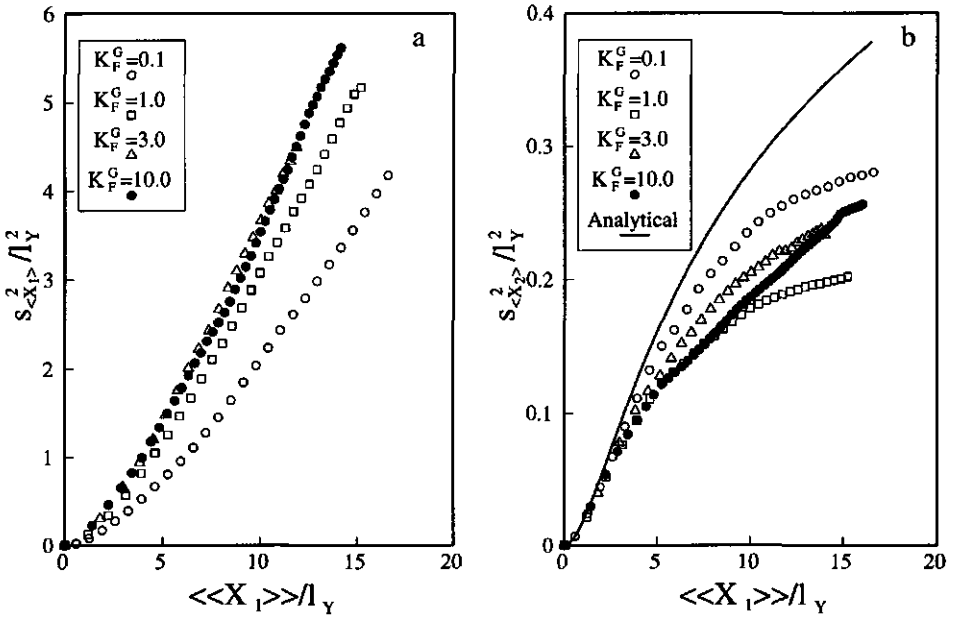

Figure 8.11 Variance of longitudinal (*a*) and transverse (*b*) plume position for physically and chemically heterogeneous case ($\sigma_Y^2=\sigma_W^2=0.2$) for various mean adsorption coefficients (n=0.65); Solid line in (*b*) is analytical result from Dagan (1989).

The behaviour of the mean adsorption coefficient in Figure 8.11 shows different effects on the variance of the plume position than on the expected plume dimensions. In the longitudinal direction, we see relatively small differences between the cases with low K_F^G values and the cases with large adsorption. We are dealing with two opposite effects. On one hand we have an increasing $s^2_{\langle X1\rangle}$ if the effect of nonlinearity reduces, i.e. if K_F^G becomes small (compare results of Figure 8.10*a*). On the other hand, an increasing coefficient of variation of $\tilde{R}$ if K_F^G increases will cause a larger variation of the plume position. This effect was demonstrated for linear adsorption by Bellin *et al.* (1993) and Bosma *et al.* (1993). The latter effect plays a role for the cases with small mean adsorption coefficients, i.e. K_F^G=0.1 and K_F^G=1.0. For larger K_F^G values this effect can be ignored, and minor differences are apparent. In the transverse direction there is also a reducing effect of nonlinear adsorption. This effect, however, is not so unequivocal as in the longitudinal direction.

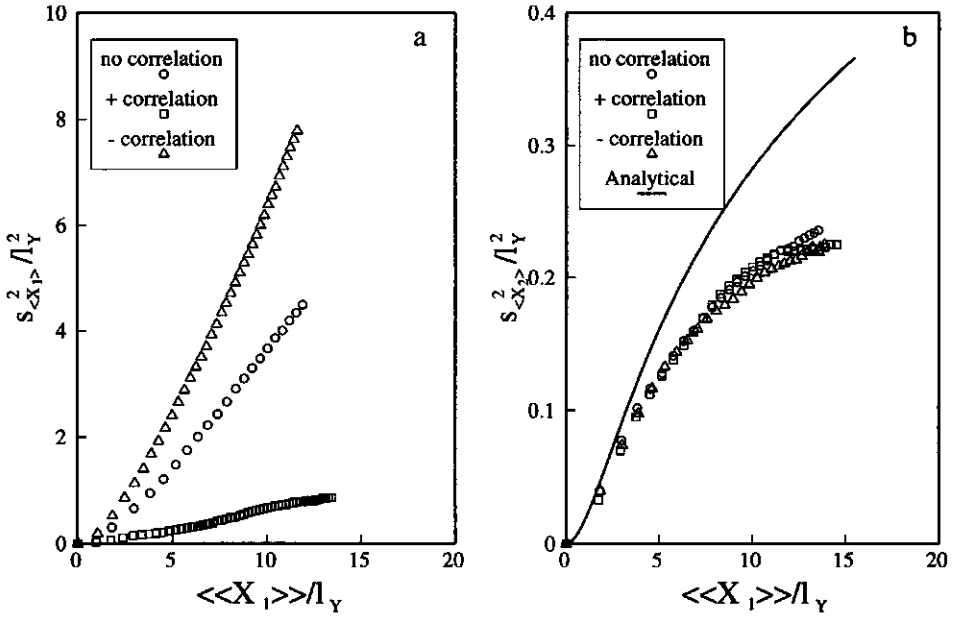

Figure 8.12 Variance of longitudinal (*a*) and transverse (*b*) plume position for physically and chemically heterogeneous case ($\sigma_Y^2=\sigma_W^2=0.2$) with correlated and uncorrelated K_H and K_F^G (n=0.65, K_F^G=3); Solid line in (*b*) is analytical result from Dagan (1989).

The effect of correlation can be seen in Figure 8.12. In the longitudinal direction the variation of the plume position is enhanced if K and K_F are negatively correlated. If K and K_F are positively correlated, the effects of physical and chemical heterogeneity are opposite, resulting in small $s^2_{\langle X_1 \rangle}$ values. In fact, in this case the effect of chemical heterogeneity, and therefore the effect of nonlinearity, is minimized. This causes $s^2_{\langle X_1 \rangle}$ values of the same order of magnitude as the trajectory covariance of the positively correlated linear case of Bosma *et al.* (1993). Results for the uncorrelated and negatively correlated cases reveal the same pattern as findings of the linear case of Bosma *et al.* (1993), although nonlinearity has reduced the values of the variances. This reduction is also visible in the transverse direction (Figure 8.12*b*). Small differences are apparent between the correlated and uncorrelated cases. These may be attributed to the minor differences in expected longitudinal plume shapes, given in Figure 8.7*a*.

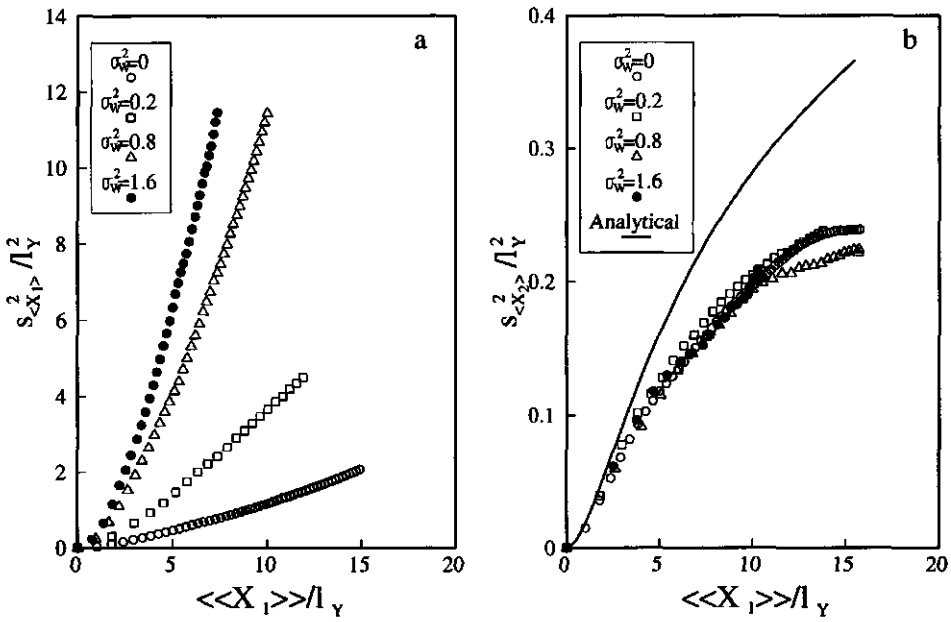

Figure 8.13 Variance of longitudinal (*a*) and transverse (*b*) plume position for physically heterogeneous case (σ_Y^2=0.2) for various degrees of chemical heterogeneity (n=0.65, K_F^G=3); Solid line in (*b*) is analytical result from Dagan (1989).

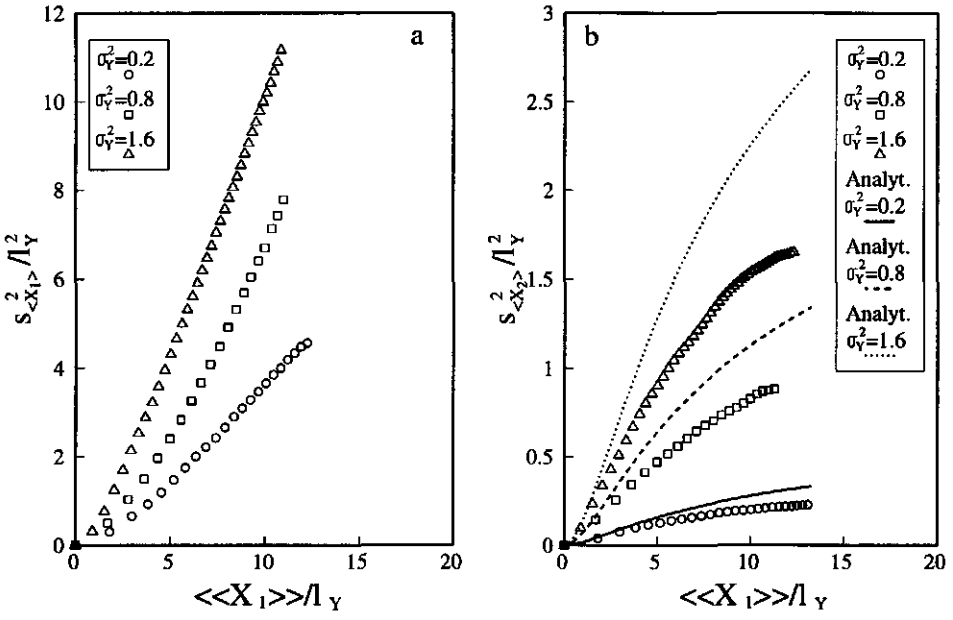

Figure 8.14 Variance of longitudinal (*a*) and transverse (*b*) plume position for chemically heterogeneous case (σ_w^2=0.2) for various degrees of physical heterogeneity (n=0.65, K_F^G=3); Solid lines in (*b*) are analytical results from Dagan (1989).

Increasing variances of the mean plume centroids with increasing physical and chemical heterogeneity can be seen in Figures 8.13 and 8.14. In Figure 8.13 the effect of chemical heterogeneity is shown with a mild degree of physical heterogeneity (σ_Y^2=0.2). The effect of increasing σ_w^2 on $s^2_{\langle X_1\rangle}$ is obvious, larger chemical heterogeneity causes larger differences between plume centroids. It increases the area where the centre of mass of the plume can be located. The variance of the longitudinal plume position is, however, still smaller than for the linear case. Bosma *et al.* (1993) showed trajectory covariances for σ_Y^2=0.2 and σ_w^2=1.6 up to 30 l_Y^2, which is a considerably larger domain than the results of Figure 8.13*a*. Note that the contribution of chemical heterogeneity is of the same order of magnitude as the contribution of physical heterogeneity. In Figure 8.13*b* the insensitivity of $s^2_{\langle X_2\rangle}$ on chemical heterogeneity can be seen. Reductions with respect to the analytical solution of Dagan (1989) are due to the long plumes. Small differences between the various cases cannot be attributed to differences in

plume lengths. They can be a result of numerical inaccuracies, which become apparent because the values of $s^2_{\langle X_2 \rangle}$ are small.

The effect of physical heterogeneity on $s^2_{\langle X_1 \rangle}$ is similar to the effect of chemical heterogeneity. The variance of the mean plume position increases if σ_Y^2 increases. The order of magnitude of the results of Figure 8.14*a* is also similar to the results of Figure 8.13*a*. Figure 8.14*b* demonstrates the dominating effect of physical heterogeneity on the transverse variance of the plume centroid. A larger irregularity of the streamlines increases the longitudinal and transverse area in which the solute plume can be located. There remains, however, a small reduction of the $s^2_{\langle X_2 \rangle}$ values with respect to the analytical solutions. This reduction was also found by Bellin *et al.* (1992) and Bosma *et al.* (1993).

8.6 Conclusions

We studied the behaviour of instantaneously injected, nonlinearly adsorbing solutes in physically and chemically heterogeneous porous formations. Nonlinear adsorption was described by the Freundlich isotherm. Spatial variation of the hydraulic conductivity and the adsorption coefficient was assumed to be random. Individual plume development can be characterized by the plume centroid, given by the first spatial moment, and by the plume dimensions, i.e. the second spatial moments or trajectory covariances. In a Monte Carlo approach, as used herein, expected behaviour is obtained with the statistical mean of the spatial moments. Furthermore, the variance of the expected plume position was computed as a measure for the variation of expected plume location. We derived expressions for the limiting behaviour of the time dependence of the spatial moments in homogeneous porous media.

The combination of instantaneous injection and nonlinear adsorption causes quite deviating behaviour from the equivalent linear case. The strong adsorption of the low concentrations is responsible for a profound tail of the transporting plume. The plume spreading and the concentration dependence of the retardation coefficient have a decreasing effect on the plume velocity as a function of time. The plume dimension is primarily affected in the longitudinal direction, showing a strong increase of the expected longitudinal spatial moment with respect to the linear case. Transverse plume spreading is mainly physically determined, i.e. by

pore scale dispersion and, in case of physical heterogeneity, by irregular streamlines. Therefore, the expected transverse spatial moment is not affected much by nonlinear adsorption.

We used the analytical expressions to describe the time dependence of the plume development. We showed that limiting behaviour for a large degree of nonlinearity is reached within the displacement considered in our calculations. For the shown homogeneous case the limiting behaviour is described well by the analytical expressions. Even in case of physical and chemical heterogeneity, the derived expressions can be used to predict the time dependence of the growth rate of the plumes. The effect of nonlinear adsorption is strong, so that the numerical results agree well with the analytical expressions.

Extra calculations were performed to show the effects of various parameters, n, K_F^G, σ_Y^2, σ_W^2 and degree of correlation between K and K_F, on the plume development and on the variation of the plume position in heterogeneous domains. Generally can be concluded that the plume dimensions are dominated by the effect of nonlinear adsorption. Even for a moderate degree of nonlinearity or a moderate degree of adsorption, the expected longitudinal spatial moment is much larger than for the linear adsorption case. Furthermore, $\langle X_{11} \rangle$ is hardly affected by different degrees of heterogeneity, even for large σ_W^2 and σ_Y^2. In the transverse direction, the expected spatial moments remain small, i.e. of the same order of magnitude as for the linear case. There is a small effect of nonlinear adsorption, due to the length of the plume. A strong effect on $\langle X_{22} \rangle$ is observed for the degree of physical heterogeneity, which is caused by more irregularly shaped streamlines if σ_Y^2 increases.

In contrast, the variation of the plume position is more strongly determined by heterogeneity. There is a clear effect of nonlinear adsorption which can be attributed to the length of the plume. Compared with the linear case, the variation of the longitudinal position is reduced due to the large plumes. Negative correlation between K and K_F increases the variation between longitudinal plume positions, similar to the linear case. The effects of physical and chemical heterogeneity are of the same order of magnitude, despite the time dependency of the coefficient of variation of the retardation coefficient. In the transverse direction, the effect of nonlinear adsorption is small. There is a minor reduction of the transverse variation of the plume position with respect to linear adsorption. This effect, however, is small and cannot easily be decomposed from numerical inaccuracies. Similar to the

expected transverse plume dimension, physical heterogeneity has a large effect on the transverse plume position.

References

Bellin, A., P. Salandin, and A. Rinaldo, Dispersion in heterogeneous porous formations: statistics, first-order theories, convergence of computations, Water Resour. Res., 28, 2211-2227, 1992.

Bellin, A., A. Rinaldo, W.J.P. Bosma, S.E.A.T.M. van der Zee, and Y. Rubin, Linear equilibrium adsorbing solute transport in physically and chemically heterogeneous porous formations, 1. Analytical solutions, Water Resour. Res., 29, 4019-4030, 1993.

Boekhold, A.E., and S.E.A.T.M. van der Zee, Significance of soil chemical heterogeneity for spatial behaviour of cadmium in field soils, Soil Sci. Soc. Am. J., 56, 747-754, 1992.

Boekhold, A.E., S.E.A.T.M. van der Zee, and F.A.M. de Haan, Spatial patterns of cadmium contents related to soil heterogeneity, Water, Air, and Soil Pollution, 57-58, 479-488, 1991.

Bosma, W.J.P., and S.E.A.T.M. van der Zee, Transport of reacting solute in a one-dimensional chemically heterogeneous porous medium, Water Resour. Res., 29, 117-131, 1993.

Bosma, W.J.P., A. Bellin, S.E.A.T.M. van der Zee, and A. Rinaldo, Linear equilibrium adsorbing solute transport in physically and chemically heterogeneous porous formations, 2. Numerical results, Water Resour. Res., 29, 4031-4043, 1993.

Bosma, W.J.P., and S.E.A.T.M. van der Zee, Dispersion of a continuously injected, nonlinearly adsorbing solute in chemically or physically heterogeneous porous formations, J. Contam. Hydrol., submitted, 1994.

Bosma, W.J.P., S.E.A.T.M. van der Zee, A. Bellin, and A. Rinaldo, Instantaneous injection of a nonlinearly adsorbing solute in a heterogeneous aquifer, in: Transport and reactive processes in aquifers, edited by T.H. Dracos and F. Stauffer, pp. 411-417, A.A. Balkema, Rotterdam, 1994.

Chrysikopoulos, C.V., P.K. Kitanidis, and P.V. Roberts, Analysis of one-dimensional solute transport through porous media with spatially variable retardation factor, Water Resour. Res., 26, 437-446, 1990.

Chrysikopoulos, C.V., P.K. Kitanidis, and P.V. Roberts, Generalized Taylor-Aris moment analysis of the transport of sorbing solutes through porous media with spatially-periodic retardation factor, Transp. Porous Media, 7, 163-185, 1992.

Dagan, G., Stochastic modeling of groundwater flow by unconditional and conditional probabilities, 2. The solute transport, Water Resour. Res., 18, 835-848, 1982.

Dagan, G., Solute transport in heterogeneous porous formations, J. Fluid Mech., 145, 151-177, 1984.

Dagan, G., Flow and transport in porous formations, Springer-Verlag, Berlin, 1989.

Dagan, G., Dispersion of a passive solute in non-ergodic transport by steady velocity fields in heterogeneous formations, J. Fluid Mech., 233, 197-210, 1991.

Dawson, C.N., C.J. Van Duijn, and R.E. Grundy, Large time asymptotics in contaminant transport in porous media, Transp. Porous Media, submitted, 1994.

Destouni, G., and V. Cvetkovic, Field scale mass arrival of sorptive solute into the groundwater, Water Resour. Res., 27, 1315-1325, 1991.

Garabedian, S.P., Large-scale dispersive transport in aquifers: Field experiments and reactive transport theory, Ph.D. thesis, Mass. Inst. of Technol., Cambridge, Mass., U.S.A., 1987.

Gelhar, L.W., and C.L. Axness, Three-dimensional stochastic analysis of macrodispersion in aquifers, Water Resour. Res., 19, 161-180, 1983.

Grundy, R.E., C.J. Van Duijn, and C.N. Dawson, Asymptotic profiles with finite mass in one-dimensional contaminant transport through porous media: the fast reaction case, Q. Jl Mech. appl. Math., Vol. 47, Pt. 1, 1994.

Gutjahr, A.L., Fast Fourier Transforms for random field generation, project report, contract 4-RS of Los Alamos National Laboratory, N. M. Inst. of Min. and Technol., Socorro, 1989.

Mackay, D.M., W.P. Ball, and M.G. Durant, Variability of aquifer sorption properties in a field experiment on groundwater transport of organic solutes: methods and preliminary results, J. Contam. Hydrol., 1, 119-132, 1986.

Neuman, S.P., C.L. Winter, and C.M. Newman, Stochastic theory of field-scale Fickian dispersion in anisotropic porous media, Water Resour. Res., 23, 453-466, 1987.

Rubin, Y., Stochastic modeling of macrodispersion in heterogeneous porous media, Water Resour. Res., 26, 133-141, 1990.

Sudicky, E.A., A natural gradient experiment on solute transport in a sand aquifer: spatial variability of hydraulic conductivity and its role in the dispersion process, Water Resour. Res., 22, 2069-2082, 1986.

Tompson, A.F.B., Numerical simulation of chemical migration in physically and chemically heterogeneous porous media, Water Resour. Res., 29, 3709-3726, 1993.

Valocchi, A.J., Spatial moment analysis of the transport of kinetically adsorbing solutes through stratified aquifers, Water Resour. Res., 25, 273-279, 1989.

Van der Zee, S.E.A.T.M., Analytical traveling wave solutions for transport with nonlinear and nonequilibrium adsorption, Water Resour. Res., 26, 2563-2578, 1990*b*. (Correction, Water Resour. Res., 27, 983, 1991.)

Van der Zee, S.E.A.T.M., and W.H. van Riemsdijk, Transport of reactive solute in spatially variable soil systems, Water Resour. Res., 23, 2059-2069, 1987.

Van der Zee, S.E.A.T.M., and J.J.T.I. Boesten, Effects of soil heterogeneity on pesticide leaching to groundwater, Water Resour. Res., 27, 3051-3063, 1991.

Chapter 9

General conclusions

Crucial effects of local nonlinear adsorption on solute transport, i.e. steepening fronts and a decreasing front retardation for a degrading solute, were shown in a one-dimensional analysis. Subsequently, important effects of local linear and nonlinear adsorption on macroscopic solute spreading in heterogeneous media are demonstrated. Analytical expressions are derived for linearly adsorbing solute spreading in physically and chemically heterogeneous formations. With a nonlinearly adsorbing solute, the boundary conditions determine the effects that occur during the spreading process. It is important to make a distinction between a finite and an infinite (continuous) injection. In case of a continuous injection, a traveling wave front develops if transverse spreading is large enough. However, transverse correlation scales are too large and transverse dispersivitities too small to reach this limit under practical circumstances. Spatial variability remains the main spreading factor although front spreading is reduced compared with linear adsorption. The shape of the plume of a finite solute injection is determined by nonlinear adsorption. In that case, nonlinear adsorption causes plume tailing and a decreasing plume velocity. A mathematical analysis of plume development in homogeneous media is applicable to heterogeneous media due to the dominating effects of nonlinear adsorption. The area where the plume is located is governed by spatial variability, in spite of a small reduction compared with linear adsorption.

Summary

In the past decades, awareness has grown that we are polluting the environment. Contamination of soils and groundwater with heavy metals, pesticides and other organic and inorganic solutes has become a major environmental issue. If contaminants reach a soil or groundwater system, they are subject to a number of dynamic processes. Biological, chemical and physical processes have an effect on the behaviour of the contaminants. Water movement may cause the contamination to be transported and spread over a certain distance. This transport behaviour is important, as it determines whether the contamination may form a risk within a relevant time scale. For example, the travel time of a contaminant to a drinking water well or surface water determines the necessity and priority of a possible remediation. Furthermore, knowledge of the transport behaviour of the solute is useful for the decision of an efficient remediation technique.

In general, contaminants or solutes are chemically reactive. They react with other substances present in the soil system to form adsorption complexes or precipitates. Adsorption causes a retardation of the solute relative to the water movement. In solute transport models, adsorption is often described as a linear relationship between the amount of solute in the liquid phase and the amount of solute in the solid phase. In reality, adsorption is influenced by many factors, such as *p*H, background concentration, competition effects between different solutes, and a limited surface available for adsorption. Consequently, a linear relationship to describe adsorption is often too simple; adsorption is a nonlinear process. In this thesis, nonlinear adsorption is described by the Freundlich equation, often used in studies related to soil and groundwater contamination. Although this relationship is a simplification of reality as well, it gives a good impression of the effects of the nonlinearity of adsorption.

An additional complicating factor in describing and predicting the movement and spreading of solutes in soil and groundwater systems is induced by the natural variation of properties. Soils are heterogeneous and this causes preferential pathways of water with dissolved contaminants. Consequently, travel times to, for example, drinking water wells can be significantly shorter or longer than predicted by using average properties. Properties that affect the movement and spreading of solutes, such as hydraulic conductivity, *p*H and organic carbon content, are spatially variable due to a spatial distribution of parent material and of the occurrence of soil forming processes.

In this thesis, the transport behaviour of reactive solutes in spatially variable porous formations is studied. The innovation is the incorporation of chemical heterogeneity in the analyses in addition to physical heterogeneity, combined with the consideration of nonlinear (bio)chemical interactions. An attempt is made to elucidate the significance of nonlinear adsorption while describing solute spreading on a larger scale, taking into account the spatial variation of the hydraulic conductivity and the adsorption coefficient.

In the first part of this thesis, transport and spreading behaviour of a nonlinearly adsorbing solute in one-dimensional columns is considered. High affinity nonlinear adsorption causes stronger binding of low concentrations than of high concentrations. Consequently, with a continuous solute injection, steep concentration fronts develop during the transport process. Theoretically, in homogeneous media these fronts approach (limiting sense) a constant velocity and a time invariant shape (traveling wave). If the solute is biodegradable (Chapter 2), for example a pesticide, the maximum concentration reduces with depth. This causes an increasing retardation factor, resulting in a decreasing front velocity. An analytical approximation for the downstream concentration front is derived, which can be used for predictions of laboratory results and for verification of numerical solutions. The results of the analytical approximation show the different behaviour of the nonlinearly adsorbing solute compared with a linearly adsorbing solute.

Differences between linear and nonlinear adsorption become more apparent when a layered column is considered (Chapter 3). In one layer the solute adsorbs according to a linear adsorption equation, whereas in the other layer adsorption is described by the nonlinear Freundlich equation. The effect of the layering order is studied and analytical approximations are derived for the downstream concentration fronts. Results show that the layering order is important to describe the

concentration front. The second (bottom) layer determines whether the front spreads (linear adsorbing layer) or steepens (nonlinear adsorbing layer) as a function of the displacement.

The unknown deterministic distributions of spatially variable properties in natural soil and groundwater systems and their uncertain effects, call for a probabilistic approach to describe heterogeneity. Using such an approach, the spatially variable property is characterized by its probability distribution function, as it can be determined by a sufficient amount of measurements. By using the statistical distribution, the results are given in statistical terms as well. Accordingly, the expected behaviour and a measure for the uncertainty can be obtained. Because predictions of concentrations are subject to a large degree of uncertainty, the results are given in terms of spatial moments. The moments characterize the expected front or plume position, and a measure for the front width and plume size.

The behaviour of a nonlinearly adsorbing solute in a chemically heterogeneous column is considered (Chapter 4). The Freundlich adsorption coefficient is assumed to be spatially variable. The column consists of many thin layers with a different adsorption coefficient for each layer. Transport calculations are performed for a large number of columns to compute the expected front position and front width as a function of time. Results show that traveling waves are expected to develop in heterogeneous columns as well. In a semi-two-dimensional field consisting of noninteracting columns, the spreading behaviour is different. Three spreading mechanisms are responsible for the field scale spreading of the solute, i.e. individual front spreading, column scale heterogeneity, and field scale heterogeneity. The column scale heterogeneity can often be ignored and spreading is dominated by field scale heterogeneity. In that case, the field averaged concentration front can be approximated by a modification of an analytical solution for linear adsorption.

In a fully two-dimensional system, i.e. a heterogeneous field with interacting columns, the effect of transverse spreading can be obtained. It turns out that with a continuously injected nonlinearly adsorbing solute (Chapter 7), transverse dispersion plays an important role. Compared with a linearly adsorbing solute, pore sale dispersion has opposing effects. Whereas it is expected that pore scale dispersion has a modest enhancing front spreading effect, with nonlinear adsorption the field scale concentration front steepens. Enhanced longitudinal spreading is resisted by the steepening effect of nonlinear adsorption, and, consequently,

transverse spreading becomes relatively more important. The transverse mixing causes a slower front spreading in the longitudinal direction. In theory, transverse spreading gives rise to the development of a traveling wave front, even in two-dimensional heterogeneous media. However, under practical circumstances, transverse spreading is too small to reach a traveling wave condition within a reasonable time scale.

An analytical solution is derived for the estimation of plume spreading for a linearly adsorbing solute in physically and chemically heterogeneous porous media (Chapter 5). Several cases of correlation between the hydraulic conductivity and the adsorption coefficient are considered. The results show that perfect negative correlation, i.e. low hydraulic conductivity and strong adsorption or high hydraulic conductivity and weak adsorption at one position, strongly enhances the plume spreading process. With perfect positive correlation, the effects of both parameters (hydraulic conductivity and adsorption coefficient) are opposite, and the results depend on the magnitude of both contributions. Numerical calculations (Chapter 6) to study the sensitivity of several field parameters point out that variation of the adsorption coefficient has similar effects as variation of the hydraulic conductivity.

If we are dealing with a nonlinearly adsorbing solute, instantaneously injected into a physically and chemically heterogeneous porous medium (Chapter 8), the plume shape is determined by nonlinear adsorption. The strong binding of the low concentrations causes tailing of the plume. The expected shape of the plume is hardly affected by spatial variability of the hydraulic conductivity and the adsorption coefficient. With an analytically derived expression for the time dependence of the growth rate of the plume, it is possible to predict the shape of the plume if one or two field observations are available.

On the other hand, both heterogeneity and nonlinear adsorption have a strong impact on the location of the plume. Due to the instantaneous injection, the maximum concentration of the plume reduces during plume displacement and spreading. Consequently, the retardation factor increases by stronger binding of lower concentrations. Therefore, in contrast with linearly adsorbing solute plumes, nonlinearly adsorbing solute plumes move with a decreasing velocity. The variance of the plume position, which is a measure for the area where the plume will be located, depends strongly on parameters describing the spatial variability of the hydraulic conductivity and the adsorption coefficient.

From this study can be concluded that nonlinear adsorption has a strong effect on solute movement and spreading in heterogeneous formations. In one-dimensional columns, the deviating behaviour from linearly adsorbing solutes is emphasized. A distinction between continuous injection and instantaneous injection is necessary, due to different spreading effects. It is shown in two-dimensional formations, that local nonlinearly adsorbing behaviour can have an important effect on field scale spreading behaviour. With a continuous injection, the behaviour on a field scale is dominated by the spatially variable property. The degree of longitudinal spreading, however, is, compared to linear adsorption, reduced due to more pronounced transverse mixing. Considering instantaneous injection, heterogeneity also determines the expected area where the plume will be located. The reduced plume velocity caused by the increasing retardation factor must be taken into account. The expected plume shape is determined by nonlinear adsorption. Strong binding of the lower concentrations causes tailing of the plumes. Several readily usable analytical expressions are derived for estimations of concentration fronts, plume shapes, plume positions, and variances of plume shapes. These expressions can be useful for first estimates in practical applications and for verification of numerical solutions and laboratory results.

Samenvatting

Gedurende de afgelopen decennia is de aandacht voor bodem- en milieuverontreiniging sterk toegenomen. Onderzoek heeft aangetoond dat de bodem en het grondwater op veel plaatsen zijn verontreinigd met zware metalen, bestrijdingsmiddelen en andere organische en anorganische stoffen. Als een verontreinigende stof de bodem of het grondwater bereikt, speelt een aantal fysische en chemische processen een rol. Als gevolg van de waterbeweging kan een verontreiniging zich verplaatsen en verspreiden. Deze verspreiding bepaalt in grote mate het risico dat een verontreiniging kan opleveren. De snelheid van verplaatsing van een verontreinigende stof in de richting van bijvoorbeeld een drinkwateronttrekkingsput bepaalt de noodzaak en de prioriteit van een mogelijke sanering. Bovendien kan met kennis van het transportgedrag van verontreinigingen een efficiënte saneringstechniek gekozen worden.

Verontreinigende stoffen zijn chemisch reactief. Zij kunnen complexen vormen met andere verontreinigingen die eventueel kunnen neerslaan, en zij kunnen reageren met de vaste fase van het poreuze medium. Dit adsorptieproces heeft een vertraging tot gevolg ten opzichte van de waterbeweging.

In het algemeen wordt bij het modelleren van stoftransport adsorptie beschreven met een lineaire relatie tussen de concentratie in oplossing en de hoeveelheid stof geadsorbeerd aan de vaste fase. Deze beschrijving is echter een vereenvoudiging van de werkelijkheid. Adsorptie wordt beïnvloed door een groot aantal factoren, onder andere de *p*H, het organisch stofgehalte, competitie tussen aanwezige stoffen en de grootte van het adsorptie-oppervlak. Dit heeft tot gevolg dat adsorptie soms beter beschreven kan worden als een niet-lineair proces. In dit proefschrift word adsorptie gemodelleerd met de Freundlich vergelijking. Hoewel ook deze relatie de werkelijkheid niet volledig weergeeft, is het wel mogelijk om

het effect van niet-lineaire adsorptie op stoftransport te bestuderen.

Een ander aspect dat het nauwkeurig beschrijven en voorspellen van transport en verspreiding van stoffen in bodems en grondwater bemoeilijkt, is de ruimtelijke variabiliteit van fysische en chemische eigenschappen. Als gevolg van plaatselijke verschillen van moedermateriaal en een van plaats tot plaats verschillende werking van bodemvormingsprocessen bestaat er grote ruimtelijk variatie van eigenschappen die het transportgedrag van stoffen kunnen beïnvloeden. De waterdoorlatendheid, de *p*H en het organisch stofgehalte zijn voorbeelden van ruimtelijk variabele eigenschappen die een groot effect hebben op de beweging en vastlegging van stoffen.

In dit proefschrift is het gedrag van reactieve stoffen in heterogene poreuze media beschreven. In de modelmatige beschrijving is ruimtelijke variabiliteit van fysische en van chemische eigenschappen in beschouwing genomen. Er wordt bovendien aandacht besteed aan de effecten van niet-lineaire adsorptie op de verspreiding van stoffen op veldschaal. De waterdoorlatendheid en de adsorptiecoëfficiënt zijn ruimtelijk variabel verondersteld.

In het eerste deel van dit proefschrift is het gedrag van een niet-lineair adsorberende stof in een één-dimensionale kolom geanalyseerd. Bij preferente adsorptie worden lage concentraties sterker gebonden dan hoge concentraties, hetgeen bij een continue bron scherpe concentratiefronten tot gevolg heeft. In homogene kolommen verandert zo'n front na verloop van tijd niet meer van snelheid en van vorm (lopende golf). Als de toegediende stof biologisch afbreekbaar is (Hoofdstuk 2), bijvoorbeeld een pesticide, dan loopt de maximum concentratie terug met de afgelegde afstand van de stof. Door de sterkere adsorptie van lage concentraties neemt de front retardatiefactor toe met de diepte, met een vertragend concentratiefront als gevolg. Dit gedrag wijkt af van het gedrag van een lineair adsorberende stof, wat ook bevestigd wordt door resultaten van een analytische benadering voor de concentratie als functie van diepte en tijd.

Een analyse met een gelaagde kolom, waarbij in één laag de stof volgens een lineaire vergelijking adsorbeert en in de andere laag de stof niet-lineair adsorbeert (Hoofdstuk 3), laat meer verschillen zien tussen een lineair en een niet-lineair adsorberende stof. Het effect van de volgorde van de lagen is bestudeerd en er zijn analytische benaderingen afgeleid voor de concentratieprofielen in de onderste laag. Deze laag bepaalt of het concentratiefront zich verbreedt (lineaire adsorberende laag) of scherp blijft (niet-lineair adsorberende laag).

Een stochastische methode is gebruikt om de ruimtelijke variabiliteit van de waterdoorlatendheid en de adsorptiecoëfficiënt te beschrijven. Zo'n methode houdt in dat de ruimtelijke verdeling van een heterogene eigenschap beschreven wordt met een kansverdelingsfunctie. Deze functie kan bijvoorbeeld bepaald worden door een aantal metingen uit te voeren. Door de kansverdeling van de ruimtelijk variabele parameters in de analyse mee te nemen, worden de resultaten ook in de vorm van statistische grootheden gegeven. De verwachte positie en een maat voor de vorm van het concentratiefront of van de pluim van de toegediende stof worden weergegeven met behulp van ruimtelijke momenten (verwachting, variantie).

In een chemisch heterogene kolom, bestaande uit een groot aantal lagen met verschillend adsorptiegedrag, is het transport van een niet-lineair adsorberende stof bestudeerd (Hoofdstuk 4). Een groot aantal kolommen zijn gebruikt om de verwachting van de frontpositie en frontbreedte te bepalen. Resultaten van frontbreedten zijn vergeleken met frontbreedten van lopende golven die ontstaan in homogene kolommen. Het blijkt dat de verwachte frontbreedte goed te beschrijven is met een equivalente homogene kolom, met andere woorden, ook in heterogene kolommen ontstaan scherpe concentratiefronten. Door een heterogeen veld te beschrijven als een groot aantal kolommen, is het mogelijk om de verspreiding van een stof in een semi-twee-dimensionaal veld te analyseren. Met deze methode wordt geen rekening gehouden met laterale menging tussen kolommen. In zo'n geval wordt de breedte van een front bepaald door drie factoren, namelijk de breedte van de fronten in de verschillende kolommen, de heterogeniteit binnen de kolommen en de variatie die bestaat tussen de verschillende kolommen. Voor een verspreiding op veldschaal speelt de interne variatie van adsorptie eigenschappen een ondergeschikte rol, deze wordt voornamelijk bepaald door de variatie tussen de kolommen. Door alleen deze spreidingsfactor in beschouwing te nemen, kan een analytische benadering gebruikt worden om veldgemiddelde concentraties als functie van diepte en tijd te bepalen.

In een volledig twee-dimensionaal domein waarbij met de interactie tussen kolommen wel rekening wordt gehouden, kan de rol van de laterale of transversale spreiding duidelijk worden (Hoofdstuk 7). Resultaten van de berekeningen laten zien dat bij een continue bron deze lokale transversale dispersie wel degelijk een rol speelt die ook op grotere schaal effecten heeft. In vergelijking met een lineair adsorberende stof heeft lokale dispersie bij niet-lineaire adsorptie tegengestelde effecten. Een verwachte kleine verbreding van het gemiddelde concentratiefront

blijft uit, er vindt zelfs een verscherping van het front plaats. Door de sterke binding van de lagere concentraties wordt de longitudinale spreiding tegengehouden. Hierdoor is de transversale spreiding relatief belangrijker en neemt de breedte van het front langzamer toe. In het limiterende geval dat de transversale spreiding zeer sterk is, ontstaat er, zelfs in een heterogeen twee-dimensionaal domein, een lopende golf. Onder praktische omstandigheden, echter, zal zo'n concentratiefront niet ontwikkelen vanwege de beperkte transversale spreiding.

Voor de verspreiding van een niet-lineair adsorberende stof in een fysisch en chemisch heterogeen poreus medium is een analytische oplossing afgeleid (Hoofdstuk 5). Verschillende vormen van mogelijke correlatie tussen de waterdoorlatendheid en de adsorptiecoëfficiënt zijn in beschouwing genomen. Met behulp van numerieke berekeningen (Hoofdstuk 6) is de gevoeligheid van een aantal parameters geanalyseerd, die de mate van adsorptie en ruimtelijk variabiliteit beschrijven. De resultaten laten zien dat bij gelijke mate van variatie van fysische en chemische parameters de effecten van beide spreidingsfactoren gelijk zijn. De numerieke resultaten blijken goed voorspeld te kunnen worden met behulp van de analytische oplossing.

In het geval van een instantane bron van een niet-lineair adsorberende stof in een fysisch en chemisch heterogeen poreus medium (Hoofdstuk 8) wordt de vorm van de pluim sterk bepaald door de niet-lineaire adsorptie. Door de sterke binding van lage concentraties hebben de pluimen een lange vorm. Met behulp van wiskundige analyse, geldig voor een homogeen medium, kan de groei van deze pluimen als functie van de tijd worden voorspeld. De analyse is ook goed bruikbaar in heterogene domeinen door de dominante effecten van niet-lineaire adsorptie op de verwachte pluimvorm.

De lokatie van de pluim wordt daarentegen sterk beïnvloed door de heterogeniteit. De grootte van het gebied waar de pluim na verloop van tijd aangetroffen kan worden, wordt bepaald door de mate van ruimtelijke variabiliteit van de waterdoorlatendheid en de adsorptiecoëfficiënt. Daarbij moet wel rekening gehouden worden met de afnemende snelheid van de pluim als gevolg van de toename van de retardatiefactor bij afnemende concentraties (niet-lineaire adsorptie).

Van dit onderzoek kan geconcludeerd worden dat niet-lineaire adsorptie een groot effect heeft op transport en verspreiding van stoffen in heterogene media. In één-dimensionale kolommen zijn verschillen met een lineair adsorberende stof

aangetoond. Een onderscheid tussen een continue bron en een instantane bron is noodzakelijk vanwege de verschillende spreidingseffecten die een rol spelen. Bij een instantane bron neemt de maximale concentratie van de bewegende pluim af, waardoor retardatiefactor toeneemt gedurende de verplaatsing. Dit heeft tot gevolg dat de pluim met een afnemende snelheid door het poreuze medium beweegt. Bij een continue bron speelt dit geen rol. Bij beide bronnen heeft lokale niet-lineaire adsorptie gevolgen voor de spreiding op grotere schaal. Bij een continue bron treedt er frontspreiding op door de heterogeniteit, maar als gevolg van de prominente rol van transversale dispersie is de toename van de frontbreedte kleiner dan bij een lineair adsorberende stof. Dit betekent dat er ook in twee-dimensionale domeinen scherpe fronten ontstaan. Bij een instantane bron wordt de verwachte vorm van de pluim in grote mate bepaald door niet-lineaire adsorptie, ook in heterogene domeinen. De pluimen hebben een lange vorm door de sterke binding van de lage concentraties. Waar de pluim na verloop van tijd aangetroffen kan worden, wordt voornamelijk bepaald door de mate van heterogeniteit. Een aantal analytische uitdrukkingen is afgeleid voor concentratiefronten, pluimposities en pluimvormen. Deze uitdrukkingen kunnen nuttig zijn voor voorlopige schattingen en voor verificaties van numerieke modellen en experimentele resultaten.

Curriculum vitae

Willem Jan Pieter Bosma werd op 31 oktober 1965 geboren in Amersfoort. Na zijn VWO eindexamen in 1983 vertrok hij naar de Verenigde Staten om een jaar te studeren aan 'Occidental College' in Los Angeles. Een van de hoogtepunten van dat studiejaar was het werk dat hij verrichtte voor de organisatie van de Olympische Spelen van 1984. Bij terugkomst in Nederland in september 1984 begon hij de studie bodemkunde aan de Landbouwuniversiteit Wageningen. Tijdens zijn studie heeft hij stages gelopen bij Cornell University in de Verenigde Staten en bij het MARIN (Maritime Research Institute) in Wageningen. In 1990 studeerde hij met lof af met de afstudeervakken wiskunde, operationele analyse, bodeminventarisatie en bodemverontreiniging.

In september 1990 kreeg hij een aanstelling als assistent in opleiding bij de vakgroep Bodemkunde en Plantevoeding van de Landbouwuniversiteit. Gedurende de vier jaar die volgden heeft hij onderzoek uitgevoerd op het gebied van de bodem- en grondwaterverontreiniging, waarvan de belangrijkste resultaten in dit proefschrift zijn beschreven. In het kader van zijn onderzoek heeft hij in 1992 vier maanden doorgebracht aan de Universiteit van Trento in Italië. In juni 1993 is hij in de Universiteitsraad van de Landbouwuniversiteit gekozen, waarin hij onder meer actief is in de commissie studentenvoorzieningen (CSV) en de commissie financiën en planning (CFP). In augustus 1993 haalde hij zijn motorrijbewijs.